Abstract

Compositae plants of the genus *Erigeron* have *ca.* 390 species, widely distributed in most temperate regions around the world. *Erigeron annuus* (L.) Pers. (fleabane) is one of the most valuable plants in this genus, used in Chinese folk medicine to treat indigestion, malaria, enteritis, hepatitis and hematuria increasingly since the 1970s. However, it is not an indigenous species in China and has not been officially recorded in the Chinese Pharmacopeia. Very little research has been published on its biological activity and no activity against MRSA has been reported. In this research, whole plant material was collected in Shanghai, China and its chemical composition, antibacterial activity, DNA gyrase inhibitory activity and mutagenicity assessment were evaluated on isolated compounds and extracts.

Chapter I is an introduction to the plant *E. annuus.* A review of the literature relating to phytochemical studies and their biological applications is given.

Chapter II describes the phytochemical separation of *E. annuus.* An ethanolic extract of the whole plant was suspended in water and partitioned against hexane, ethyl acetate and butanol respectively. Various chromatography techniques of column chromatography, preparative TLC, flash chromatography, HPLC, gel column filtration, solid phase extraction and also recrystallization methods were used in the separation process.

Chapter III describes the antibacterial studies on *E. annuus.* Minimum inhibitory concentration assays were used in order to search for potential antimicrobial agents. Isolated compounds and fractions were tested against two Gram-negative and three Gram-positive wild type strains and a methicillin-resistant *Staphylococcus aureus* (MRSA) strain. Two compounds were found to have inhibitory activity against MRSA, while four hexane, one ethyl acetate and four butanol fractions showed inhibitory

activity against both Gram-positive and Gram-negative wild type strains.

DNA gyrase is a type II topoisomerase, unique in prokaryotes, that regulates bacterial DNA topology structures. It is a good target for antibacterial agents. Potential gyrase inhibitors can be identified in DNA gyrase supercoiling assays against Gram-negative and Gram-positive gyrase. Chapter IV discusses the DNA gyrase inhibitory activity of isolated compounds and fractions. Five compounds, five ethyl acetate and three butanol fractions showed gyrase inhibitory activity and the IC_{50} of three of the compounds was evaluated.

The final part of this thesis is a mutagenicity assessment of the plant extracts against *Saccharomyces cerevisiae ade2*. Mutagenicity tests were carried out against a haploid *Saccharomyces cerevisiae ade2* (mating type **a**). However, the maintenance of the red mutant was difficult, and the background mutation frequency was very high giving inconsistent test results. During the tests, some cytotoxicity was observed in the hexane fractions which had a major influence on the cell survival rate.

This study has demonstrated for the first time that *E. annuus* contains compounds with antibacterial activity against MRSA and inhibitory activity against DNA gyrase. Two of the compounds, erythrodiol and 4-pent-3'-ne-1'-ynyl-pyran-2-one were isolated from this plant for the first time, and both compounds were active against the MRSA strain. DNA gyrase inhibitors were also found including one naphthoquinone derivative and one 1, 4-benzopyrone derivative. This research supports the traditional use of *E. annuus* as a folk herbal medicine in China to treat fever and infections such as malaria, diarrhea, gingivitis, gastroenteritis. Further investigation of this plant's biological activity is warranted.

Acknowledgements

There are many people to whom I would like to express my deepest gratitude for their considerable help along this journey, but first and foremost my supervisor Dr. E. Smith for her guidance, suggestions, valuable discussions and patience throughout this research study. I would also to express my gratitude to Professor S.W. A. Bligh, for her kind and helpful guidance in the first three years chemistry research. Many thanks are due to my second supervisor Dr. K. White and Dr. S. Atchia, for their constructive advice and support. I express my sincerest gratitude to my former lecturers Dr. D. Spillane, Dr. D. Green and Dr. M, Shepherd who have supported and taught me a great deal of knowledge in science at undergraduate level. I would also like to add thanks to Dr. N. Wardle for his valuable suggestions and many patient talks. Many thanks must also go to Professor Z. T. Wang, Dr. L. Yang, Dr. T. Wu, Dr. S. Z. Zheng and Dr. L. H. Wu from Shanghai University of Chinese Traditional Medicine for their great advice and academic support on the chemical study of my research.

I would like to express my deep gratitude to all the technicians in the Londonmet Science Centre; to Mr. J. Crowder, Dr. B. Awamaria, Mr E. Coleman, Dr. J. Morgan and Mr O. Erkek, for their technical assistance and support in the NMR, HPLC laboratories and microbiological experiments. Without their help, I would never have made it this far. I would like to thank all my former colleagues and all my research partners in the lab: Dr. X. B. Pan, Dr. G. Y. Chen, Dr. Y. C. Yang, Dr. E. Welbeck, Dr. O. Ogegbo, Dr. Y. Z. Xu, Xin Yu, Ali and Miao.

Finally I would like to thank my family for their support and understanding during my research, which has enabled me to complete this work.

<div align="right">Yifan Zhang</div>

Dedications

I wish to dedicate my research to the development of traditional Chinese herbal medicine.

Declaration

I declare that whilst studying for the Doctorate in Chemistry at London Metropolitan University, I have not been registered for any other award at another university. The work undertaken for this degree has not been submitted elsewhere for any other awards. The work contained within this submission is my own work and, to the best of my knowledge and belief, it contains no material previously published or written by another person, except where due acknowledgement has been made in the text.

Yifan Zhang

September 2014

Abbreviations and Symbols

>	Greater than
<	Less than
°C	Degree Celsius
δ (ppm)	Chemical shift (in parts per million)
^{1}H-NMR	Proton nuclear magnetic resonance
^{13}C-NMR	Carbon nuclear magnetic resonance
ABC	Bacterial efflux pump:
	ATP-binding cassette superfamily
ACTs	Artemisinin-combination therapies
ADP	Adenosine diphosphate
AGEs	Advanced glycation end products
AIR	5'-phosphoribosylaminoimidazole
AMP	Adenine monophosphate
ATCC	American Type Culture Collection
ATP	Adenosine triphosphate
CoA	Coenzyme A
CA-MRSA	Community-associated MRSA
$CDCl_3$	Deuterated chloroform
cfu	Colony forming units
CYP450	Cytochrome P450 monooxygenase enzyme system
Da	Dalton
D_2O	Deuterated water
DMSO	Dimethyl sulfoxide
DNA	Deoxyribonucleic acid
DTT	Dithiothreitol
EDTA	Ethylenediaminetetraacetic acid
EMS	Ethyl methanesulfonate
EtOAc	Ethyl acetate
EtOH	Ethanol
GC-MS	Gas chromatography-mass spectrometry
gDNA	Gate-DNA
HA-MRSA	Healthcare-associated MRSA
HPLC	High performance liquid chromatography
IC_{50}	Half maximal inhibitory concentration

LC-MS	Liquid chromatography-mass spectrometry
LLE	Liquid-liquid extraction
LPS	Lipopolysaccharides
m/z	Mass-to-charge ratio
MATE	Bacterial efflux pump:
	Multidrug and toxic compound extrusion family
MeOH	Methanol
MFS	Bacterial efflux pump:
	major facilitator superfamily
MF	Mutation frequency
MHB	Müller hinton broth
MIC	Minimum inhibitory concentration
min	Minute
MRSA	Methicillin-resistant *Staphylococcus aureus*
MTT	Thiazolyl blue tetrazolium bromide
MV	Minimal plus vitamin medium
MV+ade	Minimal plus vitamin and adenine medium
NAG	B-acetylglucosamine
NAM	N-acetylmuramic acid
NCYC	National Collection of Yeast Cultures
NMR	Nuclear magnetic resonance
ODS	Octadecylsilyl
Pal	Peptidoglycan-associated lipoprotein
PBPs	Penicillin-binding proteins
PCR	Polymerase chain reaction
PRPP	Phosphoribosyl pyrophosphate
RNA	Ribonucleic acid
RND	Bacterial efflux pump:
	Resistance-nodulation division superfamily
SPE	Solid phase extraction
SMR	Bacterial efflux pump:
	Small multidrug resistance
TAE	Tris-acetate-EDTA buffer
tDNA	Transfer DNA
TIC	Total ion chromatogram
TLC	Thin layer chromatography
UV	Ultraviolet
TMS	Tetramethylsilyl

YEA	Yeast extract agar
YEL	Yeast extract liquid medium
YEAD	Yeast extract adenine dextrose medium
YEPDA	Yeast extract peptone adenine dextrose medium

Table of Contents

List of Figures

<u>Chapter V:</u>

<u>Chapter VI:</u>

List of Tables

1. Chapter I: Introduction

1.1 Introduction

1.1.1 Traditional medicine

The earliest surviving records of medicine are from the ancient Egyptian civilization. The first records of ancient traditional medicine date back to 2900 BC in the form of clay tablets created by the Egyptian people. Western approaches to medicine are very different to those originating in the East (Rustamadji, 2000). The first record of Chinese Materia Medica was documented in 1100 BC in the book of <wu shi er bing fang> (containing of 52 prescriptions) (Cragg and Cragg, 2001). Unlike the western medicinal system, applications of Chinese medicines were performed under the instruction of the basic theory of traditional Chinese medicine in clinic (Li et al., 2014). The traditional Chinese medicine had many forms such as decoction, vinum and ointment. The most commonly used Chinese medicines were decoctions, but the chemical compositions and preparation methods could be different according to the different diagnosis of individual patient. Commonly, more than two herbs were used in one prescription and the final chemical components of the decoction were unclear. Sometimes the side effects of the decoctions were serious, as they might be contaminated with heavy metals or produce toxins during the preparation procedures (Yu et al., 2011, Sreejith et al. 2014). It is necessary to evaluate the validity of phytochemicals from herbal medicine, eliminating the risk of treatments and optimizing the applications.

1.1.2 Phytochemicals

Plants produce phytochemicals with a variety of structures and functions. They provide a wide range of foods, medicines and dietary supplements for humans (Osbourn and Lanzotti, 2009). They have numbers of biochemical functions, which had been proven to be effective against a range of human diseases. For example, over 200 years ago, the isolation of the first pharmacologically active compound from

Papaver somniferum was achieved by Germany scientist Friedrich Wilhelm Adam Sertürner. He successfully isolated and purified morphine in 1804 and published his findings in the German *Journal der Pharmacie* for the first time. As a consequence of this research, morphine became widely used from 1815 (Schmitz, 1985), the discovery of morphine initiated a new era of drug development. As a drug precursor (Hamilton and Baskett, 2000), morphine and other opioids were modified to reduce the side-effects, improve the drug's effectiveness. Those semi-synthetic drugs include dihydromorphine, hydromorphone and heroin (Khazir et al., 2013, Klous et al., 2005).

Phytochemicals had been isolated from natural plant sources and used to treat diseases instead of using mixed herbal decoctions. They provide a more precise treatment for certain diseases, for example, artemisinin, a first line anti-malarial drug, was first separated in 1972 from *Artemisia annua* L., and used for treating *Plasmodium falciparum* caused malaria (Tu, 2011). The synthesized derivatives of artemisinin are also used in artemisinin-combination therapies (ACTs) against all types of malaria (Gubaev et al., 2009). It could inhibit the early stages of plasmodium development in the red blood cells by inactivation of the PfATP6 calcium pump on the cell membrane (Haynes and Krishna, 2004, Shandilya et al., 2013). Another famous anti-malarial compound is quinine from genus *Cinchonas* which has been used in malarial treatment since the 1960s (Daikos et al., 1961). Quinine and its derivatives had been used as first line antimalarial agents almost 400 years until quinine resistance became widespread after 1950s (Achan et al., 2011).

1.1.3 Secondary metabolites

Plant cells can produce two types of metabolites: primary and secondary metabolites. A large proportion of phytochemicals are secondary metabolites, as they are produced by plants to defend themselves against pests and diseases and to adapt to their living environments. Unlike primary metabolites, secondary metabolites are not necessary for plant survival, but important for plant bioactivities (Leicach and Chludil,

2014) and benefits (Muller-Waldeck et al., 2010). For example, gibberellins are a type of plant hormones that can regulate plant growth (Martin and Hine 2008); *Cinnamomum camphora* can produce camphor, which they secreted to repeal the pests which used as an insect repellent agent and pesticide by human (Martin and Mcferran, 2008).

1.2 *Erigeron annuus* (L.) Pers

Erigeron annuus (L.) Pers (also known as Herb of Annual Fleabane) belongs to the Compositae family, genus *Erigeron* (Stace, 1992). It is native to North America and was introduced to China in the 17th century. Since then, it has become popular in domestic gardens (Edwards et al., 2006).

Figure 1.1 *Erigeron annuus* (L.) Pers. Copied from the web page (Pflanzenbilder, 2014).

Erigeron annuus (L.) Pers (Figure 1.1) is a biennial herbaceous plant, 20-100 cm in

height with sparsely haired erect stems and alternate leaves (Daniel and Austin;, 2004). Small clusters of daisy-like white flowers 1.5 cm in diameter occur at the apex of the plant. The flowers' blooming period begins in early summer and continues until late autumn (Gedvilaite and Sasnauskas, 1994). The achene is covered with fine hair (ChineseAcademyofSciences, 1985).

1.2.1 Phytochemicals form *E. annuus*

Phytochemicals from *E. annuus* can be sorted into three major classes: terpenes (including sesquiterpenes, diterpenes and triterpenes); steroids; and flavonoids. Sesquiterpenes have been reported as the main constituents in this plant (Iijima et al., 2003a) showed in Table 1.1 (Table 1.1).

Table 1.1 Phytochemicals isolated from *E. annuus*

Terpenoids
Sesquiterpenes (Li et al., 2005, Iijima et al., 2003a)
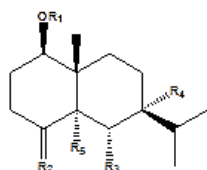
R₁=H, R₂=CH₂, R₃=H, R₄=OH, R₅=H, 1β,7α-dihydroxyeudesman-4(15)-ene;
R₁=H, R₂=O, R₃=OH, R₄=H, R₅=H,
   (1R,5S,6S,7S)-1β,6α-dihydroxyeudesman-5-one;
R₁=β-D-Glu, R₂=CH₂, R₃=OH, R₄=H, R₅=H,
   1β-O-β-D-glucopyranosy-6α-hydroxyeudesman-4(15)-ene;
R₁=H, R₂=CH₂, R₃=OH, R₄=H, R₅=H, 1β,6α-dihydroxyeudesman-4(15)-ene;
R₁=H, R₂=CH₂, R₃=H, R₄=H, R₅=OH, 1β,5α-dihydroxyeudesman-4(15)-ene
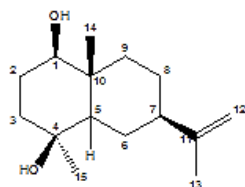
1β,4β-dihydroxyeudesman-11-ene
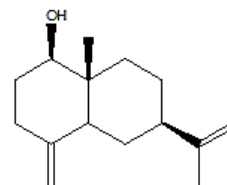
1β-hydroxyeudesman-4(15),11-diene

Sesquiterpenes (Li et al., 2005, Iijima et al., 2003a)
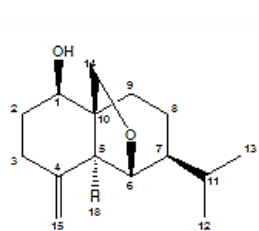
6β,14-epoxyeudesman-4(15)-ene-1β-ol
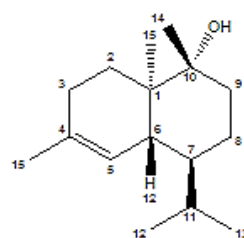
10α -hydroxycadin-4-ene-15-ol
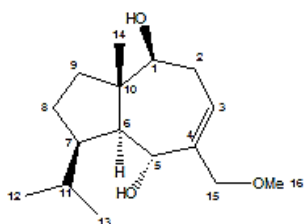
15-methoxyopposit-4-ene-1β –ol
oppsit-4(15)-ene-1β,11-diol
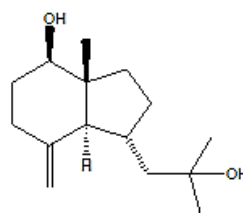
15-methoxyisodauc-3-ene
-1β,5α–diol
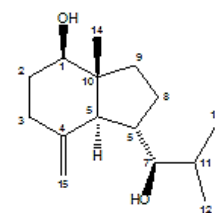
(7R*)-opposit-4(15)
-ene-1β,7-diol
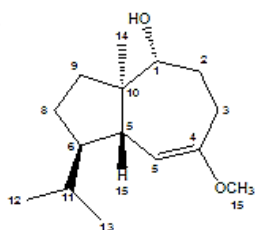
1α-hydroxyisodauc-4-ene-15-ol
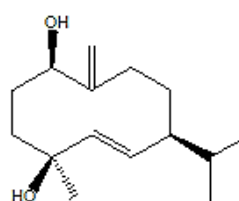
(5E)-germacra-5,10(14)-dien-1β ,4β-diol
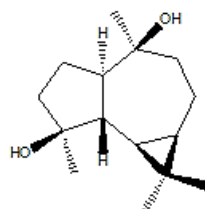
aromadendrane-4β,10β-diol
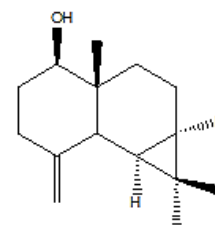
β-maaliene

Diterpene (Iijima et al., 2003a)
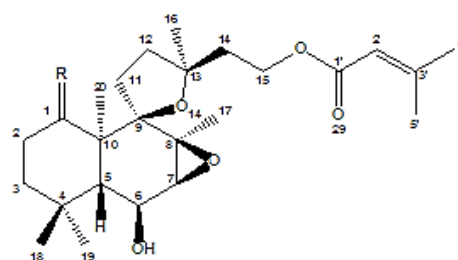
R=O, Philadelphinone
R=H, erigerol

Triterpenes (Li et al., 2004)
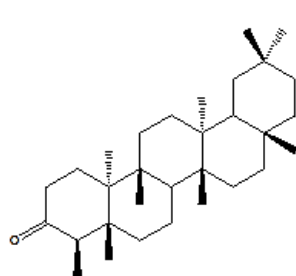
friedela-3-one (friedelin)
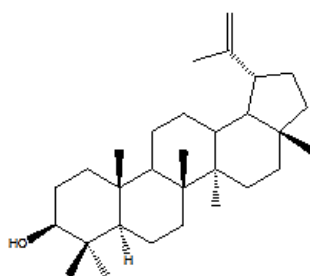
lupeol
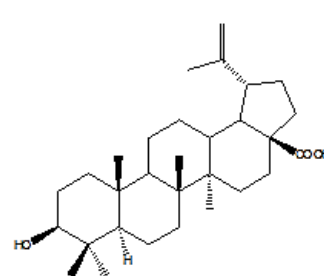
betulinic acid
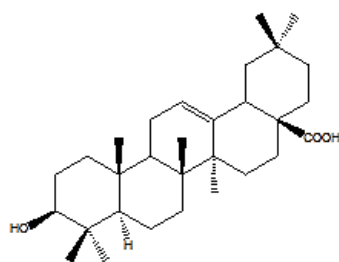
oleanolic acid
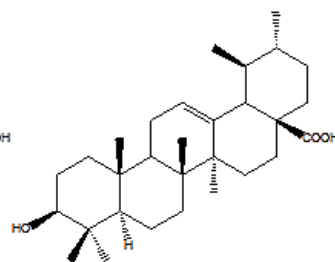
ursolonic acid
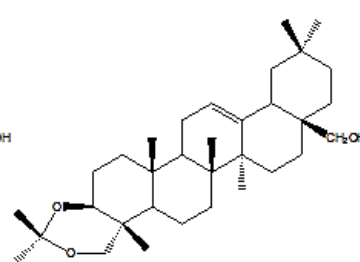
olean-12-ene-28-ol-3β,23
dihydroxy acetonide
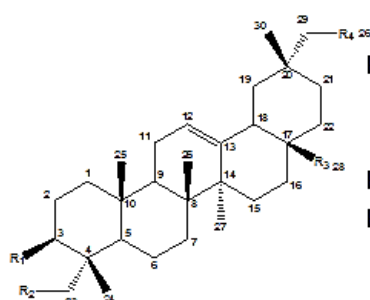
$R_1=R_2=OH, R_3=COOH, R_4=O-β-D-Glu$),
29-O-β-D-glucopyranosyloxy-3β,23-dihydroxyolean-12-ene-28-oic
;
$R_1=R_2=OH, R_3=CH_2OH, R_4=H$, olean-12-ene-3β,23,28-triol;
$R_1=OH, R_2=H, R_3=CH_3, R_4=H$, olean-12-ene-3β-ol

Sterols (Mohamed and Abd, 2006, Kim et al., 2005)
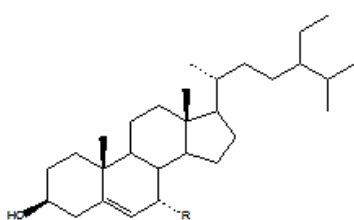
R=H, β-sitosterol
R=OH, stigmast-5-ene-3β,7α-diol
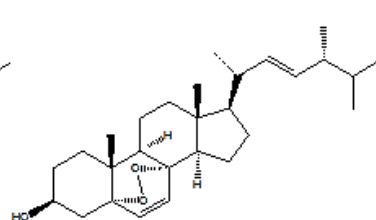
ergosterol peroxide
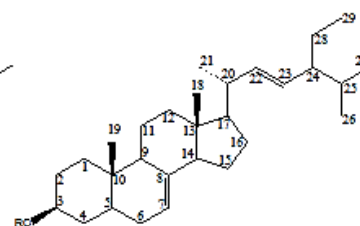
R=H, stigmast-7,24-dien-3β-ol
R=β-D-Glu, 3β-O-D-glucopyranoside-
stigmast-7,24-diene
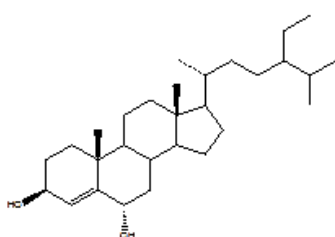
stigmast-4-ene-3β,6α-diol

7

Flavonoids (Mohamed and Abd, 2006, Jang et al., 2010, Yoo et al., 2008)
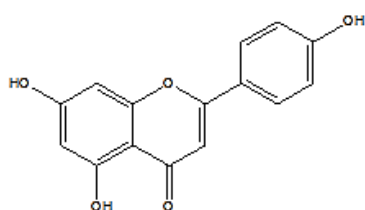
apigenin
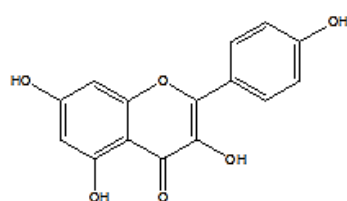
kaempferol
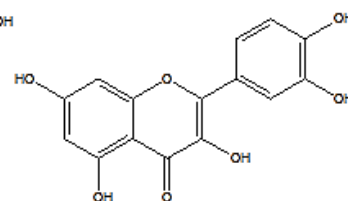
quercetin
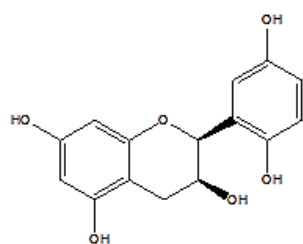
(2S,3S)-3,5,7,2',5'-
Pentahydroxyflavan
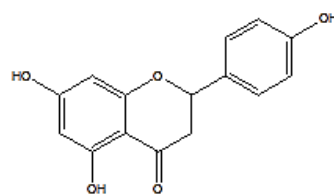
naringenin
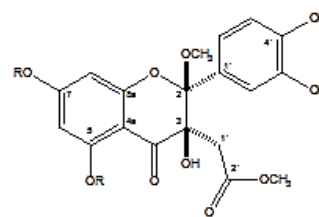
erigeroflavanone
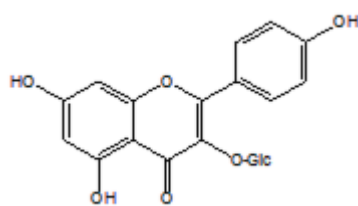
astragalin
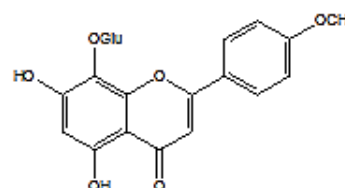
isoscutellarein-4-methyl ether 8-O-b-D-gcuronide

Caffeic acid and derivatives (Jang et al., 2010)
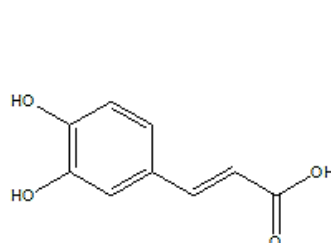
caffeic acid
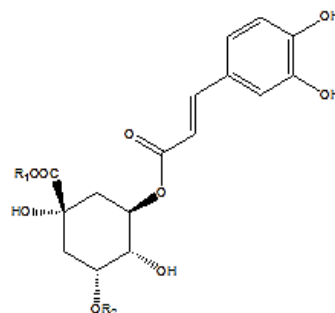
R₁=R₂=H, 3-caffeoylquinic acid
R₁=CH₂, R₂=Caf, 3,5-di-o-caffeoylquinic acid methyl ester

3,5-di-O-caffeoyl-epi-quinic acid

8
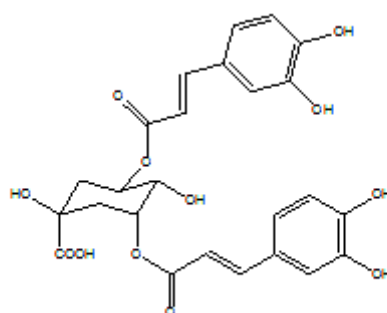
γ-pyranone derivatives (Hashidoko, 1995, Li et al., 2006)
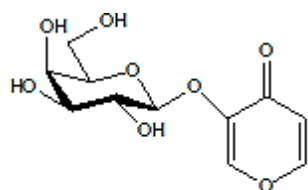
3-hydroxyl-g-pyranone
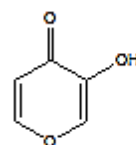
3-hydroxy-pyran-4-one

Cyclopentenone Derivatives (Iijima et al., 2003b)
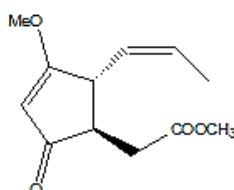
erigerenones   A
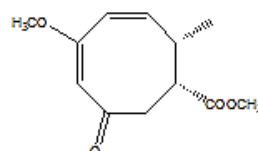
erigerenone B

Others (Li et al., 2006, Yang et al., 2008)
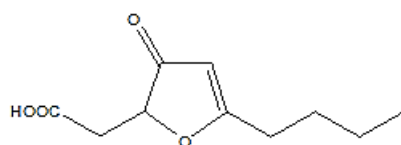
(5-butyl-3-oxo-2,3-dihydrofuran-2-yl)-acetic acid
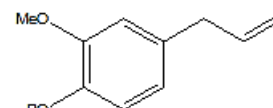
R=Glu, 1-O-β-D-(6'-O-β-D-glucopyranosyl)-
2- methoxy-4-propenylbenzene
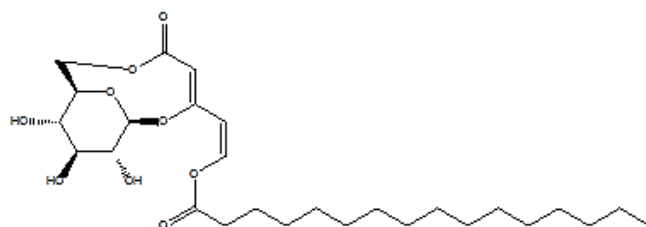
monosaccharide erigearide

Glu: glucuronoyl

Compounds isolated from the aerial part of this plant include: sesquiterpenes (Mishima et al., 2005, Nazaruk and Kalemba, 2009, Ragasa et al., 1997, Li et al.,

2005, Iijima et al., 2003a); triterpenes (Li et al., 2004); flavonoids (Mohamed and Abd, 2006); caffeic acid (Jang et al., 2010) and its derivatives (Jang et al., 2008, Mishima et al., 2005); monosaccharide derivatives; polyacetylenic compounds (Pieribattesti et al., 1981); cyclopentenone derivatives (Iijima et al., 2003b) and γ-pyrone derivatives (Hashidoko, 1995). Saccharides or polysaccharides were discovered in the roots of *E. annuus* (Roberfroid, 2005). In addition, over 60 constituents from the volatile oil of the whole plant were identified by Lis and Kumar (Lis et al., 2011, Kumar et al., 2014).

1.2.2 Bioactivities of *E. annuus*

E. annuus has been used as a folk medicine in southern China, India and some other Asian countries (Chinese Materia Medica, 1985). It is also commonly described as an ornamental plant and is used for improving soil conditions (Liu et al., 2008).

1.2.2.1 Medical use

E. annuus has some medical applications that have been reported in treating diseases in south China. In some villages in Zhejiang, Anhui and Hubei provinces in China, the local physicians told the malarial patients to chew on the aerial part of the plant or to ingest the water/ethanolic extracts of the *E. annuus* (100 g dried plant extracted by 300 mL solvent) 2-4 hours before the paroxysm. It has been used for treating malarial fevers caused by *Plasmodium vivax* and *Plasmodium falciparum*. (Shanghai Scientific Technological Publishers, 1985, Chinese Academy of Sciences, 1985). The medicinal applications of this plant were first published in the 1970s in many Chinese folk medicine books by the local health committees, including treating diarrhea (Revolutionary Health Committee of Zhe jiang Province, 1970); gingivitis (Nanjing Military Ministry of Health, 1969, Fan and Zhu, 1975); gastroenteritis (Revolutionary Health Committee of Anhui Province, 1975); hepatitis; and cholecystitis (Shanghai People's Publishing House, 1972). However, mechanisms for these medicinal usages are still unstudied.

1.2.2.2 *In vitro* test activities

Antimicrobial activities were reported on the essential oils from flower, leaf, stem, and root extracts of *E. annuus.* The oils showed inhibitions at concentration of 153.2-660.0 µg/mL against fungal pathogens such as *Fusarium oxysporum, Helminthosporium maydis, Rhizoctonia solani, Alternaria solani* and *Sclerotinia sclerotiorum,* compared to fungicide carbendazim (IC$_{50}$ 33.7-38.7 µg/mL)(Kumar et al., 2014). The flower extract also had been used in the synthesis of Ag-nanoparticle as a reducing and a capping agent against *B. linens* and *S. epidermidis* (Velmurugan et al., 2014).

An ergosterol peroxide isolated from the flower extract might be used as a potential anti-hypercholesterolemic and anti-atherogenic agent. It was proven to have inhibitory activity against cholesterol acyltransferase (ACAT) by the acylating of cholesterol to cholesteryl esters in rat liver cells. From the cholesterol research results of Kim and Brown, the inhibitory value was observed at 51.6± 0.9% at 0.23 mM, compared to the positive control oleic acid anilide 45.2± 1.4 % at 0.3 mM (Kim et al., 2005, Brown et al., 1975).

Moreover, compounds separated from *E. annuus* were reported to have anti-cancer activities. Ethanolic extracts of *E. annuus* are tested for antiproliferative and antiprotein-glycation activities in a variety of cancer cell lines, including MCF7 (breast epithelial adenocarcinoma) cells. The IC$_{50}$ were observed using MTT assay at 62.54±1.63 µM (Kim and Kim, 2003). Caffeic acid and it's derivatives were isolated from the EtOAc extract of *E. annuus* according to Jang's research, it had inhibitory activity against Advanced Glycation End products (AGEs). The best inhibitory activity was recorded at IC$_{50}$ 12.8 µM for O-caffeoylquinic acid methyl ester, even better than the positive control aminoguanidine 961 µM (Jang et al., 2008, Jang et al., 2010).

The antioxidant property had also been reported for the methanolic and butanol extracts of *E. annuus.* The antioxidant assay-guided fractionation led to an isolation of

three antioxidant compounds: apigenin, quercetin-3-O-glucoside and caffeic acid (Lee and Lee, 2006). The activity had been reported in another research that a flavanone derivative erigeroflavanone was separated from the flower's ethyl acetate extract, it was proven to have potential cytoprotective effects against hyperglycemia-induced oxidative mouse mesangial cell death (Kim et al., 2009).

Germination inhibitory activity was found in *E. annuus* in field tests. *E. annuus* is a hardy plant, tolerant of a wide range of soil conditions including gravels and clay. It can spread aggressively and compete for resources with other plants in its vicinity (Ling and Chen, 1985,Shanghai Scientific Technological Publishers, 1985, Trtikova, 2009). The mechanism of the competitive growth was studied and a compound (5-Butyl-3-oxo-2,3-dihydrofuran-2-yl)-acetic acid was isolated from the flower. It was proven to be a strong inhibitor in plant growth by suppressing the germination. According to Oh's study, the extract showed 50% inhibitory effects on the germination of lettuce seeds at the concentration 2.13± 0.03 mM (Oh et al., 2002).

E. annuus was also reported to be used as a biological control for pests. The volatile extract from this plant could attract the females *Lygus* and female *Peristenus. relictus* (Halloran et al., 2013)*.*

1.2.2.3 *In vivo* test activities

According to Jo's research, oral administration of 0.3 g/k the methanolic root extract of *E. annuus* had anti-inflammatory effects against the carrageenan-induced acute paw edema in rat and could suppress the activation of rat macrophages (3 and 10 µg/mL) (Jo, 2013).

1.3 Aim and objectives

E. annuus is a common plant although it is not officially recorded in the China Pharmacopeia, its extracts have been used as folk medicines in many treatments. Few results of the chemical components have been published, very little research has been published on the antimicrobial activity and no reports of antibacterial activity against Methicillin-resistant *Staphylococcus aureus* and DNA gyrase inhibitory activity have been published yet. The aim of this research was to investigate the chemical composition of this plant and look for potential antibacterial agents through bioassay guided fractionations.

In order to study the antibacterial activity of *E. annuus*, enthanolic crude extract of whole plant was made, and then partitioned using hexane, ethyl acetate and butanol. Antibacterial assays and DNA gyrase supercoiling assays were employed in this research to guide the separation. It was an efficient approach to narrow down the range of fractionation.

The aim of the antimicrobial study was to identify the antibacterial agents from the active fractions, and bioassay guided fractionations against wild type *Salmonella enterica, Micrococcus luteus, Enterococcus faecalis, Staphylococcus aureus, Escherichia coli* and Methicillin-resistant *Staphylococcus aureus.*

Selected fractions from the antibacterial research were tested for DNA gyrase inhibitory and mutagenicity activities. The antibacterial mode of action would be studied by exhibiting DNA gyrase inhibition during the DNA gyrase supercoiling assays. The evaluation of the mutagenicity assessment of the potential antibacterial agent will be carried out against a yeast strain.

2. Chapter II: Chemical separations of *Erigeron annuus* (L.) Pers

2.1 Introduction

E. annuus is a hardy plant that can be found around the world. It is not a widely used herb and only a few reports have been published on its chemical compositions and biochemical activities. In previous studies of this plant researchers extracted the dry plant material of *E. annuus* by soaking in solvent and left at room temperature. the crude extract frequently partitioned into 4-6 main fractions using increasing polarity of solvents. Hexane, chloroform, diethyl ether, ethyl acetate, n-butanol and water are the six most frequently used solvents (Yoo et al., 2008, Oh et al., 2002, Mohamed and Abd, 2006).

In order to extract all types of compounds from *E. annuus*, different solvents were selected. According to Lijima and Mohamed's research, terpenes and flavonoids were two major classes of compounds in *E. annuus.* Terpenes were found in the hexane or chloroform fractions (Iijima et al., 2003a), while flavan derivatives were commonly found in ethyl acetate and butanol soluble fractions (Mohamed and Abd, 2006). Extraction and separation methods for other plants of the *Erigeron* genus can also help to build up the appropriate separation methods of *E. annuus.* For example, scutellarin could be isolated from methanol extract of *E. multiradiatus* on macroporous resins and Sephadex LH-20 columns (Luo et al., 2008); terpenoids and steroids could be obtained from diethyl ether and ethyl acetate extracts of *E. naudini*, and separated over silica columns. In the meantime, other separation methods had been involved in previous research publications. For example, scutellarin was separated from *E. breviscapus* by using high-speed counter-current chromatography (HSCCC), which is a liquid-liquid partition chromatography without any solid stationary phase (Gao et al., 2006). Crude saponins would precipitate out from the hot butanol extract of *E. naudini* in the cooling process after hot solvent distillation (Pieribattesti et al., 1981).

2.2 Materials and instruments used in both China and UK

Plant collection, crude extraction and large scale separation of the *E. annuus* extract were accomplished at Shanghai University of Traditional Chinese Medicine, Shanghai, China. Further chemical separations and identification works were carried out in London Metropolitan University, London, UK. The time line is shown in Table 2.1.

Table 2.1 Research locations and timeline.

	Locations	
	China	**UK**
Date	Sep.2010-Jan.2011	Jan.2011-Dec.2013

2.2.1 Materials and instruments in China

95% ethanol was purchased from Sino-Pharm Chemical Reagent Co., Ltd. Reagent grade methanol, hexane, ethyl acetate butanol, dichloromethane and chloroform were purchased from Fisher Scientific, China. HPLC- grade water (resistivity=18.2 mΩ) was prepared using Millipore Mili-Q purification system, Milipore Corp., New Bedford, MA. Silica gel 100-400 mesh (pore size 60 Å.) for flash chromatography and silica gel TLC plates were obtained from Qingdao Haiyang Chemical Company, China. Sephadex^{TM} LH-20 was purchased from GE Healthcare, Sweden.

HPLC analysis was carried out on an Agilent 1100 series: the system was equipped with a G1379A degasser, G1311A Quat pump, G1313A auto sampler, G1316A column and ChemStation software. TSK-GEL ODS-100V 5µL, 4.6 cm x 25 cm column was purchased from TOSOH, China. Flash chromatography was carried out on Dr Flash-II from LISUI (Shanghai) Chemical Engineering Co., Ltd with 3 kg capacity superclass column DN100 x 500 mm.

Plant material *E. annuus* (L.) Pers. was authenticated by Dr Li Hong Wu (Shanghai University of Traditional Chinese Medicine), collected from Zhangjiang High Technology Park, Shanghai Pudong district, China. Plants were carefully washed to get rid of the soil and dried at room temperature. Once dried, the whole plant was ground into powder and 9 kg powder was obtained.

2.2.2 Material and instruments in UK

Reagent grade methanol, hexane, ethyl acetate butanol, dichloromethane, chloroform, DMSO, iso-propanol, HPLC and LC-MS grade methanol and acetonitrile, were purchased from Fisher Scientific, Loughborough, UK. Silica gel 200-300 (ALUG®, SIL G/UV 254 Kieselgel) and silica gel TLC plates (coated with 0.2 mm silicagel 60 Å pore size, F_{254}) were obtained from Fisher Scientific, Loughborough, UK. Sephadex™ LH-20 was purchased from GE Healthcare, Sweden. MCI GEL® CHP20P (75-150 µm, 400-600 Å pore size) was purchased from Sigma-aldrich, Poole, Dorset, UK. Eppendorf centrifuge tubes were used for fraction collections and were obtained from Hamburg, Germany. BÜCHI rotary evaporator R-210, equipped with vacuum pump V-700 and heating bath B-491 was used for solvent evaporation, Flawil, Switzerland.

HPLC separation and fractionation were carried out on Dionex, Agilent and PerkinElmer HPLC systems. The Dionex (Camberley, UK) HPLC system was equipped with P680 HPLC pump, ASI-100 auto sampler, thermostatted column compartment TCC-100, UV D340U detector and Chromeleon™ workstation; Agilent 110 series (Santa clara, USA) system was equipped with G1379A degasser, quat-pump, auto sampler, column oven and ChemStation LC3D; PerkinElmer (Cambridge, UK) HPLC system was equipped with series 200 auto sampler, pump, UV/Vis detector, column oven and Total-chrom workstation Version 6.3.1. Semi-prep column (250 X 8 mm, 100-10 C18) for fractionation was purchased from KNAVER, Berlin, Germany.

HPTLC CAMAG system was equipped with ATS 4 auto-sampler, CAMAG TLC Scanner 3, ADC 2, TLC Visualizer and winCATs workstation, Hungerford, UK.

Flash chromatography separation was carried out on 971-Fp flash purification system, with repacked super flash column SF10-4 g, SF15-12 g, and SF25-4 g, Varian, Agilent, Wokingham, UK.

The SPE separation was carried out using vacuum manifold chamber and columns (strata SI-1 silica column, 55 µm, 70 Å, 10 g/ 60 mL Giga tubes), which were purchased from Phenomenex, Macclesfield, UK.

GC-MS was carried on Trace DSQ GC 2000 series gas chromatography (ThermoQuest Corp, San Jose, CA, USA), interfaced with a TriPlus autosampler and joined to a quadruple mass spectrometer operated in electron impact (EI) ionization mode at 70 eV electron energy with browser software version 1.4 SRI. The NIST mass spectral search program for the NIST/EPA/NIH mass spectral library was version 2.0a, built in January 2002.

LC-MS was carried on an automated Dionex/LC Pickings HPLC system consisting of Famos micro auto sampler connected to an Ultimate™ plus HPLC system (Camberley, UK). Separations were achieved on Phenomenex column- Luna C8 (2), 3 µm, 150 x 2.0 mm with a gradient elution condition. LC system was coupled with a Waters Micromass Quadrupole Time of Flight Micro™ spectrometer V4.1, Waters Inc. 2005, Milford, UK, with a MassLynx V4.1 work station. NMR spectrometer was from Bruker®, AV-500. NMR results were processed using MestReNova©, version 6.1.0-6224, 2010 Mestrelab Research S.L.

2.3 Plant extraction

The extraction of 9 kg plant powder was carried out at the Institute of Chinese Materia Medica, Shanghai University of Traditional Chinese Medicine, in January 2010. Due to health and safety requirements, 9 kg plant powder was divided into five portions, and each portion was soaked with 18 L of 95% ethanol in 20 L high-density polyethylene solvent buckets. All five buckets were left at room temperature for 2 weeks, during which the supernatant from each bucket was sucked into a rotary evaporator with a 5 L capacity round bottom flask. Solvent were removed using rotary evaporation at 40°C and fresh solvent was poured back into the buckets for further extractions. After removing the solvent, crude extract was obtained in a dark oily paste format at the bottom of the round bottom flask.

The second part of extraction was liquid-liquid partition. In order to separate the crude extract into different groups, 4 L distilled water was added into the round bottom flask and heated on a water bath at 40 °C. The condensed crude extract was suspended into water to form a dark oily suspension. Liquid-liquid extraction (LLE) of the water suspension was carried out using n-hexane, ethyl acetate and n- butanol successively. The 4 L suspension was divided between two 5 L glass separating funnels, 1 L hexane was added to each funnel to extract: the step was repeated with 4 x 1 L hexane for each funnel. The funnels were gently shaken and left on the rack for 30 min to let the emulsified layer disappear, followed by removing the water layer through the tap at the bottom. Then the process was repeated using ethyl acetate and n-butanol respectively. After separation, organic solvents were recycled and the condensed extracts were weighed, labeled as hexane (H), ethyl acetate (E), butanol (B) and water extracts (W).

2.4 Chromatographic separation methods

2.4.1 Thin layer chromatography (TLC)

Analytical thin layer chromatography (TLC) was used to characterize the fractions eluted from other chromatographic separations, such as flash, solid phase extractions and gel column filtrations. Silica coated aluminum analytic plates were used and samples were spotted along the baseline using capillary tubes, which was 1 cm from the bottom edge. Before each elution, a small amount of developing agent was poured into the tank for chamber saturation with a depth less than 1 cm. Filter papers were used to wrap the inner surface of the tank to help saturate the chamber when the developing solvent was not very volatile. Plates were removed from the tank when the solvent front reached 1 centimeter from the upper edge of the plate. The results were recorded under UV/fluorescent wavelength 254 and 366 nm. Fractions with same TLC profile were combined.

Preparative TLCs were carried out using several 20 x 20 cm aluminum analytical TLC plates. In order to gain a better separation, elution for each sample was repeated twice on the same plate with same mobile phase. Samples were spotted onto the plates as a single line along the baseline with capillary tubes. Approximately 10 mg of sample could be loaded onto one 20 cm x 20 cm plate each separation. After viewing the results under the UV wavelength 254 and 366 nm, bands with good separation were scraped off the plate and soaked in the most polar solvent choosing from the mobile phase. The amount of the solvent was at least ten times more than the volume of the silica. The solvent was removed by rotary evaporation, and the purity of the residue was checked with analytical TLCs before carrying out structure elucidation.

2.4.2 Flash chromatography

Normal-phase and reverse-phase flash chromatography were used in the separation of extracts. Flash chromatography technique was invented and described in 1978 by W. C. Still (University of Columbia) as a rapid and economical way to achieve separations of phytochemicals. It was designed with a pressurized eultion system, and the mobile phase was pumped through a pre-packed column at a high flow rate (Alcock et al., 1983, Still et al., 1978). A pre-packed flash column was made of superglass packed with silica gel for normal phase separation, or octadecylsilyl (ODS) for reverse phase separation. For example, silica was packed using the dry method for a large column with capacity beyond 500 g, and the wet pack method was more convenience for smaller columns with a capacity under 50 g. Wet packing method was the only way to prepare a reverse phase column. ODS were pre-treated with 50% acetonitrile and 50% water, before being packed into the column.

Sample inlet methods were different due to the different packing methods of the flash columns: for the wet pack, the samples were directly injected onto the column from the top. As for the dry packed columns, the samples must be absorbed by the silica gel first, and then loaded as part of stationary phase on the top of the column before sealed the top tap of the superglass column.

Equilibration time was varied due to the different particle size of the stationary phase, different solvent and different elution methods. Step gradient elution was normally used to achieve better separation and group the compounds into different fractions according to their polarity. For example 100% hexane to 100% ethyl acetate solvent system was used for hexane and ethyl acetate extracts, while 5% methanol to 100% methanol with deionized water was used for reverse-phase elution of the butanol and water extracts. The ODS used in this research was one year old, and it was preserved in 100% acetonitrile and purged with water: acetonitrile 1:1 (v/v) before the elution.

2.4.3 Solid phase extraction (SPE)

Solid phase extraction (SPE) was used to separate fractions obtained from flash chromatography and column separations. The SPE columns were pre-packed with silica as stationary phase in syringe-shaped cartridges, which were connected to a negative pressure chamber. Samples could be loaded as concentrated as possible in liquid form on the top of the column, in order to achieve a good separation. A 10 g capacity column could be loaded with no more than 250 mg sample. The column could be wetted with 10% ethyl acetate in hexane and equilibrated with 100% hexane. Negative pressure of the chamber was controlled by a vacuum pump which connected to the chamber through the vacuum port with a gauge. Fractions were collected using the boiling tubes on the rack inside the chamber. Each fraction could then be dried and elution profiles were produced using TLC. Fractions with the same profile were combined.

2.4.4 Silica column separation

Silica gel column separation was the most traditional method used to purify non-polar compounds from plant extracts. Glass analytical columns with a diameter from 5 mm to 25 mm were used for fraction purification in this study. All the columns were packed with wet silica slurry, which was prepared in mobile phase 24 hours before the separation. Samples were loaded onto the silica gel at the top of the column. After sample loading, a piece of glass wool was added to the top of the column to protect the integrities of stationary phase; solvent was then carefully poured into the column. Particle size of the stationary phase could affect the retention time: if necessary, a manual air pump could be added on top of the column to force the solvent through the column. Elution gradient could be adjusted by changing the ratio of different solvents in mobile phase, and the fractions were collected from the bottom tap.

2.4.5 Sephadex gel column filtration

Sephadex[TM] LH-20 was used to purify the sub-fractions which only contain one or two components. Sephadex LH-20 is a cross-linked dextran gel, prepared by hydroxypropylation of Sephadex G-25, which is composed of macroscopic beads synthetically derived from the polysaccharide, dextran (HealthcareGE, 2006). It is frequently used in the separation of natural products due to its broad spectrum of solvent tolerance (Chen and Wang, 2009, Murphy and D'Aux, 1975). Before packing the column, the Sephadex G-25 powder needed to be swollen for at least three hours without stirring at room temperature. The extent of swelling depended on the different mobile phase, and in this study, 50% dichoromethane with 50% methanol was used (Seki and Sugase, 1969). The columns used in Sephadex gel column filtration were glass columns with a diameter of 5 mm. After packing with the Sephadex slurry, 2-3 bed volumes of mobile phase were used for equilibration before sample loading. If new solvent was added to the column, re-equilibration with at least 2 bed volumes was necessary.

2.4.6 MCI gel column filtration

MCI gel[®] (MCI GEL is a registered trademark of Mitsubishi Chemical Corp.) CHP20P is a macroporous adsorptive resin, a popular support material which is widely used to purify fractions from reverse-phase flash separations. CHP20P gel separation mechanism is based on polyaromatic adsorbent resin (Sigma-AldrichCHP20Pdatasheet). Pigments such as chlorophylls could be easily adsorbed and removed from the top of the column when eluted with 100% water to 100% methanol. Acetone was often used to clean the column after each elution, as pigments and non-polar compounds can be removed by acetone; 2-3 bed volumes equilibrium would be needed before starting another elution. MCI gel column needed to be kept sealed and wet.

2.4.7 High performance liquid chromatography (HPLC)

Three different HPLC systems, Agilent, Dionex and PerkinElmer, were used in this research in both China and UK. For sample separation and fingerprint chromatogram works, micro-column and analytical columns were used. The HPLC results were also displayed as 3D pictures recorded by photodiode array detectors (Agilent and Dionex). Fractionation works were mainly carried out on the PerkinElmer system with a semi-prep column and fractions were collected manually.

2.5 Identification Methods

2.5.1 Gas chromatography-Mass Spectrometry (GC-MS)

Gas chromatography-mass spectrometry (GC-MS) was used for analysis of volatile fractions, eluted from the hexane extracts using SGE analytical GC capillary column BPX5 (30m x0.25 mm, 5% phenyl polysilphenlene siloxane). It was operated by Mr. Osman Erkek, technician of London Metropolitan University. Peaks identified in total ionic currents flow chromatograms were given selecting mass spectrums of each compound. An electron-impact ionization system with ionization energy of 70 eV was used. Total GC run time was 35 min for each fraction. The identification of each peak was assigned by comparison of the mass spectra fragmentation patterns in NIST/EPA/NIH mass spectral library version 2.0a, built in January 2002.

2.5.2 Liquid chromatography Mass spectrometry (LC-MS)

LC-MS was carried out on an automated Dionex/LC Packing HPLC system coupled with Micromass Quadrupole Time of Flight Micro[TM] spectrometer (Waters[®]). It was used for identifying the molecular weight of compounds isolated from the butanol

extracts. A gradient elution was started with 100% 0.5% formic acid in water to 100% methanol. Positive ion mode electrospray ionization was used for Q-Tof-MS and it was calibrated with Naics test solution set (Waters API test solution Kit, NaI: 2 µg/µL, CsI: 50 ng/µL). The capillary voltage, sample cone voltage and extraction cone were set at 3000 V, 30 V and 3V respectively. Source temperature was set at 150 $^{\circ}$C. Collision energy was set at 3 V. 10-20 µL of each sample was injected, and total ion current chromatogram was displayed and extracted-ion chromatogram was processed using MassLynx 4.1 software.

2.5.3 Nuclear magnetic resonance (NMR)

Nuclear magnetic resonance spectroscopy was used for structure elucidation, ^{1}H-NMR, ^{13}C-NMR, HMQC and HMBC spectroscopic analyses were carried out in deuterated water (D_2O) and deuterated chloroform ($CDCl_3$). It was operated by Mr. John Crowder, NMR technician of London Metropolitan University.

2.6 Results and Discussion

2.6.1 Pre-separation study

In order to extract the whole plant without destroying the compounds, the total extraction was carried out by soaking the ground plant material into the solvent at room temperature. Pre-separation study was carried out in China. According to the previous research, *E. annuus* contains volatile oil and thermally labile compounds (eg. ergosterol peroxide) (Nazaruk and Kalemba, 2009, Kim et al., 2005), the temperature for solvent evaporation was set below 40 $^{\circ}$C. Methanol and 95% ethanol were used in extraction, the recovery is compared in Table 2.2 below:

Table 2.2 Compare of the recovery of methanol and ethanol extraction.

Solvent	Plant material (g)	Weight of Extract (g)	Recovery %
MeOH	12.1364	8.9499	73.74
EtOH 95%	12.5290	10.4947	83.76

Plant material was extracted by ultrasonication in the room temperature for 30 min in both solvents. From the research data, using 95% ethanol could give a higher recovery, up to 83.76%. After removing the solvent, both extracts were dissolved in MeOH at the same concentration and their chromatographic finger-print profiles were compared using reverse phase HPLC.

HPLC results obtained from Agilent 1100 analysis are shown in Figure 2.1. The 3D plot of EtOH extract is displayed in Figure 2.1 **A** from UV wavelength 200 to 360 nm. There were many strong absorption peaks observed at lower wavelength, and the baseline was not clear. In order to compare the chromatographic finger-print profiles of EtOH and MeOH extracts, five monitoring wavelength were selected at 210, 240, 254, 320 and 360 nm. Same elution method (TSK-GEL ODS 4.6 cm x 25 cm; flow rate: 1 mL/min; 30 $^{\circ}$C; deionized water and MeOH from 1:0 to 0:1; 60 min) was applied in both elutions. The chromatograms from this finger-prints analysis are compared in Figure 2.1 **B** and **C.**
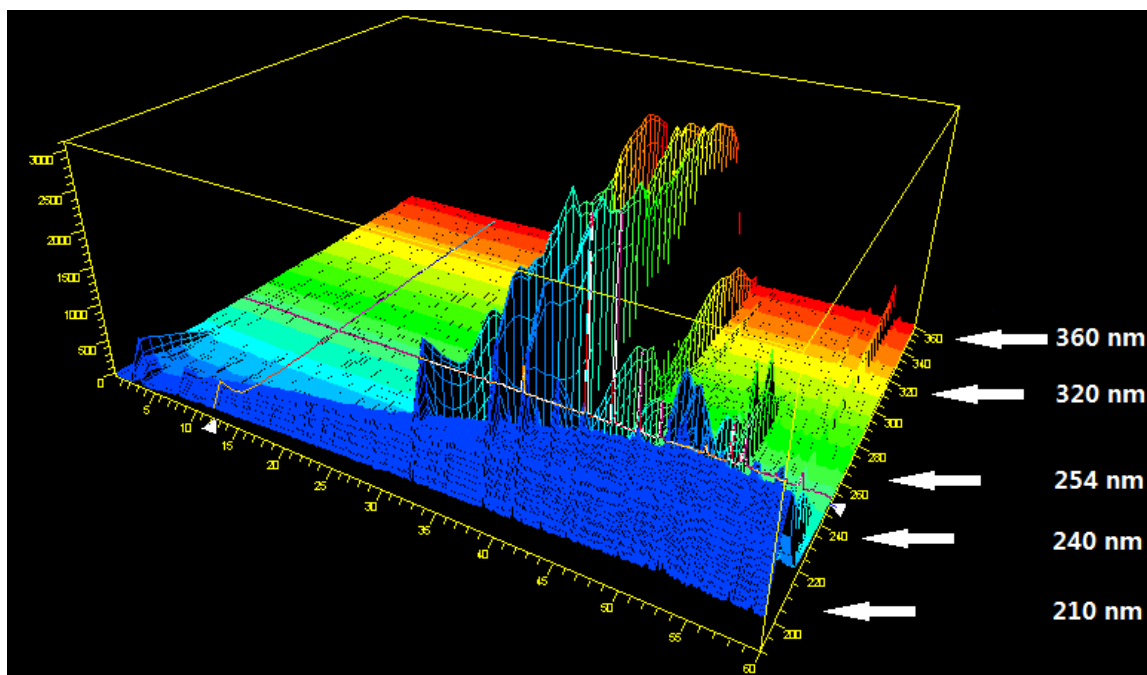
A. 3D plot of EtOH extract from UV wavelength 200-360 nm.
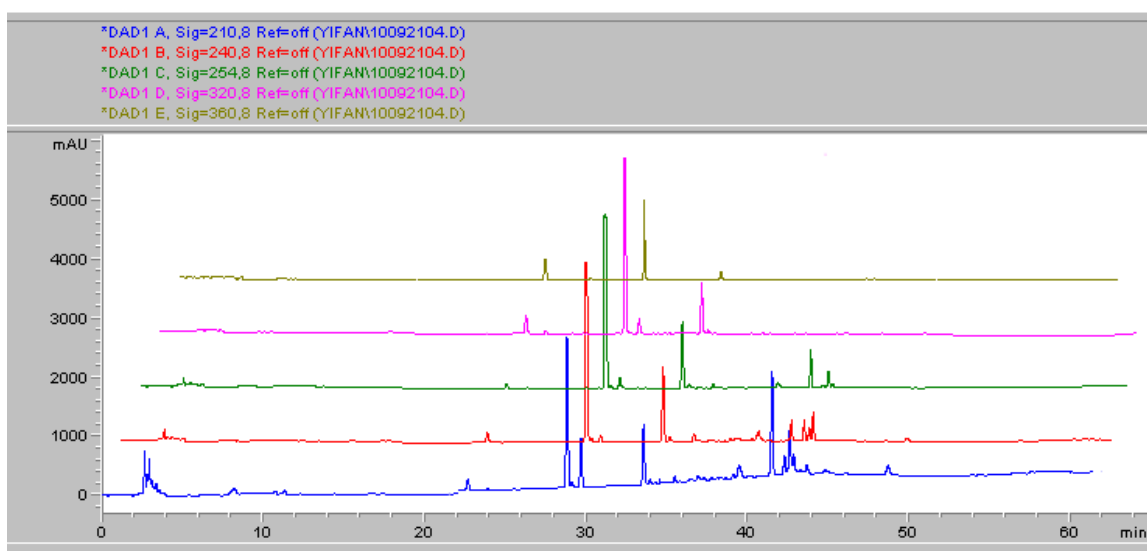
B. HPLC chromatogram of MeOH extract at UV wavelength 210,240,254,320,360 nm.
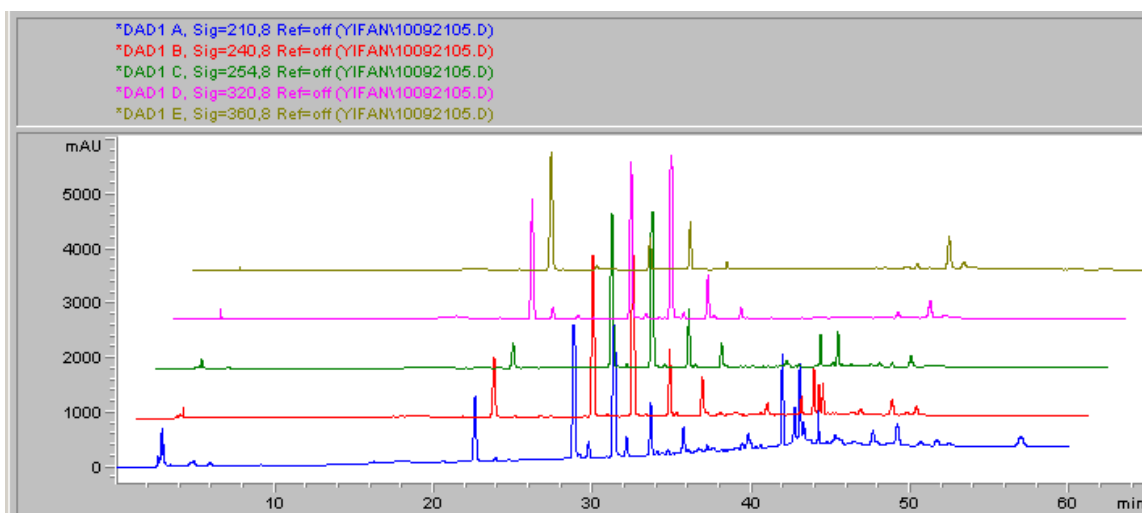
B. HPLC chromatogram of EtOH extract at UV wavelength 210,240,254,320,360 nm.

Figure 2.1 Chromatographic finger-print analysis of *E. annuus* extracts*.*

Main peaks showed same retention times at 28.9, 29.9, 33.8 and 41.8 min in both chromatograms, an extra peak showed in the EtOH extract sample at retention time of 31.8 min. More peaks were observed in the EtOH extract chromatogram, indicated that better recovery could be obtained by using 95% ethanol. Thus, 95% ethanol was selected for the large scale plant extraction.

2.6.2 Extraction of *E. annuus*

Extraction of large scale plant material was carried out on 9 kg ground *E. annuus* using 95% ethanol. Dark oily paste crude extract 747.6 g was obtained and suspended in deionized water. Liquid-liquid partition was then carried out using hexane, ethyl acetate and butanol against the water suspension respectively. Four extracts were obtained. The weight of each extract is showed below in Table 2.3.

Table 2.3 Weight of different extracts

Sample name	sample weight (g)
Hexane extract (H)	214.6
EtOH extract (E)	105.1
Butanol extract (B)	65.3
Water extract (W)	289.6
Total	674.6
Recovery (%)	90.2

The total weights of all four extracts were 674.6 g, total recovery was 90.2% from the crude EtOH extract. The organic solvents were removed by rotary evaporation and the water extract was freeze-dried. Once the extracts dried, they were all stored at -20 ºC.

2.6.3 Separation of hexane extracts

The hexane extract was a dark oily paste, to get a further separation, 214.6 g extract was dissolved in EtOAc and mixed with 200 g silica gel to make the sample in powder format for large scale silica column elution. After evaporated the EtOAc, the sample was loaded on top of the silica gel column (100-200 mesh) and flash chromatographed from 100% petroleum ether to 100% EtOAc using gradient elution.

Nine fractions were obtained from the flash chromatographic separation (H1 to H9), and H5 was further fractionated (H5-1 to H5-9). Compounds H4 and H7 were precipitated out in the separation procedures and they were purified by repeatedly silica column separations and MCI gel filtrations. White oily precipitations were found in fractions H5-1 and H5-2, compound H5-1-1, H5-1-2 and H5-2 were isolated from those white precipitations over the silica column separations.
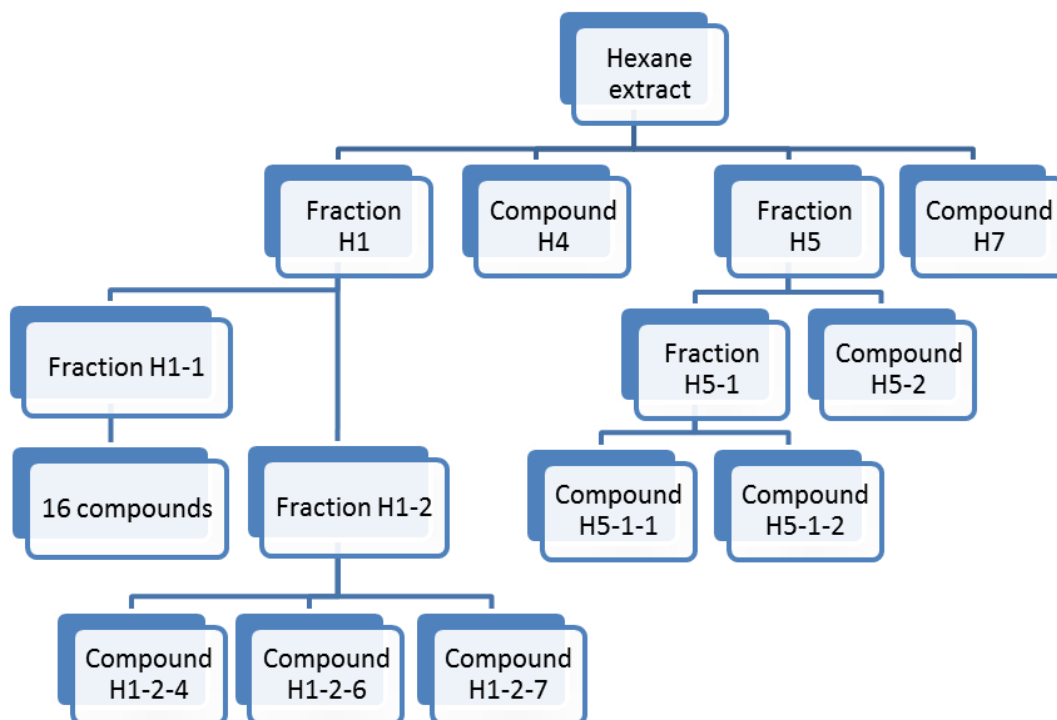
Figure 2.2 Separation of hexane extract.

Fraction H1 was a brown oily paste, approximately 500 mg of H1 was used during each solid phase extraction separation. Nine fractions were collected and fractions H1-1 and H1-2 were further separated.

Fraction H1-1 was an orange oil, it was analyzed by GC-MS and 16 compounds were identified. Fraction H1-2 was separated repeatedly over silica column and preparative TLC separation, finally seven fractions were obtained, and their TLC profiles are showed in Figure 2.3. The amount of compound H1-2-4, H1-2-6 and H1-2-7 were enough for the biological assays and their structures were elucidated using NMR and GC-MS.
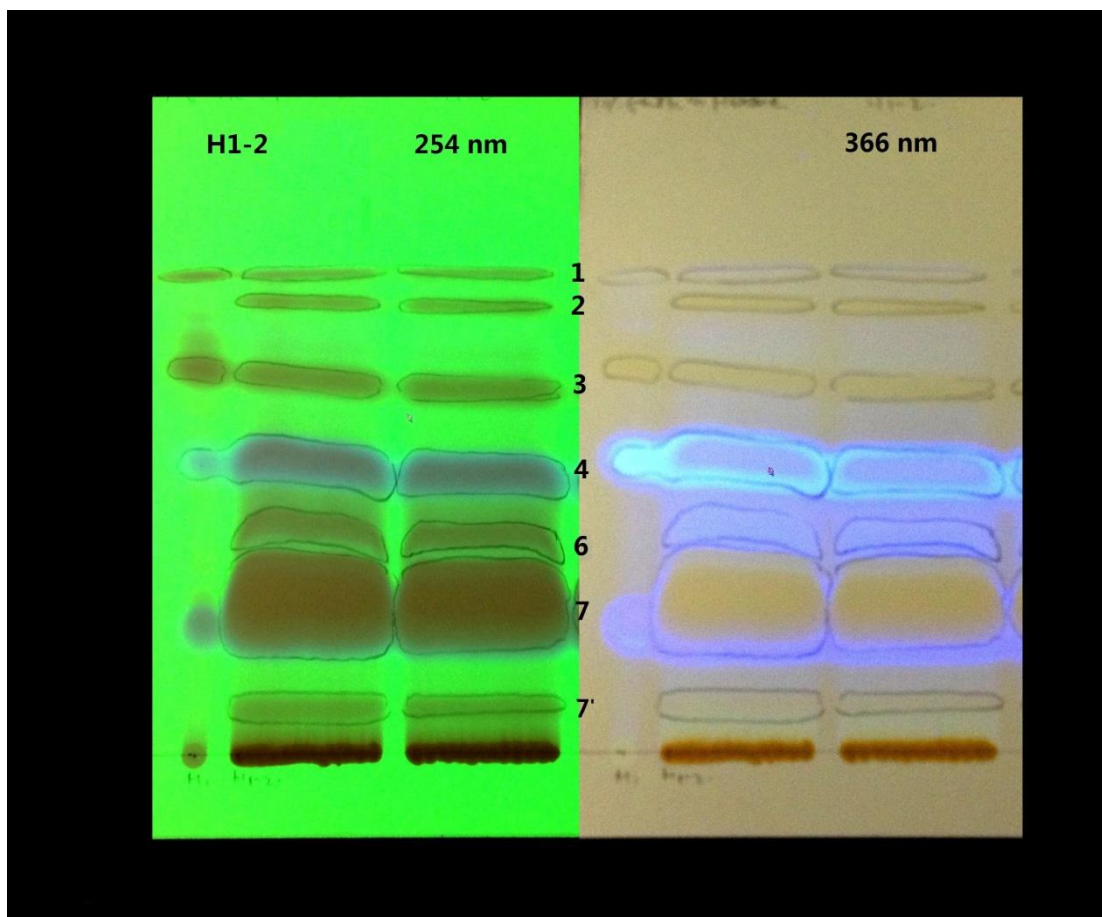
Figure 2.3 TLC of fraction H1-2 (Mobile phase: EtOAc: Hexane, 1:9 v/v).

2.6.3.1 Fraction H1-1

Fraction H1-1 was an orange oil which had been eluted with 100% hexane. It was analyzed by GC-MS, the mass spectra fragmentation patterns were matched through the NIST/EPA/NIH mass spectral library version 2.0a; the closest matches are listed below:
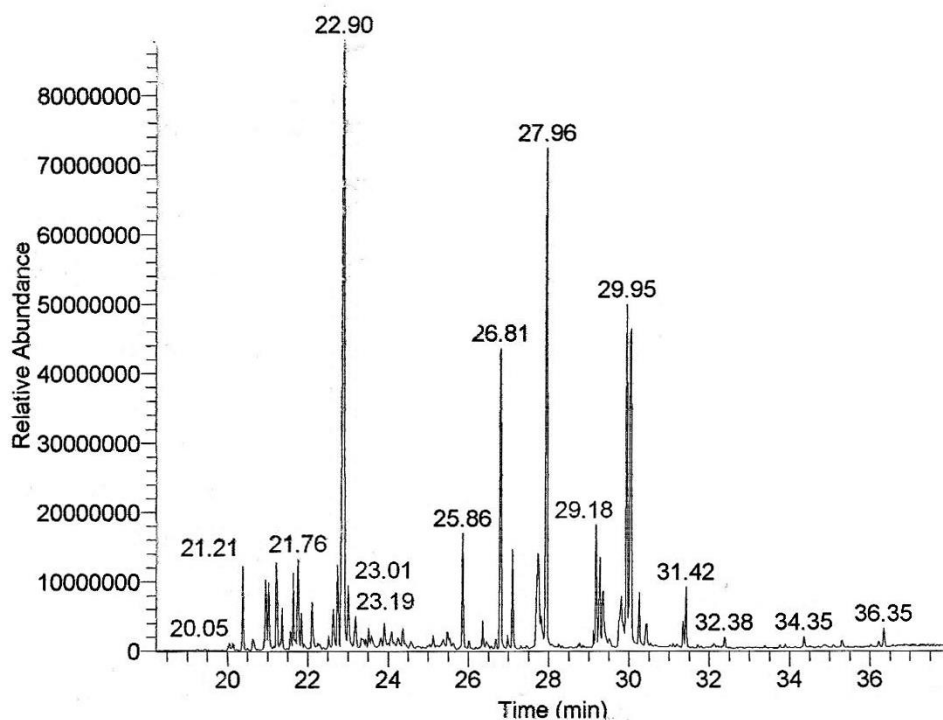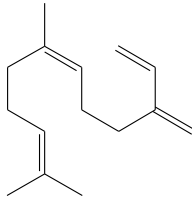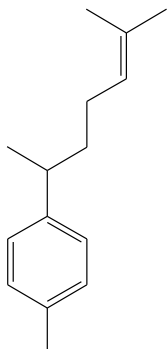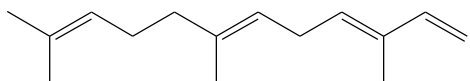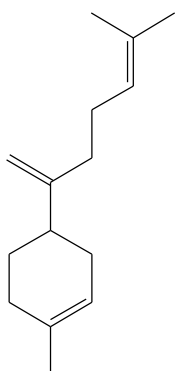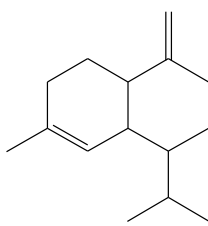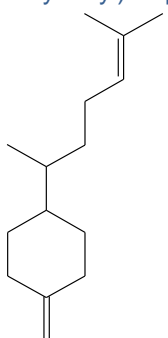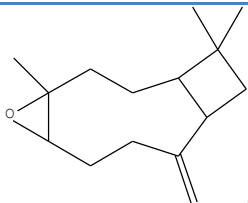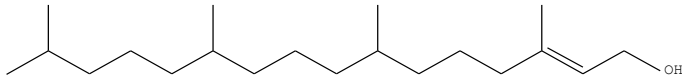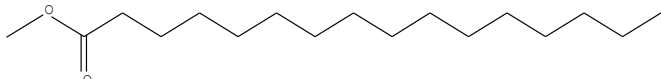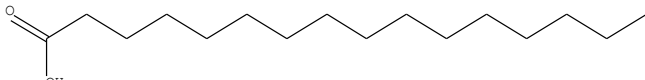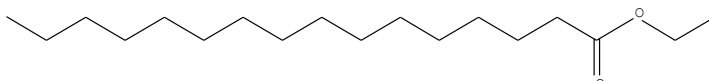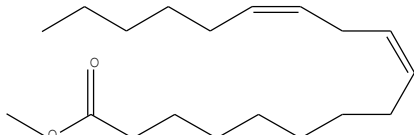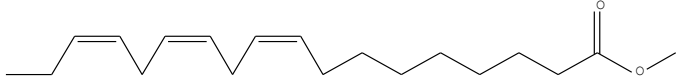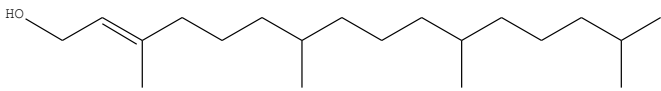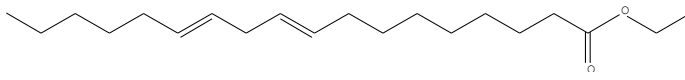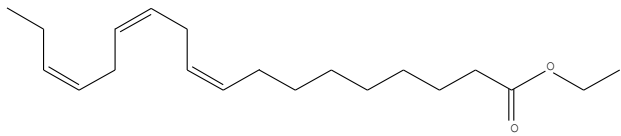
Figure 2.4 Gas chromatogram of fraction H1-1.

Sixteen compounds were identified by matching the known compounds structures through the mass library (compounds have match factors above 800 were listed). Most of them were terpenes, polyunsaturated fatty acids and their esters (Table 2.4).

Table 2.4 Compounds characterized from fraction H1-1.

Retention Time(min)	Closest Matching Structure/Name	Match factor	Molecular formula and Mass (*m/z*)
20.38	 7,11-dimethyl-3-methylene-(Z)-1,6,10-dodecatriene	926	$C_{15}H_{24}=204.35$

| 20.95 | | 925 | $C_{15}H_{22}=202.34$ |

1-(1,5-dimethyl-4-hexenyl)-4-methyl-benzene

| 21.21 | | 916 | $C_{15}H_{24}=204.35$ |

α-farnesene

| 21.36 | | 911 | $C_{15}H_{24}=204.35$ |

1-methyl-(S)-4-(5-methyl-1-methylene-4-hexenyl)-cyclohexene

| 21.56 | | 917 | $C_{15}H_{24}=204.35$ |

1,2,3,4,4α,5,6,8α-octahydro-7-methyl-4-methylene-1-(1-methylethyl)-naphthalene

| 21.64 | | 909 | $C_{15}H_{24}=204.35$ |

3-(1,5-dimethyl-4-hexenyl)-6-methylene-cyclohexene

22.74		920	$C_{15}H_{24}O=220.35$
	aryophyllene oxide		
25.86	3,7,11,15-tetramethyl-2-hexadecen-1-ol	880	$C_{20}H_{40}O=296.53$
27.10	methyl hexadecanoate	921	$C_{17}H_{34}O_2=270.45$
27.73	n-hexadecanoic acid	867	$C_{16}H_{32}O2=256.42$
27.96	hexadecanoic acid	915	$C_{18}H_{36}O_2=284.48$
29.18	methyl-(9Z,12Z) -octadecadienoate	931	$C_{19}H_{24}O_2=284.39$
29.28	methyl-(9Z,12Z,15Z)- octadecatrienoate	883	$C_{19}H_{32}O_2=292.46$
29.36	ethyl-9,12-octadecadienoate, phytol	906	$C_{20}H_{40}O=296.53$
29.95	9,12-octadecadienoate	919	$C_{20}H_{36}O_2=308.50$
30.05	ethyl-(9Z,12Z,15Z)- octadecatrienoate	888	$C_{20}H_{34}O_2=306.48$

H1 and H1-1 had some antibacterial activities, however the amount for H1-1 was less than 5 mg, further chemical separation was not carried out on H1-1. Most of the compounds had been identified were terpenes, unsaturated fatty acids (UFAs) and

their esters. UFAs were reported to have inhibitory activity against wild type bacteria (Desbois and Lawlor, 2013), one compound eluted at 29.36 min, possessed a high matching factor to the known compound phytol. According to Inoue's research, phytol had a inhibitory activity against *Staphylococcus aureus* at the concentration of 20 µg/mL (Inoue et al., 2005). However, other antifungal activity had been reported, but none of those compounds were identified in this research. For example, in a study of essential oils from *Erigeron* species, essential oil of *E. annuus* was found highly active against fungi *Fusarium. oxysporum*, *Curvularia. lunata* and *Albugo. candida*. The IC_{50} was obtained from 153-660 µg/mL compared with fungicide carbendazim at 33.7-38.7 µg/mL (Kumar et al., 2014).

2.6.3.2 Compound H1-2-4

Compound H1-2-4 was separated from fraction H1-2. It was light green in colour, and showed d blue fluorescence under UV wavelength 254 and 366 nm (Figure 2.3).

^{1}H NMR, ^{13}C NMR and 2D HMQC spectra of H1-2-4 are showed in Figure 2.5 and 2.6 (500 MHz, CDCl$_3$). In the ^{13}C NMR spectrum, 27 carbon peaks were counted, and compared to the DEPT, one methyl peak at δ14.14 and two quaternary carbon peaks at δ155.91 and 178.49 were identified.

Figure 2.5 ^{1}H NMR spectrum of compound H1-2-4.

In ^{1}H NMR spectrum, a doublet at δ 7.32-7.34 was assigned to a sp[2] hybridization carbon (C=CH-), correlated with carbon peak at δ 141.85 through HMQC (Figure 2.7). Peaks between δ 5.26-6.24 and 1.5-2.7 in proton spectrum might be caused by the vinyl methylene protons in the alkyl chain. Six protons were integrated at δ 2.29 for a triplet, they were assigned to three methylene groups (-CH_2-). Other signal peak correlations could not be identified as there were too many impurity peaks showing in the spectrum, which was likely to be caused by contamination with other compounds. The solvent peaks at δ 1.25 and 7.19 were solvent peaks (caused by EtOAc and $CHCl_3$ respectively).
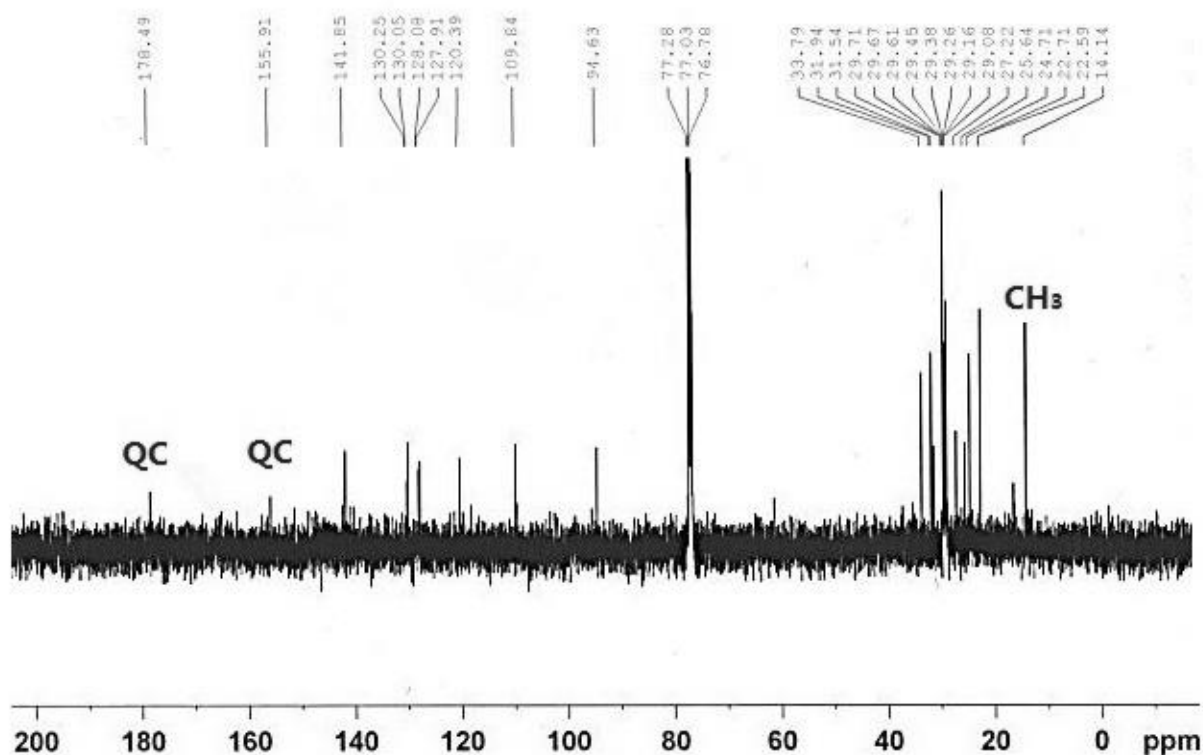
Figure 2.6 ^{13}C NMR spectrum of compound H1-2-4.
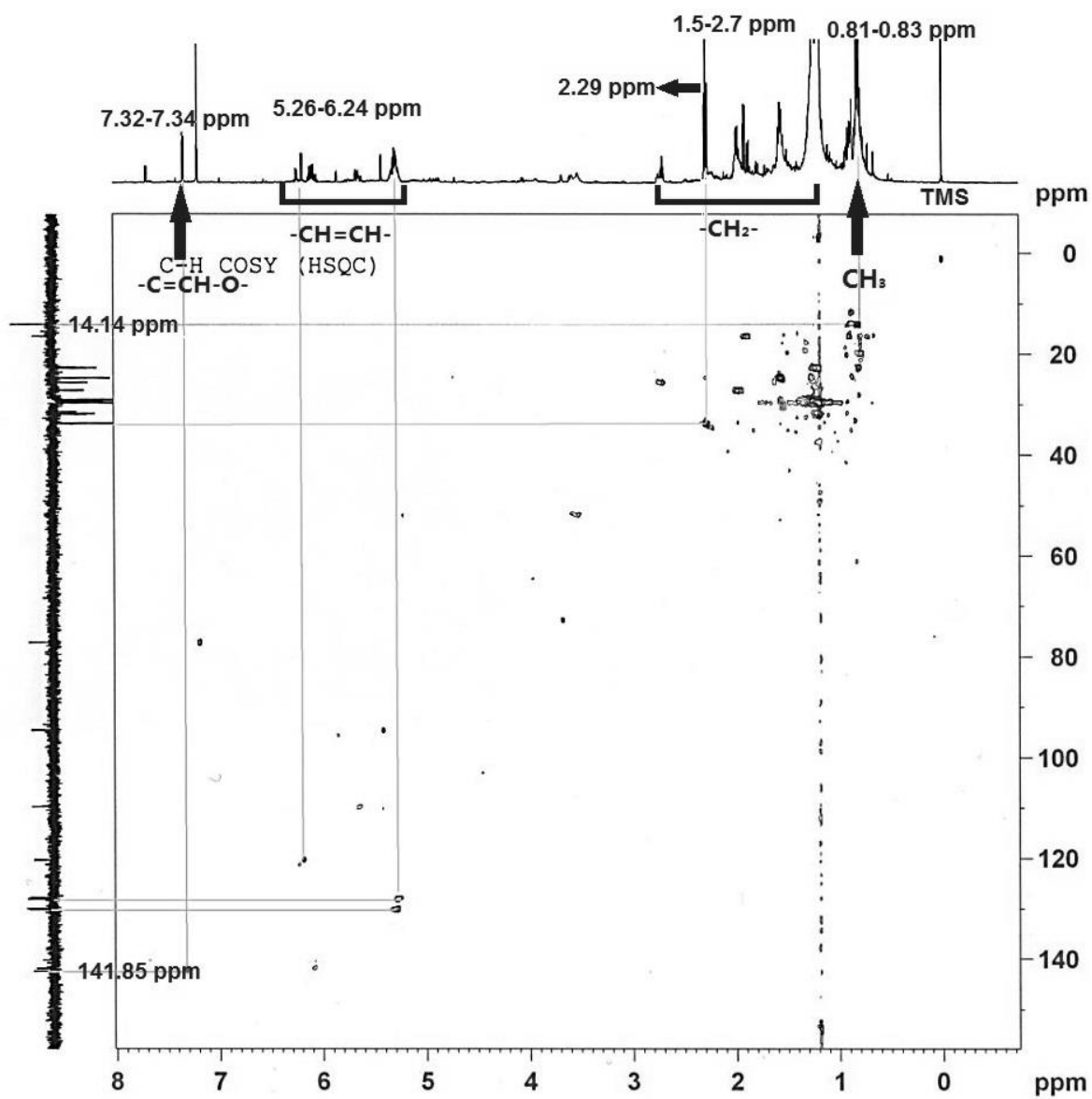
Figure 2.7 HMQC spectrum of compound H1-2-4.

The proposed structure is showed in Figure 2.8 **A**, two quaternary carbons were labelled as carbon 1 and 2. The C-H correlation was showed in HMQC (Figure 2.7), however, not enough sample was left for HMBC and the structure of alkyl chain could not be fully elucidated, a close match of structure was proposed by software ChemDraw®.
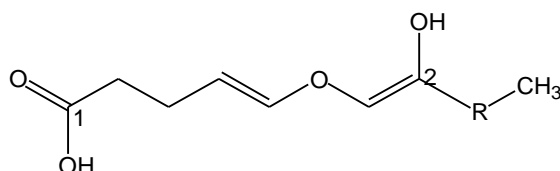
A. Proposed structure of compound H1-2-4.
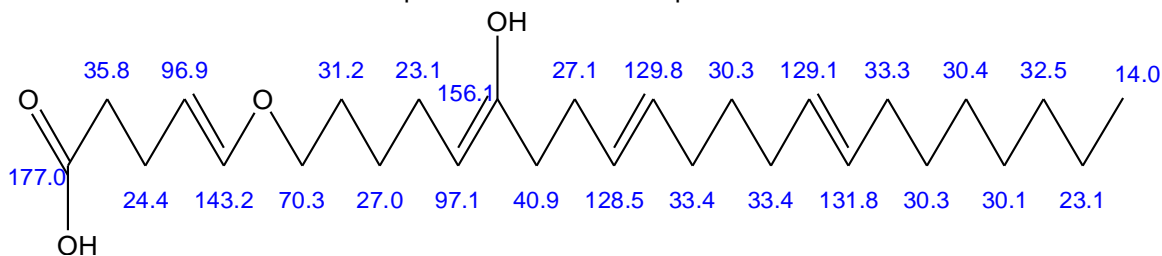
B. ^{13}C NMR chemical shifts of 5-(6-Hydroxy-docosa-5,9,14,20-tetraenyloxy)-pent-4-enoic acid.
Figure 2.8 Proposed structures of compound H1-2-4, approximated by ChemDraw®.

The estimated chemical shifts for terminal methyl group in ^{13}C NMR was at δ 14.0 and chemical shift for quaternary carbons showed at δ 156.1 and 177.0, matched very closely to the NMR data from this study, δ 14.14, 155.91 and 178.49 respectively. The estimated sp^2 and sp^3 carbon peaks in the alkyl chain were showed between δ 20-40 and 120-140, however, position and number of the double bonds could not be determined. The unknown portion was shown as R in Figure 2.8 A, it could be a saturated carbon china ($-(CH_2)_n-$) or had double bonds somewhere in the chain structure. H1-2-4 was suggested to be a fatty acid with an alkoxy group, this type of compounds have not been reported yet from *E.annuus.*

2.6.3.3 Compound H1-2-6

Fraction H1-2 also yield compound H1-2-6. Compound H1-2-6 was a deep green paste, and showed deep blue fluorescence under UV wavelength 254 and 366 nm (Figure 2.4).
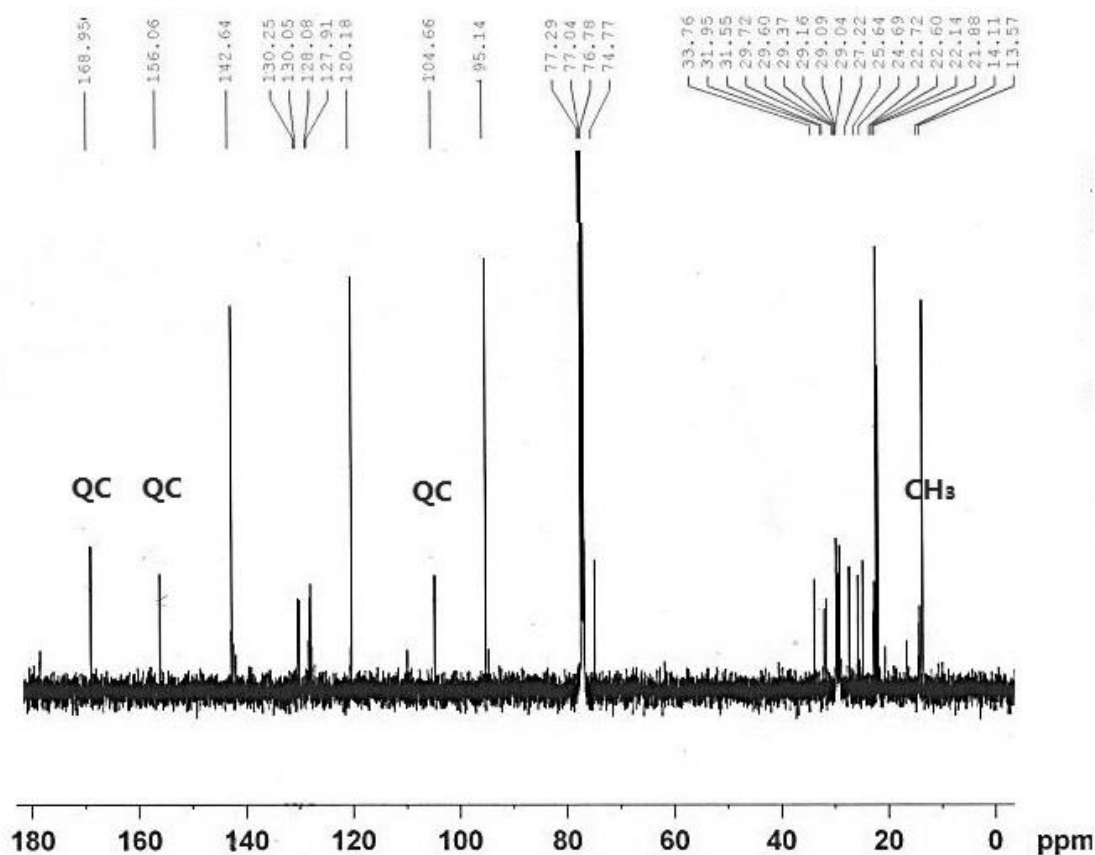
Figure 2.9 ^{13}C NMR spectrum of compound H1-2-6.

^{1}H NMR, ^{13}C NMR spectra of H1-2-6 are showed from Figure 2.9 to 2.11(500 MHz, CDCl$_3$). Twenty-eight carbon peaks were counted according to the ^{13}C NMR spectrum, three quaternary carbons were observed at δ 104.66, 156.60 and 168.95 after comparing to the DEPT, the quaternary carbons are labeled in Figure 2.9 as QC. The peak showed at 168.95 indicated a carboxyl group; one terminal methyl group peak was observed at δ 13.57 (Figure 2.9).
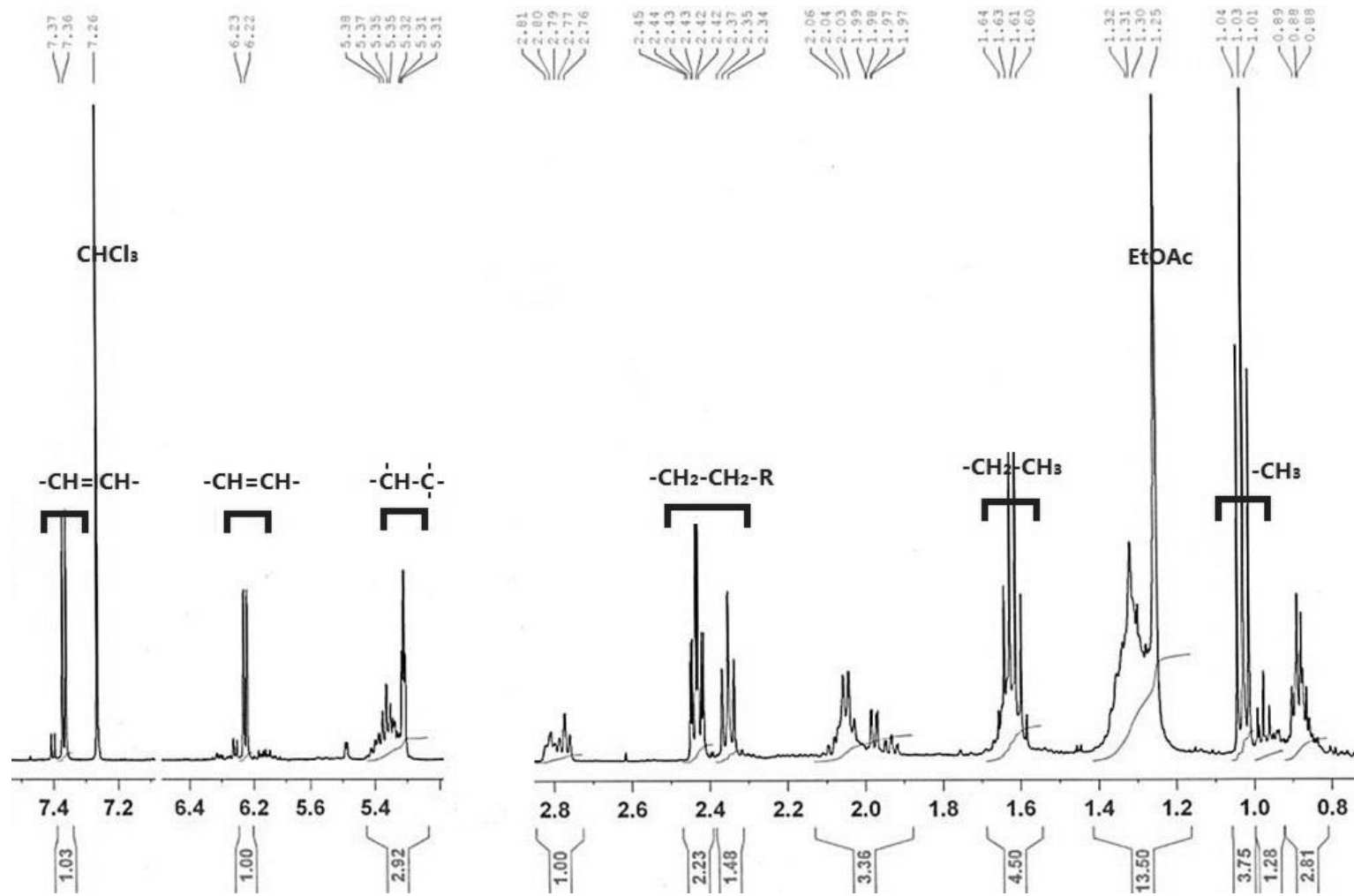
Figure 2.10 ^{1}H NMR spectrum of compound H1-2-6.

In the ^{1}H NMR spectrum, the peak at δ 1.03 was assigned to the methyl group, it splits into a triplet indicating that the adjacent carbon group might be a methylene group. Many multiplets between δ 1.5 and 2.8 were in different scale, suggested that this sample might not be pure. An alkyl side chain structure was involved. Peaks at δ 5.32, 6.22 and 7.36 represented vinyl protons in the alkyl side chain (Figure 2.10). EtOAc and CHCl$_3$ peaks were observed at δ1.25 and 7.19 respectively.
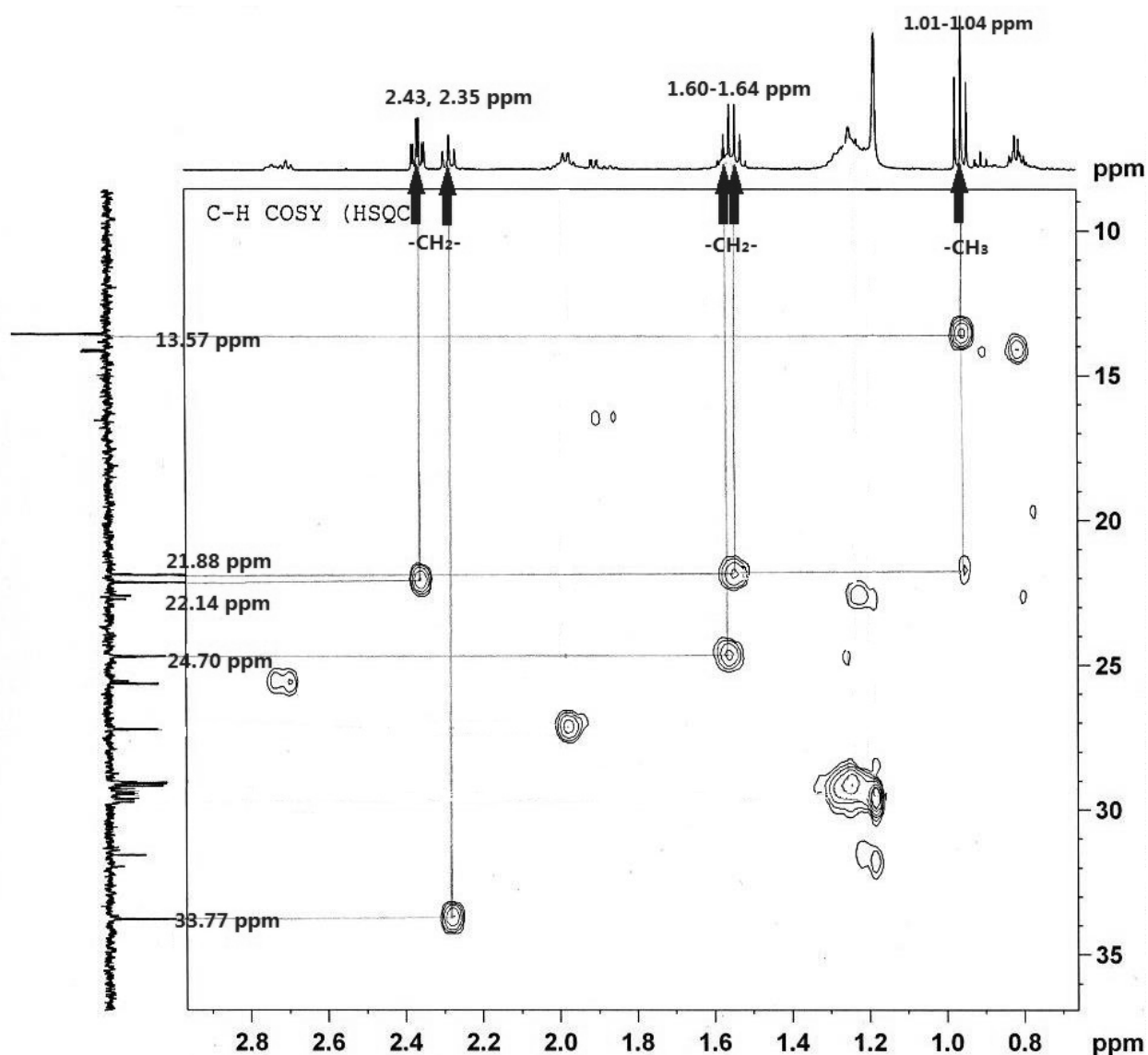
Figure 2.11 HMQC spectrum of compound H1-2-6 (^{13}C NMR: δ10-35; ^{1}H NMR: δ 0.8-2.8).
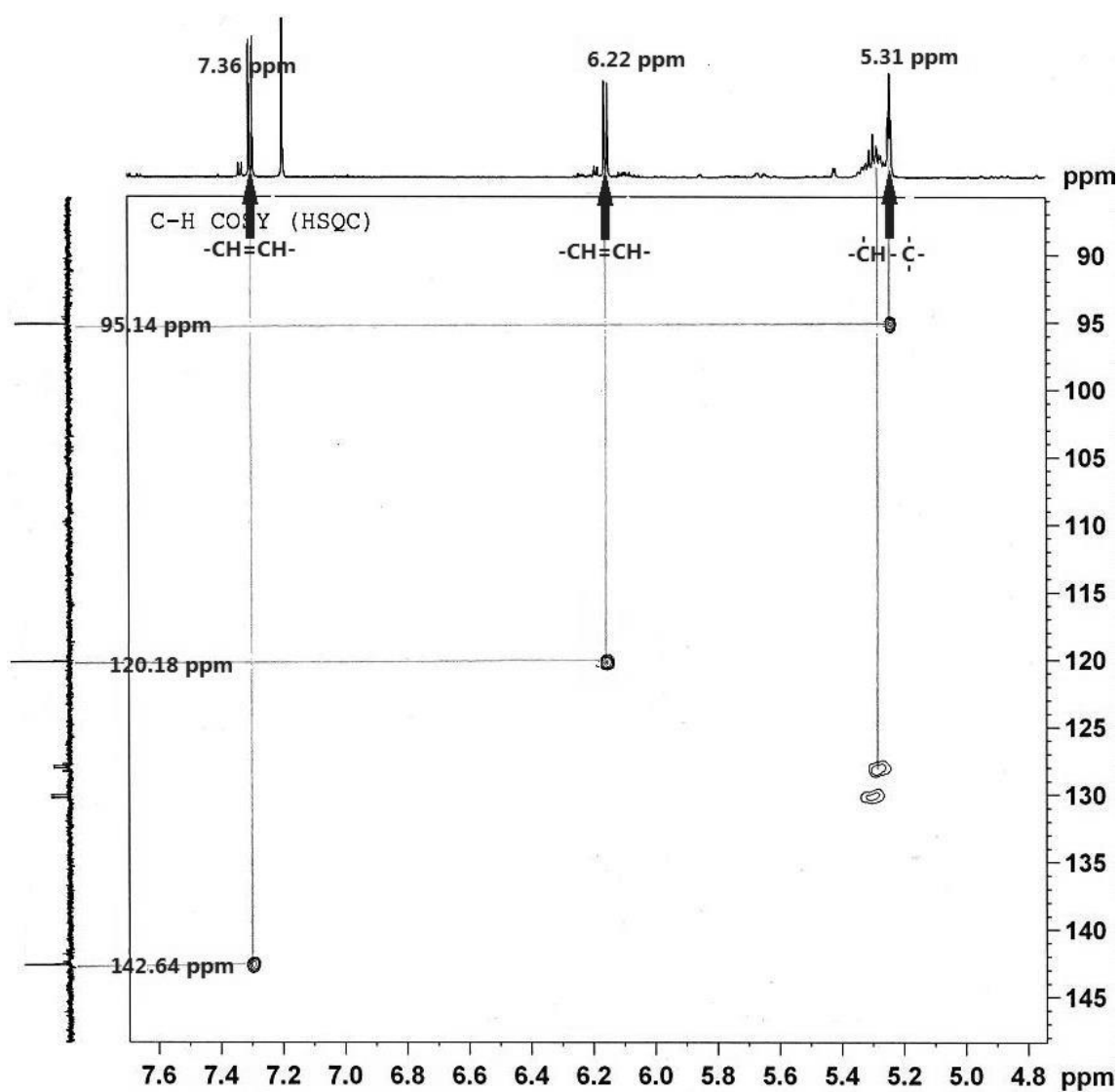
Figure 2.12 HMQC spectrum of compound H1-2-6 (^{13}C NMR:δ 90-145; ^{1}H NMR : δ 4.8-7.6).
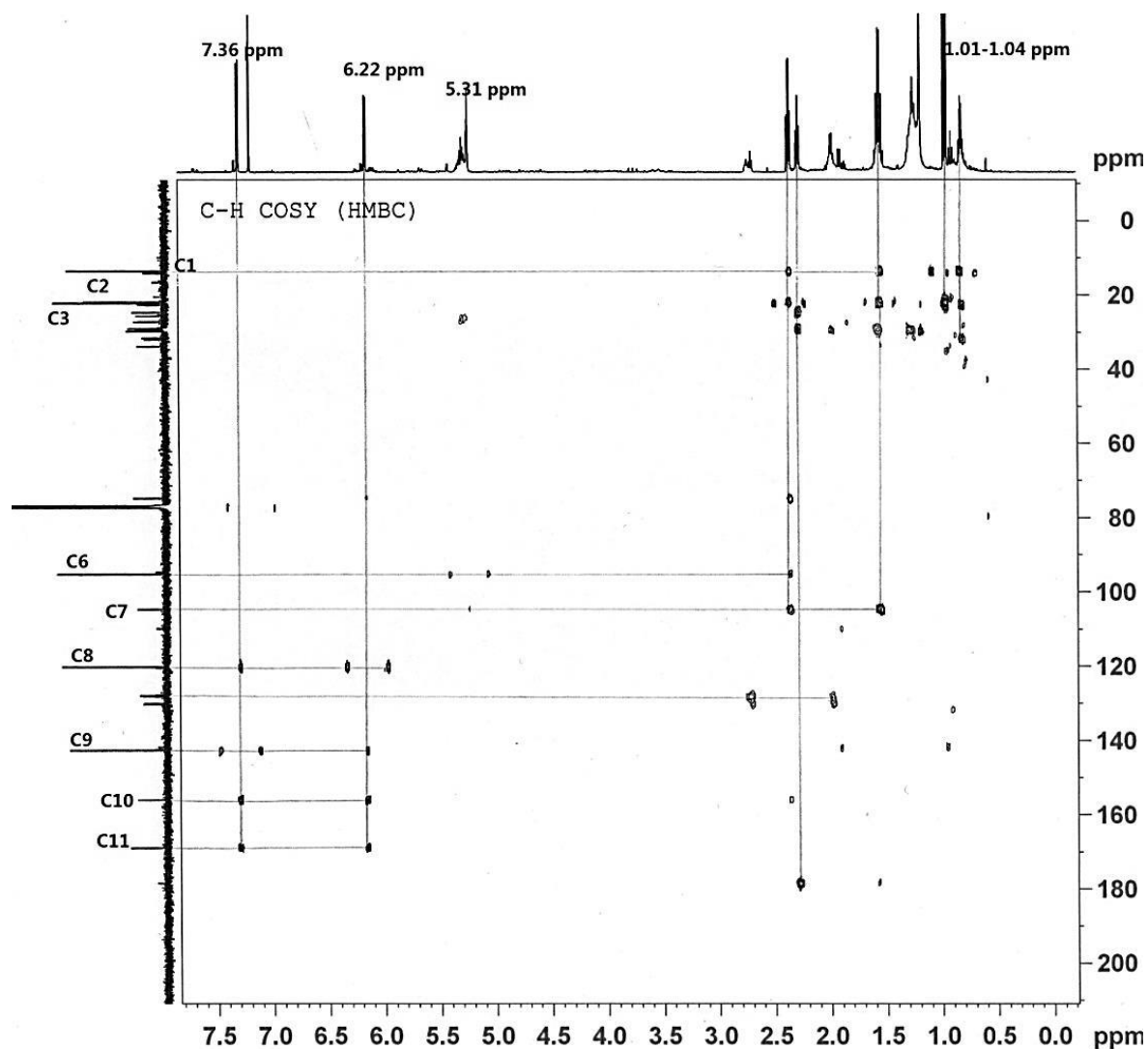
Figure 2.13 HMBC spectrum of compound H1-2-6.

Correlations from 2D NMR spectra HMQC and HMBC are showed in Figure 2.11 to 2.13. The two quaternary carbons were both correlated with H8 and H9, suggested that these four carbons were on a ring structure. The estimated chemical shifts were compared in Table 2.5, estimated ^{13}C-NMR chemical shift had a good match with for C10 and C11 at the δ 165 and 147 respectively (compare to δ 168.95 and 142.65 for H1-2-6).

Table 2.5 HMQC and HMBC correlations of compound H1-2-6.

	δ ^{13}C (ppm)	δ^{1}H (ppm)	Proposed structure	HMBC Correlation
1	13.57	1.01-1.04	-CH$_3$	H2,3
2	21.88	1.60-1.63,	-CH$_2$-	H1, 4
3	22.14	2.43	-CH2-	
4	24.70	1.62-1.64	-CH$_2$-	H5
5	33.77	2.35	-CH$_2$-	H1
6	95.14	5.31		H3
7	104.66		quaternary carbon	
8	120.18	6.22	-CH=CH-	H9
9	142.64	7.36	-CH=CH-	H8
10	156.06		quaternary carbon	H8, 9
11	168.95		quaternary carbon	H8, 9
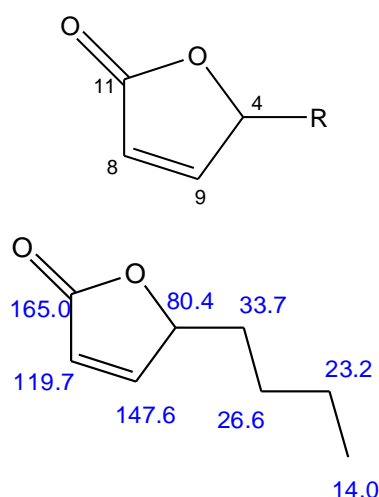
Figure 2.14 Proposed structure and estimated ^{13}C NMR chemical shifts of compound H1-2-6.

However, number and the positions of methylene group could not be determined (R group in Figure 2.14), because the sample contains many impurities thus further structure investigation is warranted. The ^{13}C chemical shifts estimation was carried out using a butyl group, proposed structure was showed as a butyrolactone. Butyrolactone has not been reported from the *Erigeron* genus yet.

2.6.3.4 Compound H1-2-7

Compound H1-2-7 was a brown powder, it gave brown colour under UV wavelength

254 nm and blue florescence under UV wavelength 366 nm (Figure 2.3). From the mass spectrum, molecular ion was observed at *m/z* 160 (Figure 2.15), and the mass loss between fragment peak *m/z* 160 and 131 was suggested to be a carbonyl group plus proton (-HC=O).

Unknown: H1-2-7#909 RT: 23.50
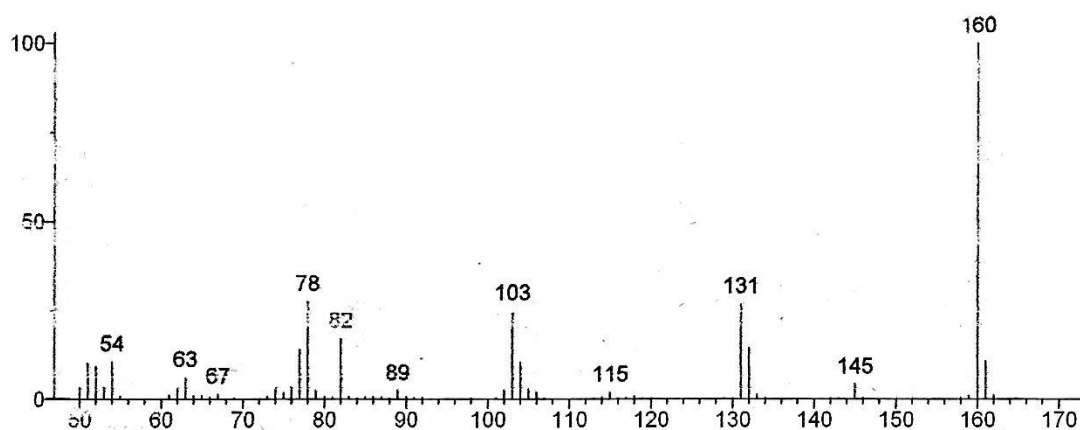
Figure 2.15 MS spectrum of compound H1-2-7.

^{1}H NMR and ^{13}C NMR spectra of H1-2-7 are showed in Figure 2. 16 and 2.17 (500 MHz, $CDCl_3$). From the ^{13}C NMR spectrum, 10 carbon peaks were counted, after comparing with the DEPT, one methyl peak at δ 16.52 and four quaternary carbon peaks at δ 87.98, 99.34, 155.91 and 168.83 were identified (Figure 2.16). No negative peaks found in DEPT, suggested that there were no methylene groups.
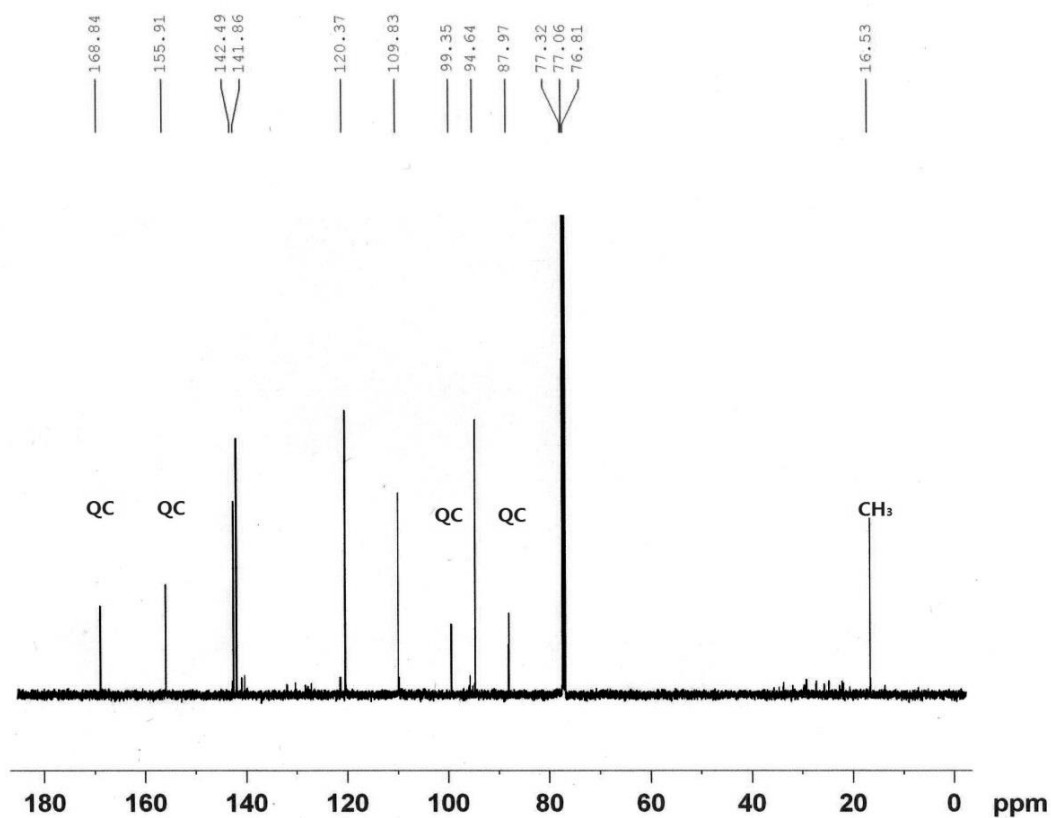
Figure 2.16 [3]C NMR spectrum of compound H1-2-7.

In the ^{1}H NMR spectrum (Figure 2.17), the peak at δ1.98 was assigned to a methyl group, it split into a doublet indicated that there was only one proton attached to the adjacent carbon, therefore the methyl group might link to a double bond (=CH-CH$_3$). Doublet showed at δ 7.38-7.42 suggested an aromatic structure of H1-2-7.
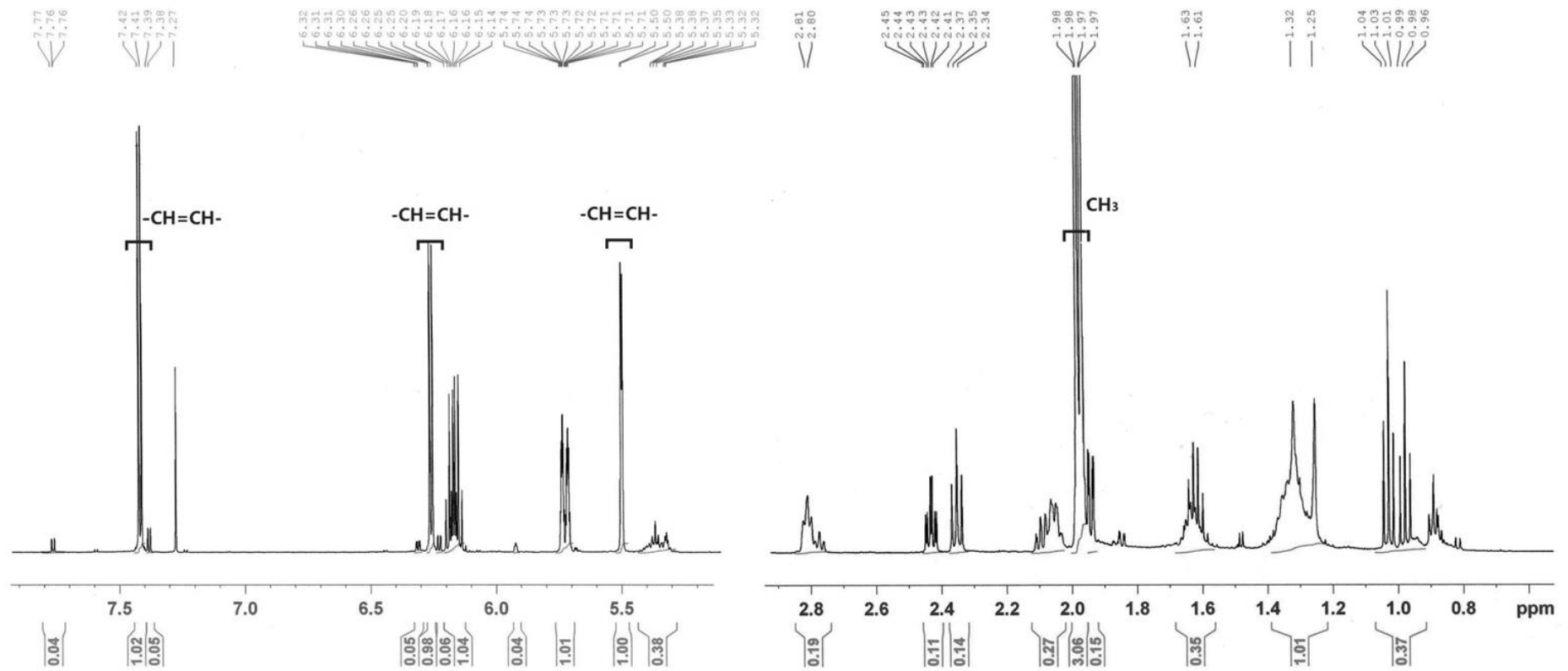
Figure 2.17 ^{1}H NMR spectrum of compound H1-2-7.
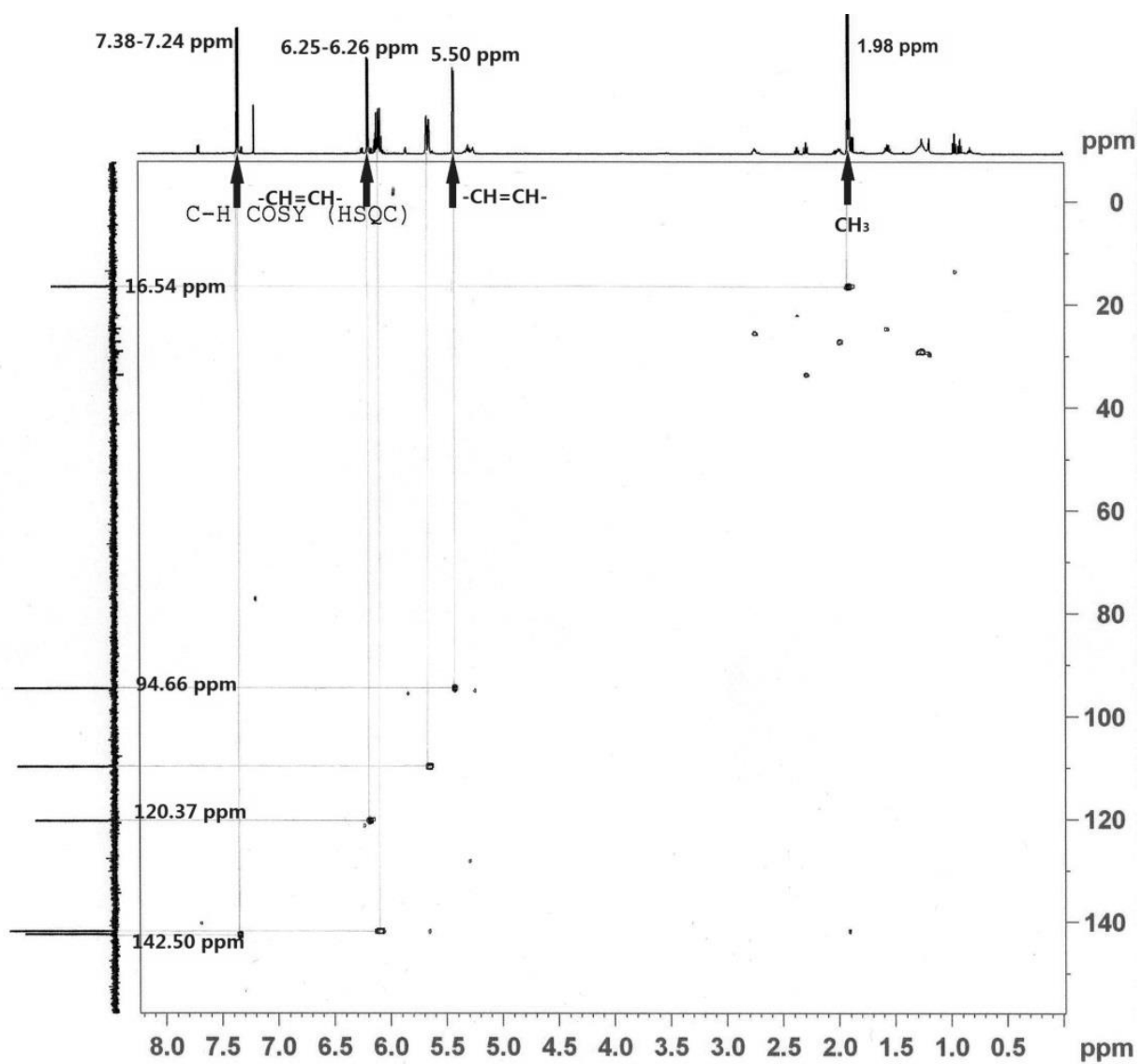
Figure 2.18 HMQC spectrum of compound H1-2-7
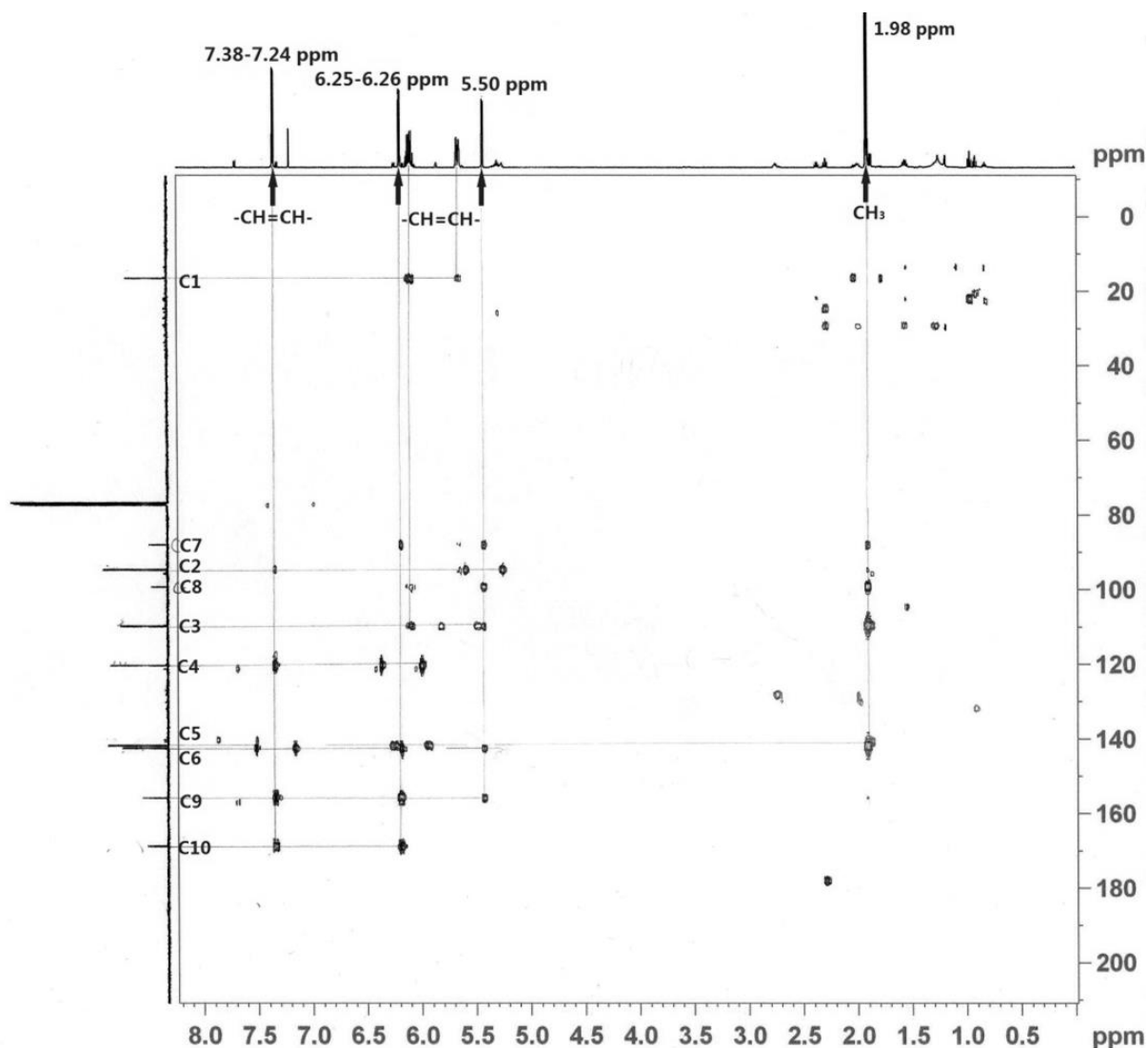
Figure 2.19 HMBC spectrum of compound H1-2-7.

The C-H correlations were obtained from HMQC and HMCB spectra (Figure 2.18 and 2.19). Carbon C7 and C8 had chemical shifts at δ 87.97 and 99.35, which were likely caused by sp hybridization, an acetylene bond. C8 had a correlation with H1 in HMBC, suggested that the terminal methyl group might be attached or two bonds away from the acetylene carbon. C7 correlated with H1 and H2, and the correlation to H1 was weaker than it of C8, suggested the C8 was at the far end (from the ring structure) of the alkyl chain. The other two quaternary carbons C9 and C10 were both correlated to H4 and H6, indicating that these four carbon atoms were likely on the same ring structure.

The C-H correlations were compared in Table 2.6, and the proposed structure of H1-2-7 was showed in Figure 2.20: a 2-pyrone derivative, 4-pent-3'-ne-1' -ynyl-pyran-2-one. However, many impurity peaks were observed in the ^{1}H NMR spectrum, sample H1-2-7 was not pure and the structure elucidation result might be

compromised, and more purification procedures were warranted.

Table 2.6 C-H correlations of compound H1-2-7.

	δ ^{13}C (ppm)	δ^{1}H (ppm)	Proposed structure	HMBC correlations
1	16.52	1.98	CH$_3$	H3, 5
2	94.64	5.50-5.55	-CH=CH-	H6
3	109.83	5.71	-CH=CH-	H1
4	120.36	6.25	-CH=CH-	H6
5	141.84	6.14	-CH=CH-	H1,3
6	142.49	7.38	-CH=CH-	H1, 2, 5
7	87.97		quaternary carbon	H1, 2
8	99.35		quaternary carbon	H1, 2
9	155.91		quaternary carbon	H2, 4, 6
10	168.84		quaternary carbon	H4, 6
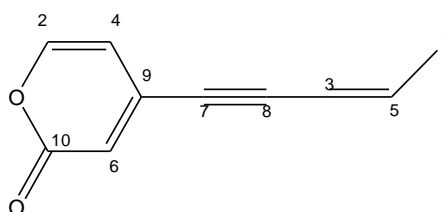
Figure 2.20 Proposed structure for compound H1-2-7.

Other type of pyrone have been reported in the *Erigeron* genus, especially 4- pyrones (Yue et al., 1994, Li et al., 2005, Mathela D. K. et al.,1984), and two polyacetylenic esters: lachnophyllum ester and matricariaester were reported from the *E.annuus* by Kumar (Kumar et al., 2014), which might be the product of 2-pyrone's ring open reaction. Both 2-pyrone and 4-pyrone structure carry one oxygen atom and a ketone functional group, which would be considered to be part of coumarin and chromone motif.

2.6.3.5 Compound H4

Compound H4 was obtained from hexane fraction H4 when eluted by petroleum ether ethyl acetate (3:1, v/v), it was then purified by recrystallization. Compound H4 was a white needle crystal, and 50 mg of H4 was collected. NMR spectra of H4 was clear and full structure of H4 was elucidated.
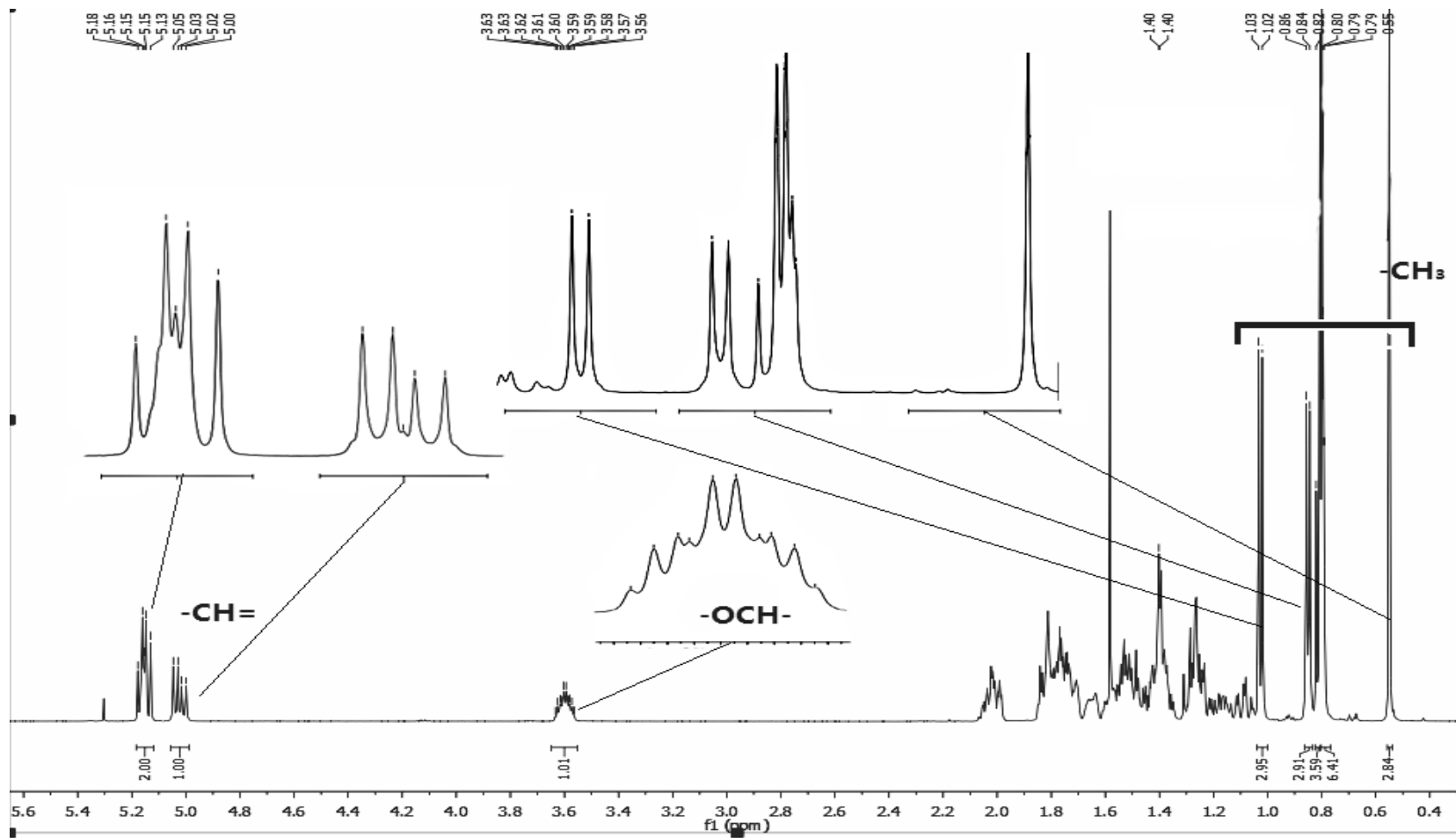
Figure 2.21 ^{1}H-NMR spectrum of compound H 4.
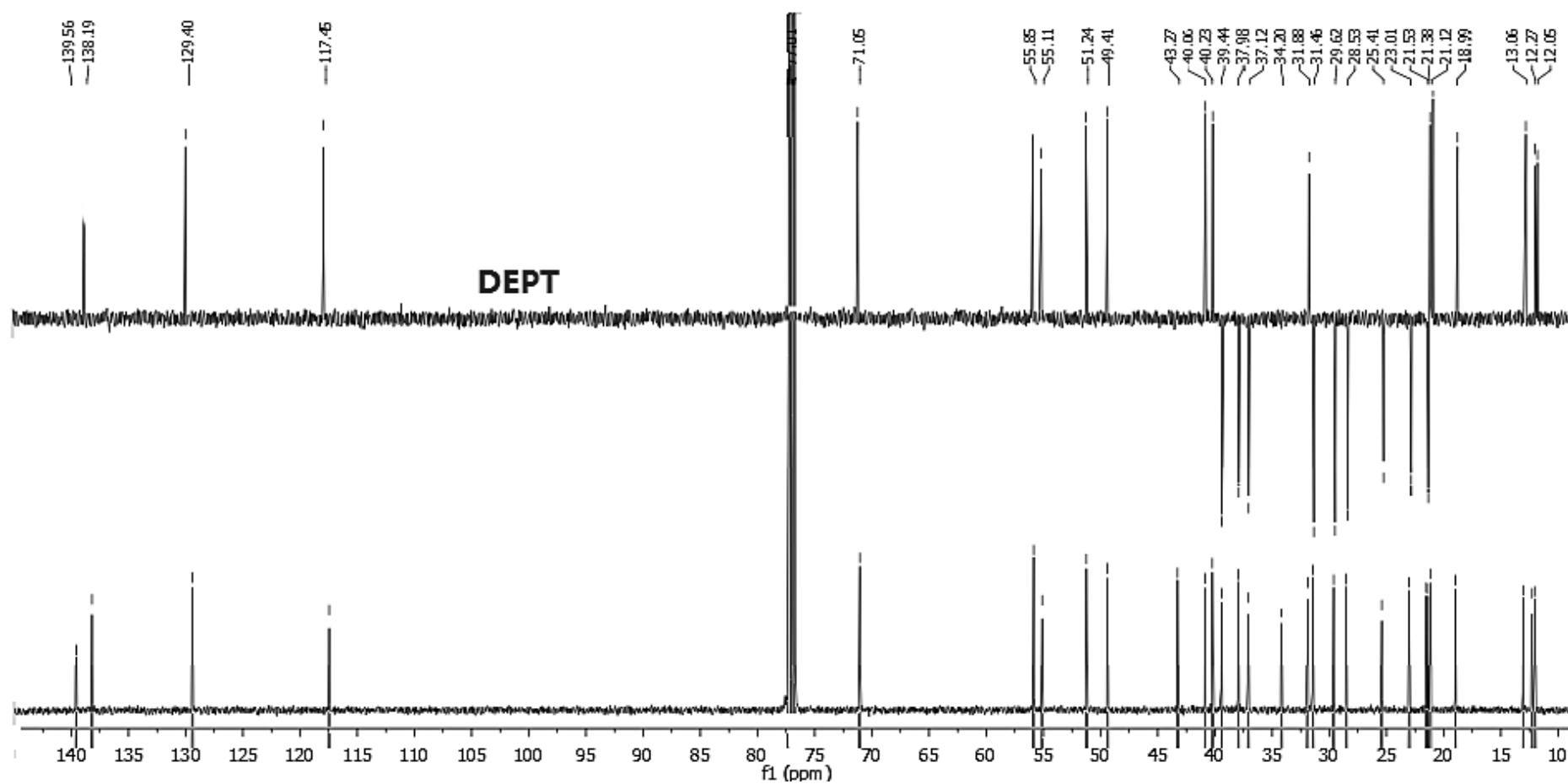
Figure 2.22 DEPT135 and ^{13}C NMR spectra of compound H4.

From the ^{1}H NMR spectrum of compound H4 (Figure 2.21), there were six methyl peaks in at δ1.03 that assigned to six methyl groups in the suggesting structure, they were H21 (δ 1.03), H26 (δ 0.85), H29 (δ 0.82), H27 (δ 0.81), H19 (δ 0.80), and H18 (δ 0.55). Doublelts and multiplets observed between δ 4.9 and 5.2 were assigned to the unsaturated side chain in the molecule, they could be the signal of three carbon double bonds.

Twenty nine carbon atom peaks were counted from the ^{13}C NMR spectrum (Figure 2.22) and only twenty six of them showed in the ^{13}C DEPT NMR spectrum, which indicated that there were three quaternary carbon atoms in the structure (C8, 13 and 20) From the ^{13}C and DEPT NMR spectra, nine methylene (-CH$_2$-) groups and six methyl (-CH$_3$) groups were counted respectively.
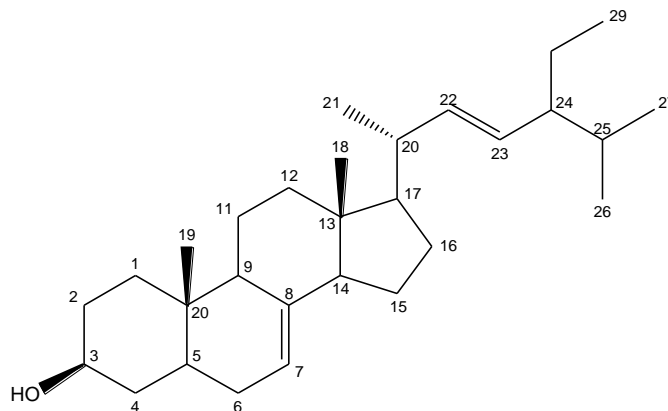
Figure 2.23 Proposed structure of compound H4, α-spinasterol.

The 2D NMR HMQC and HMBC correlations of compound H4 are showed in Figure 2.24 and 2.25. Six eligible carbon peaks were identified from the ^{13}C spectrum. Carbon peak at δ 12.27 (C18) was assigned to H18 (δ 0.55), it was coupled with H12, H17 and H14 (three bonds) and adjacent to C13 which indicated that the adjacent quaternary carbon was C13 (δ 139.56). Another methyl peak at δ12.05 (C19) correlated with proton peak H19 (δ 0.7), was adjacent to quaternary carbon C10 (δ 43.27). Carbon peak at δ 21.38 (C21) correlated with H21, H21 split into a doublet indicated that the adjacent carbon C20 had one proton attached. C21 was coupled with H17 and H22 (three bonds) and H20 (two bonds). Carbon peak at δ 21.12 correlated with H26 (δ 0.85) which was a doublet split by coupling with H25 (single proton), and C26 was coupling with H24 and H27 in three bonds. Carbon peak at δ 18.99 was correlated with H27, and peak C27 was coupled with H24 and H26 in three

bonds. Carbon peak at δ 13.06 was correlated with H29 which split into a triplet by coupling with C28. The rest correlations of each identified peaks are listed in Table 2.7.
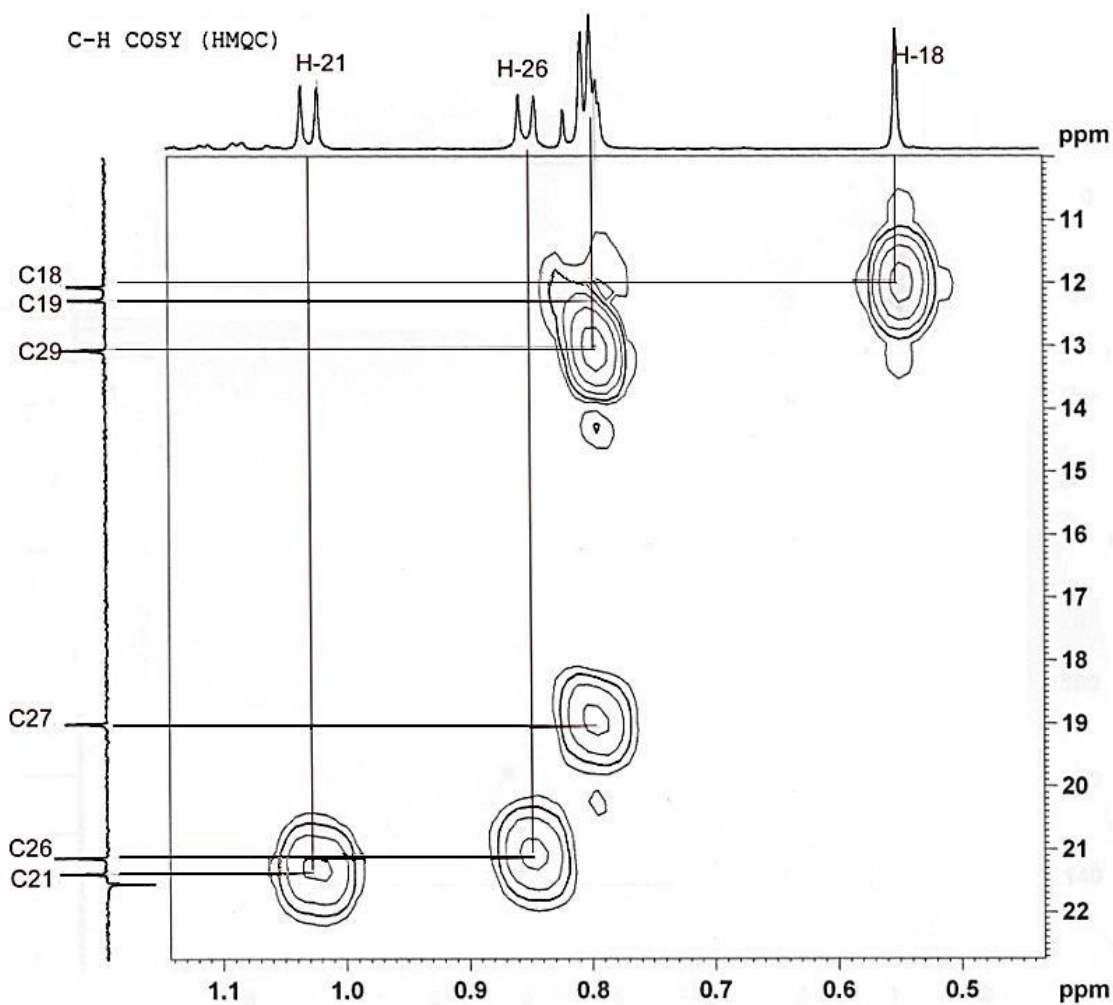
Figure 2.24 HMQC spectrum of compound H4,α-spinasterol.
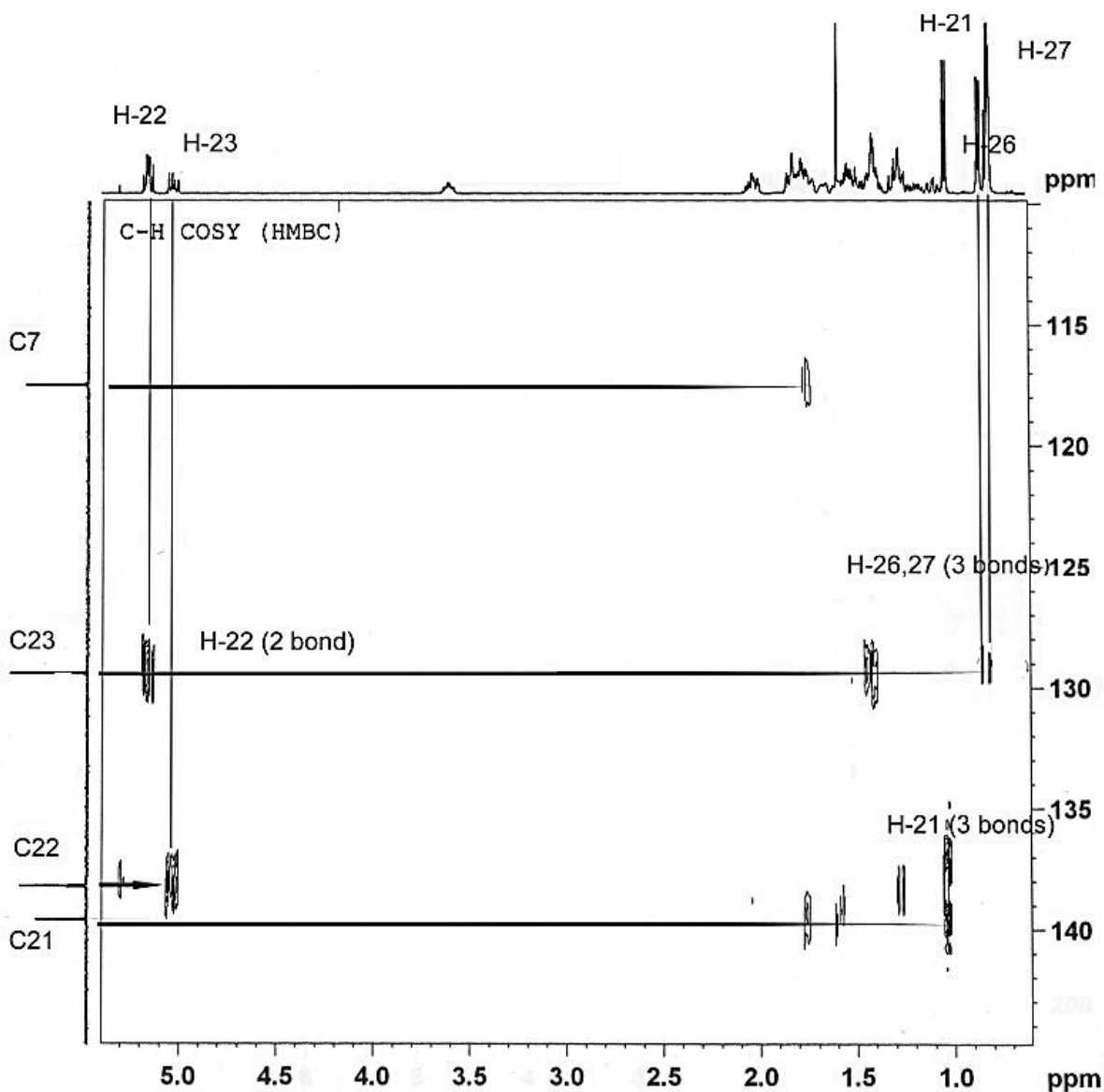
Figure 2.25 HMBC spectrum of compound H4, α-spinasterol.

The C-H correlations are listed in Table 2.7. Two double doublets at the low field (> 5 ppm) were caused by the two vinyl protons from the double bond in the side chain (H22 and H23 in ^{1}H NMR, Figure 2.21). Because they had a similar chemical environment, their chemical shifts were very close, the chemical shifts were C22 at δ 138.19 and C23 at δ 129.40. There was another proton peak identified at the same chemical shift H7 at δ 5.15, it was assigned to carbon C7 (δ 117.45) and coupled with a methylene group in HMBC.

Table 2.7 NMR data of compound H4 and α-spinasterol

C	δ ^{13}C^a (ppm)	δ ^{13}C^b (ppm)	δ^{1}H^c (ppm)	m, *J*(Hz)	HMBC correlations Two bonds (three bonds)
1	37.1	37.12			H-2, 10, (H-3,5,9,19)
2	31.5	31.46			H-1, 3, (H-4, 10)
3	71.1	71.05	3.59	m, 5	H-2, 4, (H-1, 5)^d
4	38.0	37.98			H-3, 5, (H-2, 6, 10)
5	40.2	40.23			H-4, 6,10, (H-1, 3, 7, 9, 19)
6	29.6	29.62			H-5, 7, (H-4, 8, 10)
7	117.4	117.45	5.15	s	H-6, 8, (H-5, 9, 14)
8	139.6	139.56			H-9, 14, 12, (H-11, 6, 15)
9	49.4	49.41			H-8,10,11, (H-1, 5, 12, 14, 7, 19)
10	34.2	34.20			H-1, 5, 9, 19, (H-2, 4, 6, 11)
11	21.5	21.53			H-9, 12, (H-8, 10, 12)
12	39.4	39.44			H-11, 13, (H9, 14, 18)
13	43.3	43.27			H-18, 12, 14, 17, (H-11, 15, 16, 20)
14	55.1	55.11			H-15, (H-7, H-9, H-12, H-17, H-18, H-16)
15	23.0	23.01			H-14, 16, (H8, 13, 17)
16	28.5	28.53			H-15, 17, (H-13, 14, 20)
17	55.9	55.88			H-13,16, 20, (H-18, 12, 14, 15, 21, 22)
18	12.0	12.05	0.55	s	H-13, (H-12, 14, 17)
19	13.0	13.06	0.79	s	H-10, (H-1, 5, 9)
20	40.8	40.68			H-21, 22, 17, (H-13, 16, 23)
21	21.4	21.38	1.02	d, 10	H-20, (H-17, 22,)
22	138.2	138.19	5.816	dd, 10	H-20, 23, (H-21, 17, 24)
23	129.4	129.40	5.02	dd, 5	H-22, 24, (H-20, 28, 25)
24	51.2	51.24			H-23, 28, 25, (H-22, 26, 27, 29)
25	31.9	31.88			H-24, 26, 27, (H-23, 28)
26	21.1	21.12	0.85	d, 10	H-25, (H-27, 24,)
27	19.0	18.99	0.80	d, 10	H-25, (H-26, 24,)
28	25.4	25.41			H-24, 29, (H-23, 25)
29	12.2	12.27	0.81	t, 10	H-28, (H-24)

a ^{13}C NMR of spinasterol (Kongduang   et al., 2008, De-Eknamkul and Potduang, 2003, Ragasa et al., 2012), 150 MHz, CDCl$_3$.
b ^{13}C NMR of H4, Bruker, 500 MHz, CDCl$_3$.
c   Assignments by ^{1}H–^{1}H COSY spectrum.
d   Assignments by HMBC spectrum.

The NMR data of compound H4 showed a good match with NMR data of α-spinasterol, the structure is shown in Figure 2.23, the NMR data used in Table 2.7 was published by Schlitzer (Schlitzer, 2007).H4 belongedto Δ^7-sterol family, they are phytosterols distributed widely throughout the plant kingdom. Compound α-spinasterol is known to be involved in the stabilization of cell membranes and possesses an additional unsaturation double bond in the side-chain of the molecule (Kongduang et al., 2008, Dewick, 2001).

2.6.3.6 Fraction H5-1

Fraction H5-1 was sent for GC-MS analysis, it was a colorless oil and 2 mg of H5-1 was obtained when eluted H5 with petroleum ether ethyl acetate 4:1(v/v). Two compound H5-1-1 and H5-1-2 were identified using GC-MS.
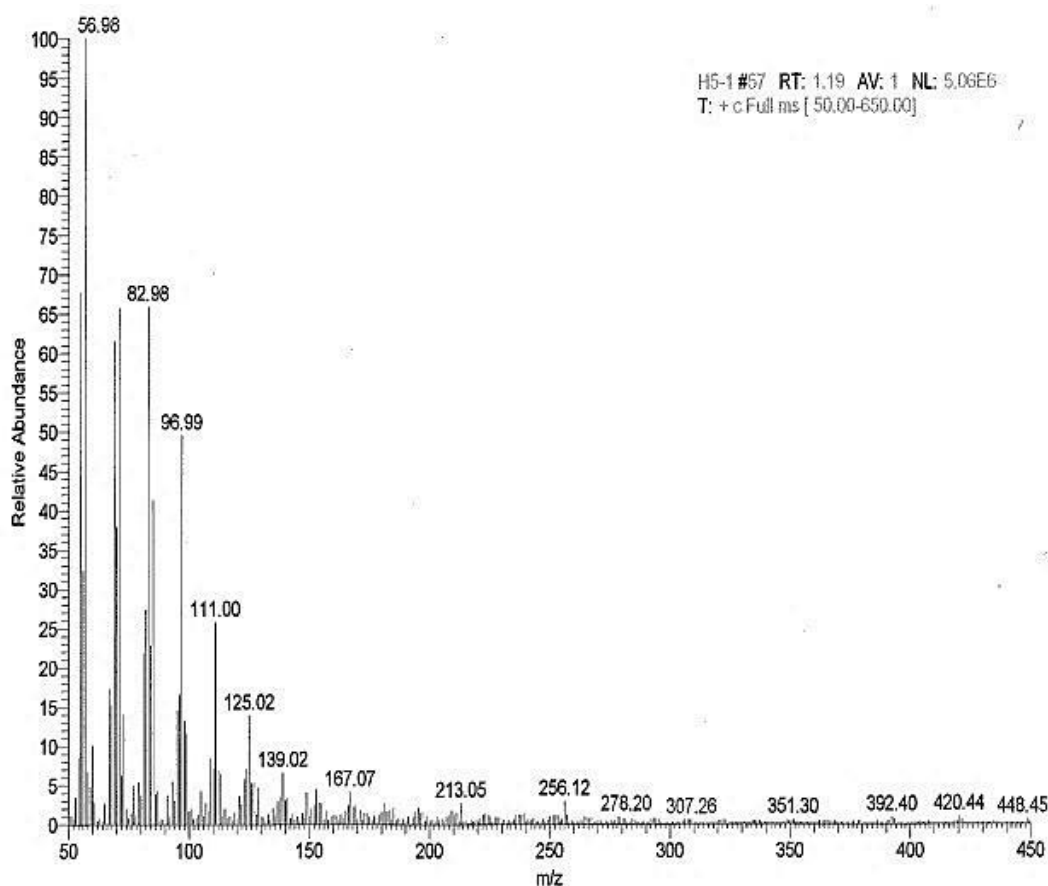
Figure 2.26 MS spectrum of compound H5-1-1, eluted at 1.19 min from GC.

From the mass spectrum of H5-1-1 (Figure 2.26), the molecular ion peak for compound H5-1-1 was observed at *m/z* 256 and base peak was observed at *m/z* 56.98. The base peak was suggested to be a -$(CH_2)_3CH_3$ group and *m/z* 14 difference between peaks from *m/z* 83 to *m/z* 167 suggested those fragmentations were seven

methylene groups. The mass difference between *m/z* 56.98 and 82.98 was 26 units mass lost indicating that the structure contained a double bond (-CH=CH-). Fragment peaks from *m/z* 213 to *m/z* 256 suggested to be a - $(CH_2)_2CH_3$ group (43 mass units). Compound H5-1-1 was an aliphatic compound, however, more sample was required for further structure elucidations.
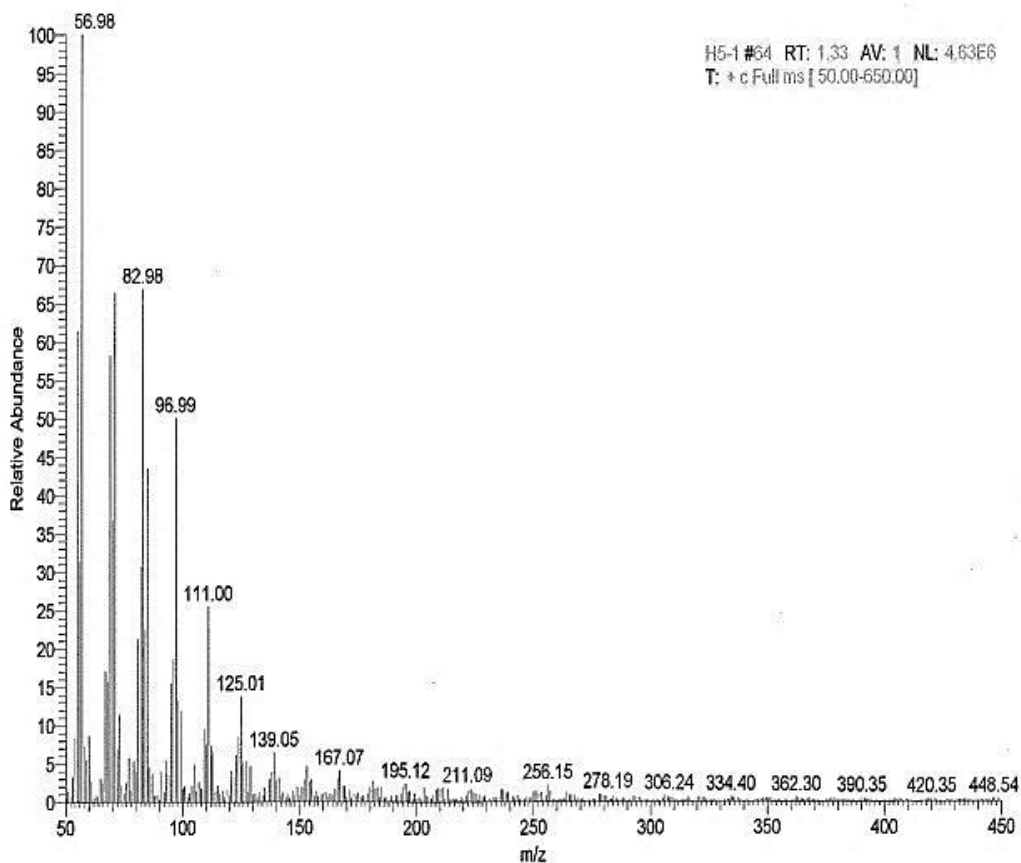
Figure 2.27 MS spectrum of compound H5-1-2, eluted at 1.33 min from GC.

The molecular ion peak of compound H5-1-2 (Figure 2.27) was found at *m/z* 256.15. Mass of the base peak was observed at *m/z* 56.98 which might be share the same fragment structure as H5-1-1, $-(CH_2)_3CH_3$. The mass difference between *m/z* 56.98 and 82.98 was 26 mass units indicating a double bond in the structure. Counting from the fragment peak *m/z* 82.98 to the *m/z* 195.12, six *m/z* 14 peaks (methylene groups) were found. Difference between *m/z* 211.09 and *m/z* 256.15 was 45 mass units which suggested to be a carboxyl group. The compound was proposed to be gondoic acid $C_{20}H_{20}O_2$ which molecular weight was *m/z* 256.42 (Liu et al., 2011, Lwata et al., 2011). More samples are needed for further structure elucidation for the position of the double bond.

2.6.3.7 Compound H5-2

Compound H5-2 was a white powder (5 mg) obtained from petroleum ether ethyl acetate elution (4:1,v/v). It was further purified by silica gel columns (400 mesh).The mass spectrum of H5-2 is shown in Figure 2.28.
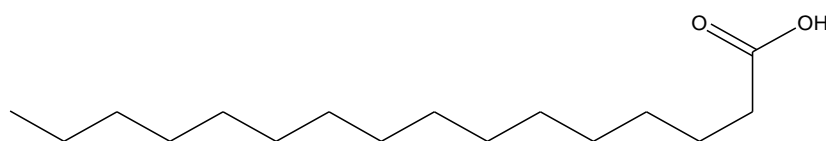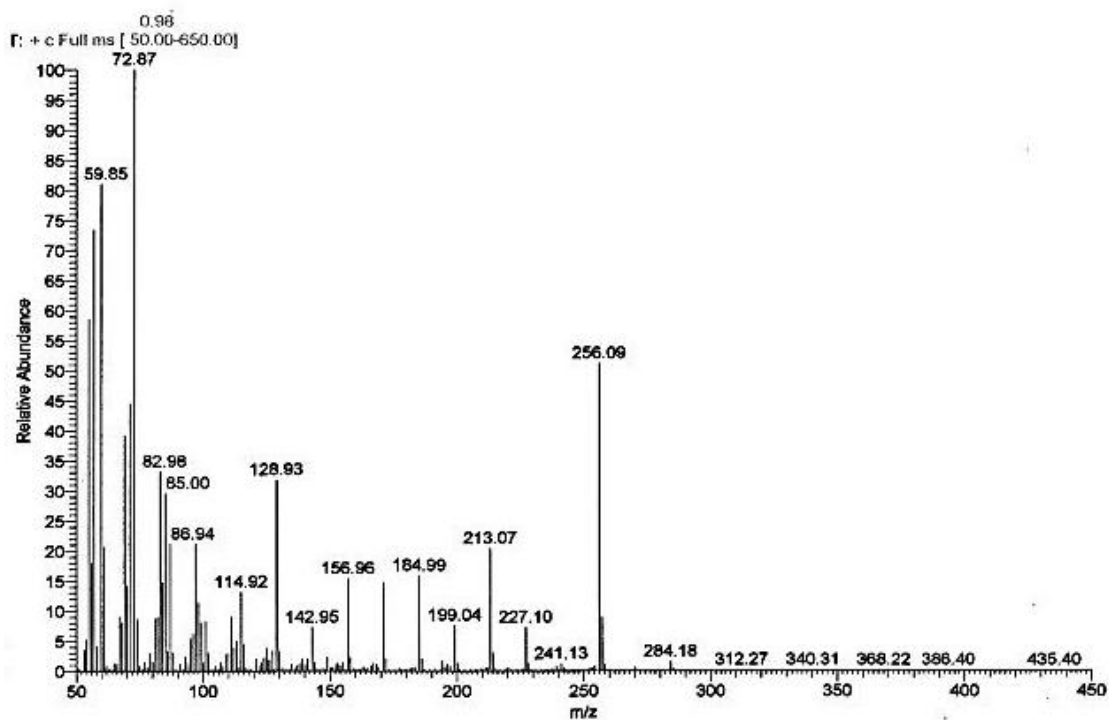
Figure 2.28 **A.** MS spectrum of compound H5-2. **B.** Structure of hexadecanoic acid.

Molecular ion peak of compound H5-2 was observed at *m/z* 256 and the base peak was observed at *m/z* 72.87. Fragment ion peak *m/z* 59.85 was indicated a -CH$_2$COOH group. From the peak *m/z* 59.85 to the peak *m/z* 241.13, twelve methylene groups were counted. From peak *m/z* 241.13 to *m/z* 256.09, the mass unit loss was 15 *m/z*, suggested to be a methyl group.
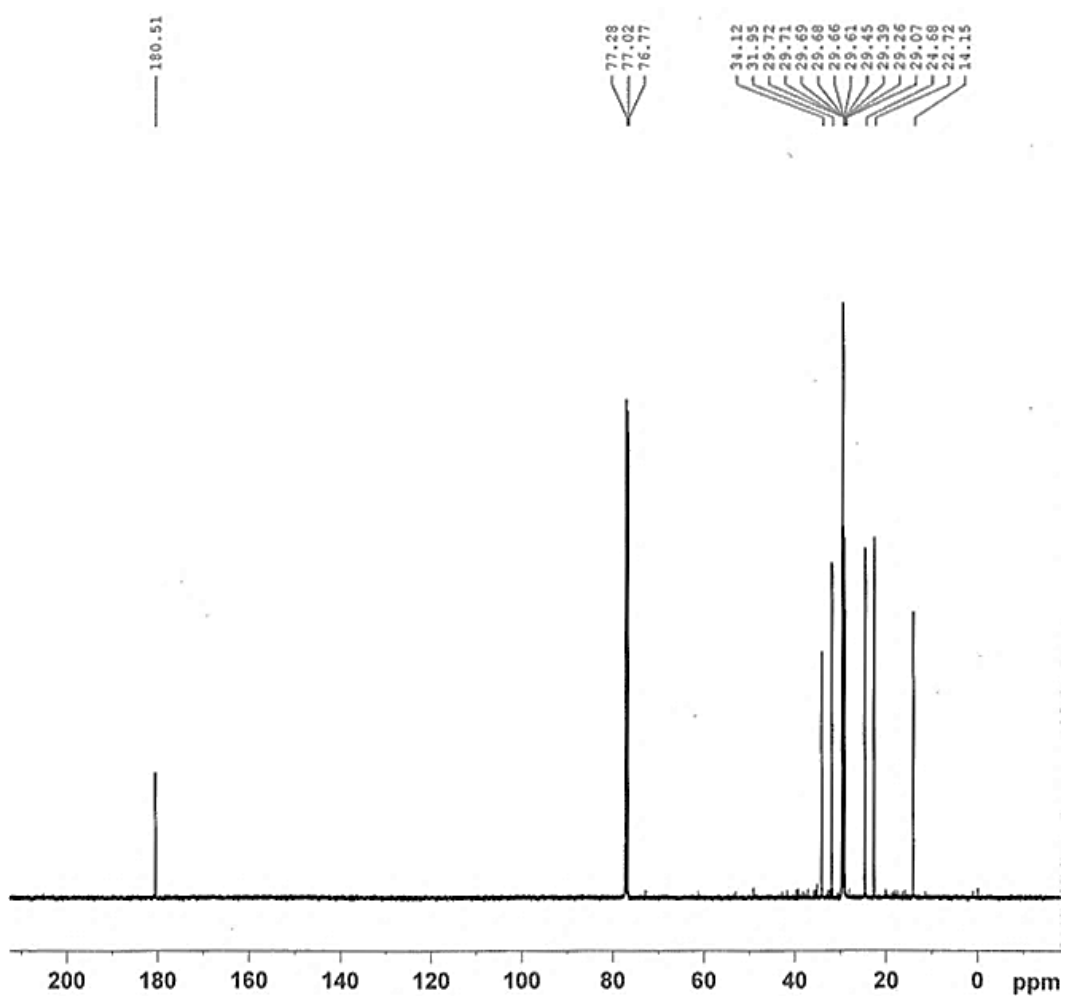
Figure 2.29 ^{13}C NMR spectrum of compound H5-2.

Sixteen carbon peaks were identified from the ^{13}C NMR of H5-2 and one methyl peak at δ 14.15 and fourteen methylene peaks (between δ 22.72 and 34.13 p) were counted after comparing with the DEPT.
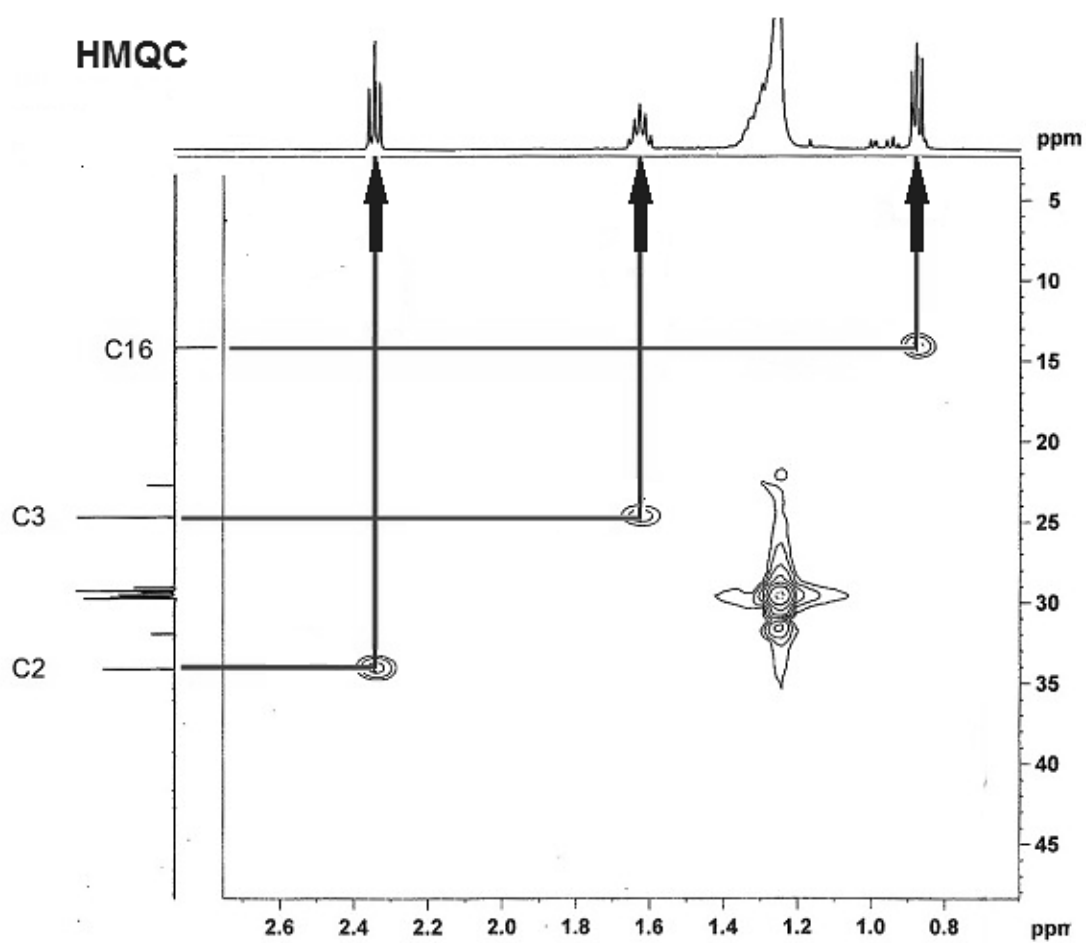
Figure 2.30 HMQC spectrum for compound H5-2.
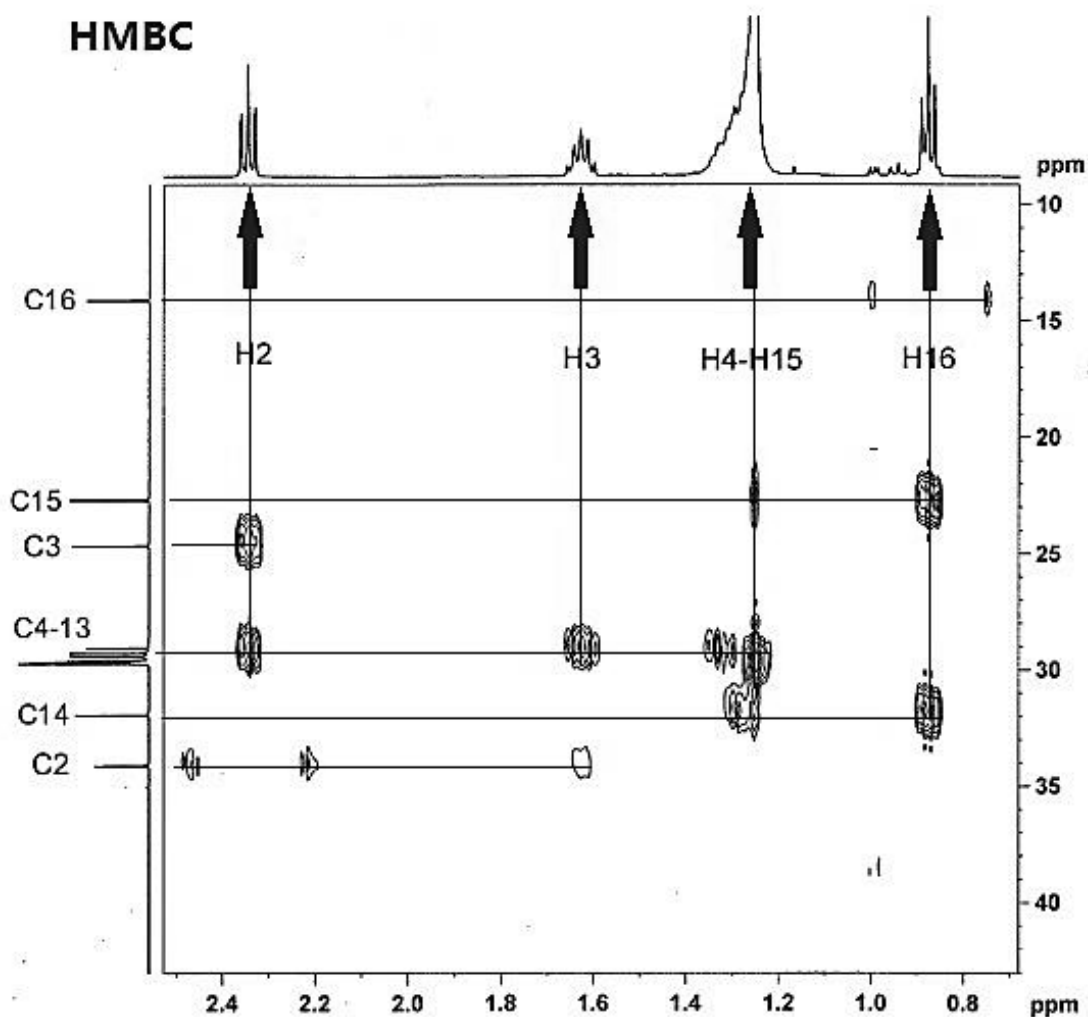
Figure 2.31 HMBC spectrum for compound H5-2.

According to the HMQC and HMBC spectra of H5-2 (Figure 2.30 and 2.31), a triplet at δ 0.83 in ^{1}H NMR spectrum was assigned to the methyl group, another triplet at δ 2.33 was observed. The oxygen atom in the carboxyl group applied a descreening magnetic field that caused the peak appeared in the low field, indicating those protons might be close to a carboxyl group. The quintuplet in ^{1}H NMR at δ1.63 was assigned to the methylene group C3 (Figure 2.30), the protons were correlated with a methylene carbon in HMQC, and also coupling with the carboxyl group in bonds (Figure 2.31). The rest of the saturated aliphatic chain structure on the molecule contained thirteen methylene groups (counted from the mass spectrum), the proton NMR peaks for them appeared as a multiplet at around δ 1.25 (C4-13). The suggested structure for H5-2 was hexadecanoic acid (Figure 2.28 **B**), $C_{16}H_{32}O_2$, *m/z* 256.42.

2.6.3.8 Compound H7

Compound H7 was a white precipitate (6 mg) eluted with petroleum ether and ethyl acetate (1:7, v/v) over silica gel column. Due to the seven characteristic methyl signals from ^{1}H-NMR spectrum (δ 0.7-1.2, Figure 2.32), compound H7 was considered to be a pentacyclic triterpenoid.

There were three main classes of skeletons of pentacyclic triterpenoid, oleanane skeleton, ursane skeleton, and lupane skeleton (Wu and Wu, 2003). For lupane, CH_3-30 (atom number showed in Figure 2.33) was connected to a double bond, the methyl protons will coupling with the double bond and the CH_3-30 showed a broad peak in ^{1}H- NMR. In ^{1}H- NMR spectrum of H7, there was no broad peak showed, that indicated the compound H7 did not have a lupane skeleton. There was a multiplet showed between δ 5.0 and 5.4, indicated that there was a single double bond structure at C12. If there was a diene in the structure, the chemical shift of the proton peak would move to the lower field, might be beyond δ 5.5, due to the descreening effect of the double bond. The compound H7 suggested being a 12-oleanene or a 12-ursanene.
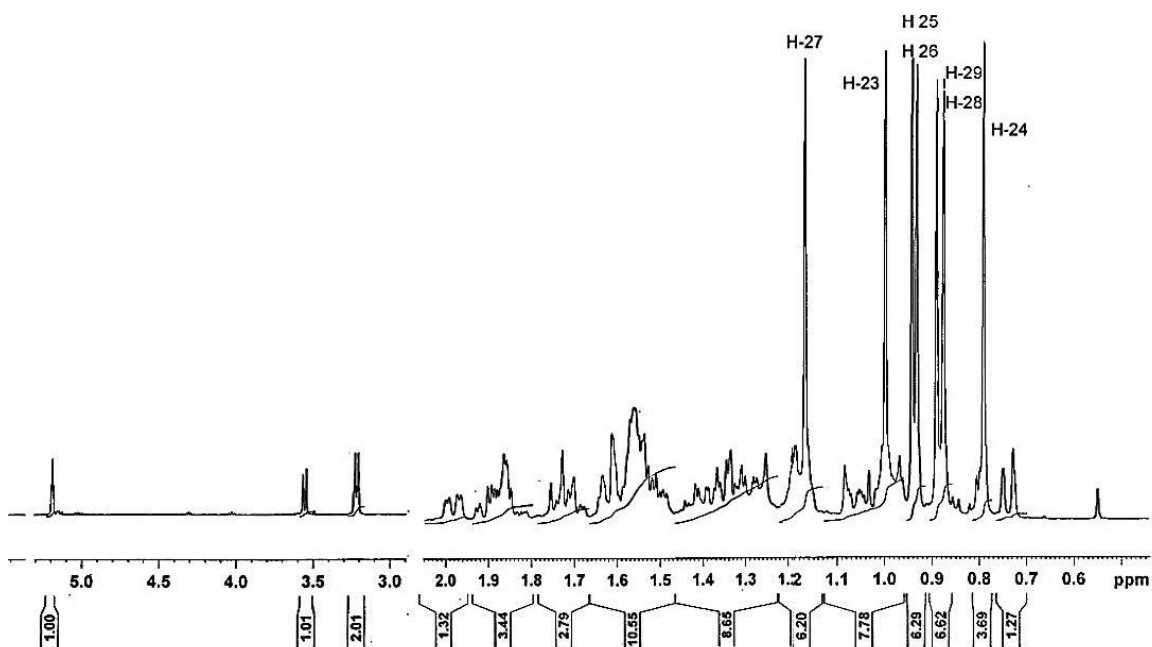
Figure 2.32 ^{1}H NMR spectrum of compound H7.

.
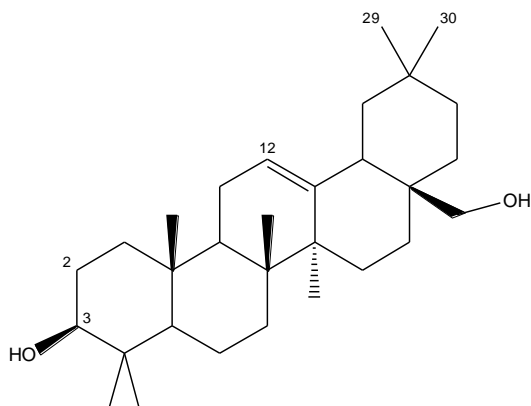
Figure 2.33 Proposed structure of compound H7, erythrodiol.

In the[13]C NMR spectrum, thirty-four carbon atoms were counted and seven of them were quaternary carbon compared with the DEPT (Figure 2.34), which both the 12-oleanene or a 12-ursanene structure have seven quaternary carbons. However, the chemical shift of the C12 and C13 were different: Chemical shifts of C12 and C13 of 12-oleanene was at δ 122~124 and δ143~144, while chemical shifts of C12 and C13 of 12-ursanene was δ 124~125 and δ 139~140 (Wu and Wu, 2003). Compound H7 was suggested to have a 12-oleanene skeleton (Figure 2.33).
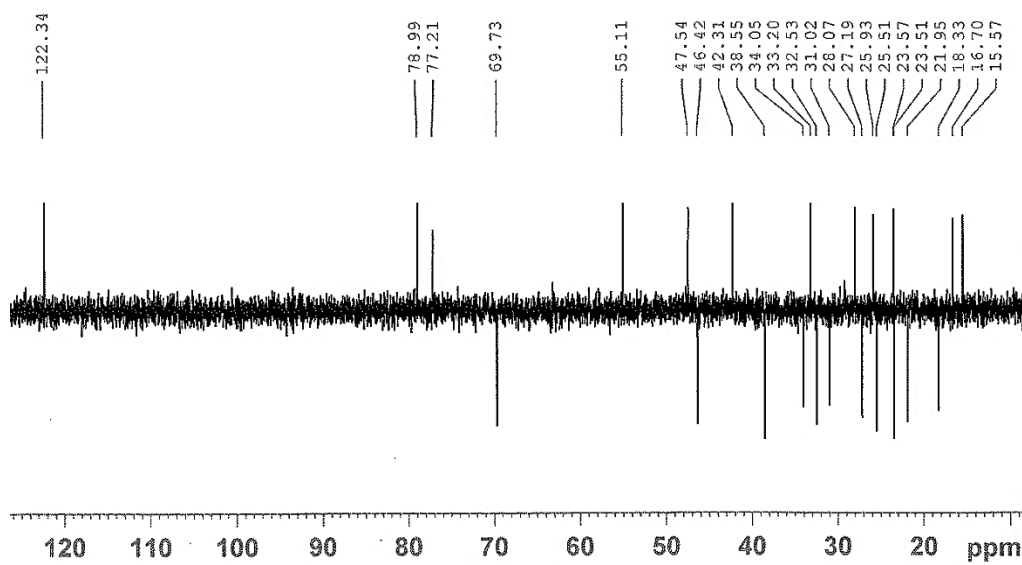
A. ^{13}C NMR spectrum of compound H7.
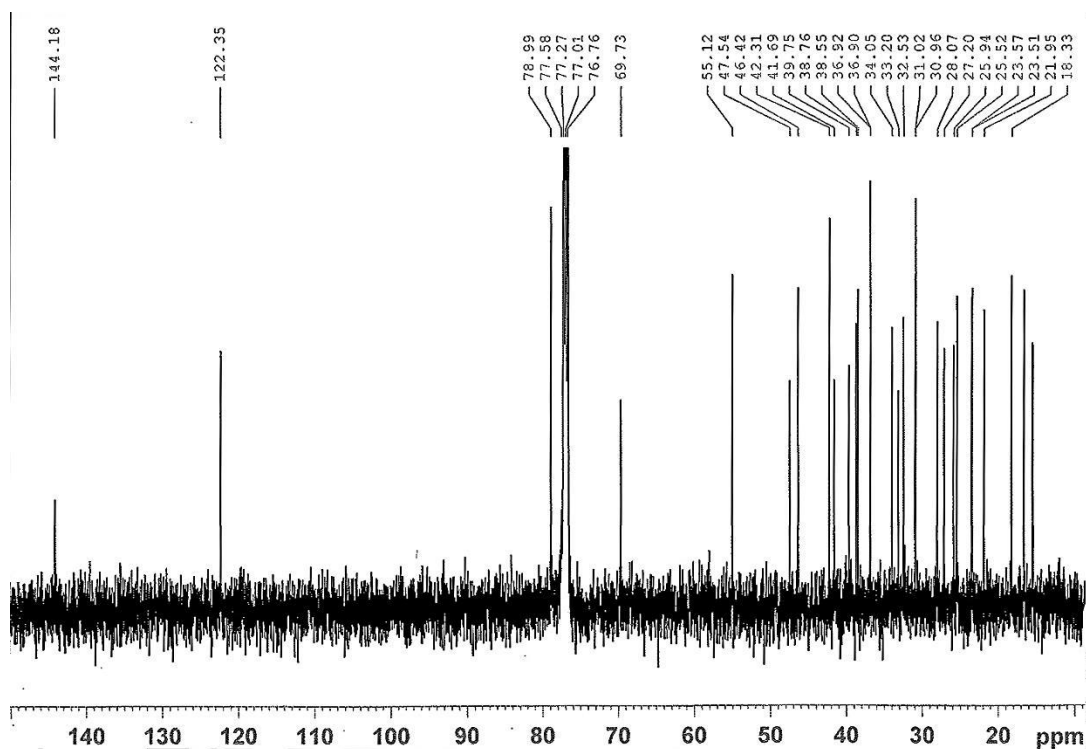
B. DEPT of compound H7.
Figure 2.34 DEPT and ^{13}C NMR spectra of compound H7.
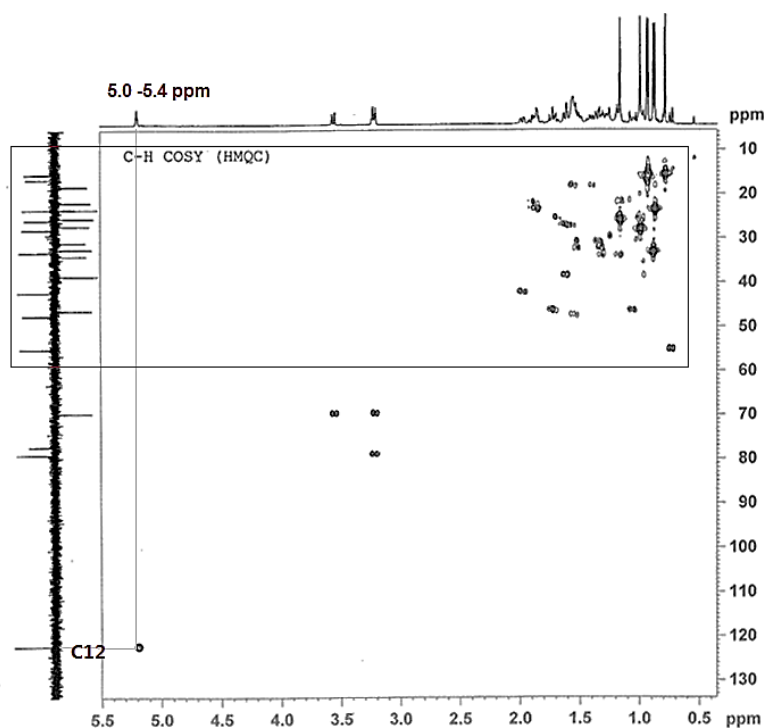
A. HMQC spectrum for compound H7. The framed area was showed in **B.**
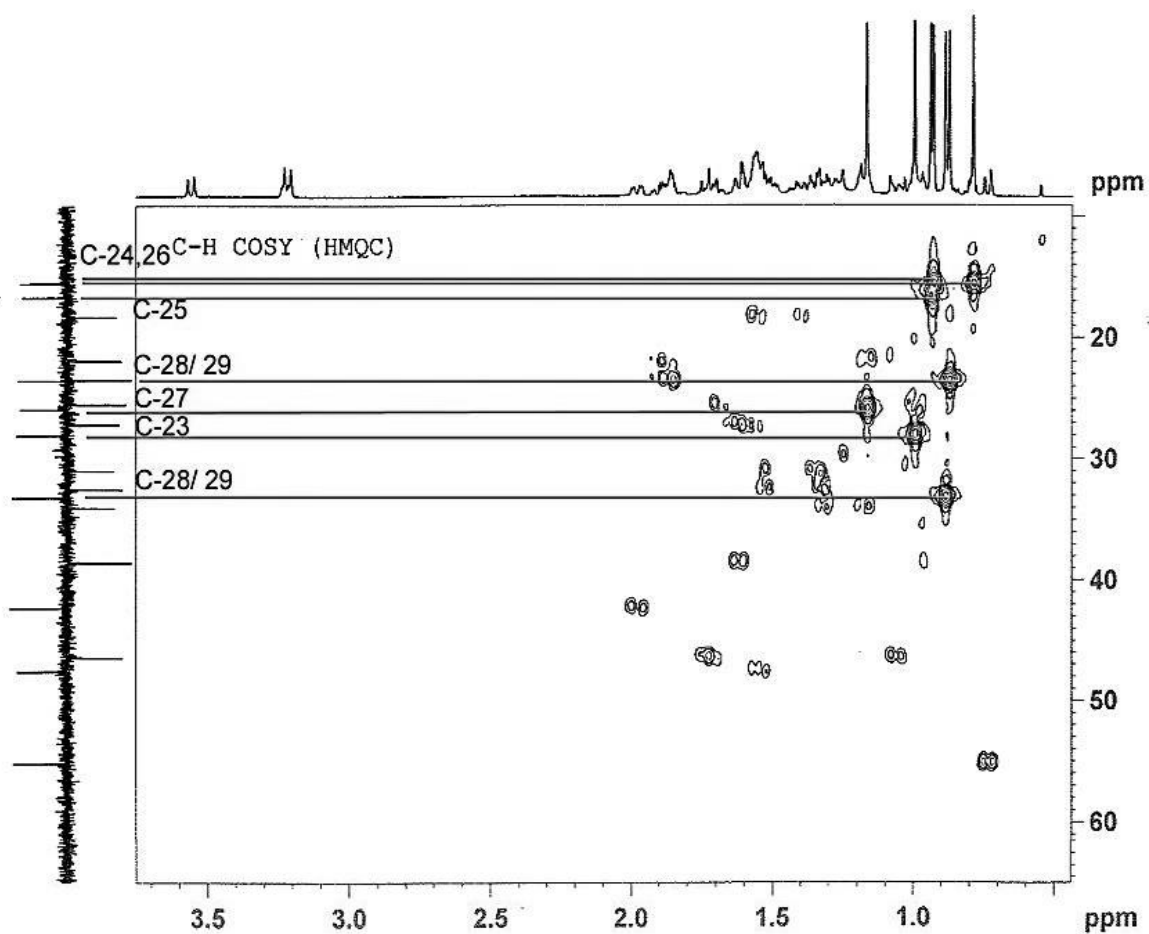
B. HMQC spectrum of compound H7. (^{13}C NMR: 20-80; ^{1}H NMR: 0-3.6).

Figure 2.35 HMQC spectra of compound H7.

Table 2.8 NMR data of H7 and erythrodiol.

C	δ ^{13}C (ppm)[a]	δ ^{13}C (ppm)[b]	δ^{1}H (ppm)	m, J(Hz)
1	38.6	38.55		
2	27.2	27.20		
3	79.0	78.99		
4	38.8	38.76		
5	55.2	55.12		
6	18.4	18.33		
7	32.6	32.53		
8	39.8	39.75		
9	47.6	47.54		
10	36.9	36.92		
11	23.6	23.57		
12	122.3	122.35		
13	144.2	144.18		
14	41.7	41.69		
15	25.6	25.52		
16	22.0	21.95		
17	36.9	36.90		
18	42.3	42.31		
19	46.5	46.42		
20	31.0	31.02		
21	34.1	34.05		
22	31.0	30.96		
23	15.5	25.58	0.79	s
24	28.1	28.07	1.00	s
25,26	15.5, 16.7	15.52,16.70	0.94	d, 5
27	25.9	25.94	1.17	s
28	69.7	69.73		
29, 30	33.2, 23.6	33.20, 23.57	0.88	d, 5

[a] ^{13}C NMR of erythrodiol, 100MHz, CDCl$_3$ (Kagawa et al., 1998).

[b] ^{13}C NMR of compound   H7, 500 MHz, CDCl$_3$.

From the HMQC of H7 (Figure 2.35), the proton peak at δ 5.0-5.04 assigened to C12, it coupled with the double bond on the ring structure and split into a multiplet. The peak was in low field because of the descreening effect of lone pair electron on the oxygen atom. The NMR data of H7 was compared with NMR of erythrodiol published by Kagawa (Kagawa et al., 1998), and H7 showed a good match to erythrodiol, $C_{30}H_{50}O_2$, *m/z* 442.72.

2.6.4 Separation of butanol extract

Fractions from butanol extracts were separated by reverse phase flash chromatography ten fractions were collected and fraction B3 were further separated over preparative reverse phase HPLC, 14 and 19 fractions were collected from B2 and B3 respectively. The fractions were freeze dried and their structures were educated by 1H NMR specrutm.

2.6.4.1 Compound B3-1

B3-1 was a white powder, 0.8 mg was isolated from the fractionation and the ^{1}H NMR was run in D_2O. The post-processing water peak suppression ^{1}H NMR spectrum is shown below (Figure 2.37).

From the ^{1}H NMR spectrum of B3-1, many impurity peaks showed this sample might not pure. Singlet at δ 2.28, 4 triplets between δ 3.47 and 3.95 were suggested to be the signals of -CH_2- groups or protons which had the same chemical environments on a glucose ring. The other two triplets from δ 3.71 to 3.95 showed characteristic signals for -OCH_3 groups; each triplet integrated for 3 protons. The singlet at δ 5.09 was possibly the anomeric proton on the glycosyl group. The singlet at δ 8.46 was in a very low field that might cause by the strong electron-withdrawing effect from an oxygen atom on the aromatic ring structure. A triplet at δ 6.51 was likely to be caused by aromatic protons, hypothetically, if the multiplet between δ 7.22 and 7.43 were triplets that the proposed structure of the compound is showed in Figure 2.36.
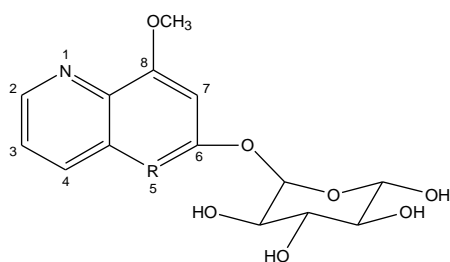
No.	^{1}H NMR chemical shift (ppm)	Estimated value (ppm)
2	8.76	8.73
3	7.22-7.43	7.30
7	6.51	6.65
Glu	3.47, 3.61, 3.74,	3.49-5.41
Ring -CH_2-	3.93	

Figure 2.36 Proposed structure of compound B3-1.
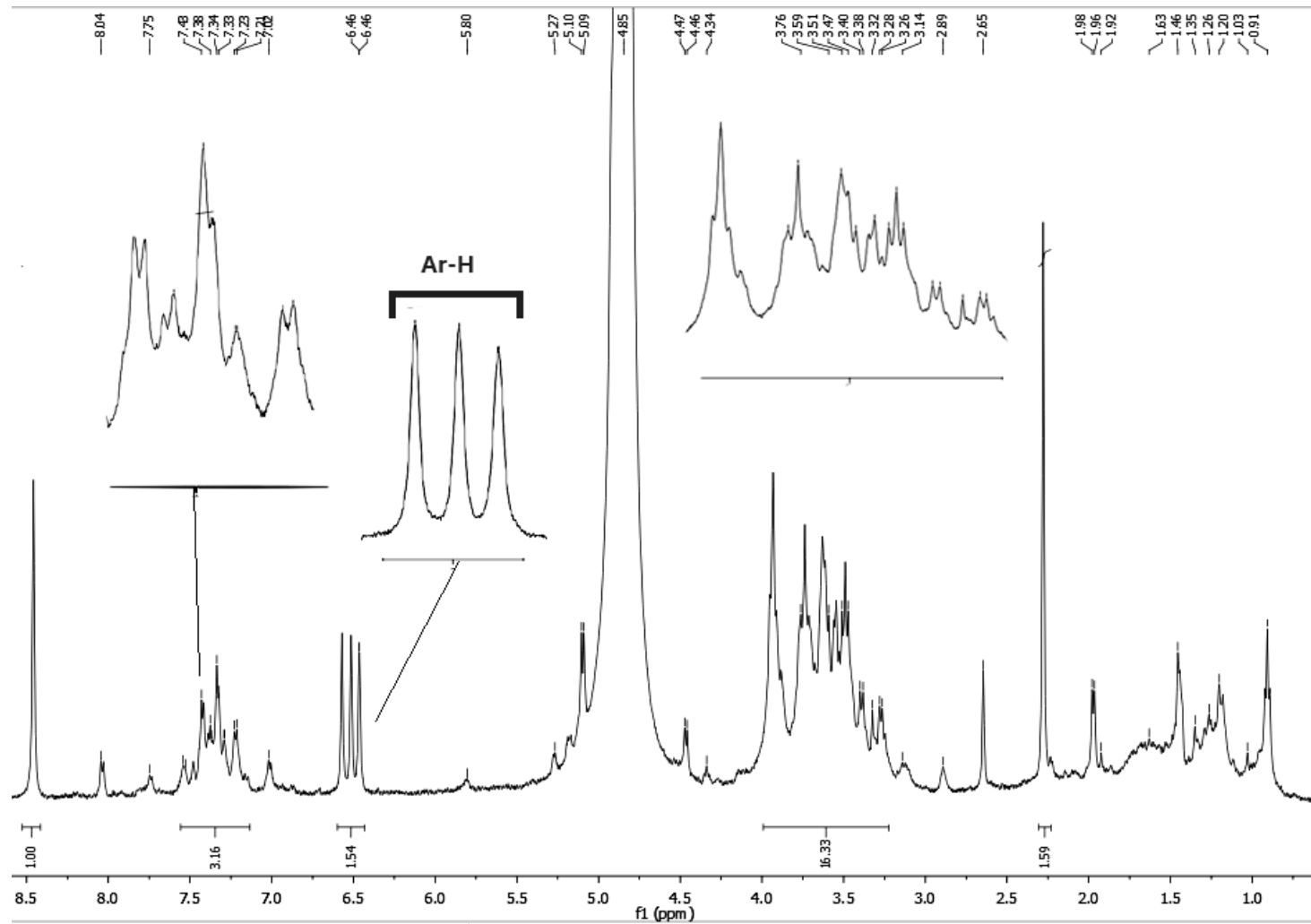
Figure 2.37 ^{1}H NMR spectrum of compound B3-1.

The ^{13}C chemical shifts of the proposed structure was estimated by ChemDraw$^{®}$ (Figure 2.37) and the estimated values were compared with ^{1}H NMR data in Figure 2.36.The nitrogen was a strong electro-withdrawing group that, the proton attached to the carbon next to it could resonate at very low field, such as δ 8.73 showed in estimation results.
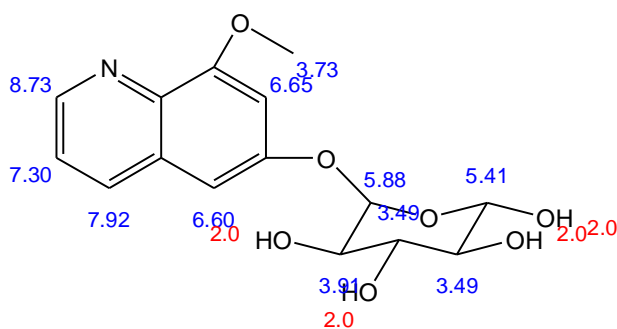
Figure 2.38 Estimation ^{1}H NMR chemical shift of compound B3-1 (Estimation Quality: blue = good, magenta = medium, red = rough).

This was a close match to the peak seen at δ 8.46 in the ^{1}H NMR of B3-1. The substitution at position 5 (labeled as R in the proposed structure). The estimated chemical shift of hydroxyl groups were shown roughly at δ 2, which could not be observed in the original NMR data, since the spectrum was run in D_2O, deuterium could exchange for the hydrogen in hydroxyl groups. The proposed structure for compound B3-1 was a glycoalkaloid as shown in Figure 2.38. Glycoalkaloids have not been previously reported from the genus *Erigeron*. They are usually toxic and act like neural toxins to humans (Cantwell, 1996). To confirm the hypothesized deduction, the compound could be run on TLC and sprayed with Dragendorff's reagent. Dragendorff's reagent detects the presence of alkaloids giving an orange to red colour, therefore an orange or red band should be observed.

2.6.4.2 Compound B3-7 and B3-8

Fraction B3-7 and B3-8 were brown pastes 0.5 mg and 0.3 mg were isolated from the HPLC fractionation respectively.

The post-processing ^{1}H NMR is shown below in Figure 2.40. The doublet at δ 3.36 was integrated as 1 proton, and the compound contained at least six aromatic protons: two doublets at δ 6.36, δ 7.63 and two doublets at δ 6.94, δ7.58. Two triplets from δ 5.43 to δ 5.56 might be caused by the protons on the double bond. As the peaks below δ 4.00 might be caused by the methylene groups or methoxyl groups. More sample was needed for further structure elucidation.
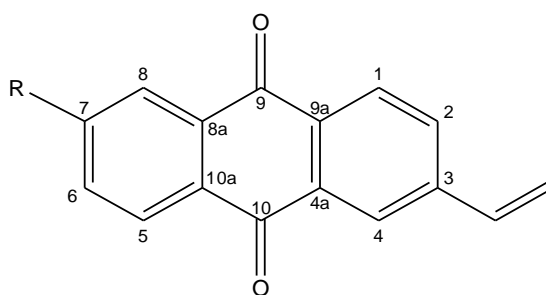
A. Proposed structure for compound B3-7.
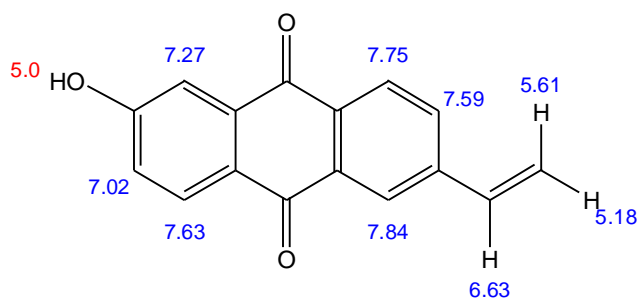
B. Estimated ^{1}H NMR chemical shift of compound B3-7.

Figure 2.39.Proposed structure and estimated ^{1}H NMR chemical shift of compound B3-7.

The proposed structure of B3-7 is shown in Figure 2.39 as an anthraquinones (9,10-Anthraquinone), which could explain why there were two split singlets at δ 6.94 and δ 7.58. The peak at δ 7.58 could be affected by an electron withdrawing group (R in the proposed structure) attached to the aromatic ring. ^{1}H NMR of the structure was estimated by the program ChemDraw®, the estimated chemical shifts are shown in Figure 2.39 **B.** and data is compared in Table 2.9.
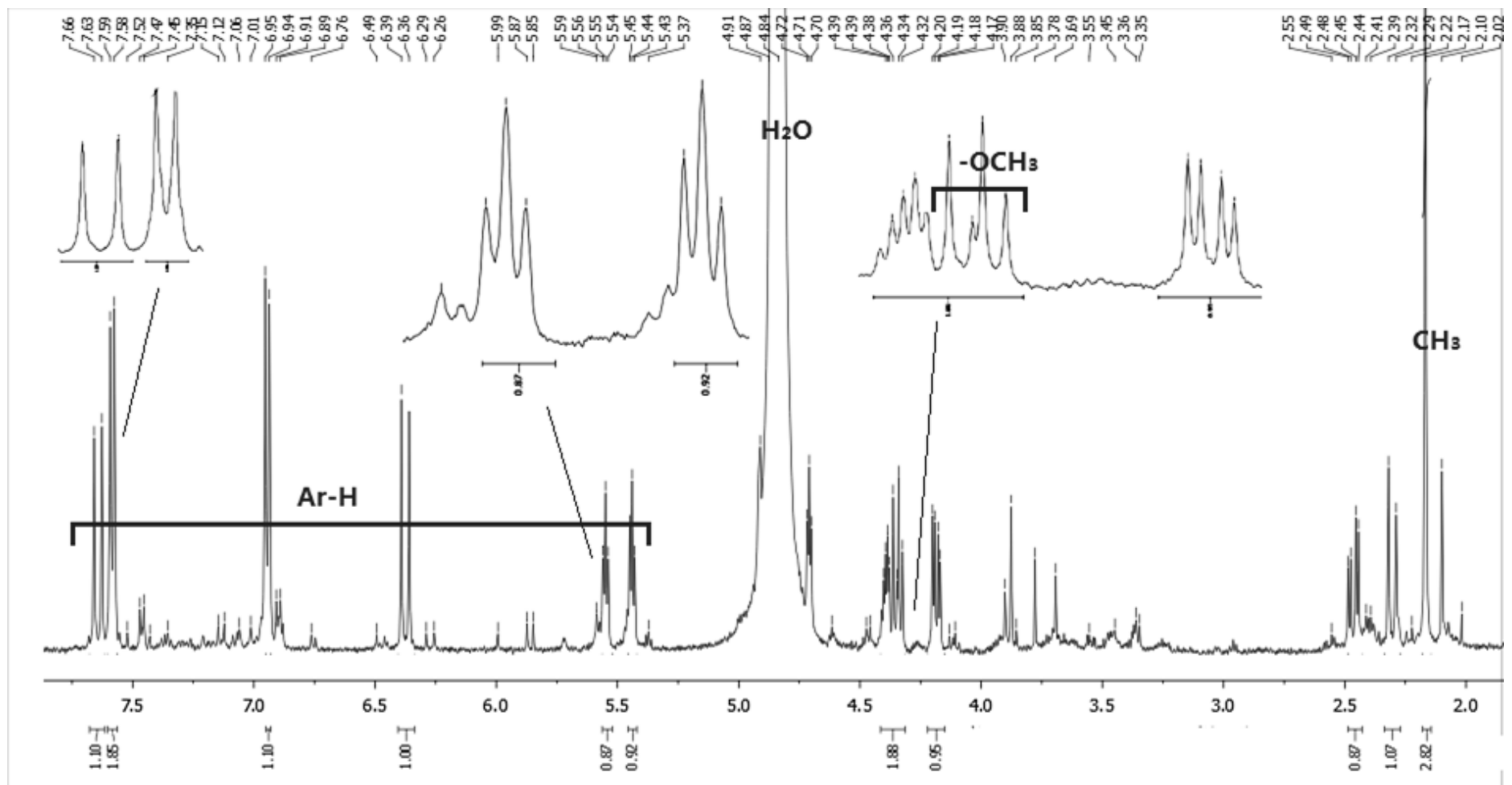
Figure 2.40 Post-processing water peak suppression ^{1}H NMR spectrum of compound B3-7.

Table 2.9 Estimation chemical shifts and chemical shifts of compound B3-7.

No.	^{1}H NMR chemical shift (ppm)	Estimated value (ppm)
1	7.59	7.75
2	7.58	7.59
4	7.66	7.84
5	7.63	7.63
6	6.36-6.39	7.02
8	6.94-6.95	7.27

Fraction B3-8 was also suggested to be a quinone derivative after comparing the ^{1}H NMR spectra with compound B3-7. However, due to the limited amount of sample collected, the NMR spectra for B3-8 was not very clear, only few peaks could be assigned. More samples were request for further structure elucidation. The proposed structure of B3-7 was a close match to anthraquinone ring. Six aromatic proton peak from δ 7.02 to 7.87 were matched the peaks from δ 6.36 to 7.63 in the ^{1}H NMR spectrum of B3-7, and also matched the double bond attached to the ring structure.

Anthraquinone was abundant in *Polygonaceae* plants, like genus *Reynoutria Houtt.* and *Rheum* (Babu, et al., 2003.), and it was also found in some of the genus in Compositae family, such as genus *Gynura* (Seow et al, 2013), and *Gnaphalium* (Zheng et al, 2013), for example, emodin and physcioin were isolated and elucidated from *Gnaphalium affine* D. Don, they had been proved to have anti-inflammatory activity (Xi et al, 2011). However, no reports have been published for discovery the anthraquinones from genus *Erigeron* yet.

2.6.4.3 Compound B3-9

Fraction B3-9 was a brown paste, 0.8 mg B3-9 was isolated. The proposed structure of B3-9 is shown in Figure 2.42 **A** as a benzopyrone based analogue. The structure was estimated by the program ChemDraw®.

The ^{1}H NMR of B3-9 is shown in Figure 2.41. Four aromatic protons were identified from δ 5.48 to 7.07. Singlet at δ 5.48 was assigned to the proton on the pyrone ring H3. The double doublet at δ 6.38-6.49 was assigned to H8 on the benzene ring, it was adjacent to another aromatic proton, and spit into a doublet and due to the effect of the adjacent oxygen atom, the peak was split into double doublet.
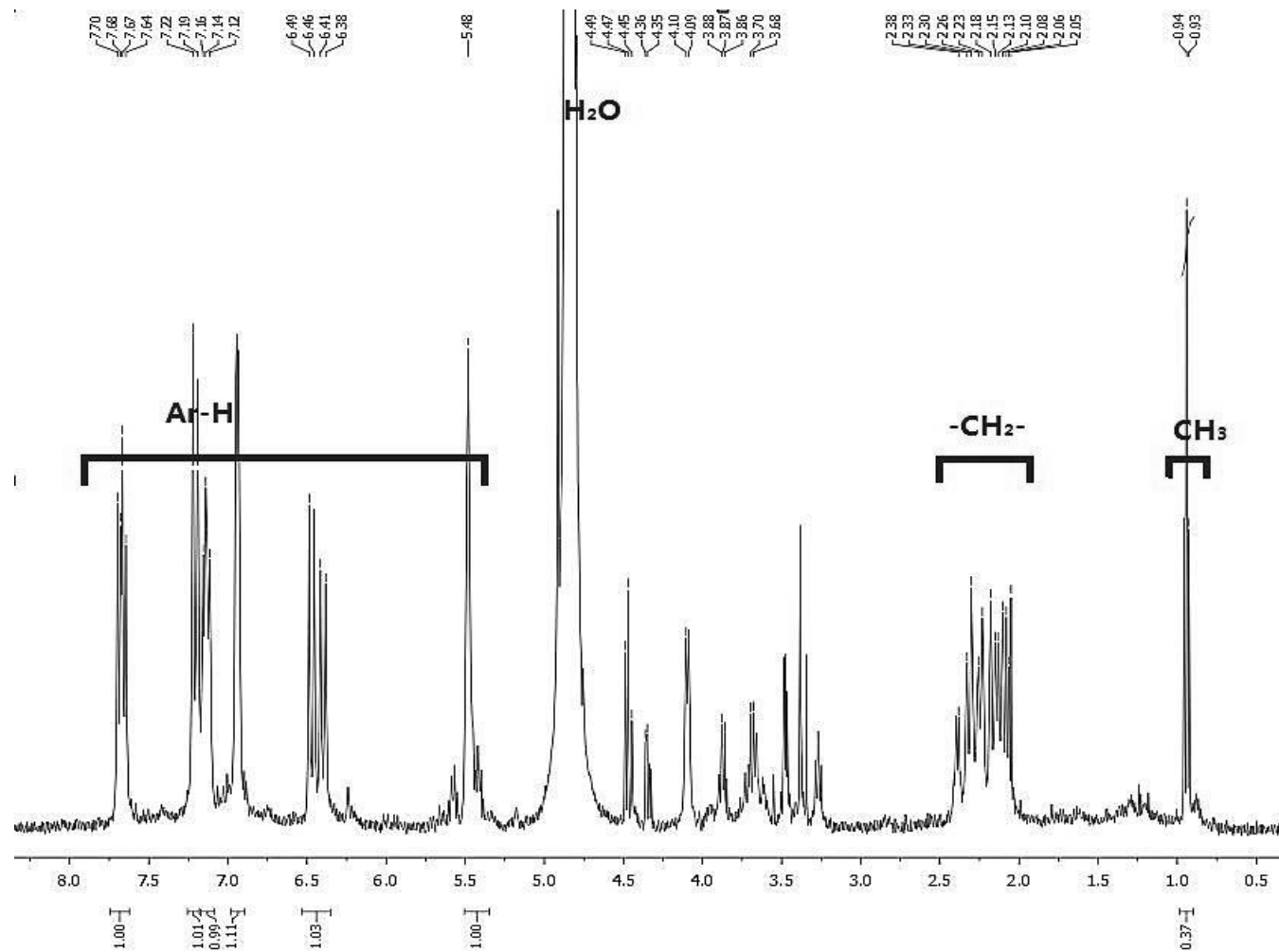
Figure 2.41 ^{1}H NMR spectrum of compound B3-9.

Two triplets at δ 7.12-7.14 were assigned for aromatic protons, chemical shift for H7 and H6 and the H5 were observed from δ 7.19-7.22. One terminal methyl peak was observed at δ 0.93, and there were massive multiplets between δ 2 and 4.5 indicated that the 2 position substitution might be an alkyl side chain.
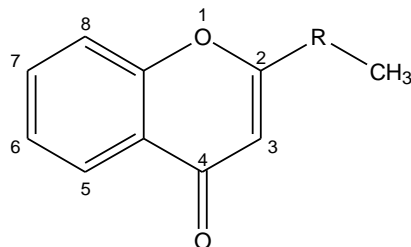
A. Proposed structure of compound B3-9.
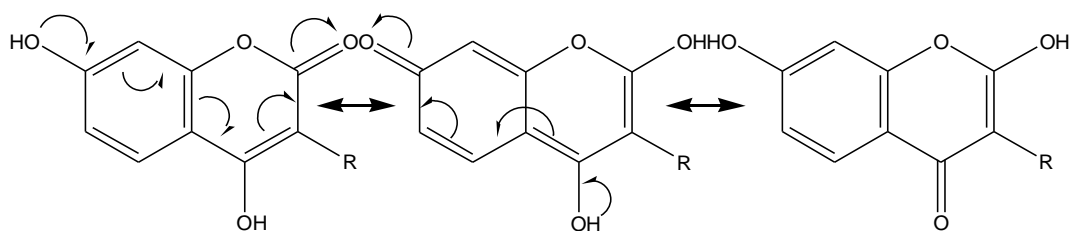
B. C$_4$-OH coumarin isomer.
Figure 2.42 Proposed structures of compound B3-9 and coumarin tautomerism.

B3-9 could also be an isomer of C$_4$-OH coumarin. According to the previous studies of the tautomers, if a hydroxyl group is substituted at position 7 in a C$_4$-OH coumarin, the coumarin undergoes a tautomerism (Figure 2.41 **B**): the proton dissociates from the hydroxyl group and the phenoxide anion conjugates with the benzene ring forming 2, 7 -diyhdroxy chromone. This tautomerism is acid or base catalyzed, affected by solvent, pH value, and temperature (Porter and Trager, 1982, Alok et al., 2004).

2.7 Conclusion

Chemical compositions of hexane and butanol extracts from *E. annuus* were investigated. Sixteen compounds were identified from the volatile hexane fraction H1-1 using GC-MS method. The structures of isolated compounds were elucidated using MS and NMR spectroscopy. Five compounds were fully elucidated including gondoic acid (H5-1-2); hexadecanoic acid (H5-2); α-spinasterol (H4); erythrodiol (H7) and 4-pent-3'-ne-1'-ynyl–pyran-2-one (H1-2-7). The structures of the rest of the isolated compounds were not fully elucidated because the small amount of the samples isolated was not enough for further analytical analysis.

3. *Chapter III: Antibacterial activities of Erigeron annuus*

3.1 Introduction

Microorganisms can produce many products including food supplements, organic acids, functional proteins and antibiotics. The antibiotics in clinical use which are derived from nature are all produced by bacteria and fungi; rather than being plant derived (Perry et al., 2002c). Many plants contain antimicrobial compounds and are widely used in traditional medicines around the world to fight infections (Srivastava et al, 2014).

The increasing trend of drug-resistant pathogens has demonstrated that new antimicrobial agents with new motifs are urgently needed. Plants contain a wide variety of secondary metabolites which have therapeutic values and could provide new aspects for investigation. Plant antimicrobial agents include flavonoids, alkaloids, terpenes, coumarins, phenolics and polyphenols (Savoia, 2012). An example is terpinen-4-ol, a monoterpene from *Melaleuca alternifolia* which is the main active ingredient of tea tree oil. This compound has modulation effects when applied with antibiotics against the resistant bacterial strains (Hammer et al, 2012); Another example, berberine, an isoquinoline alkaloid from the genus *Berberis,* is used as broad spectrum antimicrobial in traditional medicine in China. Berberine showed synergism with conventional antibiotics including oxacillin and ampicillin. It is also used as a substrate in studies on resistance-modifying agents and in the detection of efflux pump inhibitors (Abreu et al, 2011). The potential uses of phytochemicals as antimicrobial agents should be further evaluated.
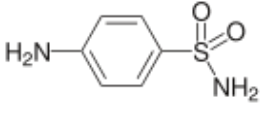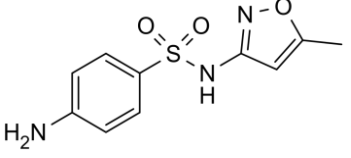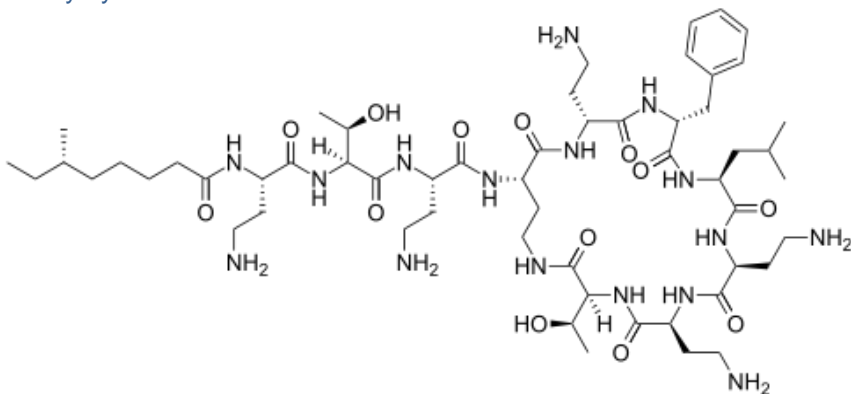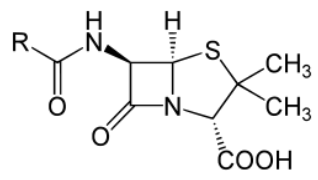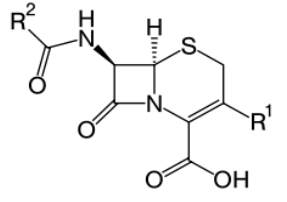
3.1.1 Antibiotics

In the modern history of pharmacy, antimicrobial (anti-infective) agents were first described in the 19th century (Cassell, 2001), as a variety of chemicals that had been proved to have therapeutic functions (Saga and Yamaguchi, 2009), and defined as antibiotics by Selman Waksman in 1941 (Waksman, 1941, Waksman, 1943, Waksman, 1947)The first known natural antibiotic was beta-lactam antibiotic penicillin, discovered from *Penicillium notatum* by Alexander Fleming (Fleming, 1929), who shared a Nobel Prize in 1945 for these pioneering contributions to his field (Fleming, 1945). The first synthetic antibiotics were a series of compounds called sulfonamides, discovered by Gerhard Domagk in 1932; he received his Nobel Prize in 1939 (Domagk, 1895). Sulfonamide antibiotics have a broad antimicrobial spectrum, and they competitively inhibit the growth and multiplication of bacteria by inhibiting the

dihydropteroate synthetase activity in the folate synthesis pathway (Cohen and Cluff, 1961, Domagk, 1950).

Antibiotics are either bacteriostatic or bactericidal. They are generally well-characterized and target the microbes in many aspects, including interfering with the folate pathway, inhibiting bacterial membrane function, inhibiting the cell wall, protein, and nucleic acid synthesis (Cuddy, 1997, Kohanski et al., 2010). Some well-known antibiotics and their modes of action are listed in Table 3.1.

Table 3.1 Modes of action and structures of antibiotics.

Mode of action	Classification of antibiotics*	Characteristic Structure of examples	
Inhibition of folate metabolism	Sulphonamides (Henry, 1943)	Sulfanilamide	Sulfamethoxazole
Inhibition of membrane function	Polymyxins (Aronson et al., 2006b)	Polymyxin B	
Inhibition of cell wall synthesis (peptidoglycan synthesis)	B-lactam antibiotic (Lee et al., 2001)	Penicillins	Cephalosporins

Glycopeptides   Vancomycin (Newsom, 1982)
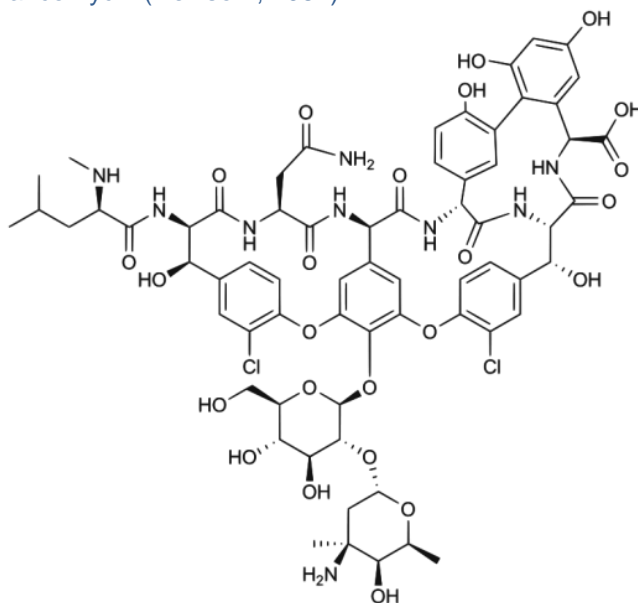
| **Inhibition of protein synthesis** | Aminoglycosides (binding to 30S ribosomal subunit)(Phillips, 1982) | |
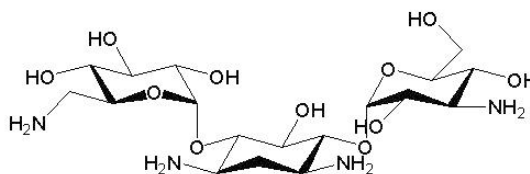
Macrolides (binding to 50S ribosomal subunit)(Blondeau, 2002)

Erythromycin
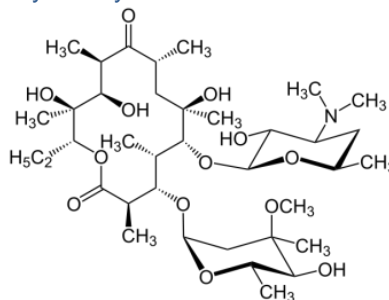
Clarithromycin
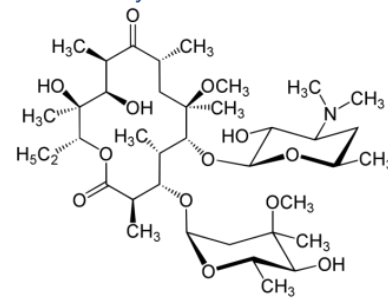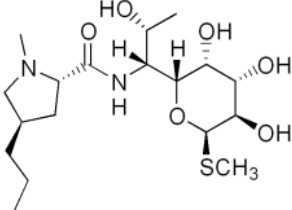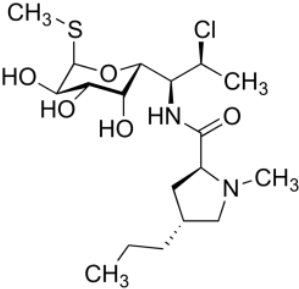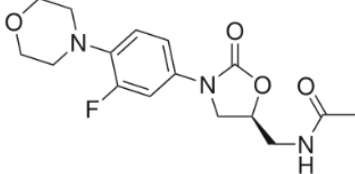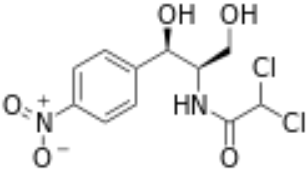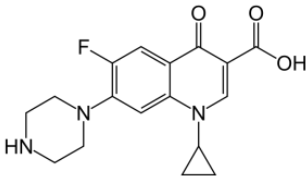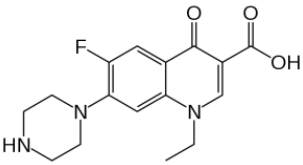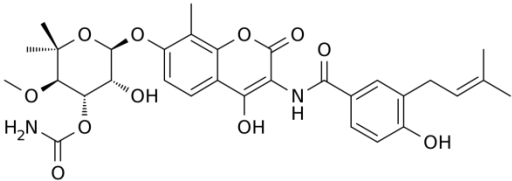
Tetracyclines (binding to 30S ribosomal subunit)(Nelson and Levy, 2011)

Tetracycline

Doxycycline

Lincosamides (binding to 50S ribosomal subunit)(Aronson et al., 2006a)	Lincomycin	Clindamycin
Oxazolidinone (binding to 50S ribosomal subunit)(Diekema and Jones, 2001)	Linezolid	
Phenicols (binding to 50S ribosomal subunit)	Chloramphenicol (Weeks, 1980)	
Inhibition of DNA replication (topoisomerase inhibitors)	Quinolones (Neu, 1988) Ciprofloxacin	Norfloxacin
	Aminocoumarins (Anderle et al., 2008) Novbiocin	

*: The categories of well-known antibiotics and their mode of actions had published (Torrence and Isaacson, 2003, Walsh, 2000).

In addition, some small antibiotic families have their own mode of action. For example, the ansamycin family, including streptovaricins and rifamycins, are particularly effective against mycobacteria and can interact with the bacterial DNA-dependent

RNA polymerase (Milavetz and Carter, 1977, Wehrli et al., 1968).

3.1.2 Bacterial structures

Bacteria are prokaryotic organisms. According to the different compositions of cell walls (Betsy and Keogh, 2005), they can be classified into Gram-positive bacteria and Gram-negative bacteria using the Gram staining test (Friedman et al., 1995). As the bacterial cell wall is outside the cytoplasmic membrane (blue plasma membrane, Figure 3.1), it provides protection to the cells against osmotic stress and invasions from the antibiotics. It also provides rigidity and shape to the cells. The cytoplasmic membrane and the cell wall are usually described together as the cell envelope, and most of bacteria have a polysaccharide layer outside the cell envelope called the capsule (Kasper, 1986). Different cell wall compositions between Gram-positive and Gram-negative bacteria are compared in Figure 3.1.
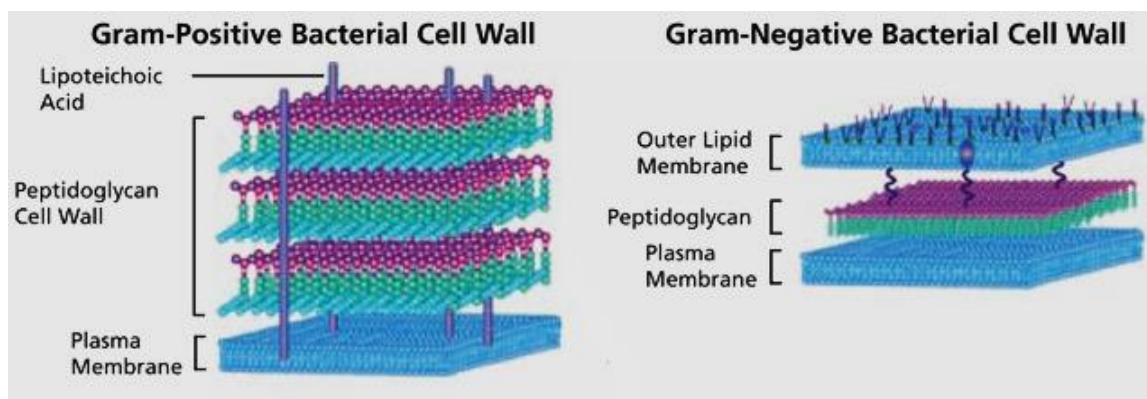
Figure 3.1 Gram-positive and Gram-negative bacterial cell walls. Gram-positive bacterial cell wall (left) consist of thick peptidoglycan layers; Gram-negative bacteria cell wall (right) consist of an outer lipid membrane and a thin peptidoglycan layer (Sligma-Aldrich, 2014).

Gram-positive bacteria cell walls are thicker than the Gram negative cell walls, as the main component of the cell wall is peptidoglycan, which takes about 40%-80% of the cell wall's dry weight, depending on different species. The rest of the cell wall components are teichoic acids, teichuronic acids and lipopolysaccharides (Stewart Tull, 1980). The Gram-positive call wall contains several layers of peptidoglycan which consist of two types of amino sugars, N-acetylmuramic acid (NAM) and N-acetylglucosamine (NAG) (Perry et al., 2002b). They link to each other by β-1,4 glycosidic bonds, which are the cleavage site for lysozyme. N-acetylmuramic acid

links to peptide at the carboxyl group of the D-lactic acid residue (Figure 3.2, orange bonds); the peptide links to a pentaglycine bridge through a diamino acid (L-lycine, in Figure 3.2). The pentaglycine can join two peptides together from glycan chain a and chain b (blue structures in Figure 3.2) to form an amino sugar backbone. This pentaglycine cross-link bridge can be used to distinguish the Gram-positive from Gram-negative peptidoglycan, which the glycan chain a and chain b link together directly without a pentaglycine cross-link bridge in Gram-negative cells(Schleifer and Kandler, 1972).
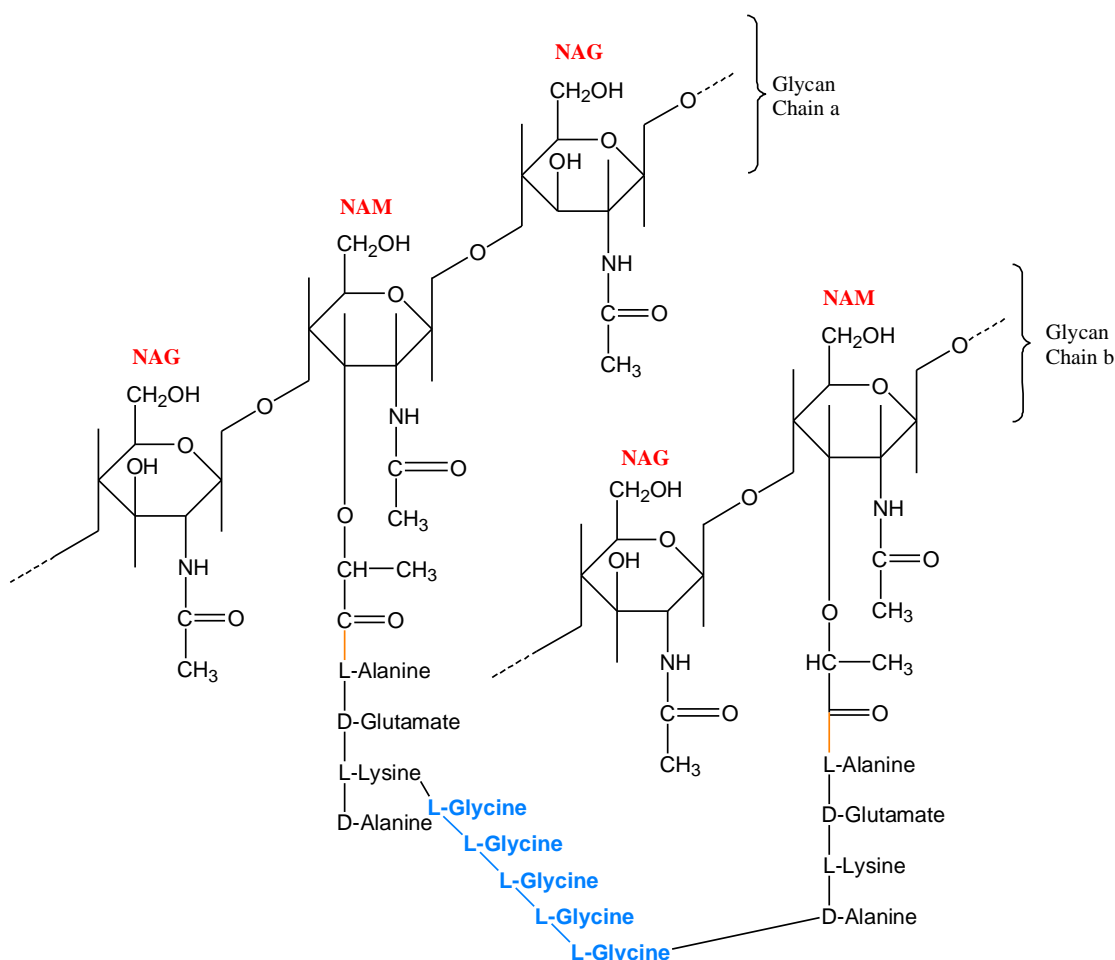
Figure 3.2 Peptidoglycan of Gram-positive bacterial cell wall. N-acetylmuramic acid (NAM) and N-acetylglucosamine (NAG); Pentaglycine of glycine is shown in blue.

The Gram-negative bacterial cell wall is more complicated than the Gram-positive cell wall. It has an outer membrane which is similar to the cytoplasmic membrane but contains fewer proteins. Lipopolysaccharides (LPS) are covalently attached to the outer membrane on the surface, which consists of a lipid A (red in Figure 3.3) and a polysaccharide (green in Figure 3.3). Polysaccharides are often used to distinguish

different classes of Gram-negative bacteria. The LPS is also known as endotoxin; it can induce an inflammatory response when released from the cell wall (Silverman and Ostro, 1999).

The outer membrane contains proteins called porins, which are selective and permeable transport proteins that can facilitate the influx of antibiotics or nutrients (Nikaido and Vaara, 1985). For example, the trimeric porin OmpF of *Escherichia coli* is a well-studied, non-specific transport channel that allows low molecular weight solutes passage across the outer membrane (Mahendran et al., 2010, Agafitei et al., 2010). There is another type of low molecular weight lipidpolypeptides, called Peptidoglycan-associated lipoprotein (Pal), which exists on the outer membrane towards the peptidoglycan layer (purple in Figure 3.3). The N-terminal end of the lipoprotein is a hydrophobic fatty acid chain, anchoring the protein down to the membrane. The C-terminal region attaches to the peptidoglycan covalently at the biamino acid (Lazzaroni and Portalier, 1992).
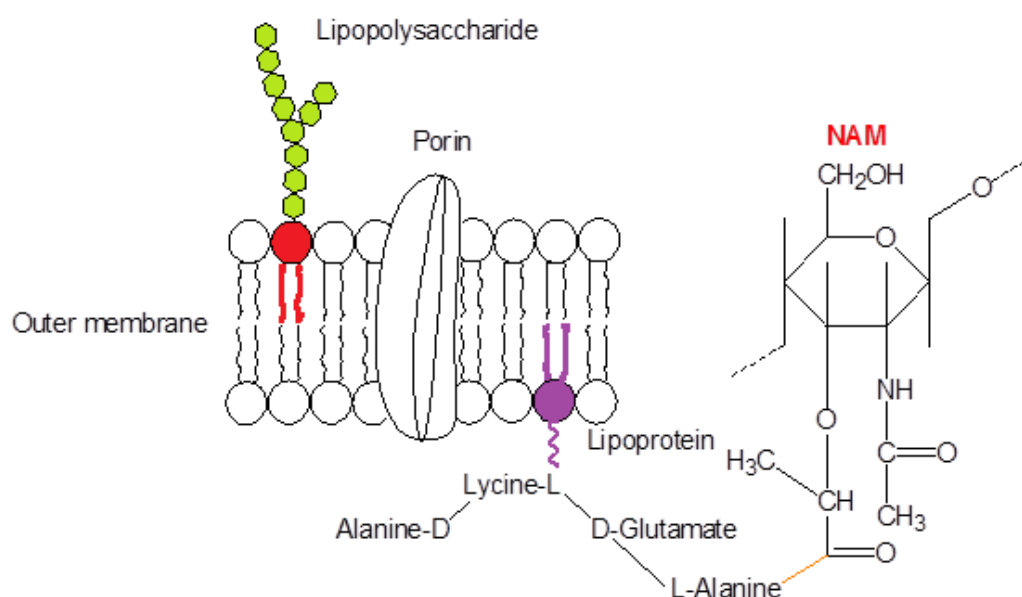
Figure 3.3 Outer membrane of Gram-negative bacteria covalently bonds to peptidoglycan through Pal.

The space between the cytomembrane and outer membrane in the Gram-negative bacteria envelope is called the periplasmic space: it contains variety of enzymes, proteins and a thin peptidoglycan layer (Bowden, 1990). The peptidoglycan consists

of only 5% of the cell wall's dry weight and it attaches to many lipoproteins from the outer membrane. The breakdown of antibiotics are located in periplasmic space (Anba et al., 1988), for example, protease III is an Mg^{2+}-dependent endopeptidase of *Escherichia coli* (Cheng, 1979*)* it can cleavage a small amount of polypeptides which are involved in bacterial metabolism (Kemshead and Kemshead, 1976).

3.1.3 Bacterial pathogens

Pathogenic bacteria can be classified into three categories: obligate, accidental and opportunistic pathogens (Perry et al., 2002a). Obligate pathogens live only inside the host cells. During the transmission to new host cells, they can be attacked by the host's immune system and cause symptoms of disease, such as *Mycobacterium tuberculosis* species (Comas et al., 2010). The accidental pathogens exist wildly in nature and the survival of the pathogen is not dependent upon the host cells. It will only cause severe diseases if it accidentally enters the host, such as *Clostridium tetani* (Agrawal, 1995)*.* The opportunistic pathogens can be transmitted between the healthy cells without causing disease; however, if the host is unhealthy or the immune system is not functioning properly, the bacteria can cause an infection, such as the *Staphylococcus* species (Latorre et al., 1993).

The pathogenesis virulence factors are described as substances that are produced by pathogens to facilitate the adhesion, colonization and invasion of the host cells (Wilson et al., 2002). Pathogens can also produce toxins, including endotoxins and exotoxins. Exotoxins are proteins released from the live bacteria in certain species and endotoxins are a lipopolysaccharide complex (Figure 3.3) in Gram-negative bacteria cell walls, regardless of different species, and only released on lysis of the bacteria cells. The exotoxins are heat labile (60 °C- 80 °C) and immunogenic sensitive, while the endotoxins are heat stable (>250 °C), endotoxins also can cause weakly immunogenic respond and caused a fever in the host (Baron, 1996).

3.1.4 Antibiotic-resistance and antibiotic-resistance strains

One consequence of the development of antimicrobial agents since the 1930s is the increasing threat antibiotic-resistance poses to public health

(CentersforDiseaseControlandPrevention, 2014). Sulfonamides-resistance, the first known antibiotic-resistance, was discovered in the 1950s when several *Escherichia coli* resistant mutants were isolated and the modes of action resistance were studied (Pato and Brown, 1963). The resistant mechanisms of commonly used antibiotics are listed below in Table 3.2.

Table 3.2 Resistant mechanisms of commonly used antibiotics (Adapted from Davies's publication, Davies, 2010).

Antibiotic family	Effect on bacteria	Targets	Resistance mechanisms
Sulfonamides	Bacteriostatic	Folate metabolism	Efflux, modify target
β-lactam antibiotics	Bactericidal	Peptidoglycan biosynthesis	Hydrolysis, efflux, modify target
Glycopeptides	Bacteriostatic	Peptidoglycan biosynthesis	Reprogramming peptidoglycan biosynthesis
Aminoglycosides	Bactericidal	Protein synthesis	Phosphorylation, acetylation, nucleotidylation, efflux, modify target
Macrolides	Bacteriostatic	Protein synthesis	Hydrolysis, glycosylation, phosphorylation, efflux, modify target
Tetracyclines	Bacteriostatic	Protein synthesis	Monooxygenation, efflux, modify target
Lincosamides	Bactericidal	Protein synthesis	Nucleotidylation, efflux, modify target
Phenicols	Bacteriostatic	Protein synthesis	Acetylation, efflux, modify target
Quinolones	Bactericidal	DNA replication	Acetylation, efflux, modify target
Rifamycins	Bactericidal	Protein synthesis	ADP-ribosylation, efflux, modify target
Oxazolidinones	Bacteriostatic	Protein synthesis	Efflux, modify target
Pyrimidines	Bactericidal	Folate metabolism	Acetylation, efflux, modify target

General resistance mechanisms of the commonly used antibiotics include: enzyme

inactivation; target alteration (modification of the target site or overproduction of the target); decreasing cell permeability; and efflux (Davies and Davies, 2010). For example, the β-lactam resistant strains share the same resistant mode of action by inactivating or reducing the antibiotic activity, breaking the β-lactam ring, causing the modification of the PBPs and the efflux of the antibiotic molecule (Sun et al., 2014).

The first bacterial enzyme discovered with the ability to destroy β-lactam antibiotics is β-lactamase, produced by the *amp* gene (Abraham and Chain, 1940). Production of β-lactamase is the most important and most common resistance found in both Gram-positive and Gram-negative bacteria (Jacoby, 2009). It can hydrolyze the β-lactam ring and deactivate the antibiotic molecule (Lee et al., 2001). In some Gram-negative resistant strains, β-lactam antibiotics were also found to be bonded by β-lactamase, and the complex was trapped in the periplasmic space (Antunes et al., 2011).

Another important drug resistant mechanism is to modify the bacterial enzymes. For example, beta-lactam antibiotic is a well characterized antibiotic family that can bind and deactivate the penicillin-binding proteins (PBPs), which are a group of enzymes responsible for the polymerization of peptidoglycan in both Gram-positive and negative bacterial cells (Bush, 1995). These proteins function as transpeptidases, carboxypeptidases and transglycosylases. Transpeptidase (green in Figure 3.4) can catalyze the final transpeptidation step in peptidoglycan synthesis (Georgopapadakou, 1982). The β-lactam antibiotics can mimic the NAM D-Ala-D-Ala terminal (C-terminal) peptide residue and bind to the transpeptidase covalently at transpeptidase residue Ser_{403} (Figure 3.4). The β-lactam-PBP adduct is stable, and the enzyme is deactivated. In that case, the cross-link of the NAM and pentaglycine bridge (Gram-positive bacteria) or peptide residue on another NAM (Gram-negative bacteria) will not form. Deactivation of the transpeptidase leads to the termination of peptidoglycan synthesis, and eventually the death of the bacteria cell (Otero et al., 2013).
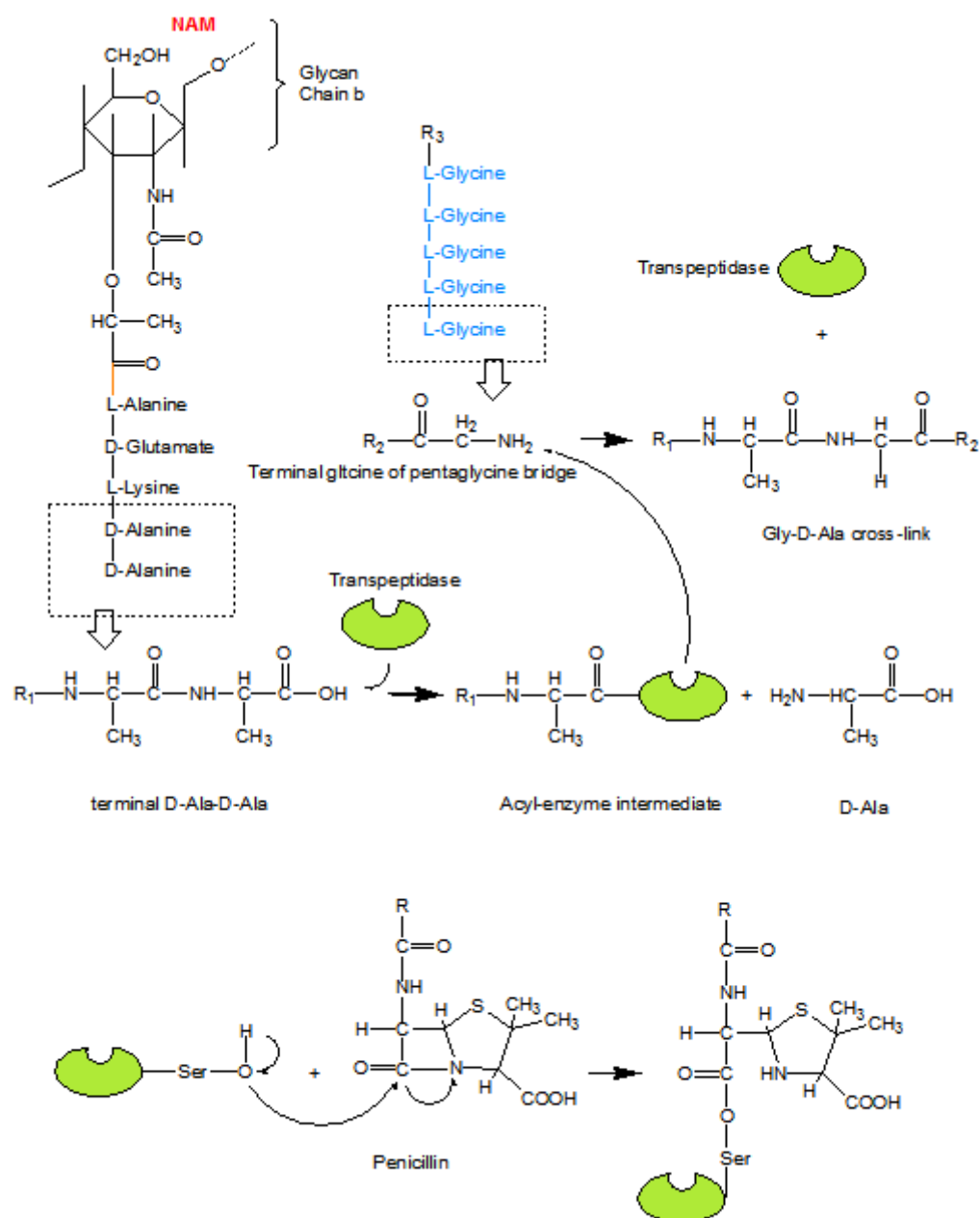
Figure 3.4 Transpeptidase function in Gram-positive bacteria and the acylation of serine by penicillin antibiotics, adapted from Lee's publication (Lee, 2003).

Some organisms also can efflux the antibiotic molecules from the periplasmic space back through the cell wall. The efflux pumps have been classified into five families, including: ATP-binding cassette (ABC) superfamily; the major facilitator superfamily (MFS); resistance-nodulation division (RND) superfamily; the small multidrug resistance (SMR) family; and the multidrug and toxic compound extrusion (MATE) family. ABC efflux pumps are ATP-dependent multidrug transporters with the ability to export a broad spectrum of compounds (Lubelski, 2007). MFS pumps are single-polypeptide transporters and only transport small solutes. This can be

regulated by chemiosmotic ion gradient (Pao, 1998). RND efflux pumps act as drug anti-porters and they are wildly present in Gram-negative bacteria (Nikaido and Nikaido, 2009). SMR efflux pumps are homodimer proteins, such as EmrE, found in *E.coli*. They only efflux the compounds into the periplasmic space, and then the compounds can be picked up by RND pumps (Jack et al., 2001). MATE efflux pumps are narrow spectrum transporters and they export multiple cationic-toxic compounds (eg. fluoroquinolones) (Kuroda, 2009).

Table 3.3 Skeleton of different β-lactam antibiotics*.

Penicillin

Cephalosporin

Carbapenem

Monobactam
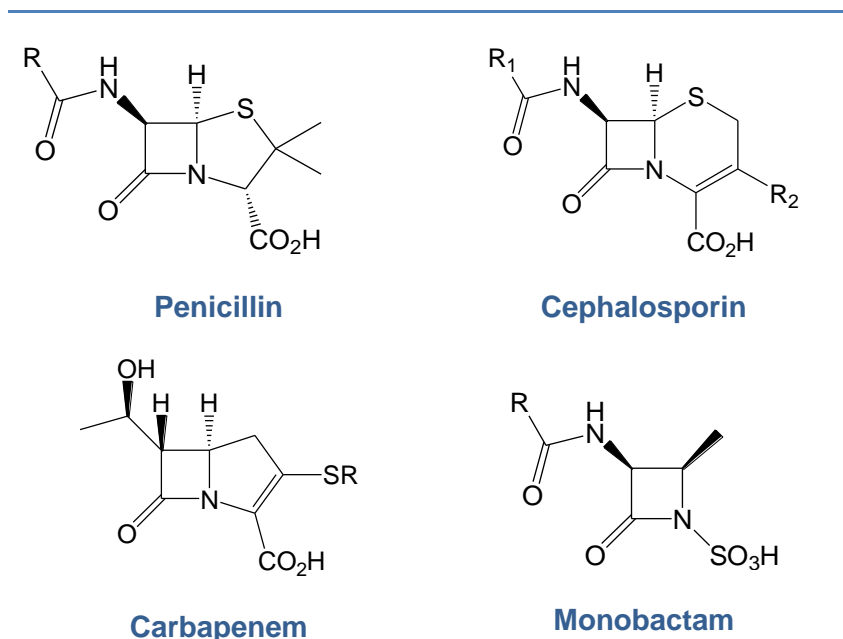
*: Structures of the different β-lactam antibiotic classes (Worthington and Worthington, 2013).

Methicillin-Resistant *Staphylococcus aureus* (MRSA) strains are those *S.aureus* strains that have developed β-lactam antibiotic resistance. Those β-lactam antibiotics (Table 3.3) include penicillins (methicillin, oxacillin), cephalosporins (cefepime, ceftaroline), carbapenems (imipenem, meropenem) and monobactams (tigemonam, nocardicin A) (Evans et al., 2014). The resistant strains carry a *mecA* gene, transferred by *Staphylococcal* cassette chromosome *mec* (*SCCmec*) chromosome. The *mecA* gene encodes protein PBP2a, which has three domains: transpeptidase domain, allosteric domain and an N-terminal extension residue. According to Otero's research, when the transpeptidase domain and allosteric domain are occupied in PBP2a, a series of conformation changes would take place and allow the muramic acid saccharide to enter inside. Therefore the cross-link of peptidoglycan could still proceed (Oteroa et al., 2013, Leski, 2005, Fuda et al., 2005).

Two types of MRSA: health care-associated MRSA (HA-MRSA) and the community-associated MRSA (CA-MRSA). The HA-MRSA causes infections among patients who have contacts with hospitals or healthcare facilities, such as surgery and hospitalization; while CA-MRSA infections are most frequently spread through direct skin contacts (Benoit et al., 2008, Huang, 2006). Many tests are used for the detection of MRSA infection: traditional disk diffusion and screening, *mecA* PCR-based amplification (Araj et al., 1999) and colorimetric cycling probe technology (Bekkaoui et al., 1999). However, HAMRSA infection is often found in less healthy patients, and those patients who have open wounds are more susceptible to MRSA infection {Kallen, 2010 #4112}. Often, MRSA strains exhibit multidrug resistant profiles, such as kanamycin and erythromycin resistance (Bobba et al., 2011). The appearance of multi-drug resistant (MDR) strains could be the consequence of regular exposure to different types of antibiotics (Alekshun and Alekshun, 2007). Nonetheless, there is promising news that Dalvance™ (dalbavancin) was approved by the US Food and Drug Administration earlier this year to treat acute bacterial skin infections against susceptible gram-positive bacteria including MRSA (Fox, 2014). Dalbavancin is a mixture of semisynthetic lipoglycopeptides derived from vancomycin (Figure 3.1), it interferes with cell wall synthesis by binding to the D-Ala-D-Ala peptide, and preventing cross-link of peptidoglycan in the Gram-positive bacterial cell wall (DurataTherapeutics, 2014).

3.2. Minimum inhibitory concentration (MIC) assay

3.2.1 Material and Strains

Nutrient agar, nutrient broth, Ringer's solution tablets and Müller- Hinton broth (MHB) were purchased from Oxiod microbiology, Thermo Fisher scientific, Loughborough, UK. Thiazolyl blue tetrazolium bromide (3-[4,5-dimethylthiazol-2-yl] -2,5-diphenyltetrazoliium bromide, MTT), tetracycline, oxacillin, ciprofloxacin, norfloxacin, erythromycin, novobiocin and dextrose were purchased from Sigma-Aldrich® Dorset, UK. Ninety-six well microtitre plates were purchased from NunIcon™ brand, Sigma-Aldrich®.

Gram-negative strains *Escherichia coli* (*E.coli*) NCIMB 1119 and *Salmonella enterica* (*S.enterica*) ATCC 14579/4601217, Gram-positive strains *Micrococcus luteus* (*M. luteus*) ATCC 49732/4604080, *Enterococcus faecalis* (*E.faecalis*) ATCC

29212/4807030 were obtained from Culti-Loops®, Remel, Lenexa, USA. Gram-positive strains *Staphylococcus aureus* (wild type) ATCC 25923 (*S.aureus*) and Methicillin-Resistant *Staphylococcus aureus* ATCC 33591 (MRSA) were obtained from Oxoid, Culti-Loops®, Dartford, Kent, UK. The depositor of the MRSA strain ATCC 33591 was S. Schaefler: the multi-resistant MRSA strain was obtained from A. W. Jackson, Ramsey St. Paul Hospital, Saint Paul, USA (Schaefler, 1979).

3.2.2 Method

MRSA related antibacterial works were carried out in the biohazard Level 2 lab with a Level 3 cabinet. All equipment was sterilized with 70% industrial methylated spirit before and after use. Nutrient agar, cation-adjusted Müller- Hinton broth and saline solution were autoclaved using pasteurization at $121^{o}C$, 15 min.

Ninety-six well microtitre plates were used for the tests. The prepared concentration of test samples were 512, 256, 128, 64, 32, 16, 8, 4, 2, and 1 µg/mL in 3% DMSO. The turbidity of inoculum was compared with McFarland standard 1.0 ($1X10^8$ cfu/mL) and diluted with Müller- Hinton broth 8 times before inoculation. Tetracycline, oxacillin, ciprofloxacin, norfloxacin, erythromycin, novobiocin were dissolved in DMSO and diluted with MHB to the initial concentration used as positive controls. DMSO in Ringer's solution was used as negative control. All controls and test samples were diluted within the two hours before each test.

Strains were prepared from the freeze-dried culture loops. Overnight cultures of each strain were grown on nutrient agar plates. Colonies were transferred from the agar plates into 10 mL Ringer's solution with a sterilized loop. The turbidity of bacterial suspensions were compared with a McFarland standard 1.0 ($1X10^8$ cfu/mL). Bacterial suspension was further diluted with Ringer's solution to make the concentration around 5 x 10^5 cfu/mL.

During the assay, 125 µL of MHB was dispensed into wells 1-11 of each 96-well microtitre plates (Figure 3.5), followed by dispensing of 125 µL positive controls and test samples in well 1, the assay for each sample were carried out in duplicate. Two fold serial dilutions across the plate from well 1 to well 10 were made, while well 11 was omitted. The final volume from the two fold dilution was dispensed into row 12.

125 µL of bacterial inoculum were added into wells from row 1 to 11.   Row 11 was the bacterial growth control and row 12 was the sterile control (Figure 3.5). Entire preparation works and MIC tests were operated in a safety cabinet.
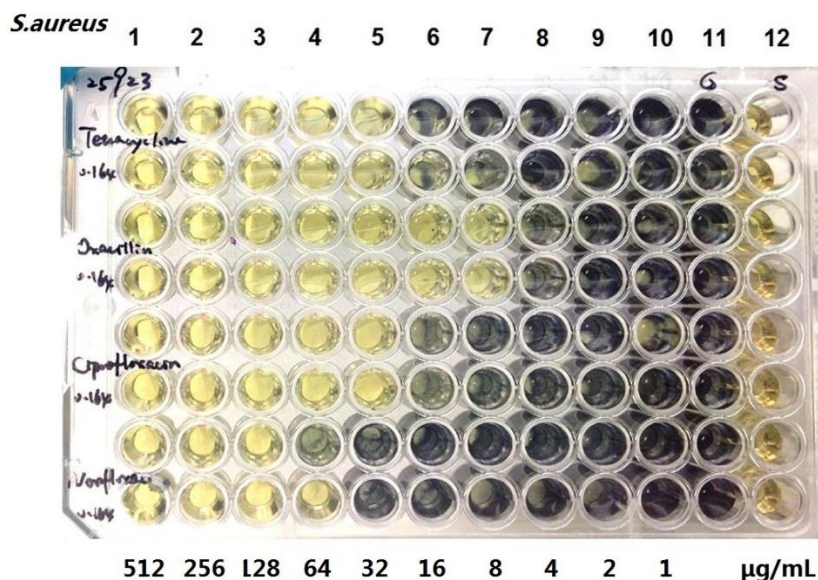
Figure 3.5 Ninety-six well microtitre plates in MIC assays.

All of the 96-well microtitre plates were incubated at 37 ^{o}C for 24 hours. After incubation, 20 µL of 5 mg/mL methanolic MTT solution was dispensed into every well of the test plates to give the bacterial growth result reading.

3.3 Results and Discussion

3.3.1 Screening of fractions against wild type strains

All MIC tests results were confirmed by duplicate experiments. For the wild type strains, tetracycline was used as positive control at the start concentration of 512 mg/mL; while for *S. aureus* tetracycline, oxacillin, erythromycin, ciprofloxacin, norfloxacin and novobiocin were used as positive control, concentrations were set at 5.12 mg/mL. The hexane extract (H) and its 18 hexane fractions (H1~3, H4~9, H5-1-9) were tested against five selected strains (Table 3.4). Fractions H1, H2, H3 and H4 showed some anti-bacterial activities against the Gram-negative strains. The best inhibitory concentration against *E. coli* was 128 µg/mL (H1, H2, H3, H4), while the best inhibitory concentrations against *S. enterica* strain was 128 µg/mL (H 1, H3, H4) as well. Candidates H1, H2, H3, H4, H5-1, H5-1 and H6 showed inhibitory activity on Gram-positive strains. *M. luteus* was sensitive to the test candidate H1-4, while the best MIC value was observed at 32 µg/mL.

Table 3.4 The MIC values of hexane fractions (µg/mL).

Strains	Test samples																	
	T	H1	H2	H3	H4	H6	H7	H8	H9	H5-1	H5-2	H5-3	H5-4	H5-5	H5-6	H5-7	H5-8	H5-9
E. coli	8	128	256	128	128	>512	>512	>512	>512	>512	>512	>512	>512	>512	>512	>512	>512	>512
S. enterica	32	128	>512	128	128	>512	>512	>512	>512	>512	>512	>512	>512	>512	>512	>512	>512	>512
M. luteus	2	32	256	64	64	>512	>512	>512	>512	>512	>512	>512	>512	>512	>512	>512	>512	>512
S .aureus	0.3	128	>512	128	256	256	>512	>512	>512	512	128	>512	>512	>512	>512	>512	>512	>512
E. faecalis	64	>512	256	256	>512	>512	>512	>512	>512	>512	>512	>512	>512	>512	>512	>512	>512	>512

T: Positive control, tetracycline.

Fractions H1, H3, H4, H6, H5-1 and H5-2 showed mild inhibitory activity against *S. aureus*; the wild type *S. aureus* is very sensitive to tetracycline; the MIC value for positive control was 0.3 µg/mL. Other fractions did not show any inhibition in the assay.

Apart from the fractions, some isolated compounds were tested in the antibacterial assays from the phytochemical research. However, most of them showed no activity against the selected strains. For example, many unsaturated fatty acids from the whole plant of *E. annuus* were identified, including myristic acid, oleic acid and linoleic acid. Meanwhile, one sterol, α-spinasterol, was isolated and tested against the selected strains and no antibacterial activities were found. Alpha-spinasterol belongs to Δ^7-sterol family and is known to have anti-inflammatory activities (Jeong et al., 2010). It is also a part of the plant cell components involved in plant metabolism.

Fraction H1 and H4 were separated, fraction H4-2-1 showed MIC at 16 μg/mL and 32 μg/mL against wild type *S.aureus* and MRSA respectively; and fraction H4-2-3 showed MIC at 32 μg/mL against both strains. However, full structure elucidations were not obtained from the phytochemical study.

The ethyl acetate crude extract was fractionated into 12 fractions. E1 was the most active fraction, demonstrating inhibitory activities at the concentration of 128 μg/mL against Gram-negative strain *E.coli,* and Gram-positive strain *S. aureus* (Table 3.5). The MIC value for E1 on *M. luteus* and *E. faecalis* was 256 μg/mL. Fraction E2, E5, E7 and E8 showed mild inhibitory activity against *M. luteus* and fraction E2 also showed some inhibitory activity against *E. faecalis*. Other test samples did not show any obvious activity during the tests.

Table 3.5 The MIC values of ethyl acetate fractions (µg/mL).

Strains	Test samples												
	T	E1	E2	E3	E4	E5	E6	E7	E8	E9	E10	E11	E12
E. coli	8	**128**	>512	>512	>512	>512	>512	>512	>512	>512	>512	>512	>512
S. enterica	32	>512	>512	>512	>512	>512	>512	>512	>512	>512	>512	>512	>512
M. luteus	2	**256**	**256**	>512	>512	**256**	>512	**256**	**256**	>512	>512	>512	>512
S. aureus	0.3	**128**	>512	>512	>512	>512	>512	>512	>512	>512	>512	>512	>512
E. faecalis	64	**256**	**256**	>512	>512	>512	>512	>512	>512	>512	>512	>512	>512

Through the antibacterial tests screening, active fractions were identified from hexane and ethyl acetate extracts: fractions H1-4 and E1 were active on both Gram-positive and Gram-negative strains. MIC results of wild type *S. aureus* fractions were used as comparison when testing the resistance profile of the selected MRSA strain. Fractions H1, H2, H3 and H4 were chosen to carry out further separations.

The MIC value of butanol fractions are listed in Table 3.6. Compared to the hexane and ethyl acetate extracts, butanol fractions had only mild inhibitory activity against the selected strains, except for fraction B1, which had a MIC value of 128 μg/mL against *M. luteus*. Fractions B1, B5, B6, B10 showed mild inhibitory activity against Gram-negative strains at the concentration of 256 μg/mL.

Table 3.6 The MIC values of butanol fractions (μg/mL).

Strains	Test samples										
	T	B1	B2	B3	B4	B5	B6	B7	B8	B9	B10
E. coli	8	**256**	>512	>512	>512	**256**	**256**	>512	>512	>512	**256**
S. enterica	32	>512	>512	>512	>512	>512	>512	>512	>512	>512	>512
M. luteus	2	**128**	>512	>512	>512	**128**	**256**	**256**	>512	**256**	**256**
S. aureus	64	>512	**256**	**256**	**256**	**256**	**256**	>512	**256**	>512	>512
E. faecalis	58	>512	->512	>512	>512	->512	**256**	>512	>512	>512	>512

All of the butanol fractions showed Gram-positive bacterial inhibition, fraction B1, B5 B6 and B10 also showed inhibition on Gram-negative bacterial strains. Few bioactivities on the butanol plant extracts have been published. According to the Chinese folk medicine book <Zhejiang common used herbal medicine> whole plant butanol and water extracts had been used for treating diarrhea (Revolutionary Health Committee of Zhejiang Province, 1970), gingivitis (Nanjing Military Ministry of Health, 1969, Fan and Zhu, 1975), gastroenteritis (Revolutionary Health Committee of Anhui Province, 1975), hepatitis, and cholecystitis (Shanghai People's Publishing House, 1972). According to these books, the plant extract was ingested by patients after boiling with water or soaking with ethanol. These traditional methods were very common and simple, the administration of polar solvent extracts suggested that, the polar fractions from this plant might be the key to its medical use.

In order to isolated the active compounds from butanol fractions, the fragmentation of butanol fractions was carried out on HPLCs. Fraction B2 and B3 were fractionated, and compounds were isolated by fraction collections (the structure information could be found in chapter II). However, after the structure elucidation, isolated compounds were sent for DNA gyrase supercoiling assay directly, due to the limited amount of each compound.

Table 3.7 The MIC values of water fractions (µg/mL).

Strains	Test samples								
	T	W	W1	W3	W4	W5	W8	W9	W10
E. coli	8	>512	>512	>512	>512	>512	>512	>512	>512
S. enterica	32	>512	>512	>512	>512	>512	>512	>512	>512
M. luteus	2	>512	>512	>512	**256**	>512	>512	>512	>512
S. aureus	0.3	>512	>512	>512	>512	>512	>512	>512	>512
E. faecalis	64	>512	>512	>512	>512	>512	>512	>512	>512

MIC values of water fractions are shown in Table 3.7. Most of the water fractions were not active in the MIC assay, and the only active found in water fractions was W4, at 256 µg/mL against *M. luteus*.

3.3.2 MIC of selected fractions

3.3.2.1 Positive controls susceptibility tests

Methicillin-Resistant *Staphylococcus aureus* ATCC 33591 is a resistant strain against beta-lactam antibiotics, which include penicillin methicillin, dicloxacillin, nafcillin, oxacillin, and cephalosporins. It was isolated in 1975 with penicillin, erythromycin and tetracycline resistant marker (Schaefler, 1979). In order to confirm the multi-drug resistant susceptibility profile, six antibiotics from different antibiotic families were tested. Wild type *Staphylococcus aureus* (ATCC 25923) were also tested along with the MRSA (ATCC 33591) strain. The starting concentrations for the antibiotics are listed in Table 3.4 in the preparation section. MIC results are shown in Table 3.8 below.

Table 3.8 Resistance profile of MRSA (ATCC33591).

Antibiotics	MRSA	*S.aureus*
Tetracycline	**256 µg/mL**	0.32 µg/mL
Oxacillin	**128 µg/mL**	0.08 µg/mL
Ciprofloxacin	0.32 µg/mL	0.32 µg/mL
Norfloxacin	1 µg/mL	1.28 µg/mL
Erythromycin	**> 512 µg/mL**	0.64 µg/mL
Novobiocin	0.02 µg/mL	0.16 µg/mL
DMSO	>3.13%	3.13 %

Ciprofloxacin could not be dissolved completely in DMSO, so it remained as a suspension when the MIC tests were carried out. Compared with wild type *S.aureus* strain test results, the β-Lactam antibiotic resistance feature was observed in Methicillin-resistant *S. aureus* strain ATCC 33591 and it was resistant to oxacillin at 128 μg/mL. The rest of the resistant susceptibility profile for ATCC 33591 was identified in erythromycin (>512 μg/mL) and tetracycline (256 μg/mL) (Bold in Table 3.8).

The expression of tetracycline resistance of MRSA was reported by Trzcinski using polymerase chain reaction (PCR) for the expression and detection of resistant determined genes (Trzcinski, 2000). Two mechanisms of the tetracycline resistance were published: activate the bacteria cell efflux pump (encode by tetracycline efflux resistance gene *tetK and tetL*) and reinforce the protection of ribosomals (ribosome protection proteins encode by *tetM or tetO genes*)(Donhofer et al., 2012). In this assay, the MIC value detected against tetracycline was at 256 μg/mL, indicated this strain (ATCC 33591).

The MIC value for erythromycin was >512 μg/mL in this assay, suggesting that this MRSA strain was strongly resistant to the macrolides antibiotics. There were three ways that bacteria became resistant to macrolide antibiotics: drug target modification (methylation or mutation of ribosomal); efflux; and drug deactivation (Leclercq, 2002).. The resistance genes for erythromycin were *ermB, ermC and msrA* confirmed by PCR analysis by Ding. *msrA* gene encodes macrolide efflux pump which belongs to the ABC transporter family; while genes *ermB, ermC* encode ribosome-RNA methylase and preventing the drug binds to rRNA (Ding et al., 2012).

The MIC values for MRSA against ciprofloxacin, norfloxacin and novbiocin were ≤ 1μg/mL almost the same compared with the wild type strain, which indicated that the MRSA resistant profile did not include quinolone and aminocoumarin antibiotics.

3.3.2.2 Selected fractions against MRSA and *S.aureus*

From the MIC results of the fractions above, nine fractions had been selected to test against the MRSA strain. They were fractions H1, H3, H4, H5-1, H5-2, B1, E1, E8, and E12. The starting concentration used was 512 μg/mL.

Table 3.9 MIC values of selected fractions against MRSA and wild type *S.aureus*, test sample starting at 512 μg/mL.

Candidates	MRSA	*S.aureus*
Oxacillin	256 μg/mL	0.32 μg/mL
Tetracycline	256 μg/mL	0.64 μg/mL
Novobiocin	0.04 μg/mL	0.16 μg/mL
H1	**128 μg/mL**	**125 μg/mL**
H3	512 μg/mL	256 μg/mL
H4	512 μg/mL	256 μg/mL
H5-1	256 μg/mL	512 μg/mL
H5-2	256 μg/mL	**128 μg/mL**
B1	512 μg/mL	512 μg/mL
E1	**128 μg/mL**	**128 μg/mL**
E8	>512 μg/mL	>512 μg/mL
E12	>512 μg/mL	>512μg/mL

According to the MIC results from Table 3.9, fraction H1 and E1 had inhibitory activity against both strains at 128 μg/mL. Since only a small amount of E1 was abstracted, no further study was carried out on fraction E1. In order to concentrate the activity, and remove those inactive components in the fraction H1, it was then separated into nine sub-fractions and labelled as H1-1 to H1-9. The MIC results are shown in Table 3.10.

Table 3.10. MIC values for H1 fractions against MRSA and wild type *S.aureus*, test sample starting at 512 µg/mL.

S.aureus	MRSA	*S.aureus*
Oxacillin	256 µg/mL	0.16 µg/mL
Tetracycline	256 µg/mL	0.32 µg/mL
Novobiocin	0.02 µg/mL	0.16 µg/mL
Fraction H1-1	512 µg/mL	512 µg/mL
Fraction H1-2	**64 µg/mL**	**128 µg/mL**
Fraction H1-3	**64 µg/mL**	256 µg/mL
Fraction H1-4	**128 µg/mL**	**128 µg/mL**
Fraction H1-5	**64 µg/mL**	**128 µg/mL**
Fraction H1-6	**16 µg/mL**	**128 µg/mL**
Fraction H1-7	**128 µg/mL**	**128 µg/mL**
Fraction H1-8	>512 µg/mL	>512 µg/mL
Fraction H1-9	>512 µg/mL	>512 µg/mL

Compared to the MIC value of H1 at 128 µg/mL, Fraction H1-6 (47.2 mg) showed a very good inhibitory activity on MRSA strain, the MIC value was observed at 16 µg/mL. It was indicated that, the fraction H1-6 might contain anti-bacterial compounds which were not belong to penicillin, erythromycin or tetracycline family. Fraction H1-2 (946.7 mg), H1-3 (43.0mg), H1-5 (48.6 mg) showed good inhibition activity on MRSA strain at 64 µg/mL , H1-4 and H1-7 showed exactly the same MIC value as the fraction H1. Fraction H1-1, H1-8 and H1-9 showed no obvious activity. According to the test results, the MRSA seem to be less tolerable than the wild type strain when tested against H2, H3, H5 and H6. This might be because the fractions contain certain types of compounds that could target the proteins encoded by resistant genes: for example, inhibition of PBP2a protein could cause the termination of bacterial cell wall synthesis and lead to cell death.

Fraction H1-2 (946.7 mg) was enough for further separation after the antibacterial assays, seven fractions were obtained from H1-2. Concentrated antibacterial activity was observed in fraction H1-2-6 and H1-2-7. After purification, structures of compound H1-2-6 and H1-2-7 were elucidated.

3.3.2.3 Compound H1-2-6 against MRSA and *S.aureus*

Fraction H1-2-6 had a MIC value against MRSA and wild type *S.aureus* at 64 µg/mL and 256 µg/mL respectively. Compound H1-2-6 is a white paste; its proposed structure is a butyrolactone derivative (Figure 3.6 **A**).
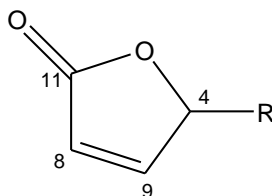
Figure 3.6   Proposed structure of compound H1-2-6.

The proposed structure was a butyrolactone. Number and the positions of methylene group could not be determined, because the sample contains many impurities and further structure investigation was warranted.

Acyl-homoserine lactones molecules could mediate the bacterial quorum sensing, by interfering with bacterial communication (Diggle and Crusz, 2007). Some butyrolactone derivatives such as 2-isocapryloyl-3-hydroxy-methyl -butyrolactone and N-(3-Oxo-octanoyl)-L-homoserine lactone (Luo, 2003) were also share the same mode of action. They mimicked the signaling molecules and bind to the bacterial receptor (inducer)(Bassler, 1999).

3.3.2.4 Compound H1-2-7 against MRSA and *S.aureus*

Compound H1-2-7 was proposed to be a 2-pyrone derivative: 4-pent-3-ene-1'-ynyl--pyran-2-one (Figure 3.7). The MIC value of H1-2-7 against both MRSA and wild type is 128 µg/mL.
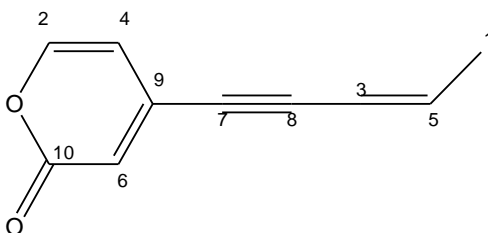
Figure 3.7 Proposed structure of compound H1-2-7.

Compound H1-2-7 did not possess very good antibacterial activity, which might be because the hydrophobic side chain on the position 4 is highly hydrophobic and may

not interact with the transport proteins on the cell membrane. This compound has a pyrone motif, which can be found in a number of phytochemicals such as coumarins. The bioactivities and synthesis route of a series of 4- substituted pyrones were published by Fairlamb (Fairlamb et al., 2004). The antibacterial activities of substituted-6-methyl-2-pyrones were reported using disk diffusion tests, where the diameter of zone of inhibition was 21-34 mm against *S.aureus* .

3.4 Conclusions

In this antibacterial research, two compounds were shown to have inhibition against MRSA: Compound H1-2-6 was suggested to be a butyrolactone derivative. It had the five-membered lactone ring and might be able to mimic the signaling molecules in bacterial quorum sensing system and interfere with bacterial communications. In this study, the compound 4-pent-3'-ne-1'-ynyl–pyran-2-one with a six-membered lactone ring was isolated. Both lactones have antibacterial activity against the MRSA strain. Their mode of action is not known, but they might both act as compounds which could block bacterial quorum sensing. They carry the same antibacterial motif as other some other classes of antibiotics, for example, coumarins. However, the sample isolated from this research was not enough for further investigation of inhibitory mechanisms.

In addition, forty-six fractions from *E. annuus* extract were examined and screened by their bacterial inhibitory activity. Nine fractions (H1, H2, H3, H4, E1, B1, B5, B6, B10) were confirmed to have inhibitory activities against the Gram-negative strains.

4. Chapter IV: DNA gyrase inhibitory activity of *Erigeron annuus*

4.1 Introduction

Topoisomerases are enzymes that regulate the topology of DNA molecules by breaking the DNA strands. There are two types of topoisomerases, type I and type II (Forterre et al., 2007). Type I topoisomerases are monomeric and can induce an ATP-dependent relaxation of the DNA double helix by breaking, passing and rejoining a single strand DNA (Pommier, 1998, Reguera et al., 2006). Type II topoisomerases can transiently break both strands of DNA by passing another segment through, rejoining the break (Watt and Hickson, 1994) and releasing the DNA supercoiling.

The unwound topological structure of DNA molecule is recognisable by the twist of the DNA helix and the number of times the double helix crosses over itself around its helical axis (Wu and Wu, 1996); together they constitute the DNA supercoil (Figure 4.1) described using linking numbers. DNA supercoiling is important to reduce the length of DNA molecule so that a large amount of genetic material can be compacted inside a single cell. Type II DNA topoisomerase are ubiquitous ATP-dependent enzymes in prokaryotes, lower eukaryotic and mammalian organisms (Burden and Osheroff, 1998). It has two subclasses: type IIA (topoisomerase II or gyrase, and topoisomerase IV) and type IIB (topoisomerase VI)(Watt and Hickson, 1994). Type IIA topoisomerase is essential in DNA growth-dependent processes (McClendon and Osheroff, 2007, Roca, 2009); it can relax the DNA supercoiling by breaking both strands and facilitate the replication and transcription process (Mukherjee et al., 1993).. Type IIB topoisomerases are heterodimers and their function mode is similar to that of type IIAs, but they have only been found in archaea and some higher plants.

During the DNA replication and transcription process, DNA double helix is unwound by helicase to form a tracking complex and each DNA strand is a template (Figure 4.1). In most prokaryotic circular DNA molecules, torsional strains are increased on both single strands and the rest of the double helix during DNA replication and transcription. In addition, they can be released by topoisomerases catalyzed unknotting decatenation and supercoiling (Watt and Hickson, 1994).

DOUBLE HELIX DNA MOLECULE
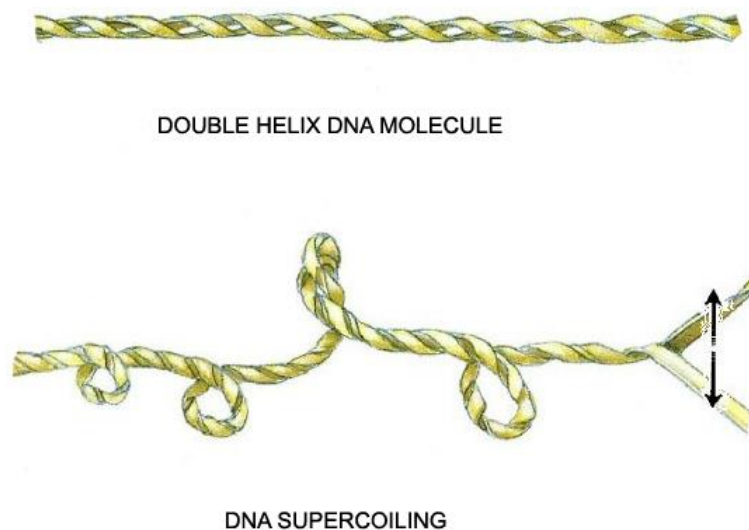
DNA SUPERCOILING

Figure 4.1. DNA supercoiling.

DNA gyrase is a unique type IIA on, replication and recombination in most bacteria. It allows both DNA chains to have free negative supercoils and relax the DNA double helix, so that the replication of DNA can continue. DNA gyrase is present in bacteria and some lower eukaryotes, like yeast, which makes it a good target for many antibiotics (Maxwell, 1997, Watt and Hickson, 1994) .

4.1.1 DNA gyrase structure

Gyrase is a heterotetramer, it has an A_2B_2 primary protein complex structure, containing equivalent amounts of protein A (GryA) and B (GryB) encoded by *gyrA* and *gyrB* genes (Adachi et al., 1987). It containing four subunits (Figure 4.2), two GyrA subunits (97 kDa each) and two GyrB subunits (90 kDa each)(Janid et al., 1993). Protein A (GyrA) (A protein in Figure 4.2) consists of an amino-terminal domain (59 kDa) and a carboxyl-terminal domain (33 kDa) (Hockings and Maxwell, 2002). The amino-terminal domain (GyrA59) is involved in DNA breakage and the reunion process, while the carboxyl-terminal domain (GyrA33) is involved in wrapping, binding,

and stabilizing the enzyme-DNA complex (Maxwell, 1997, Heddle et al., 2004, Corbett et al., 2004).
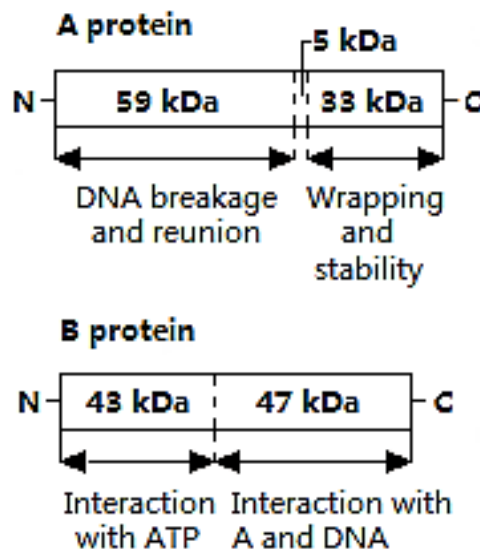
Figure 4.2 DNA gyrase constitution, adepted from Maxwell's publication (Maxwell, 1997).

Protein B (GyrB) consists of two different domains: amino-terminal domain (GyrB43) and carboxyl-terminal domain (GyrB47) (Heddle et al., 2004). The GyrB43 is fully active as an ATPase and very thermally stable (Akanuma et al., 2011b, Friedman et al., 1995), while GyrB47 can interact with GyrA33 and DNA and ensure the stability of the gyrase-DNA complex (Akanuma et al., 2011a, Ali et al., 1995).

The complex operates three different protein interfaces: N-gate, DNA-gate and C-gate (Illustrated in Figure 4. 3). These protein gates were the functional portions which could bond or grab the DNA molecules.
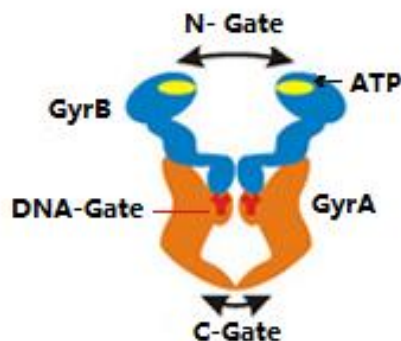
Figure 4.3 Three protein interfaces (N-gate, DNA-gate and C-gate) adapted from Gubaev's publication (Gubaev et al., 2009).

Subunit GyrB form a N-gate through which the other DNA strand (tDNA segment) can enter in the heterotetramer (Gubaev et al., 2009), C-gate is formed by subunit GyrA. The yellow spot shown in Figure 4.3 is the ATP binding site in GyrB (Basu et al., 2012), and tyrosines is shown as red spots in Figure 4.3 which gDNA can covalently attach to it and form a 5'-phosphotyrosine intermediate.

4.1.2 DNA gyrase function mode

Gyrase can change the topology of double-stranded DNA by a strand-passage mechanism (Martin and Dagmar, 2011). The original state of the N-gate is open (state 1 in Figure 4.4) and the gDNA segment binds to the DNA-gate forming an intermediate (two light gray arms area in state 2 Figure 4.4). The second DNA segment, transfer DNA (tDNA segment, black in state 2 Figure 4.4) binds to the GyrB, enters the N-gate and induces a nucleotide dimerization on the N-gate in GyrB (blue in state 2 in Figure 4.4).

Two molecules of ATP bind to the GyrB and the 5' -end of DNA binds to the tyrosines to form a covalent phosphotyrosine bond this binding can cut the gDNA segment (gray lane in state 3 Figure 4.4) and a four-base gap is generated, resulting in the closure of the N-gate. The tDNA becomes trapped in the complex and then passes through to enter the C-gate (state 3 in Figure 4.4).

The rejoining of gDNA leads to the opening of the C-gate, and in the meantime, the N-gate stays closed and forms a closed protein-operated pocket during the passage (state 4.4 in Figure 4.4).

Once the passage is completed, a GyrB47 catalyzed ATP hydrolysis is required and ADP and inorganic phosphate are released from the GyrB (Jensen et al., 1995). This leads to a reopening of the N-gate (state 5 in Figure 4.4) and tDNA leaves the complex completely (Kampranis et al., 1999). The heterotetramer resets to the initial state.
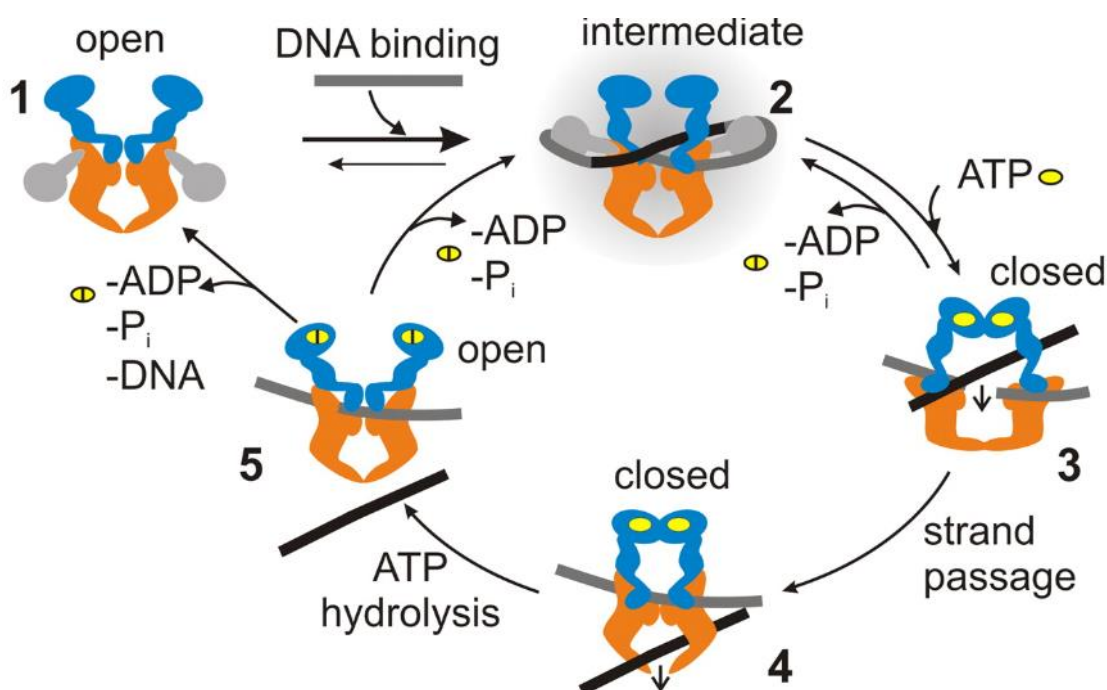
Figure 4.4. DNA-induced strand passage, directly copied from Gubeava and Klostermeier's publication (Gubaeva and Klostermeier, 2011).

In the entire strand pass through process, GyrA33 domain helps the tyrosine bind with gDNA, and helps the complex to capture the tDNA. The process introduces negative supercoils and decreases the linking number by 2 (Basu et al., 2012, Corbett et al., 2004).

4.1.3 Gyrase inhibitors

DNA gyrase has been identified as a good drug target in many therapies, since it plays an important role in bacterial DNA topological modifications (Maxwell, 1997).

There are many gyrase inhibitors which can be classified into three categories by their inhibitory modes of actions (Claudio et al., 2013): DNA-gate inhibitors, ATPase-domain inhibitors and the inhibitors that can form a cleavage complex. The most famous gyrase inhibitor family is the quinolone family.
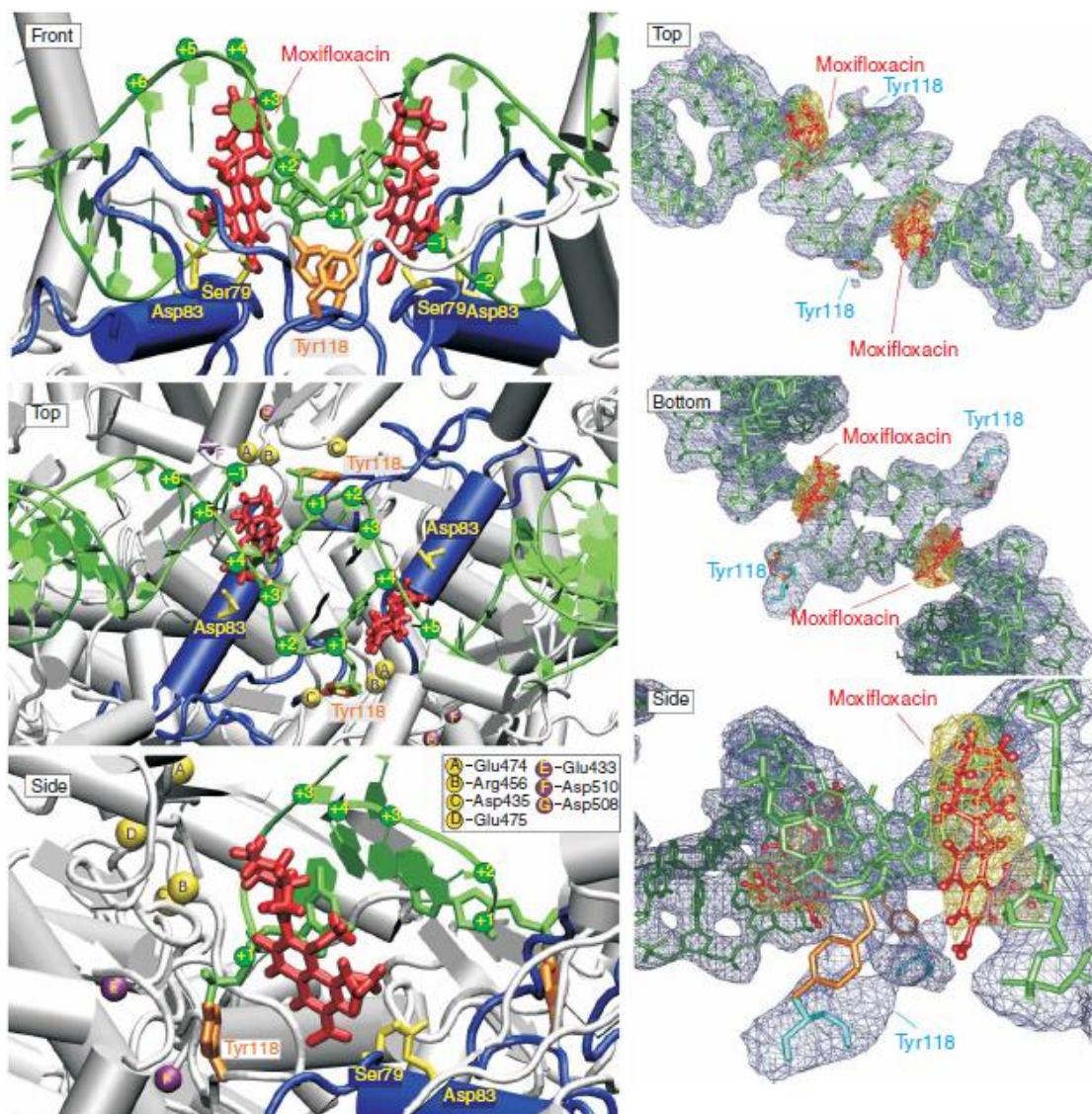
A. Mechanism of quinolone gyrase inhibitor.

(a) : Front, top and side views of quinolone cleavage complex. Moxifloxacin is shown in red, DNA helices are shown in blue, g-DNA is shown in green, the active site tyrosines (Tyr119) is shown in orange, the sites responsible for drug resistance are shown in yellow and the magnesium ion is shown in purple (b): Top, bottom and side views of the cleaved g-DNA residue. Moxifloxacin is shown in red, DNA is shown in green, active site tyrosines in shown in orange. Directly copied from Laponogov's publication (Laponogov et al., 2009).
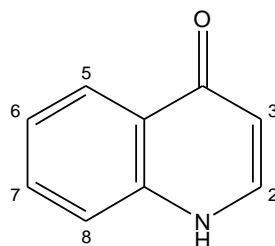
B. 4-oxo-1, 4-dihydroquinolane skeleton.
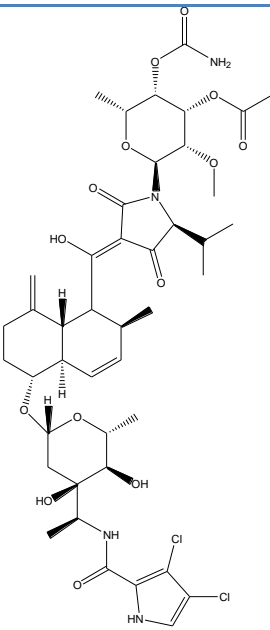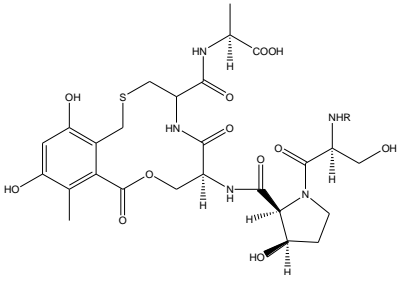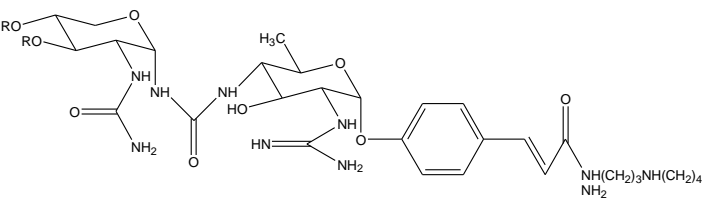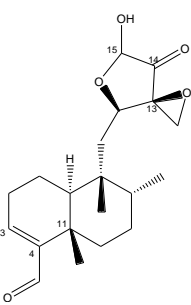
Figure 4.5 Quinolone gyrase inhibitor.
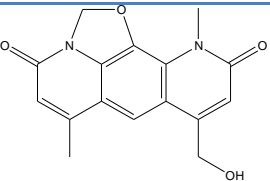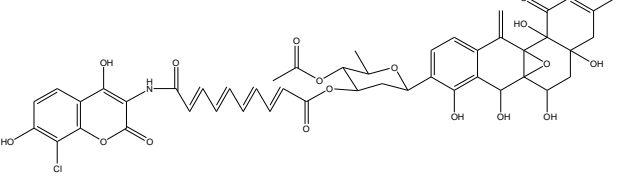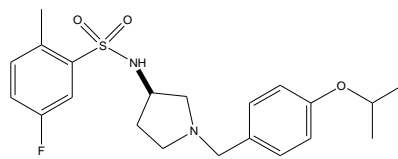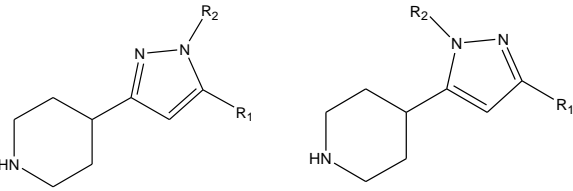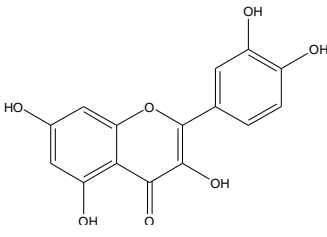
Quinolones are DNA-gate inhibitors, one of the most powerful classes of antibiotics, and have been used in clinic since 1967. They have a 4-oxo-1, 4-dihydroquinolane skeleton (Figure 4.5 **B**), include moxifloxacin, ciprofloxacin, nalidixic acid, norfloxacin, and oxolinic acid (Kim et al., 2011, Malik et al., 2011, Faye and Anthony, 2001). The structural based function mode was unknown until 2009. The quinolone-gyrase binding complex is shown in Figure 4. 5 **A**. There is a 4 base pair gap between the gate DNA (blue) and Try188 (orange) after the gate DNA and Tyr188 residues of the enzyme covalently link together at the 5' phosphate terminal of the DNA and hydroxyl oxygen of the Tyr188 residues (P-O bond). At this point DNA is pulled away, a covalent enzyme-DNA cleavage complex is formed. Two molecules of moxifloxacin (red) intercalated in the 4 bp gap on each DNA strand prevent the rejoining of the DNAs and stabilize the complex (Laponogov et al., 2009, Faye and Anthony, 2001, Sissi et al., 2001). The fluoroquinolones, quinazolanediones and isothiazolones families are quinolone derived families and share the same mode action of inhibition (Oblak et al., 2006, Hockings and Maxwell, 2002, Malik et al., 2011).

Another famous gyrase inhibitor family is the coumarin family, including novobiocin, clorobiocin and coumermycin. They are ATP analogues and bind to or bind near to the ATP binding site of the GyrB subunit. For example, novobiocin (Streptonivicin) was reported in the 1950s (Smith et al., 1956) as a powerful antibiotic. The gyrase inhibitory activity was then studied that novobiocin could bind to 24kDa N-terminal fragment of GyrB with hydrogen bindings (Lewis et al., 1996); the 24KDa fragment is inside the 43KDa N-terminal domain which is the site of ATP hydrolysis (Heide, 2013, Ali et al., 1993, Gilbert and Maxwell, 1994, Janid et al., 1993).

There are many other inhibitors which do not belong to the quinolone or coumarin families; they are listed in Table 4.1 below:

Table 4.1.Gyrase inhibitors.

Type	Antibiotics	Structure	Binding Method
Kibdelomycin			GyrB inhibitor (Singh et al., 2012, Phillips et al., 2011, Sawa et al., 2012).
Cyclothialidines	Cyclothialidine 14-benzoyl-cyclothialidine	ATPase inhibitor (Nakada et al., 1994).	
Cinodine	Cinodine	DNA-gate inhibitor (Osburne et al., 1990, Greenstein et al., 1981).	
Clerocidin	Clerocidin		DNA-gate inhibitor, induce gyrase-mediated DNA damage (Gatto et al., 2001).
Albicidin	Albicidin	Unknown structure	DNA-gate inhibitor, form a cleavage Intermediate (Hashimi et al., 2007, Royer and Costet, 2004).

Nybomycin	Nybomycin	DNA-gate inhibitor (Hiramatsu et al., 2012).
Simocyclinone D8		Binds to the N-terminal GyrA domain (Flatman et al., 2005)
Gyramides		ATPase inhibitor (Rajendram et al., 2014).
Pyrazole derivatives		Unknown (Tanitame et al., 2004).
Quercetin derivatives		ATPase inhibitor and interact with DNA (Tan et al., 2009, Plaper et al., 2003)
Macromolecular inhibitors	YacG GyrI MurI Qnr/MfpA	DNA binding (Sengupta and Nagaraja, 2008, Chatterji and Nagaraja, 2002, Sengupta et al., 2006, Tran et al., 2005).
Macromolecular inhibitors	microcin B17 microcin CcB microcin ParE	DNA-gate inhibitor, stabilizing covalent complex (Maxwell, 1997).

There are very few natural compounds acting as gyrase inhibitors which do not belong to the quinolone or coumarin family. As listed above, quercetin derivatives have shown dual inhibition activities. They can bind to the DNA GyrB subunit inhibiting the ATPase activity and it can also interact with DNA. Though the DNA-binding mode is still not clear, the binding method was suggested by Tan that quercetin derivatives can bind to DNAs by intercalation and prevent the DNA bonds to gyrase (Tan et al., 2009, Hossion et al., 2011).

Cyclothialidine inhibits the ATPase function (Nakada et al., 1994), while compound 2,3-dihydroisoindol-1-one is structurally related to cyclothialidine; these compounds are cyclic peptides with antibacterial activity by inhibiting bacterial DNA gyrase (Lubbers et al., 2007). Cinodine is a glycocinnamoylspermidine antibiotic that can inhibit DNA gyrase in both Gram-positive and negative strains (Osburne et al., 1990, Greenstein et al., 1981). Clerocidin is a diterpenoid and can induce gyrase-mediated DNA damage and produce a cleavage between DNA and gyrase complex (Gatto et al., 2001). Albicidin is a family of potent antibacterial polypeptide-peptide phytotoxins isolated from *Xanthomonas albilaneans,* which inhibit the prokaryotic DNA replication by cleaving DNA intermediate (Hashimi et al., 2007, Vivien et al., 2007, Royer and Costet, 2004).

4.2 Material and methods

The supercoiling assay kits were purchased from Inspiralis, including, *E.coli*, *S. aureus* gyrase, DNA pBR322 (4361 base pairs (Watson, 1988)), gyrase supercoiled assay buffer and dilution buffer, Norwich, UK. (*S. aureus* DNA gyrase was purified after heterologous expression in *E.coli* and supplied as A_2B_2 complex from Inspiralis). All gyrase were aliquoted into 40 U/tube batches and stored at -85°C. DNase and RNase protease free, electrophoresis tested agarose, Tris-base, EDTA, were from Fisher Bioreagents[®], Loughborough, UK. Novobiocin, ciprofloxacin, bromophenol blue and glacial acetic acid were purchased from Sigma-Aldrich[®], Dorset, UK. HPLC-grade water (18 MΩ) was prepared using a Millipore Mili-Q purification system, Milipore Corp., New Bedford, MA. HPLC grade chloroform and n- isopentyl alcohol were obtained from Fisher Scientific, Loughborough, UK. Eppendorf centrifuge (0.5, 1.5 mL) tubes were used for incubation, Hamburg, Germany. Electrophoresis results were documented by UVP BioSpectrum[®] Imaging System, equipped with High performance transilluminators and VisionWorks[®] LS Software, Cambridge, UK. IC$_{50}$ results are digitalized by software ImageJ 1.47v, National institutes of health, USA Cures are estimated by software GraphPad Prism 6.04.

4.3 Experiment preparation

TAE buffer was prepared as a 50 X stock solution. A 1 L 50 X stock solution was

prepared by adding 242 g Tris-base, 57.1 mL glacial acetic acid and 100 mL of 500 mM EDTA (pH 8.0) solution into a 1 L volumetric flask. The final volume was fixed up to 1 liter with deionized water. This stock solution was diluted to 1 X solution with deionized water for use. Loading dye was prepared as 6 X solution containing 10 mM Tris-HCl (pH=7.6), 0.03% bromophenol blue, 60% glycerol and 60mM Ethylenediaminetetraacetic acid (EDTA). The loading dye was stored at room temperature, covered with tinfoil. Dilution buffer for DNA gyrase supercoiling assay contained 40% (v/v) glycerol, 0.6% (w/v) Tris-HCL, 0.015% (w/v) dithiothreitol (DTT) and 0.03% (w/v) EDTA. Assay buffer for DNA gyrase supercoiling assay contained 1.1 % (w/v) KOH (pH7.6), 0.2% (w/v) magnesium acetate, 0.15% (w/v) DTT, 0.1% (w/v) ATP, 10% (w/v) potassium glutamate and 0.05% (w/v) albumin. Both buffers were obtained as supercoiling assay kit from Inspiralis.

4.4 DNA gyrase supercoiling assay

4.4.1 Test candidates and controls

Sterilized 1.5 mL Eppendorf centrifuge tubes were used for making 1 mg/mL of test candidates stock solution dissolved in 100% DMSO. 0.6 µL of 10% DMSO sample solution was used in each reaction volume (30 µL, 20 µg/mL in 2% DMSO).

The DNA control contained 0.5 µL pBR322 relaxed DNA only. 100 mM novobiocin and ciprofloxacin solution were used as positive control in 2% DMSO; both drugs were diluted 500 times and the final concentration used in the test was 20 µM in 2% DMSO. 2% DMSO solution was used as negative control.

4.4.2 Titrations

Both *E.coli* and *S. aureus* gyrase were titrated using the same method. The reaction volume was 30 µL as recommended by the supplier Inspiralis. 1 U of gyrase was incubated with 0.5 µg of relaxed pBR322 DNA. Titrations for both *E.coli* and *S. aureus* gyrase were carried out using 1U to 6U of DNA gyrase. The assay started with incubating DNA gyrase with 0.5 µg of relaxed pBR322 DNA in a reaction volume of 30 µL at 37 $^{\circ}$C for 30 min in assay buffer. Reactions were stopped by taking the reaction tubes out of the water bath and treated with 20 µL of loading dye and 30 µL organic solvent (chloroform: n- isopentyl alcohol 24:1). Test tubes were mixed, excessive proteins and test compounds were extracted by the organic solvent and rejected.

The gel was prepared by dissolving 1.5 g agarose powder in 150 mL 1 X TAE (1% gel was used (Lewis, 2011)). The gel particles dispersed by heating until near boiling point. The melted gel was cooled down before pouring it into a cast and the cast was set with two 12-well combs and wrapped with tapes at the opening side. 15 µL supernatant of each candidate was loaded on the agarose gel electrophosis in 1 X TAE buffer, which was run overnight under 20 volts for 15 hours. After 15 hours, the gel was stained by soaking into 6.5 µL ethidium bromide in 100 mL of 1 X TAE buffer for 40 minutes, followed by 100 mL fresh 1 X TAE de-staining for 20 minutes.

4.4.3 Method of supercoiling assays

After the titration, *E.coli* and *S. aureus* gyrase supercoiled assays were carried out on hexane, ethyl acetate, butanol and water extracts from plant *E. annuus* following the protocol. 9 hexane extractions, 12 ethyl acetate extractions, 10 butanol extractions and 7 water extractions were tested. All test groups candidates were run on agarose gel electrophoresis in 1 X TAE buffer overnight under 20 volts for 15 hours.

4.5 Half maximal inhibitory concentration (IC$_{50}$) of selected compounds

Functional antagonist IC$_{50}$ assay was a quantitative measurement to indicate how much of a single compound was required in the inhibitory reaction. It was designed to construct a dose-response curve as a result and to test the efficiency of the

compounds under different concentrations. According to the positive controls there were 20 μM in 2% DMSO and 40 μM for the concentrations of the candidates used in the positive supercoiling assays. Selected test candidates were diluted to 300, 100, 30, 10, 3, 1, 0.3 and 0.1 μg/mL. 0.6 μL of diluted samples were added to 30 μL reaction volume using the same assay method.

Three independent experiments were carried out using the same method and material: the results from all groups were documented and digitalized using ImageJ: three sets of data of inhibition density were obtained for each gel photo; and their mean$\pm$ standard error mean (SEM) were calculated. IC_{50} was valued and the curves were estimated by plotting inhibition density against log (concentration), [μg/mL] from three groups using GraphPad Prism 5 software.

4.6 Results and discussion

4.6.1 Titration and supercoiling assay for Gram-negative gyrase

Titration result of *Escherichia.coli* gyrase from 1U to 4U units, is shown in Figure 4.6. pBR322 plasmid appears in different conformations, which gives a series of bands on an agarose gel. They are topoisomers of pBR322 (DNAs of different linking number or different conformations)(Inspiralis). The Nicked open-circular DNAs and relaxed circular DNAs have floppy structures and have difficulty in going through the agarose gel; their bands can be observed at the top of the each lane. Linear DNAs also have difficulty in passing through the agarose particles, since they are unknotted and string out between the agarose particles. However, both strands of linear DNA are cut and they can move through the agarose from one end, hence their bands migrate further than the circular DNAs. Supercoiled denatured DNAs are like supercoiled DNAs, both strands are uncut but not correctly paired (Lyubchenko and Shlyakhtenko, 1988, Sen et al., 1992). The supercoiled DNAs have very good conformation mobility; their bands can be observed at the bottom of the gel (Figure 4.6, Sc). In the titration, DNA Gyrase converts the relaxed plasmid pBR322 into a supercoiled form. The supercoiled DNA is tightly coiled and very easily passes through the agarose bundles. The supercoiled bands migrate the fastest on the electrophoresis gel, therefore their bands can be observed as the furthest single band under the UV light.
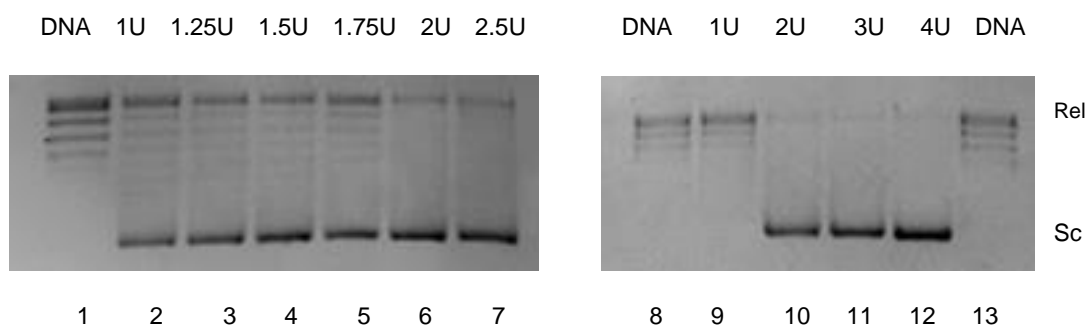
Figure 4.6 Titration *of E.coli* DNA gyrase. Rel: relaxed DNA bands, Sc: supercoiled DNA band.

From the titration result, lane 1, 8 and 13 were DNA controls, containing pBR322 plasmid only. Bands for different pBR322 topoisomers could be observed except supercoiled DNA bands. Along with the increasing concentration of the enzyme, relaxed DNA bands disappeared at 2 U of *E.coli* gyrase (lane 6) and a single supercoiled DNA band could be observed in lane 6, 7, 10, 11 and 12. Lane 6 and 10 were the cutting point of the titration, containing 2 U of enzyme.

Thirty-eight fractions from hexane, ethyl acetate, butanol and water extracts were tested against 2 U of *E.coli* gyrase at the concentration of 20 µg/mL in the supercoiling assay. The supercoiling assay result for butanol fractions are shown below in Figure 4.7.
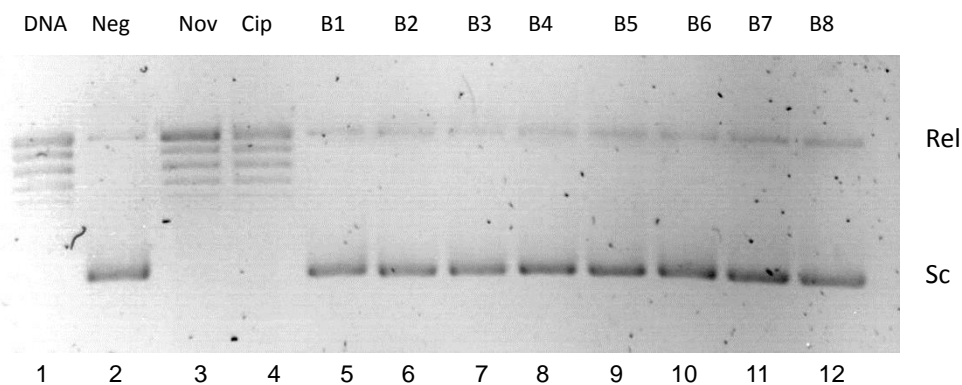
Figure 4.7 DNA supercoiling assay on fraction B1-8 against *E.coli* gyrase. Rel: relaxed DNA bands, Sc: supercoiled DNA band.

In the *E.coli* gyrase supercoiling assay, the positive controls novobiocin and ciprofloxacin (lane 3 and 4) could inhibit the gyrase function and no supercoiled DNA band was observed. Test groups from lane 5 to 12 showed negative results; compared with the negative control, they all showed a single heavy supercoiled DNA band. This indicated that all relaxed DNA had been compacted by the gyrase completely; therefore, none of the test samples were active against *E.coli* bacterial DNA gyrase.

Many black dots were observed in the result pictures. This was most likely caused by impurities in the agarose powder, for example, dust and paper fibers.

4.6.2 Titration for Gram-positive DNA gyrase

S. aureus gyrase was titrated from 0.1 U to 3 U (Figure 4.8). The pBR322 plasmid was used as the substrate in the assay.
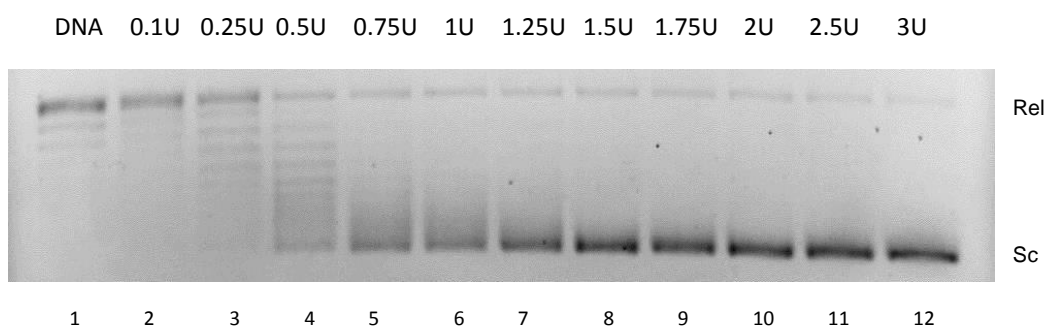
Figure 4.8 Titration of *S.aureus* DNA gyrase. Rel: relaxed DNA bands, Sc: supercoiled DNA bands.

From the *S. aureus* gyrase titration, the supercoiled DNA bands migrated as a single band observed from lane 7 to 12. However, in lane 7, the supercoiled band has a blurry edge which suggested that not all the plasmid DNA were supercoiled in the presence of 1.25 U of *S. aureus* gyrase. Thus, 1.5 U of the enzyme was used for the assay.

4.6.3 *S.aureus* DNA gyrase supercoiling assays

During the assay, fractions E3, E4, E5, E6, E11, B2, B3 and B9 showed inhibitory activity against *S.aureus* gyrase at 20 µg/mL (Figure 4.9). No activity was observed in lipophilic hexane fraction and hydrophilic water fraction groups.
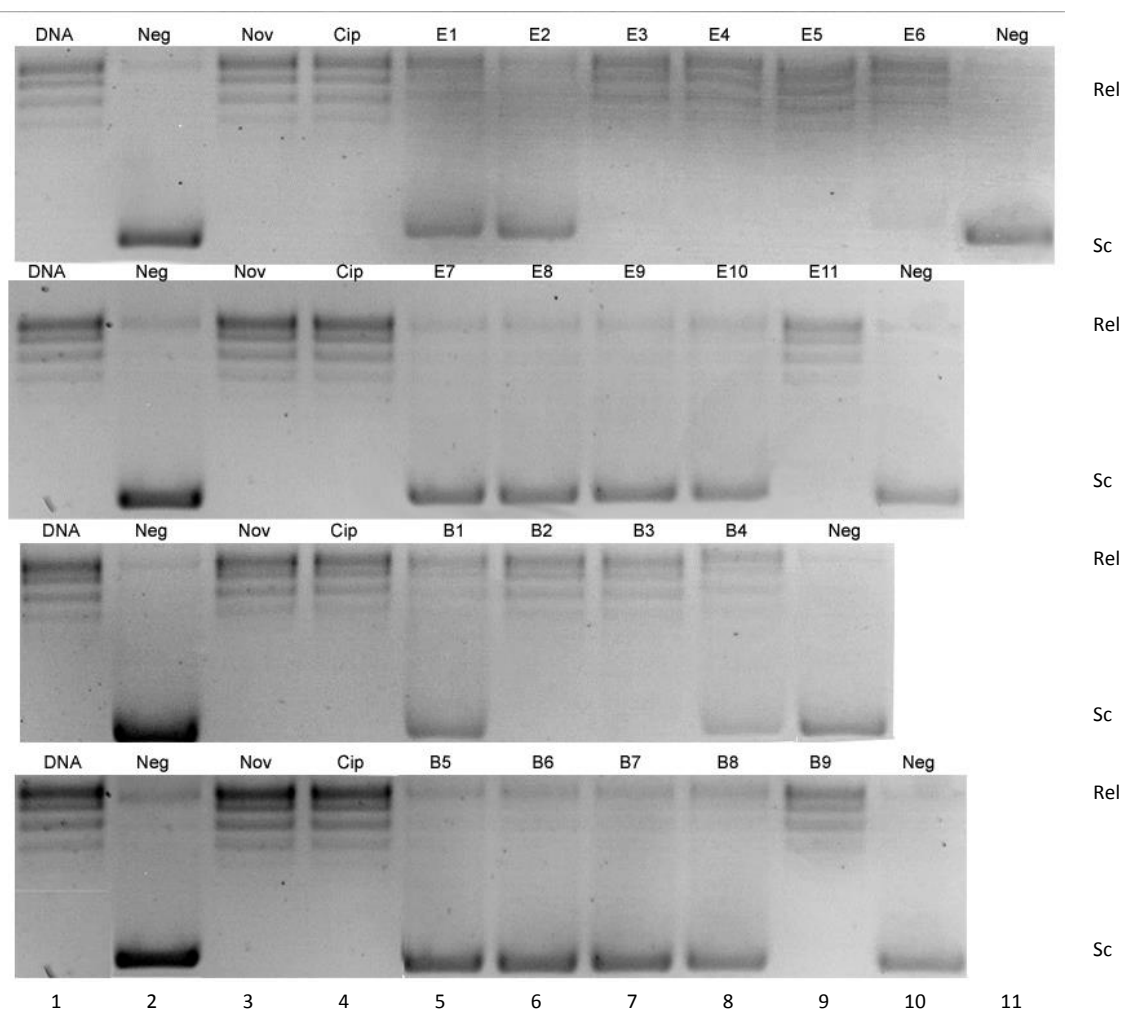
Figure 4.9. DNA gyrase supercoiling assays on ethyl acetate and butanol fractions against *S.aureus* gyrase. Rel: relaxed DNA bands (topoisomers with different configuration or linking number), Sc: supercoiled DNA bands.

In the DNA gyrase supercoiling assays of ethyl acetate and butanol fractions, the first lane was DNA control, in which all the bands for pBR322 topoisomers were observed. The second lane was the negative control. It gave a single heavy band of supercoiled DNA, which indicated that the relaxed DNA was completely supercoiled. The DNA control was repeated in the last lane on the same agarose gel. 20 µM of the gyrase inhibitors novobiocin and ciprofloxacin were used as positive controls in lane 3 and 4; the gyrase activity was completely inhibited and the DNA bands appeared like the DNA control and no supercoiled DNA band was observed.

Eight fractions from ethyl acetate extract and butanol extract: E3, E4, E5, E6, E11, B2, B3 and B9 showed inhibitory activity in the triplicated assays; no supercoiled DNA band was observed. All the bands on the left side of the gel pictures were darker; this was caused by the uneven UV light of the gel camera, as both negative controls on one gel came from the same reaction tube, but they were observed in a different intensity.

Further chromatographic separation works were carried out on eight fractions: E3, E4, E5, E6, E11, B2, B3 and B9.

4.6.4 *S.aureus* DNA gyrase supercoiling assays on isolated compounds

Fractions B2 and B3 were separated by reverse-phase HPLC; 19 and 14 peaks were collected respectively and followed by NMR structure characterization. 20 µg/m of fraction B2-3, B2-4, B2-5, B2-7, B2-9, B2-10, B2-11, B3-1, B3-5, B3-7, B3-8, B3-9, B3-10, B3-11 and B3-12 were tested in the *S.aureus* gyrase supercoiling assay, and only fraction B3-1, B3-7, B3-8, B3-9, B3-11 and B3-12 showed inhibitory activity (Figure 4.10).
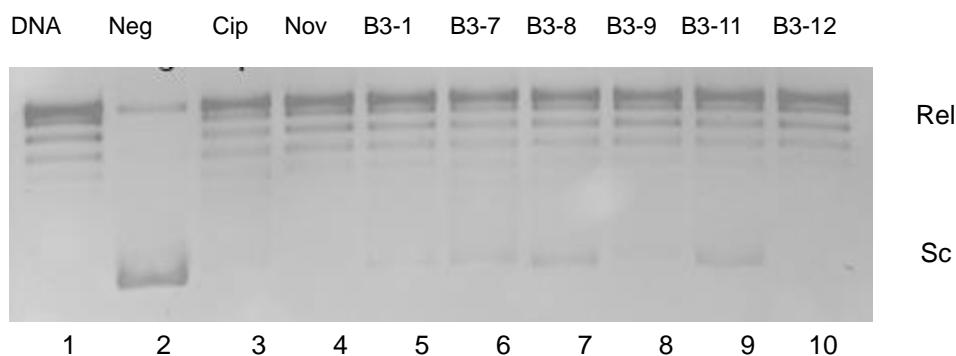
Figure 4.10 DNA gyrase supercoiling assay on B3 fractions against *S.aureus* gyrase. Rel: relaxed DNA bands, Sc: supercoiled DNA bands.

The first lane was the DNA control in which all nicked DNA and relaxed DNA bands could be observed. The second lane was the negative control. Relaxed DNAs were supercoiled by the gyrase completely, which could be determined by the single heavy supercoiled DNA band at the bottom edge of the gel. 20 µM of gyrase inhibitors novobiocin and ciprofloxacin were used as positive controls in lane 3 and 4, in which no supercoiled DNA bands were observed.

For fraction B3-1, B3-9 and B3-12, gyrase activity was likely to be inhibited completely, no supercoiled DNA bands were observed. While B3-7, B3-8 and B3-11 showed faint supercoiled DNA bands, indicated that parochial plasmid had been coiled and very blurred supercoiled DNA bands in lane 6, 7 and 9 could be observed.

4.6.4.1 Gyrase inhibitory activity of B3-1

Fraction B3-1 was a white powder separated from butanol extract. It showed good inhibition activity against *S. aureus* gyrase in the supercoiling assay. It was proved to b e a single compound from the NMR results. The proposed structure of B3-1 was estimated by the program ChemDraw® and is shown in Figure 11A.
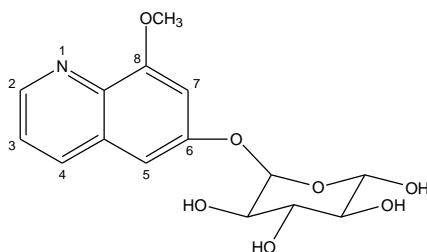
A. Proposed structure of compound B3-1.
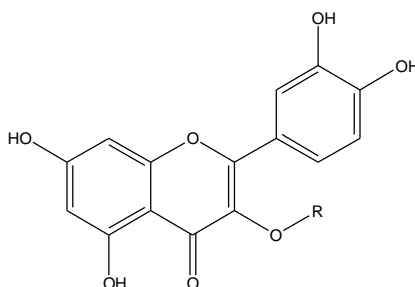
B. Structure of flavone-based analogues.
Figure 4.11 Proposed structure of B3-1 and structure of flavone-based gyrase inhibitor.

The inhibitory mode of action of B3-1 might be different depending on the different substitutions at position 1 and 5. If the atom at position 1 is an oxygen atom, then it could mimic a flavone-based gyrase inhibitor. According to Vergheses's research, the flavone-based DNA gyrase inhibitors share a motif structure shown in Figure 4.11 **B**. They have dual inhibition activities: binding to the DNA GyrB subunit inhibiting the ATPase activity (forming a stopping complex), or interacting with DNA, acting as a DNA intercalator (Verghese et al., 2013, Heide, 2013, Reece et al., 1991). The compound B3-1 could also be a quinolone derivative if a nitrogen atom substitute at position 5, a carbonyl at position 8 and the carbon double bond at position 6. The double bond conjugate with the carbonyl to form a pyridine ring, which could imitate the quinolone, acting with DNA gyrase and the DNA molecule to form the cleavage

complex.

4.6.4.2 Gyrase inhibitory activity of B3-7 and B3-8

Fraction B3-7 was a brown paste and the structure was estimated by the program ChemDraw®; the proposed structure of B3-7 is shown in Figure 4.12 **A** as an anthraquinone (9, 10 -Anthraquinone). Fraction B3-8 was also a quinone derivative but more sample was required for full structure elucidation. The proposed structure of B3-7 was a close match to anthraquinone. In the proposed structure, the chemical shift of H6 and H8 protons were high, they were most likely to be affected by the decreening effect of the R group. However, the R goupr could not be determined because of the insufficient sample for ^{13}C NMR.

A. Proposed structure of compound B3-7.
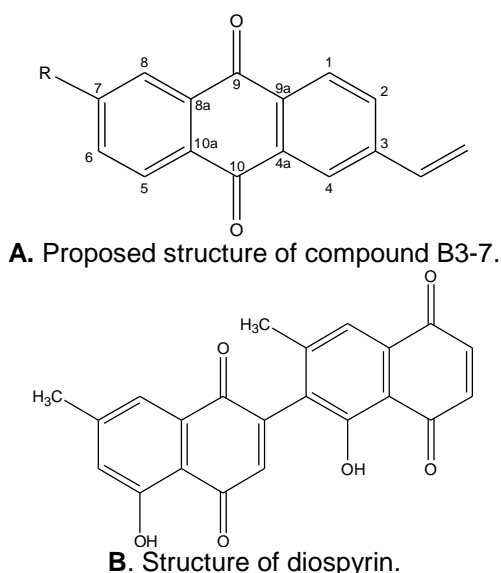
B. Structure of diospyrin.
Figure 4.12 Proposed structure of B3-7 and structure of anthraquinone.

Though there are a number of reports on the anti-bacterial activities of 1,4-naphthoquinone (Nair and Anchel, 1972, Ignacimuthu and Pavunraj, 2009, Rahmoun et al., 2012), there are few gyrase inhibitors that have been studied based on the naphthoquinone structure. For example, according to Karkare's studies, naphthoquinone diospyrin (Figure 4.12 **B**) provides a 15 µM IC_{50} value of inhibition in the gyrase supercoiling assay. It also gives a distinct inhibition mode: the binding site of diospyrin lies in the N-terminal domain of subunit B, but does not affect the ATPase. However, the mechanism of naphthoquinone-GyrB binding is not clear (Karkare et al., 2012), but the identification of the mode of action would contribute towards finding new antibacterial agents.

4.6.4.3 Gyrase inhibitory activity of B3-9

Fraction B3-9 was a brown paste, and had been identified as a single compound through the NMR elucidation. The proposed structure of B3-9 is shown in Figure 4.13 **A** as a 1, 4-benzopyrone based analogue. The structure was estimated by the program ChemDraw®.
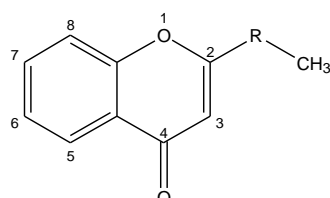
A. Proposed structure of compound B3-9.
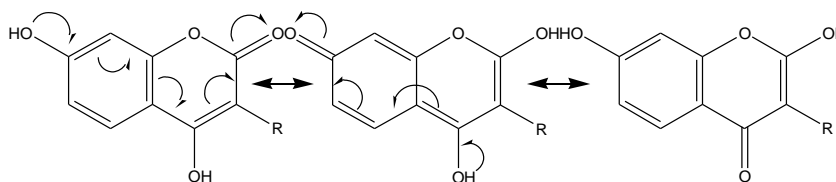
B. C_4-OH coumarin tautomerism.
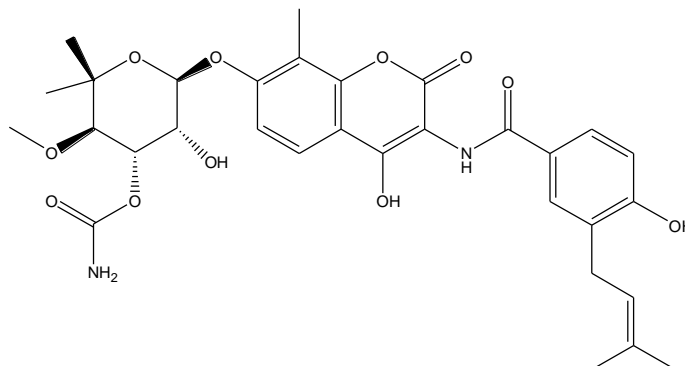
C. Structure of novobiocin.

Figure 4.13 Proposed structure of compound B3-9, C4-OH coumarin tautomerism and structure of nobobiocin.

The R group for B3-9 has not been determined. If the R group is a benzene ring, B3-9 would be a flavonoid and it would be expected to be a mode action of flavone-based analogues against gyrase. The inhibition is most likely based on their interaction with DNA. For example, a quercetin metal complex was shown to have two modes of inhibitions: DNA gyrase poison and DNA intercalator. From Verghese's research

reports, the flavone-based analogues can act as isosteric replacement for the coumarin drug, binding to the gyrase causing the deactivation of the enzyme (Tan et al., 2009, Verghese et al., 2013, Plaper et al., 2003). However, the binding mechanism is not known and the mode of inhibitory action of flavone-based compounds was only suggested by Tan as a DNA interaclator (Tan et al., 2009).

B3-9 could also be an isomer of C_4-OH coumarin. As previous studies of the tautomers have showen (Porter and Trager, 1982, Alok et al., 2004), when a hydroxyl group is substituted at position 7 in a C_4-OH coumarin, the coumarin undergoes a tautomerism (Figure 4.13 **B**): the proton dissociates from the hydroxyl group and the phenoxide anion conjugates with the benzene ring, forming 2, 7 -diyhdroxy chromone.

If the hydroxyl group is substituted at present on position 2 and 7, B3-9 could interact with the subunit B as a coumarin derivative. According to Janid and Gilberts' research, the drug-gyrase binding was studied using drug-affinity column screening, and the mode of action proposed for coumarin drugs was ATPase inhibition. Compounds like novobiocin (Figure 4.13 **C**) and coumermycin bound at the 24 kDa sub-domain in the 43 kDa N-terminal domain of GyrB to form monomer and dimer respectively, which has been detected in molecular mass studies. (Ali et al., 1995, Reece et al., 1991, Janid et al., 1993) The protein-drug binding interactions are still not clear. However, as described in Gilbert's research, only non-ionic eluent (25% v/v tertiary butanol) could be used to elute the protein-drug polymer through the coumarin-affinity column. Due to the hydrophobic nature of the protein-drug binding, the interaction was suggested to be a non-polar interaction.

4.6.5 Half maximal inhibitory concentration (IC$_{50}$) tests

The IC$_{50}$ values on the tested compound against *S.aureus* gyrase were expressed as the mean of triplicated experiments (experiment 1 to 3). Eight concentrations were selected: 300, 100, 30, 10, 3, 1, 0.3 and 0.1 µg/mL (Figure 4.14, **A**) in order to construct a dose-response curve, and IC$_{50}$ values were calculated from the dose inhibition curve. Three gel pictures were digitalized for each experiment group.
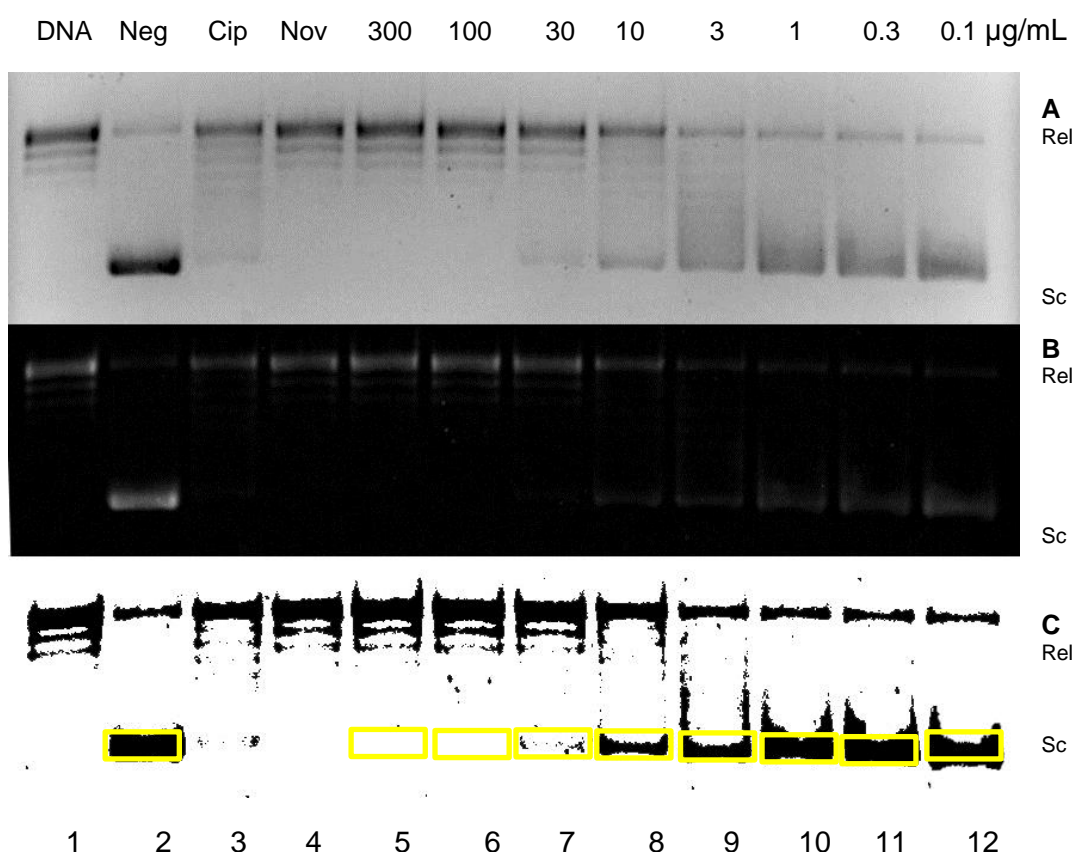
Figure 4.14 Measurement of DNA gyrase inhibition. **A.** Invert colours image; **B.** Subtract background; **C.** Adjust threshold.

The results pictures of all gels were documented and digitalized using software ImageJ® by measuring the supercoiled DNA band densities on the gel photos (yellow frame areas, Figure 4.14 **C**). The original gel photos had very noisy backgrounds, the direct measurement of lane 1 (DNA control) supercoiled DNA band density was even higher than the negative control (as can be seen, there were no supercoiled bands in

the DNA control lane). In order to eliminate the effect of the background, all backgrounds were subtracted:

Step 1: every 15 pixels of the background was subtracted into a dark background (Figure 4.14, **B**).

Step 2: the resolution was reduced to 8-bit to remove the remaining background color.

Step 3: the color threshold was adjusted to change the picture into inverted colours (Figure 4.14, **C**).

The density measurements were taken from Figure 4.14, **C** using the same size check box (W=0.6, H=0.3 mm). Before taking the measurements, picture size, quantity and colour were not changed, as this might have affected the final density value. Independent experiments were carried out testing positive control novobiocin, sample B3-1, B3-9 and B3-12 respectively using the same method and material; the results from all groups were documented and digitalized using ImageJ. Three photos from each experiment were measured, and the density mean was calculated.

IC_{50} value and the curves were estimated by plotting inhibition density against log (concentration), [μg/mL], using software GraphPad® Prism 5. The dose-response nonlinear fit curve was fitted by the software and the regression curve is shown in Figures 4.15-4.18. The X axis values are concentrations. However, since first concentration is really 0.0, the X values would be transformed to logarithms and the log (0) is not defined. Thus, a low concentration (in this case 0.01 ng/mL) is entered instead of zero.

4.6.5.1 Half maximal inhibitory concentration assay of novobiocin

The inhibition of gyrase was examined by measuring the density of supercoiled DNA bands in the presence of decreasing concentration of novobiocin (300-0.1 µg/mL). (Figure 4.15 **A**).
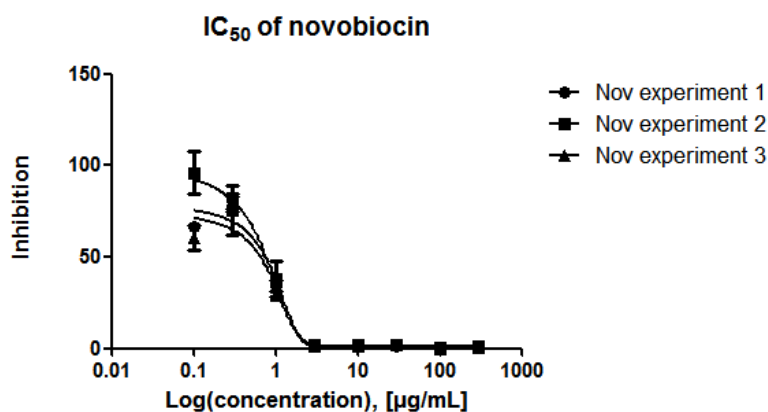
A. IC_{50} value of novobiocin.
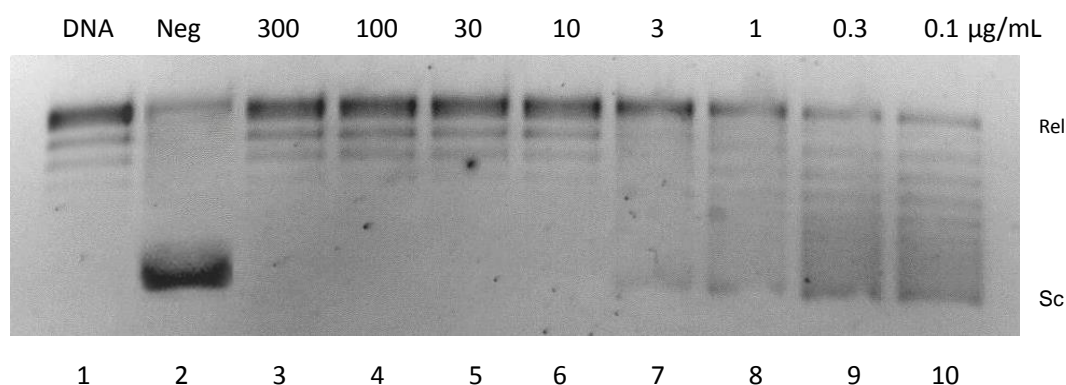
B. IC_{50} assay of novobiocin.

Figure4.15 IC_{50} assay of novobiocin; from 3.97-7.18 µg /mL. Test concentration of novobiocin was from 0.1 to 300 µg /mL on the relaxation plasmid pBR322 DNA (0.5 µg) incubating with 1.5 U of *S. aureus* gyrase. Rel, relaxed DNA bands; Sc, supercoiled DNA bands.

Novobiocin is an aminocoumarin antibiotic compound, used as positive control in this gyrase assay. The IC_{50} values of novobiocin are from 3.97 to 7.18 µg /mL. The IC_{50} value from this test was not in the same range when compared with the other published works in the gyrase supercoiling assay: Alt and their research team had tested the IC_{50} of novobiocin and other amimocoumarin drugs, obtaining 6-10 nM (3.672 ng/mL-6.12 ng/mL) inhibitory concentrations against *S. aureus* (Alt et al., 2011). However, the activity of the gyrase and the components of the assay buffer (35 mM

127

Tris-HCl (pH=7.5), 24 mM KCl, 700 mM K-Glu, 4 mM MgCl2, 2 mM DTT, 1.8 mM spermidine,1 mM ATP, 6.5% (w/v) glycerol and 0.1 mg/mL albumin) was different from this research and the activity of the enzyme was considered to be a decisive factor in the supercoiling assay.

S. aureus gyrase could be inhibited completely in the presence of a high concentration of novobiocin. From 3-300 µg/mL (Figure 4.15 **B**, lane 3-6), the nicked and relaxed DNA bands could be observed as the same as they were in the DNA control (lane 1) and there were no supercoiled DNA bands that observed in lanes 3-6. The software calculated inhibition values were tended to 0; therefore the inhibition of the gyrase was complete. From lane 7 to 10, the enzyme activity was affected by the novobiocin, the supercoiled bands observed was not clear. 0.5 µg plasmid pBR322 DNA was used as substrate; not all the plasmid had been supercoiled in lane 9 and 10 and several relaxed DNA bands were observed very clearly, representing relaxed DNAs with different linking numbers. Compared with the single heavy supercoiled DNA band in the negative control (lane 1), only partial substrates were supercoiled by the enzyme in lane 7 to 10 and no clear supercoiled bands were observed.

DNA gyrase is a validated clinical target for novobiocin, which is an aminocoumarin ATPase inhibitor (Heide, 2009). Novobiocin act by targeting the DNA gyrase ATP-binding domain GyrB or the Hsp90 C-terminal binding site (a swich control of ATPase)(Sti, 2002). This feature has been proven in many antimicrobial assays in screening a novobiocin resistance *S. aureus* strain (Mika et al., 2005). This nature of "target selection" of novobiocin is also used to overcome quinolone and other drug resistance to reduce the risk of resistance development in antibacterial combination therapies.

4.6.5.2 Half maximal inhibitory concentration assay of compound B3-1

The inhibition of gyrase was examined by measuring the density of supercoiled DNA bands in the presence of decreasing concentration of B3-1 (300-0.1 µg/ /mL). Two independent experiments were tested and the results were confirmed by constructing a dose-response curve using Prism 5 (Figure 4.16 **A**).

IC$_{50}$ of B3-1

A. IC$_{50}$ value of B3-1.

| DNA | Neg | Cip | Nov | 300 | 100 | 30 | 10 | 3 | 1 | 0.3 | 0.1 µg/mL |

Rel

Sc

1 2 3 4 5 6 7 8 9 10 11 12
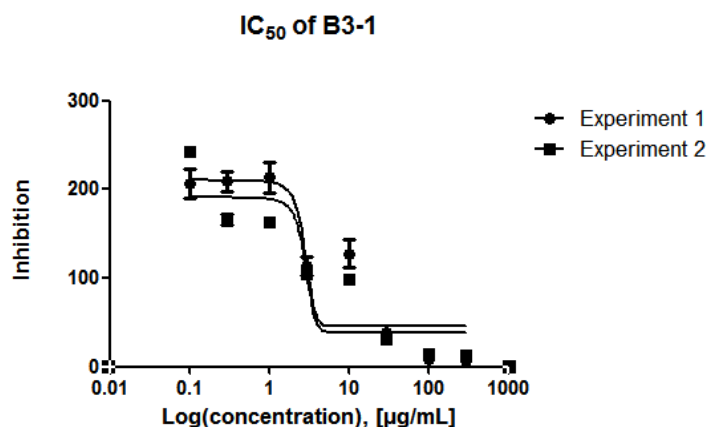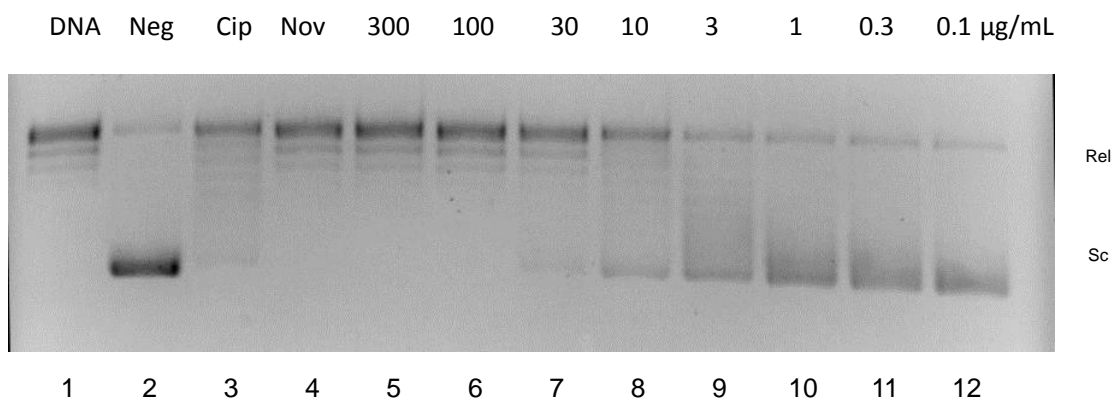
B. IC$_{50}$ assay of B3-1.

Figure 4.16. **IC$_{50}$** assay of compound B3-1; from 31.27-34.03 µg /mL. Test concentration of B3-1 was from 0.1 to 300 µg /mL on the relaxation plasmid pBR322 DNA (0.5 µg) incubating with 1.5 U of *S. aureus* gyrase. Rel, relaxed DNA bands; Sc, supercoiled DNA bands.

The calculated IC$_{50}$ value for B3-1 using dose-response curve fit analysis is from 31.27 to 34.03 µg /mL (Figure 4.16), compared with the DNA control, no supercoiled DNA bands were observed in lane 5 and 6, *S. aureus* gyrase could only be fully inhibited in the presence of a very high concentration of B3-1 (100-300 µg /mL, lane 5, 6). Supercoiled DNA bands could be observed in lane 10-12, but the edges of the supercoiled bands were indistinguishable, which indicated that the enzyme could be partially inhibited by compound B3-1. As discussed in section 4.6.4.1, the inhibitory mode of B3-1 might be different depending on the substitution atom at position 1 and 5; the compound could either mimic the structure of quinolone or quercetin derivative.

4.6.5.3 Half maximal inhibitory concentration assay of compound B3-9

The inhibition of gyrase was examined by measuring the density of supercoiled DNA bands in the presence of decreasing concentration of B3-9 (300-0.1 µg/ /mL) (Figure 4.17 **A**).
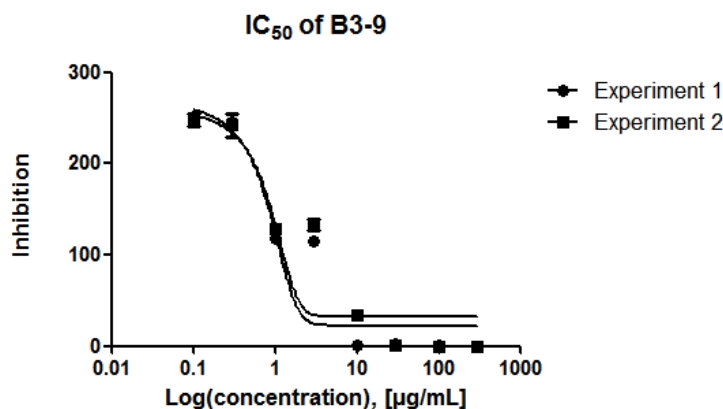
A. IC_{50} value of compound B3-9.
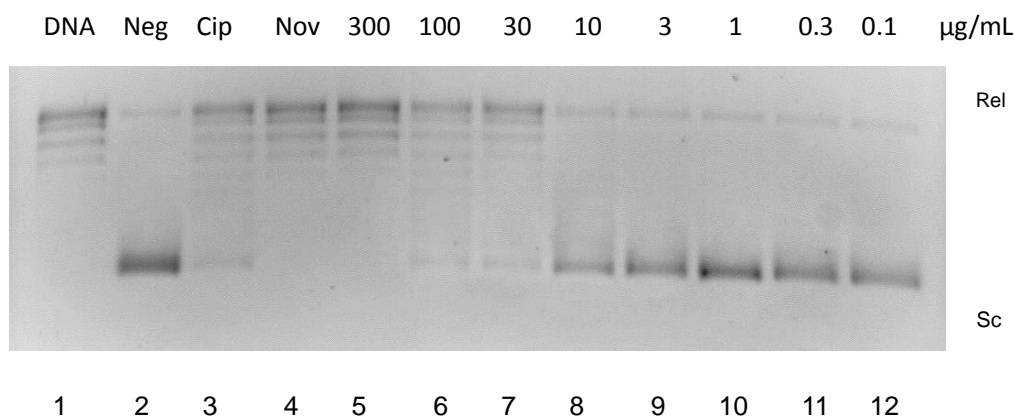
B. IC_{50} assay of compound B3-9.

Figure 4.17. IC_{50} assay of compound B3-9; from 5.39-6.18 µg /mL. Test concentration of B3-9 was from 0.1 to 300 µg /mL on the relaxation plasmid pBR322 DNA (0.5 µg) incubating with 1.5 U of *S. aureus* gyrase. Rel, relaxed DNA bands; Sc, supercoiled DNA bands.

The inhibitory activity could be observed at high concentration of B3-9, from 30-300 µg /mL, faint supercoiled DNA bands and strong relaxed DNA bands were observed in lane 5, 6 and 7, indicated that, the gyrase activity could not be inhibited or reduced by B3-9. It proposed to be a coumarin derivative and had a good IC_{50} value of 5.39-6.18 µg /mL, compared to the positive control novobiocin (3.97-7.18 µg /mL).

The mode of action of the inhibitory activity might be bound with the GyrB by interfering the ATPase activity. The interaction was between the compound and

24KDa fragment on GyrB could be intermediated by the hydroxyl groups on the proposed ring structure. The mode of action was illustrated using a known gyrase inhibitor, novoamine is shown in Figure 4.18 (Lewis et al., 1996).
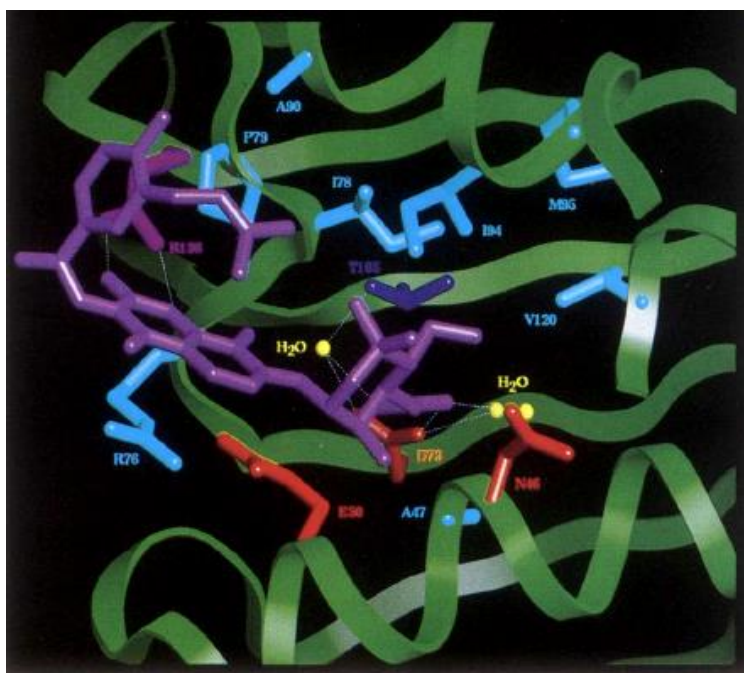
A. The substituted resorcinol structure skeleton binds to the hydrophilic protein pocket on GyrB through water-mediated hydrogen bonds systems, directly copied from Lewis's publication (Lewis et al., 1996). The structure of novobiocin is shown in purple, water molecules are shown in yellow. Directly copied from Lewis's publication.
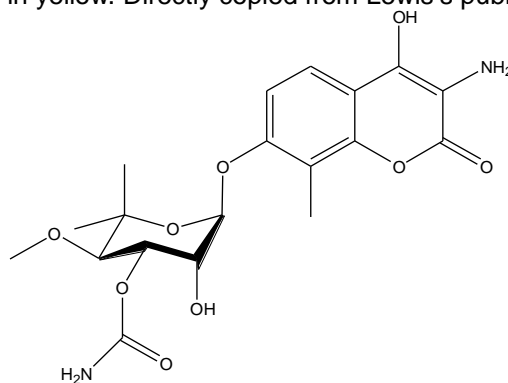
B. Structure of novoamine (Berkov-Zrihen et al., 2012).

Figure4.18 Proposed mode of action of compound B3-9 and structure of novoamine

The hydrogen bonds system of novobiocin was suggested by Althaus and showed in Figure 4.18, with three molecules of water-mediated hydrogen binding system., The resorcinol skeleton is the vital moiety that interacts with the enzyme's amino acids and interfering with the gyrase activity (Althaus et al., 1996, Reusser and Dolak, 1986). However, the sugar moiety of the structure may help the molecule structure wrap around the hydrophobic amino acids pocket of the enzyme, but play no part in anti-gyrase and anti-bacterial activities.

4.6.5.4 Half maximal inhibitory concentration assay of compound B3-12

The inhibition of gyrase was examined by measuring the density of supercoiled DNA bands in the presence of decreasing concentration of B3-12 (300-0.1 µg/ /mL). (Figure 4.19 **A**).
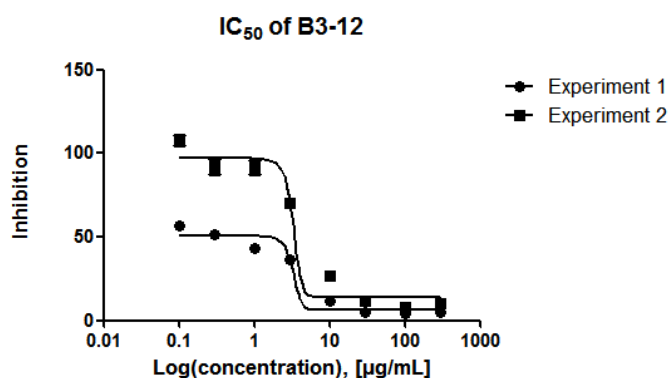
A. IC_{50} value of compound B3-12.
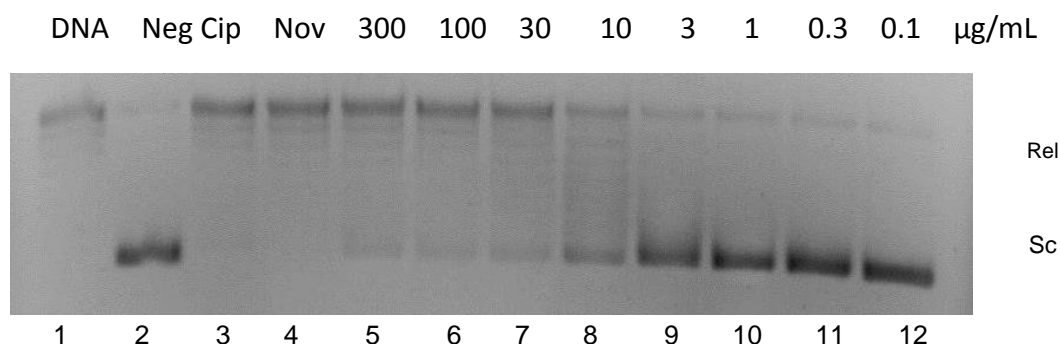
B. IC_{50} assay of compound B3-12.

Figure 4.19. IC_{50} assay of compound B3-12; from 475-2065 µg /mL. Test concentration of B3-12 was from 0.1 to 300 µg /mL on the relaxation plasmid pBR322 DNA (0.5 µg) incubating with 1.5 U of *S. aureus* gyrase. Rel, relaxed DNA bands; Sc, supercoiled DNA bands.

Gyrase activity could not be fully inhibited at the proven test concentration (300 µg /mL); some supercoiled bands could still be seen in lane 6. More relaxed DNA bands with more linking numbers could be observed in lane 6-8. In lane 9-12, a single heavy band of supercoiled DNA bands could be seen at the bottom of the gel, indicated that the sample was not active. The IC_{50} value of B3-12 was calculated from 475-2065 µg /mL, confirming that the compound B3-12 was not very active as a potential gyrase inhibitor.

4.7 Conclusion

Compounds isolated from the butanol extract from *E. annuus* exhibited potential gyrase inhibitory activity against *S. aureus* gyrase. The IC_{50} values were observed at B3-1: 31.27-34.03 µg/mL; B3-9: 5.39-6.18 µg/mL and B3-12: 475-2065 µg/mL. Compared to the positive control novobiocin 3.97-7.18 µg/m, compound B3-9 had a good IC_{50} value against *S. aureus* gyrase suggested that, the 1, 4-benzopyrone based analogue B3-9 could be used as Gram-positive bacterial gyrase inhibitor.Compounds isolated from hexane fractions this research were proven to have anti-bacterial activities against *S.aureus* strain. However, they did not show any activity in the DNA gyrase supercoiling assays.

DNA gyrase is an essential enzyme required during the replication and transcription of the bacterial chromosome. It is a natural target of antibiotics. However, the investigations of gyrase inhibitory activity of these compounds are still need to be carried out in the future and their full structure elucidation was warranted.

5. *Chapter V: Mutagenicity assays on haploid Saccharomyces cerevisiae ade2*

5.1 Introduction

5.1.1 *In vitro* mutagenicity assays

Genotoxic chemical agents can induce both direct and indirect effects in DNA, leading to somatic cell effects or heritable mutations. Most genotoxic damage can be repaired and the cells never show mutagenesis, however, some mutations may develop from this damage (Sen et al., 2011). The occurrence of mutations can be enhanced by certain compounds, and these compounds are defined as mutagens. Mutagens can be categorized into three types according to their mutagenic mechanisms: base analogues, modifying DNA and intercalating DNA.

Ethylmethane sulfonate (EMS) ($CH_3SO_3C_2H_5$) is a strong mutagen, frequently used as a positive control in mutagenicity tests. EMS is a alkylating agent that can modify the structure of guanine by adding a methyl group to the O^6 position and forming O^6-methylguanine (Rhaese and Rhaese, 1973). The O^6–methylguanine can weakly pair with thymine during DNA replication, leading to a base-pair mispairing from GC to AT (Figure 5.1 **A**).
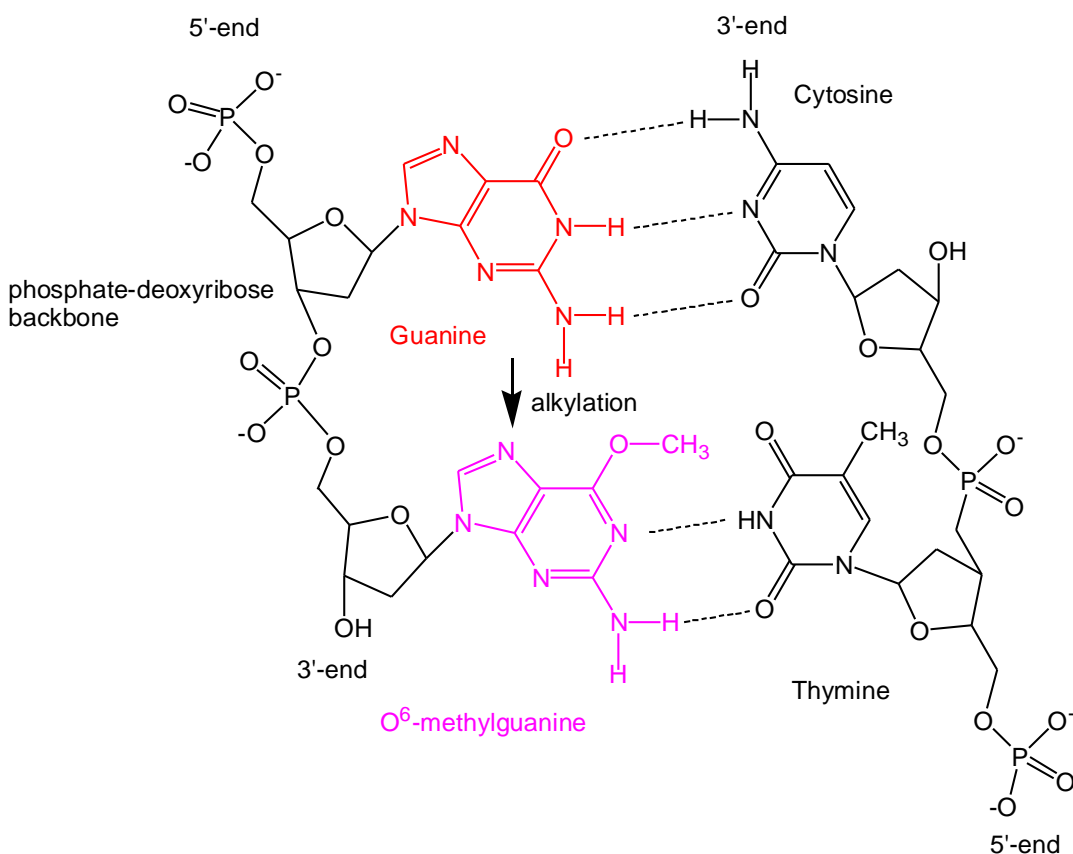
A. EMS Methylation of guanine(red) into O^6 –methylguanine (pink)(Brown and Brown, 1992).
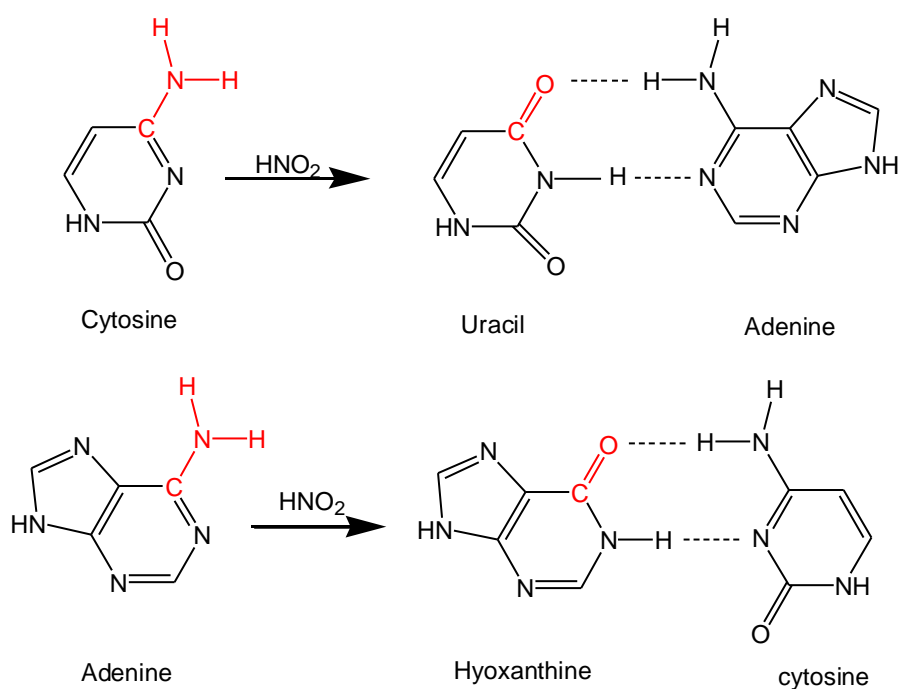
B Nitrous acid deaminates cytosine and adenine (red). Hydrogen bonds shown in dotted lines.

Figure 5.1 Modes of action of mutagen EMS and HNO_2.

Another frequently used mutagen is nitrous acid (HNO_2), which was first reported by Steinberg and Thom in 1940 when it was used as a mutagen on fungi (Steinberg, 1940). It acts through the oxidative deamination of amines to replace an amino group by a hydroxyl group (Zimmermann, 1977). For example, nitrous acid can deaminate cytosine and adenine to uracil (pair with adenine) and hypoxanthine (pair with cytosine), leading to GC to AT and AT to GA transition.

Mutagenicity assays are genetic tests for detecting mutagens which can cause heritable DNA damage in cells or organisms (Eastmond et al., 2009). *In vitro* assays include bacterial tests for gene mutations (eg. Ames tests) (Claxton et al., 2010), tests for chromosomal mutations (eg. chromosomal aberration tests) (Cao et al., 2002), and mammalian cell mutation assay (eg. comet assay) (Sasaki et al., 2007). The technique of the Ames test is simple and sensitive (Figure 5.2).

5.1.2 The Ames test

The Ames test is one of the most frequently used bacterial mutagenicity assays. It can be used to assess the genotoxicity/mutagenicity of potential carcinogens (Wexler, 2014). The procedures were described in the 1970s by Bruce Ames and his research team in the University of California, Berkeley (Ames et al., 1975, Dorothy and Bruce, 1983). Different *Salmonella typhimurium* (Joyce et al., 1975) or *Escherichia coli* amino acid auxotrophic mutants (Watanabe et al., 1998) are employed in the assay. Further mutations can restore the ability to synthesize the specific amino acid: these mutations are reverse mutations. An increase of two-fold or more in mutation frequency can suggest that a test compound is acting as a mutagen, and many mutagens have also been shown to be carcinogens. The Ames test has proven to be very sensitive and reliable in detecting mutagenic activities (Flückiger-Isler and Kamber, 2012, Lo et al., 2004, Maron et al., 1981). However, *Samonella typhimurium/ Escherichia coli* are prokaryotic, and are not a perfect model for mammalian cells. They contain only a single circular chromosome, and they cannot represent diploid cells which undergo meiosis (Masters, 1989). Supernatant fraction S9 from rat liver is often incorporated in the assay which provides a source of monooxygenase activity for the metabolic activation of pro-carcinogens (Lewis and Lewis, 2005), for example, metabolites of benzo[α]pyrene by cytochrome P450 enzymes are mutagenic and highly carcinogenic (Wong, 1998). The test is described in Figure 5.2.
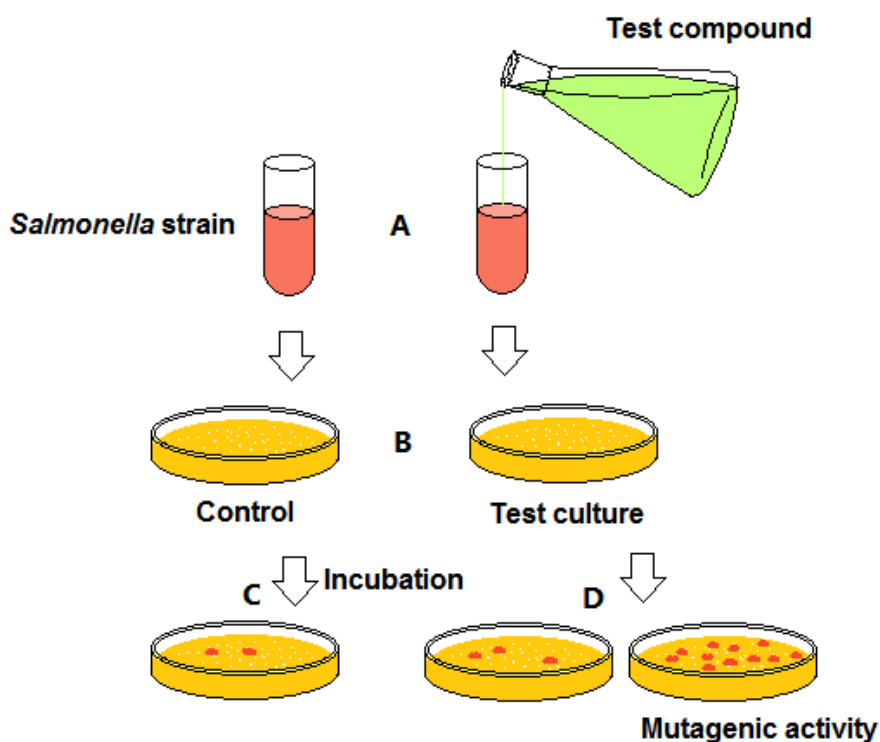
Figure 5.2 Ames test. **A.** preparation of the histidine requiring *Salmonella* strain, and the test compounds are added. **B.** plate out on glucose-minimal medium (no histidine). **C.** low back ground mutation rate of *Salmonella* His⁻ to His⁺. **D.** some compounds showed no mutagenic activity and some plates with a higher number of His⁺ colonies indicate mutagenic activity. This picture was adapted from the published book (Perry et al., 2002b).

A histidine requiring *Salmonella* strain is normally used, as it has a single mutation in the *Salmonella* genome of an enzyme involved in histidine biosynthesis. The bacterial cultures are treated with test compounds and plated on the minimal media lacking in histidine. The control has no test compounds and is plated on the same minimal media plates. After incubation, a low colony count would be expected in the control group, and it will be seen if the His⁻ *Salmonella* can mutate back to the original genotype, produce their own histidine and survive on the minimal media. If the test compound is mutagenic, an increasing frequency of back mutation colonies will be observed on the minimal media.

5.1.3 Yeast test systems

Yeast is a unicellular and uninuclear eukaryote, auxotrophic yeast strains are often used by yeast geneticists for testing mutagens (Fink, 1969). Growing yeast is rapid and simple. It provides a rapid and sensitive response to the mutagenic compounds. Mutagenicity and carcinogenicity are closely correlated (Benigni and Benigni, 2011),

and as eukaryotes, studying in yeast cells could help to discover the potential carcinogens which only showed their carcinogenicity after metabolized by cytochrome P450 system. Necessitating the testing of chemical agents to help to discover potential carcinogens. Mutagenicity tests of yeast strains share the same *in vitro* procedures (Rao et al., 2000).

.

5.1.4 *Saccharomyces cerevisiae* ade2

Saccharomyces cerevisiae, usually known as fermenting yeast, has both haploid and diploid strains (Zimmermann, 1975). The haploid cells are either an **a** or an **α** mating type. The diploid cell is formed by conjugation of an **a**-cell and an **α**-cell. In the rich medium, the yeast cells reproduce by mitosis, while under carbon and nitrogen starvation, the diploid cell undergoes meiosis to produce two **a** type spores and two **α** type spores (Figure 5.3).
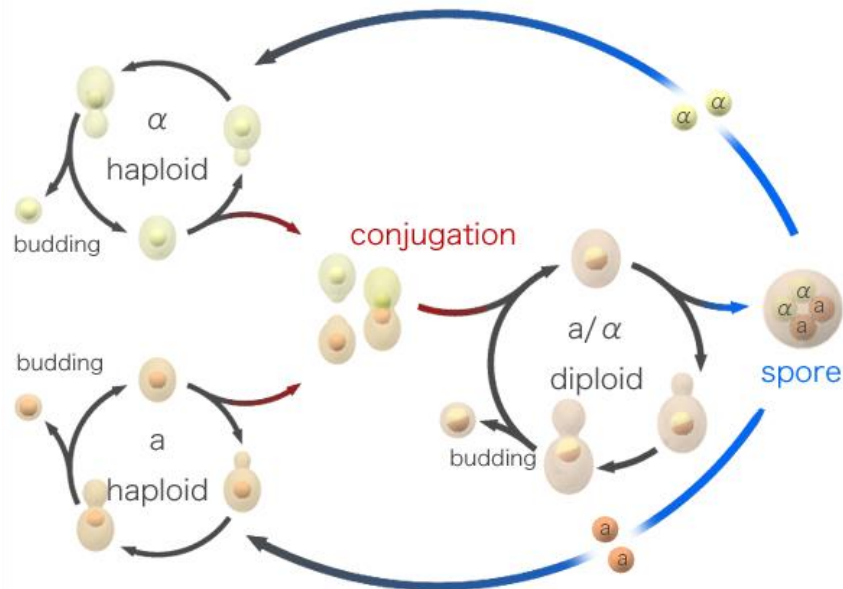
Figure 5.3 Life cycle of *Saccharomyces cerevisiae*: budding; conjugation; sporation (directly copied from *Saccharomyces* Genome Database).

Saccharomyces cerevisiae is commonly employed in eukaryotic mutagenicity tests to detect the mutagenic potential of chemical compounds. This method was first developed by Zimmermann in the 1970s (Zimmermann, 1973). Culturing yeast cells is simple, economical and rapid (Paul, 2001) , and mutagenesis could develop during

the processes of replication, recombination and repair of the yeast DNA. Additionally, *S.cerevisiae* has identical porosity in it's cell wall which, when distinguished from prokaryotic bacteria, contains more membrane protein components.
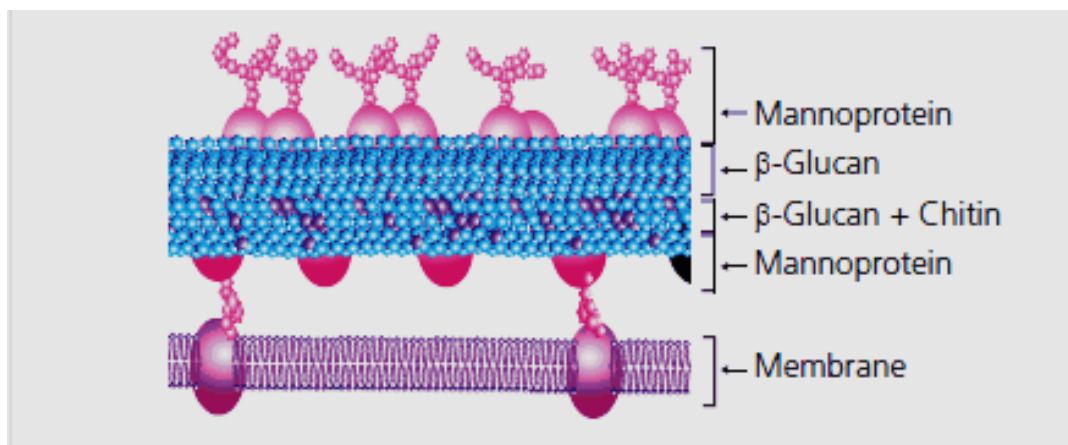
Figure 5.4 Yeast cell wall, picture copied from McClanahan's publication (McClanahan, 2009).

The cell wall makes up 15 - 30 % of the dry weight of the cell and is mostly mannoprotein and β-glucan (Lipke, 1998)(Figure 5.4). β-glucan-chitin complex is the matrix for mannoproteins and provides the skeleton of the cell wall (Kollár, 1997).

Yeast cells do not make adenine as a separate compound: the adenine appears as adenosine monophosphate (AMP) attached to the sugar-phosphate compound called phosphoribosylpyrophosphate (PRPP)(Figure 5.5). AMP is a nucleotide, a component of DNA, RNA and ATP. The synthesis of AMP requires a 12 step purine biosynthetic pathway. However, if adenine is applied in the medium, the cell can convert it to AMP by a one-step salvage pathway of purine nucleotide biosynthesis, catalyzed by adenine phosphoribosyltransferase. Wild type yeast cells are able to carry out the 12 step biosynthetic pathway, catalyzed by different gene coded enzymes, while mutants with any *adeX* gene mutations require adenine in the medium as they can convert adenine to AMP by the salvage pathway only.

Many mutants of *S. cerevisiae* have been isolated which have mutations in genes in the adenine biosynthetic pathway, and some of the genotypes are good markers for mutagenicity tests (Stotz and Linder, 1990). The *ade*2 gene encodes for AIR-carboxylase (5'- phosphoribosylaminoimidazole) which catalyzes the sixth step of the purine biosynthetic pathway in *S.cerevisiae* (Figure 5.5) (Gedvilaite and Sasnauskas, 1994). *S. cerevisiae ade*2 is unable to precede the synthetic pathway by repressing the enzyme transcription and leading to an accumulation of the metabolic

intermediate AIR. AIR can be oxidized to a red pigment giving a red phenotype to mutant colonies (K. Rébora et al., 2001).
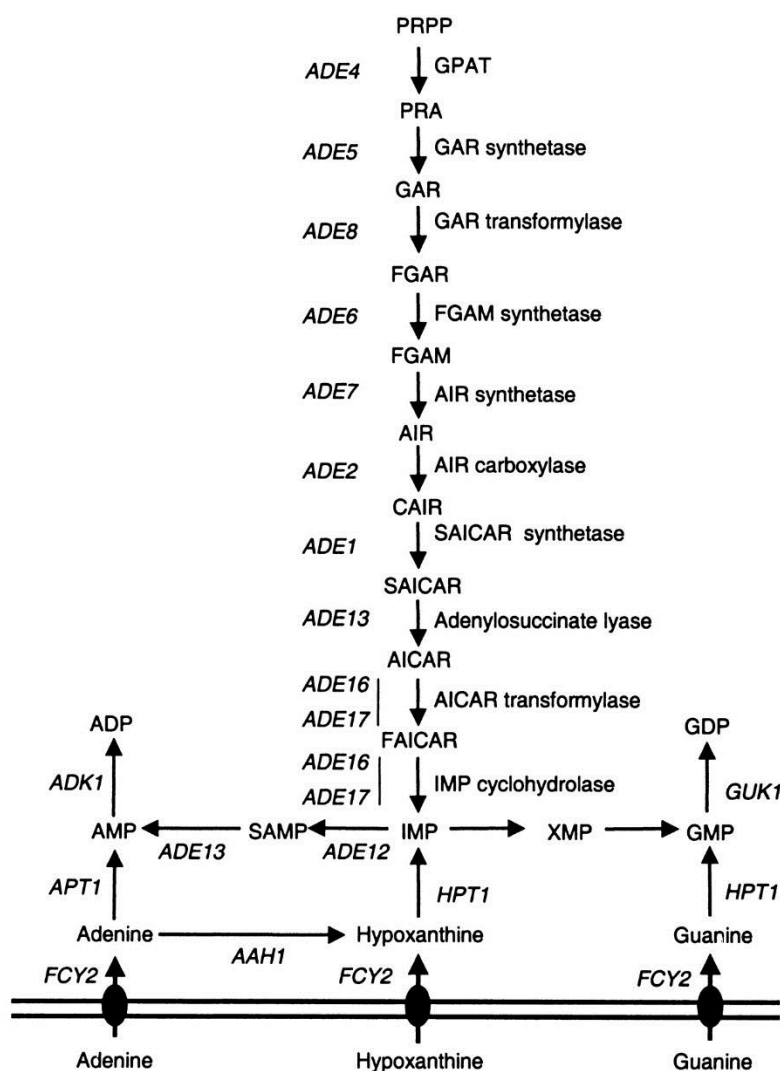
.Figure 5.5 Purine biosynthetic pathway in *S.cerevisiae.*This picture was copied from Renora's publication (K. Rébora et al., 2001).

Mutagenesis can be detected when mutagens induce a forward or reverse mutation on the synthetic pathway genes (*ade/ADE* genes)*.* For example, if the *ade2* mutant mutates backwards to the wild type by removing the repression of the *ade2* gene, the yeast cell would be able to synthesize AMP, and no more AIR accumulations would appear in the cell. The colonies would be able to grow on the adenine-limited medium, and form white colonies. Forward mutations refer to those mutations in the other genes in the purine metabolism pathway (*eg. ade8* gene in the pathway shown in Figure 5.5). The *ade2* gene will not repress in the pathway, and no more AIR will be accumulated. However, the cells still cannot synthesize AMP and the forward mutant

colonies will not grow on minimal medium. This may also lead to a change in phenotype, in which case the colony will change back to white. Strains which have auxotrophic mutations upstream in the adenine biosynthetic pathway include *S.cerevisiae ade4, ade5, ade6, ade7 and ade8.*

The prototrophic colonies for wild type *S.cerevisiae* are white; in the mutant *S. cerevisiae ade2*, the haploid *ade2* colonies are phenotypically red, while the diploid colonies may produce sectored colonies after mating. A sectoring assay is used on the detection and separation of different mutants (Gedvilaite and Sasnauskas, 1994, Abdulovic et al., 2006), and mutagenicity assays are used to characterize the mutation frequency and type of the selected mutants.

| **A** | **B** |
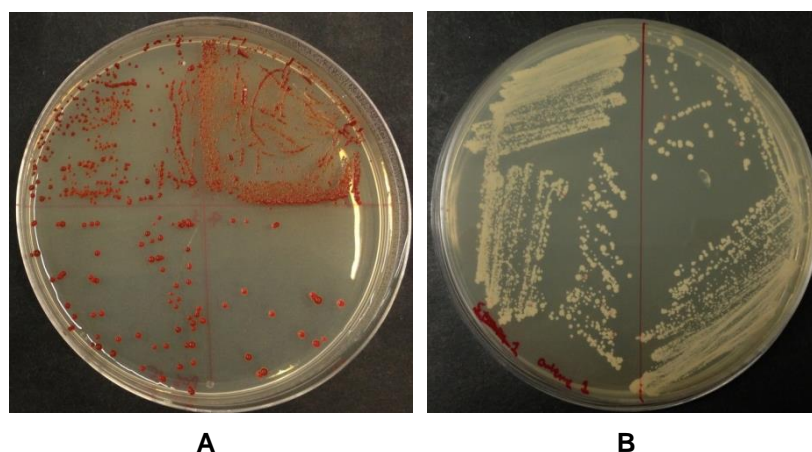
Figure 5.6 Haploid colonies of *S. cerevisiae* **A.** *ade2* mutant colonies. **B.** wild type colonies.

In the haploid strain, the wild type colonies are white and the *ade2* mutant colonies are red (Figure 5.7). This phenotypic change has been used as an assay for monitoring genetic events and will be used to determine mutagenicity in this work (Couteau et al., 2008).

5.2 Materials and Experiment preparation

Haploid adenine and tryptophan requiring *Saccharomyces cerevisiae ade2* mutant NCYC830 (mating type **a**) were obtained from the National Collection of Yeast Cultures (NCYC), Norwich, UK. Haploid adenine requiring *Saccharomyces cerevisiae ade2* mutant Ha2/WF17-3624 (mating type **a**) was obtained from Blades Biological Ltd, Cowden, UK.

Yeast extract agar CM0019, technical agar (agar No.3) LP0013 and Yeast extract LP0021, dextrose (for bacterial culture), Ringer's solution tablets BR0052 were all purchased from OXOID microbiology, Thermo Fisher scientific, Loughborough, UK. Ethyl methanesulfonate, sodium nitrite and adenine were purchased from Sigma-Aldrich® Dorset, UK. Ninety-six well plates were acquired from Nunclon™ brand, Sigma-Aldrich®. Eppendorf centrifuge (0.5, 1.5 mL) tubes were used for fraction collections and originated from Hamburg, Germany.

Different media and solutions were prepared before the mutagenicity tests. Yeast extract liquid (YEL) was made of 1% yeast extract and 2% dextrose in water. Yeast extract agar (YEA) was made of YEL supplemented with 2% agar. Extra adenine was added to YEA to allow growth of adenine requiring mutants, however, in the medium the mutant will not develop the characteristic red pigment (YEDA). Extra peptone was added to YEDA to make a very rich medium for storing yeast strains (YEPAD). Minimal plus vitamin medium was made up with minimum of chemical ingredients, include 0.52% ammonium sulfate, 2% dextrose with 2% agar in water. It is necessary to support growth of wild type yeast (MV). Minimal plus vitamins adenine medium (MV+Ade) had excess adenine added to allow growth of adenine auxotrophic mutants, however, the mutants will not develop the characteristic red pigment.

5.3 Mutagenicity assay on haploid *S. cerevisiae* ade2

5.3.1 Mutagenicity assay method

A culture of *S. cerevisiae ade2* was prepared from a freeze-dried culture, sealed in a glass ampoule. 0.5 mL of YEL was added to the dried culture, the ampoule was gently suspended and the mixture was transferred to a culture bottle containing 10 mL YEL. The culture was incubated at 25 °C for five days before the test (protocol from the NCYC).   New cultures were grown for the test from the generation 1 culture on YEA.

Ninety-six well microtitre plates were used for the tests. The designated concentration of test samples were 500, 250, 125, 62.5, 31.3, 15.6 and 7.8 µg/mL in 1% DMSO. The turbidity of inoculum was compared with McFarland standard 1.0 (1×10^8 cfu/mL) and diluted with yeast extract liquid eight times before inoculation. EMS solution and nitrous acid solution were used as positive controls at 500 µg/mL (National Toxicology Program, 2011). 1% DMSO in Ringer's solution was used as a negative control.

125 µL of YEL were dispensed to every well in 96 well microtitre plates, followed by dispensing 125 µL of controls and test samples in the first well of every two rows. Samples and controls were double diluted across the plate, followed by adding 125 mL of yeast inoculum. The plate was incubated at 28 $^{\circ}$C for 48 hours.

After 48 hours incubation, the cells in each well of the test plate were transferred into 200 µL of Ringer's solution centrifuged at 2500 r.p.m and washed twice before suspending in 200 µL of Ringer's solution. Every 20 µL of yeast suspension were diluted from 10^{-1} to 10^{-4} across 96 well plates; 40 µL of yeast suspension were spread onto two half yeast extract agar (YEA) plates for counting the white colonies; 20 µL of the suspension was spread onto a quarter platse and diluted for assessing total viable count. All test plates were incubated at 28 $^{\circ}$C for 72 hours to allow the red pigment to accumulate.

After 72 hours of incubation, colony counting of white mutants was obtained by counting the white colonies on the red adenine requiring colony backgrounds from the test plates. Enumeration from the 10^{-4} plates was used to calculate colony forming units (cfu) for red colonies in each well. The mutation frequencies were calculated as follows:

Colony forming units (cfu/ cm^3)= colony count x 1/dil. factor x 1/vol.
Mutation Frequencies (MF) = number of viable white colonies / total number of viable colonies x10^6 .

5.3.3 Characterization of mutants

After the colony counting, all agar plates were kept at 28 $^{\circ}$C for another 48 hours to let the white colonies develop. After 48 hours, white colonies from the test plates were transferred with care on to minimal medium agar (MV) and minimal medium agar +adenine (MV+ade) plates using sterilized toothpicks. Those mutants with forward mutations in the purine metabolism pathways would not grow on MV, and were still adenine requiring strains.

5.4 Results and Discussion

5.4.1 Mutagenic response of *S. cerevisiae* ade2

Extracts H1-4, E1-4, and B1-4 were tested against *S. cerevisiae ade2*. The starting concentration of each extract was the same as the positive controls (500 µg/mL in 1% DMSO). 1% DMSO was used as the negative control and samples were plated on YEA. Calculation of cfu/cm^3 was obtained from 10^{-4} dilutions. The results are presented in Table 5.1 **A-D.**

Table 5.1 Mutagenic assay against *S. cerevisiae ade2*.

A. Number of white colonies (cfu/cm^3).

Sample		7.8	15.6	31.3	62.5	125	250	500 µg/mL
Neg	Exp.1	925	700	575	1850	475	500	275
	Exp.2	400	650	300	1775	625	775	450
EMS	Exp.1	1025	1275	1675	1050	950	1050	2850
	Exp.2	875	925	2000	1275	1025	1150	1850
HNO₂	Exp.1	400	525	525	475	325	275	825
	Exp.2	175	350	250	325	525	225	475
H1	Exp.1	425	225	525	250	0	0	0
	Exp.2	25	50	275	200	275	0	0
H2	Exp.1	500	525	475	225	50	0	0
	Exp.2	+	875	1300	+	425	0	0
H3	Exp.1	475	150	75	200	50	0	0
	Exp.2	350	350	575	550	350	0	0
H4	Exp.1	300	300	50	50	0	0	0
	Exp.2	+	2250	1050	450	375	0	0
E1	Exp.1	625	25	0	2550	300	50	0
E2	Exp.1	200	150	0	175	675	50	125
E3	Exp.1	200	625	100	25	325	350	100
E4	Exp.1	0	50	1175	+	25	50	50
B1	Exp.1	2350	675	700	+	775	1025	1050
B2	Exp.1	400	25	0	175	25	0	50
B3	Exp.1	675	1000	775	1050	975	50	200
B4	Exp.1	750	475	475	1075	375	425	925

+: over growth of the mutant colonies.

Exp: experiment.

B. Number of viable cells (cfu/cm^3) X 10^6.

Sample		7.8	15.6	31.3	62.5	125	250	500 µg/mL
Neg	Exp.1	12.5	10.5	11.0	12.0	20.0	14.0	10.0
	Exp.2	17.5	10.5	12.0	12.5	16.0	7.5	12.5
EMS	Exp.1	8.5	10.0	10.5	11.0	6.0	10.0	3.0
	Exp.2	6.0	7.5	9.0	5.5	4.5	5.0	7.5
HNO$_2$	Exp.1	5.5	8.5	7.5	8.0	8.5	5.0	6.5
	Exp.2	7.0	8.0	6.0	7.5	6.0	4.5	9.0
H1	Exp.1	10.0	8.5	4.5	3.0	6.5	0.5	**0.0**
	Exp.2	9.0	4.0	5.0	6.0	7.5	1.0	**0.0**
H2	Exp.1	4.0	6.0	6.5	4.0	3.5	3.5	**0.0**
	Exp.2	13.0	10.0	12.0	12.5	10.0	2.5	**0.0**
H3	Exp.1	6.5	4.0	5.5	5.0	3.0	1.5	**0.0**
	Exp.2	9.5	10.0	10.5	12.5	9.0	2.5	**0.0**
H4	Exp.1	2.5	8.0	2.0	1.5	1.0	**0.0**	**0.0**
	Exp.2	11.0	10.0	6.0	2.5	2.5	**0.0**	**0.0**
E1	Exp.1	24.5	12.0	12.5	10.5	15.0	13.0	7.0
E2	Exp.1	8.0	5.5	4.5	12.0	3.0	4.5	0.5
E3	Exp.1	8.5	5.5	9.0	3.0	7.5	1.5	5.5
E4	Exp.1	10.0	11.5	8.5	9.5	3.0	3.0	8.0
B1	Exp.1	10.5	10.0	6.5	8.0	10.5	12.0	5.0
B2	Exp.1	7.0	4.5	10.5	8.5	7.0	5.0	2.5
B3	Exp.1	11.0	13.0	7.5	31.5	15.5	22.5	9.5
B4	Exp.1	3.0	7.0	6.0	11.0	2.0	9.5	9.0

C: Number of mutants/ 10^6 survivors.

Sample		7.8	15.6	31.3	62.5	125	250	500µg/mL
Neg	Exp.1	74.0	66.7	52.3	**154.2**	23.8	35.7	27.5
	Exp.2	22.9	61.9	25.0	142.0	39.1	103.3	36.0
EMS	Exp.1	120.6	127.5	159.5	95.5	158.3	105.0	**950.0**
	Exp.2	145.8	123.3	222.2	231.8	227.8	230.0	246.7
HNO$_2$	Exp.1	72.7	61.8	70.0	59.4	38.2	55.0	**126.9**
	Exp.2	25.0	43.8	41.7	43.3	87.5	50.0	52.8
H1	Exp.1	42.5	26.5	116.7	83.3	0.0	0.0	0.0
	Exp.2	2.8	12.5	55.0	33.3	36.7	0.0	0.0
H2	Exp.1	125.0	87.5	73.1	56.3	14.3	0.0	0.0
	Exp.2	0.0	87.5	108.3	0.0	42.5	0.0	0.0
H3	Exp.1	73.1	37.5	13.6	40.0	16.7	0.0	0.0
	Exp.2	36.8	35.0	54.8	44.0	38.9	0.0	0.0
H4	Exp.1	120.0	37.5	25.0	33.3	0.0	0.0	0.0
	Exp.2	0.0	225.0	175.0	180.0	150.0	0.0	0.0
E1	Exp.1	25.5	2.1	0.0	**242.9**	20.0	3.8	0.0
E2	Exp.1	25.0	27.3	0.0	14.6	**225.0**	11.1	**250.0**
E3	Exp.1	23.5	113.6	11.1	8.3	43.3	233.3	18.2
E4	Exp.1	0.0	4.3	138.2	0.0	8.3	16.7	6.3
B1	Exp.1	223.8	67.5	107.7	0.0	73.8	85.4	210.0
B2	Exp.1	57.1	5.6	0.0	20.6	3.6	0.0	20.0
B3	Exp.1	61.4	76.9	103.3	33.3	62.9	2.2	21.1
B4	Exp.1	**250.0**	67.9	79.2	97.7	187.5	44.7	102.8

-: cannot be calculated because of overgrowth.

D. Survival (Number of viable cells / Number of viable cells of negative control, %).

Average survivors in Negative control (x10⁶)		7.8	15.6	31.3	62.5	125	250	500 µg/mL
		15.0	10.5	11.5	12.25	18.0	10.75	11.25
EMS	Exp.1	56.7	95.2	91.3	89.8	33.3	93.0	26.7
	Exp.2	40.0	71.4	78.3	44.9	25.0	46.5	66.7
HNO₂	Exp.1	36.7	81.0	65.2	65.3	47.2	46.5	57.8
	Exp.2	46.7	76.2	52.2	61.2	33.3	41.9	80.0
Neg	Exp.1	83.3	100.0	95.7	98.0	111.1	130.2	88.9
	Exp.2	116.7	100.0	104.3	102.0	88.9	69.8	111.1
H1	Exp.1	66.7	81.0	39.1	24.5	36.1	4.7	0.0
	Exp.2	60.0	38.1	43.5	49.0	41.7	9.3	0.0
H2	Exp.1	26.7	57.1	56.5	32.7	19.4	32.6	0.0
	Exp.2	86.7	95.2	104.3	102.0	55.6	23.3	0.0
H3	Exp.1	43.3	38.1	47.8	40.8	16.7	14.0	0.0
	Exp.2	63.3	95.2	91.3	102.0	50.0	23.3	0.0
H4	Exp.1	16.7	76.2	17.4	12.2	5.6	0.0	0.0
	Exp.2	73.3	95.2	52.2	20.4	13.9	0.0	0.0
E1	Exp.1	163.3	114.3	108.7	85.7	83.3	120.9	62.2
E2	Exp.1	53.3	52.4	39.1	98.0	16.7	41.9	4.4
E3	Exp.1	56.7	52.4	78.3	24.5	41.7	14.0	48.9
E4	Exp.1	66.7	109.5	73.9	77.6	16.7	27.9	71.1
B1	Exp.1	70.0	95.2	56.5	65.3	58.3	111.6	44.4
B2	Exp.1	46.7	42.9	91.3	69.4	38.9	46.5	22.2
B3	Exp.1	73.3	123.8	65.2	257.1	86.1	209.3	84.4
B4	Exp.1	20.0	66.7	52.2	89.8	11.1	88.4	80.0

The mutagenicity tests showed inconsistent results against *S. cerevisiae ade2*, and showed high background mutation frequencies in the negative control groups. According to Ohnishi's research, the spontaneous mutation rate of haploid *S.cerevisiae* should be in the range of 10^{-7}, and the mutation rate of diploid cells could reach the range of 10^{-4} (Ohnishi et al., 2004). However, the highest background mutation frequency value was observed at 154.2×10^{-6} (Table 5.1 **C** Neg. exp. 1) in this research, which is higher than the lowest mutation frquency value in positive control nitrous acid (Table 5.1 **C** nitrous acid) and 10-fold higher than the expected value range. Further experiments were carried out to investigate these results. The highest mutation frequency value for the positive control EMS, was 950×10^{-6} (Table 5.1 **C** EMS exp. 1), while the highest mutation frequency value of nitrous acid was 126.9×10^{-6} (Table 5.1 **C** nitrous acid, exp. 1). The mutation frequency of EMS at 31.3 µg/mL was $159.5\text{-}222.2 \times 10^{-6}$ ($1.59\text{-}2.22 \times 10^{-4}$) and was ten times more effective when compared with published research: 15.44×10^{-4} at 36.18 µg/mL (Hannan, 1978). The ideal mutagen frequency values of positive controls should decrease along the dilution; however, none of the test results showed a dose-response relationship, however, there was some indication of mutagenic activity by EMS at the highest concentration.

The survival rates, listed in Table 5.1 **D**, were calculated against the number of total viable cells in the negative control. It showed inconsistent results and may have beeen affected by the overgrowth observed.

In the test candidate groups, samples H1 to H4 showed cytotoxicity against *S. cerevisiae* (see Table 5.1 **B**). According to the survival rate calculation, no yeast cells survived in the presence of 500 µg/mL of each hexane fraction Table 5.1 **D**) and no growth was observed after exposure to 250µg/mL in fraction H4. The cytotoxicity results were consistent with the antibacterial results in chapter III, and growth inhibition could be observed on both bacteria and yeast cells when the tested strains were exposed to a high concentration of fraction H1, H2, H3, and H4.The fractions may contain compounds which interfere with mannoprotein functions or inhibit glucan synthesis (Ghannoum, 1999). However, as yeasts are eukaryotes, compounds that are toxic to yeast cells may also be toxic to human cells. *In vivo* tests on antifungal drugs (eg.Fluconazole) exhibited side effects such as headache, rash, indigestion and abdominal pain were found when administrating orally (Dixon and J., 1996).

5.4.2 Characterisation of mutants

After the colony counting, all agar plates were kept at 28 $^{\circ}$C for another 48 hours to let the white colonies develop. After 48 hours, white colonies from the test plates were transferred on to minimal medium agar (MV) and minimal medium agar +adenine (MV+ade) plates with sterilized toothpicks. Double mutants will grow on MV+ade medium, but they will not show the characteristic red colour.
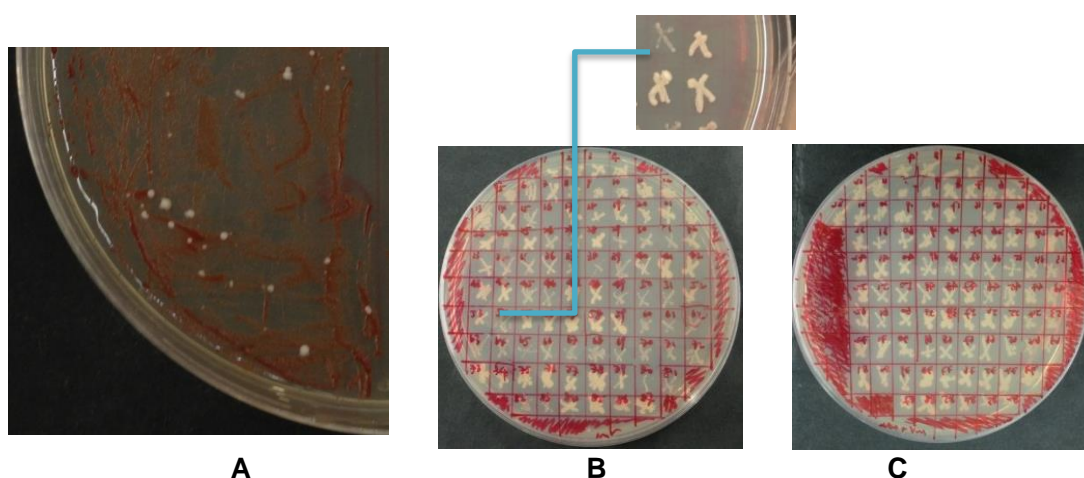
Figure 5.7 Mutants of *S. cerevisiae*. **A.** Mutants in mutagenicity test; **B.** white mutants on MV; **C.** white mutants on MV+ade.

Ethyl methanesulfonate is a strong mutagenic organic compound used as a positive control. The result is displayed in Figure 5.7 **A**. Red colonies of *S. cerevisiae ade2* were considered as background, and many white mutants were observed. They could be caused by reverse mutations at the *ade2* gene or forward mutations of other genes on the purine biosynthetic pathway (*adeX*).

The white mutants were carefully transferred using sterilized toothpicks onto the same spot on MV and MV+ade agar surface. After incubation, the test results were compared in Figure 5.7 **B** and **C**. In order to characterize the type of mutations, minimal plus vitamins medium (MV) and the minimal plus vitamins + adenine medium (MV+ade) were used. On the MV medium, the forward mutants which have *adeX* gene mutations could not grow owing to a lack of adenine. Strains with reverse mutations, which had gained prototrophy like wild type yeast cells, could synthesize AMP and appeared as white coloured colonies on the surface of the agar. 38 of the 87 separated white colonies appeared to have reverse mutations to the wild type genotype. The remaining 49 colonies only grew on MV+adenine medium, and appeared to be forward mutants which had *ade2* gene mutations or were double mutants (*ade2, adeX*).

5.4.3 Genetic stability study of *S. cerevisiae* ade2

Due to the unreliable and inconsistent mutagenicity test results shown above, further investigations were carried out. In order to eliminate variables that could affect the mutagenicity test results, different batches of test material including yeast extract, agar and buffers and different yeast culture stock (from generation 1) were used to compare the growth and spontaneous mutation rate of *ade2* mutants. Several single red colonies from the first generation culture (YEPDA showed in blue in Figure 5.9) and second generation culture (YEPDA showed in red in Figure 5.9) were spread directly onto YEA and inoculated in YEL at the same time. After 24 hours, the liquid yeast cultures were spread on the same batch of YEA plates, the YEA and YEL specimens from the first and second generation were spread onto the same plate and the differences were compared in Figure 5.9 **A**. Specimens from over-growth wells H2 (exp. 2, 62.5 and 7.8 µg/mL), H4 (exp. 2, 7.8 µg/mL), E4 (exp. 1, 62.5 µg/mL), and B1 (exp. 1, 62.5 µg/mL) in the mutagenicity tests were spread on YEA; the white colonies were isolated on YEA and MV plates.
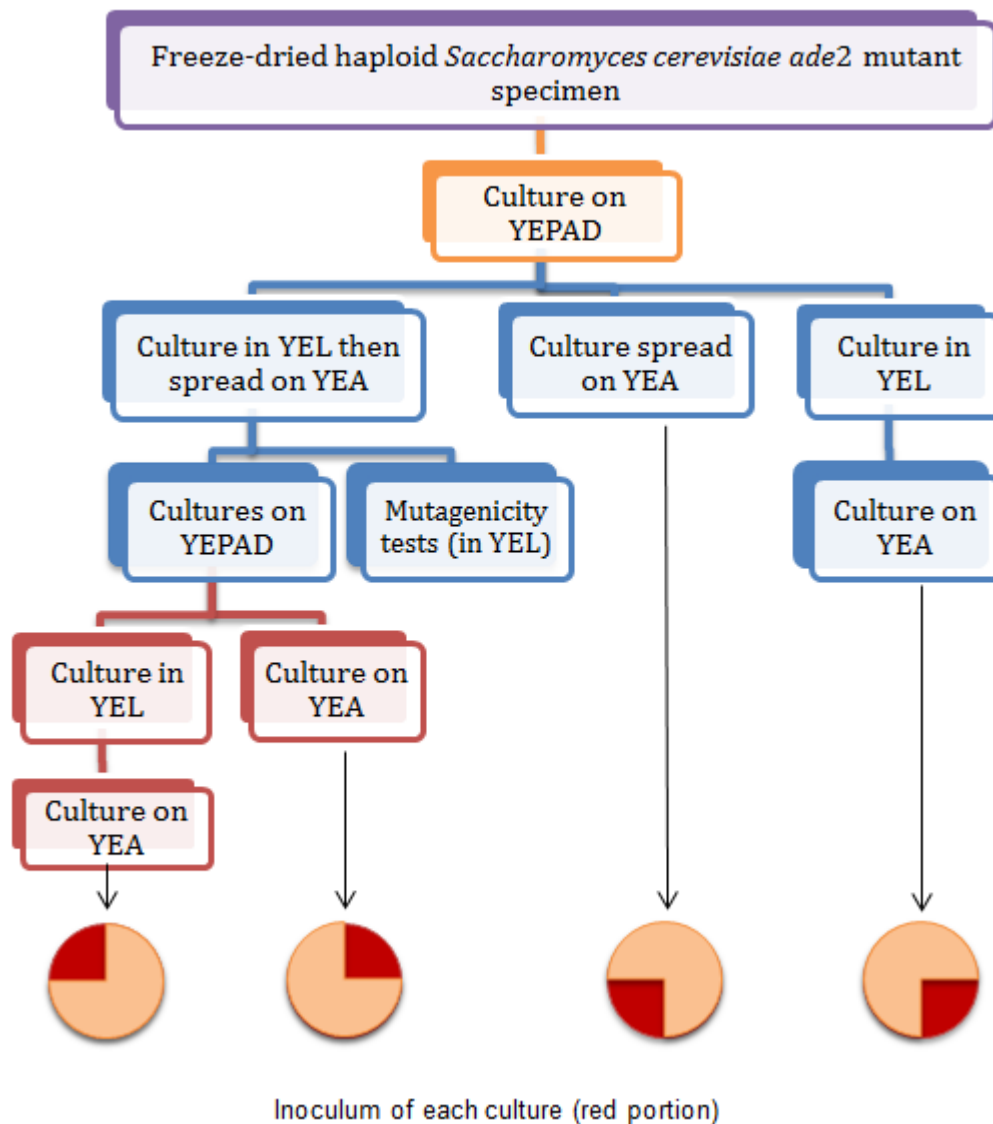
Figure 5.8 First and secondary generation cultures of *S.cerevisiae ade2*. Purple: *S. cerevisiae* specimen from NCYC; Orange: Original culture; Blue: first generation; Red second generation. Two cultures from the first generation and two cultures from the second generation were spread on the same YEA plate for comparison (Figure 5.10 A), the positions of each inoculum were showed in red portions.

After 48 hours incubation, many white colonies were observed in the YEL cultures from both first and second generation cultures (Figure 5.10 **A**, inside the blue circle). The white cells were plated on MV+ade (Figure 5.10 **B**) and confirmed that white colonies were double mutants (*ade2, adeX*), they still needed adenine to grow but did not show the characteristic red colour.
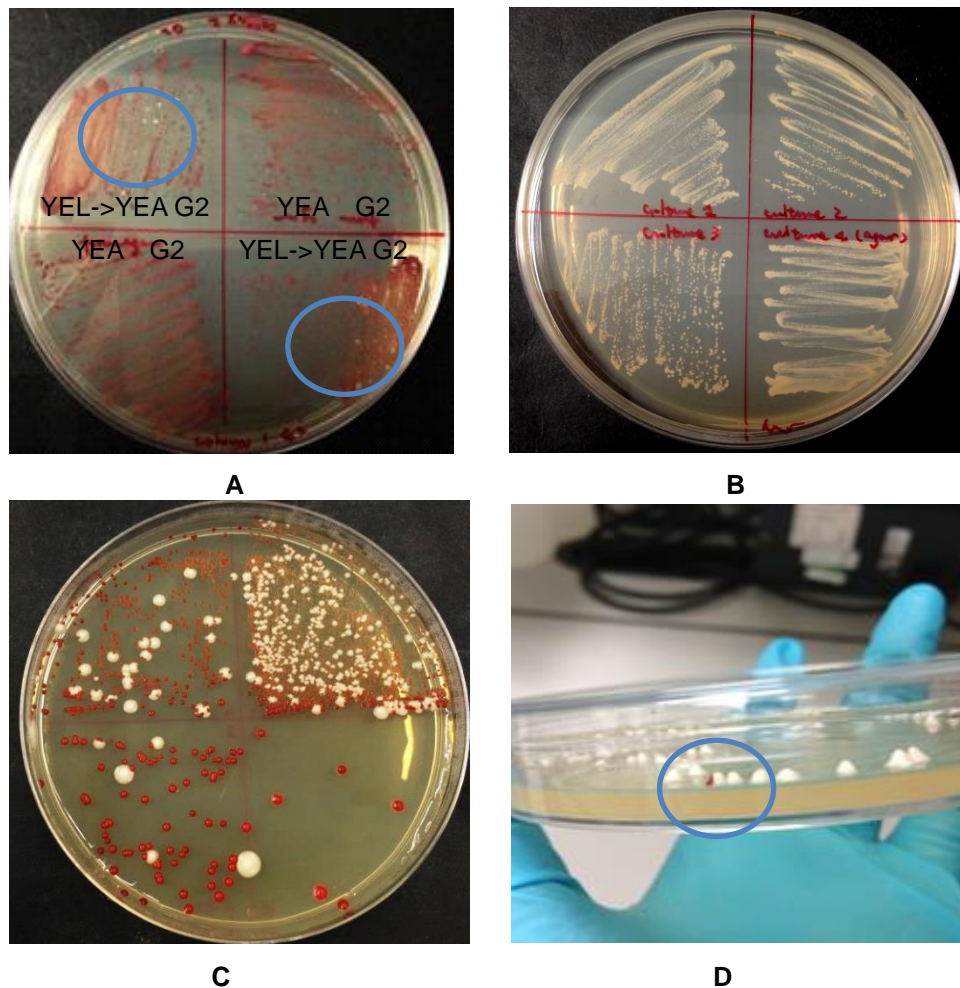
Figure 5.9 Genetic stability evaluation. **A.** First and second generation cultures from yeast extract liquid and agar, white mutants were observed in the circled area; **B.** Auxotrophic white mutants on minimum medium+ade; **C**. Dilution of new strain from YEL; **D.** Isolated white mutants on YEA, red/white sector colonies were observed in the circled area.

A new haploid *S. cerevisiae ade2* mutant strain was purchased from NCYC. The culture was incubated in YEL for 24 hours and plated onto YEA. However, many white colonies could still be seen after 48 hours of incubation (Figure 5.9 **C**), indicating that the strain had a high background mutation rate; at the same time, a sectored colony was found on one of the cultured plates (Figure 5.6 **D**). The reason for the appearance of the sectored colonies was not investigated, but research could be conducted by genetic analysis. Sectored colonies may have arisen by spontaneous mutation during colony growth. This may be due to mitotic recombination (Aguilera et al., 2000). Mitotic recombination was considered to be the primary pathway to repair DNA breaks in yeast (Paques and Haber, 1999).

5.5 Conclusion

The results of the mutagenicity assays on the haploid *S. cerevisiae ade2* strain were not conclusive. EMS which was used as a positive control, showed some evidence of mutagenic activity at the high concentrations (500 μg/mL), but the test compounds showed inconsistent mutagenic activity. Fraction H1 to H4 showed growth inhibition against *S. cerevisiae*, indicating that the hexane fraction had toxicological properties. New experimental material and new strains were tested separately in order to investigate the genetic stability of the *S. cerevisiae ade2* mutant. However, none of the tests gave a consistent result, and a high background mutation frequency suggested that this mutant was not stable and the in *vitro* test results were not reliable.

6. Chapter VI: Conclusion

The whole plant of *E. annuus* was separated using several chromatographic methods. The total crude ethanolic extract was partitioned into four major extract groups labelled as hexane extract (H), ethyl acetate extract (E), butanol extract (B) and water extract (W).

Several compounds were isolated from the *E. annuus* extracts: gondoic acid; hexadecanoic acid; α-spinasterol; erythrodiol; 4-pent-3'-ne-1'-ynyl–pyran-2-one. Structure elucidations were carried out using NMR spectroscopy and mass spectrometry. Compounds whose structures were not fully elucidated include butyrolactone derivative H1-2-6; anthraquinone derivatives B3-7, B3-8; 4-benzopyrone analogue B3-9 and compound B3-1 and B3-12. Components from volatile oily fractions of *E. annuus* were identified using GC-MS and the structures were proposed by matching the known compounds from the mass library, sixteen compounds were identified.

Two compounds were separated from this plant for the first time. Erythrodiol (Figure 6.1 **A**) was identified by comparing the NMR results to the published data. It is a naturally occurring triterpene alcohol, and showed no activity in the antibacterial and DNA gyrase assays.
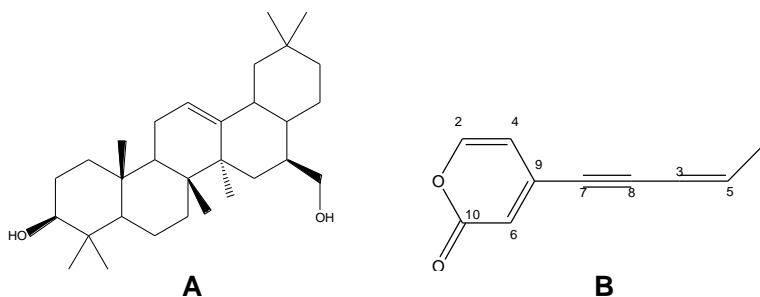
Figure 6.1 Structure of Erythrodiol, 4-but-3'-ne-1'-ynyl-6-methyl–pyran-2-one.

A 2-pyrone derivative, 4-pent-3'-ne-1'-ynyl-pyran-2-one was isolated from the hexane extract for the first time (Figure 6.1 **B**). The 4-substituted-6-methyl-2-pyrone compounds have previously been synthesized by Fairlamb. According to their publications, 4-alkynyl derivatives have inhibitory activities against several wild type bacterial and yeast strains, including *E. coli, S. aureus* and *S. cerevisiae.* But their antibacterial activity tests for those synthetic compounds were measured using disk diffusion assays, and difficult to compare with the MIC test results from this MIC assays. However, the isolated 4-substituted 2-pyrone derivative in this research had MIC value of 128 µg/mL which supported Fairlamb's findings. In addition, Fairlamb

also demonstrated that the 4-alkynyl derivatives had antitumor activity against A2780 ovarian carcinoma and K562 human chronic myelogenous leukemia cell lines *in vitro*. The IC$_{50}$ was measured from 1.8-7.0 μM against A2780 cell line and 4.0-20.3 μM against K562 cell line (Fairlamb et al., 2004).

The antibacterial activity of separated compounds from this research was evaluated against wild type *Escherichia coli, Salmonella enterica*, *Micrococcus luteus, Enterococcus faecalis, Staphylococcus aureus* and an MRSA strain. Compound H1-2-6 separated from the hexane extract showed the best antibacterial activity among all test candidates against MRSA. The MIC value was recorded at 64 μg/mL. The structure elucidation study showed this compound could be a butyrolactone derivative. Compound H1-2-7 was suggested to be 4-pent-3'-ne-1'-ynyl–pyran-2-one. (Figure 6.1 **B**). The MIC value against the MRSA strain was 128 μg/mL. In addition, forty-six fractions were tested in antibacterial assays, and this is the first report of compounds and extracts from this plant with activity against MRSA. Only the hexane fractions showed inhibitory activity against MRSA and they were fractionated to obtain the pure compounds mentioned above. Nine fractions from hexane and butanol extracts were confirmed as having Gram-negative bacterial inhibition against *E. coli* and *S. enterica,* however, further fractionation could not be carried out due to the limited amount of sample. The positive results indicate that the plant extracts should be investigated further as potential antibacterial agents.

The isolated compounds and fractions were also tested for inhibition of DNA gyrase activity. Six compounds from the butanol extract, B3-1, B3-7, B3-8, B3-9, B3-11 and B3-12, showed inhibition against *S. aureus* gyrase. The different modes of action of inhibition were suggested in accordance with the structural studies: structures of B3-1 and B3-9 were elucidated by NMR spectroscopy and mass spectrometry. Compound B3-9 had a very good IC$_{50}$ at 5.39-6.18 μg/mL compared to the positive control (novobiocin at 3.97-7.18 μg/mL). The structure of B3-9 was suggested to be a C$_4$-OH coumarin derivative and therefore may share the same mode of action of coumarin DNA gyrase inhibitors by binding to the 24kDa sub-domain of GyrB to block the ATP hydrolysis site. Compound B3-1 had an IC$_{50}$ at 31.27-34.03 μg/mL, compared to the positive control (novobiocin at 3.97-7.18 μg/mL). The other compounds B3-7, 8, 11 and 12 also showed positive activity in DNA gyrase supercoiling assays, but full structure elucidation would be needed.

Compounds B3-1 and B3-9 exhibited good gyrase inhibition. These two compounds

were isolated from fraction B3. Interestingly B3 only showed a weak inhibition against the wild type *S. aureus* and MRSA (256 µg/mL). It could be suggested that these compounds might have difficulty in reaching their gyrase target in the bacterial cell. Structure modifications on these potential antimicrobial compounds could be considered in the further investigation of this plant.

Necessitating the mutagenicity tests of chemical agents could help to discover potential carcinogens in human therapy, *E. annuus* fractions were tested in the mutagenicity assays induced in this research against *Saccharomyces cerevisiae ade2*. *S. cerevisiae* is usually known as fermenting yeast and it is a unicellular and uninuclear eukaryotic organism. *S. cerevisiae ade2* is an auxotrophic strain with red phenotype colonies. To perform the mutagenicity tests, mutants of *S. cerevisiae ade2* could be identified visually by observing white-coloured colonies, and the mutation type could be further determined using different minimal media. However, results were inconsistent and *S. cerevisiae ade2* exhibited varying mutant frequencies with test samples and the controls. A short study of the genetic stability of this strain was carried out and the results showed the red mutant had a high background mutation frequency. Hexane extracts H1 to H4 showed cytotoxicity against this yeast strain, the investigation of potential antifungal compounds were warranted in the future works.

This research supports the traditional use of the Chinese folk medicine *Erigeron annuus,* to treat infections. Compounds and extracts of *E.annuus* showed antimicrobial activity against bacteria including Gram-negative strains *Escherichia coli,Salmonella enterica*; Gram-positive strains *Micrococcus luteus, Enterococcus faecalis, Staphylococcus aureus,* and Methicillin-Resistant *Staphylococcus aureus* strain (MRSA). A mechanism experiment showed that, the isolated compounds and fractions from this plant have potential antimicrobial activity by inhibiting bacterial gyrase activity. With the increasing trend of multidrug resistant bacterial strains, further investigation will be required on the active components of this plant. For example, the study of modulation effects and potential efflux pump inhibition.

References

Abdulovic, A., Kim, N. & Jinks-Robertson, S. 2006. Mutagenesis and the three R's in yeast. *DNA Repair (Amst),* 5**,** 409-21.

Abraham, E. P. & Chain, E. 1940. An Enzyme from Bacteria able to Destory Penicillin. *Nature,* 3713**,** 837.

Abreu, A. C., McBain, A. J. & Simoes, M. 2011. Plants as sources of new antimicrobials and resistance-modifying agents. *Nat. Prod.* 29, 1007.

Achan, J., Achan, A., Talisuna, A., Erhart, A., Yeka, J., Tibenderana, F., Baliraine, P. & Rosenthal, U. 2011. Quinine, an old anti-malarial drug in a modern world: role in the treatment of malaria. *Malaria journal,* 10**,** 144-144.

Adachi, T., Mizuuchi, M., Robinson, E. A., Appella, E., O'dea, M. H., Gellert, M. & Mizuuchi, K. 1987. DNA sequence of the *E. coli* gyrB gene: application of a new sequencing strategy. *Nucleic Acids Res,* 15**,** 771-84.

Agafitei, O., Kim, E. J., Maguire, T. & Sheridan, J. 2010. The Role of *Escherichia coli* Porins OmpC and OmpF in Antibiotic Cross Resistance Induced by Sub-inhibitory Concentrations of Kanamycin. *Journal of Experimental Microbiology and Immunology,* 14**,** 34-39.

Agrawal, K. 1995. Tetanus caused by human bite of the finger. *Annals of plastic surgery,* 34**,** 201-2.

Aguilera, A., Aguilera, S. & Chvez, F. 2000. Mitotic recombination in yeast: elements controlling its incidence. *Yeast,* 16**,** 731-754.

Akanuma, S., Iwam, I. S., Yokoi, T., Nakamura, N., Watanabe, H., Yokobori, S. & Yamagishi, A. 2011a. Phylogeny-based design of a B-subunit of DNA gyrase and its ATPase domain using a small set of homologous amino acid sequences. *journal of molecular Biology,* 412**,** 212-25.

Akanuma, S., Iwami, S., Yokoi, T., Nakamura, N., Watanabe, H., Yokobori, S. & Yamagishi, A. 2011b. Phylogeny-based design of a B-subunit of DNA gyrase and its ATPase domain using a small set of homologous amino acid sequences. *J Mol Biol,* 412**,** 212-25.

Alcock, N. J., Kuhnz, W. & Games, D. E. 1983. LC/MS and MS/MS studies of natural oxygen heterocyclic compounds. *International Journal or Mass Spectrometry and Ion Physics,* 48**,** 153-156.

Alekshun, M. & Alekshun, S. 2007. Molecular Mechanisms of Antibacterial Multidrug Resistance. *Cell,* 128**,** 1037-1050.

Ali, J. A., Jackson, A. P., Howells, A. J. & Maxwell, A. 1993. The 43-kilodalton N-terminal fragment of the DNA gyrase B protein hydrolyzes ATP and binds coumarin drugs. *Biochemistry, 32***,** 2717-24.

Ali, J. A., Orphanides, G. & Maxwell, A. 1995. Nucleotide binding to the 43-kilodalton N-terminal fragment of the DNA gyrase B protein. *Biochemistry, 34***,** 9801-8.

Alok, K., Sapan, K. J. & Ramesh, C. R. 2004. A PM3 study of tautomerism in some 3,30-methylenebis [4-hydroxycoumarin] systems. *Journal of Molecular Structure, 678***,** 55-61.

Alt, S., Mitchenall, L. A., Maxwell, A. & Heide, L. 2011. Inhibition of DNA gyrase and DNA topoisomerase IV of Staphylococcus aureus and Escherichia coli by aminocoumarin antibiotics. *J Antimicrob Chemother, 66***,** 2061-9.

Althaus, I. W., Kezdy, F. J., Peterson, T., Spilman, C. H. & Reusser, F. 1996. Novenamines as inhibitors of two independent enzymes during DNA replication in a toluenized *Escherichia coli* cell system. *Biochem Pharmacol, 51***,** 1373-8.

Ames, B. N., Mccann, J. & Yamasaki, E. 1975. Methods for detecting carcinogens and mutagens with the salmonella/mammalian-microsome mutagenicity test. *Mutation Research/Environmental Mutagenesis and Related Subjects, 31***,** 347-363.

Anba, J., Bernadac, A., Lazdunski, C. & Pages, J. M. 1988. Improving the stability of a foreign protein in the periplasmic space of *Escherichia coli*. *Biochimie, 70***,** 727-33.

Anderle, C., Stieger, M., Burrell, M., Reinelt, S., Maxwell, A., Page, M. & Heide, L. 2008. Biological activities of novel gyrase inhibitors of the aminocoumarin class. *Antimicrob Agents Chemother, 52***,** 1982-90.

Antunes, N., Antunes, H., Frase, M., Toth, S. & Mobashery, S. 2011. Resistance to the Third-Generation Cephalosporin Ceftazidime by a Deacylation-Deficient Mutant of the TEM β-Lactamase by the Uncommon Covalent-Trapping Mechanism. *Biochemistry, 50***,** 6387-6395.

Aronson, J. K., Dukes, M. N. G. & Meyler, L. 2006a. Meyler's Side Effects of Drugs: The International Encyclopedia of Adverse Drug Reactions and Interactions, *Lincosamides,* 2891-2894.

Baron, S. 1996. *Medical Microbiology,* Galveston, University of Texas Medical Branch at Galveston, URL: http://www.ncbi.nlm.nih.gov/books/NBK7627/. Accessed Date: 15-06-2014.

Bassler, B. 1999. How bacteria talk to each other: regulation of gene expression by quorum sensing. *Current opinion in microbiology, 2***,** 582-587.

Basu, A., Schoeffler, A. J., Berger, J. M. & Bryant, Z. 2012. ATP binding controls distinct structural transitions of *Escherichia coli* DNA gyrase in complex with DNA. *Nat Struct*

Mol Biol, 19**,** 538-46.

Benigni, R. & Benigni, C. 2011. Mechanisms of Chemical Carcinogenicity and Mutagenicity: A Review with Implications for Predictive Toxicology. *Chemical reviews,* 111**,** 2507-2536.

Benoit, S. R., Estivariz, C., Mogdasy, C. & Pedreira, W. 2008. Community Strains of Methicillin-Resistant *Staphylococcus aureus* as Potential Cause of Healthcare-associated Infections, Uruguay, 2002–2004 *EID journal,* 14.

Berkov-Zrihen, Y., Rutenberg, R. & Fridman, M. 2012. Acylation of novobiocin by carboxylic acid anhydrides: preparation and characterization of semi-synthetic novenamines. *Tetrahedron,* 68**,** 2306-2312.

Betsy, T. & Keogh, J. 2005. Microbiology Demystified. McGraw-Hill. 70-74.

Blondeau, J. 2002. The macrolides. *Expert opinion on investigational drugs,* 11**,** 189-215.

Bobba, S., Ponnaluri, V. K., Mukherji, M. & Gutheil, W. G. 2011. Microtiter plate-based assay for inhibitors of penicillin-binding protein 2a from methicillin-resistant *Staphylococcus aureus*. *Antimicrob Agents Chemother,* 55**,** 2783-7.

Bowden, G. A. 1990. Folding and aggregation of beta-lactamase in the periplasmic space of *Escherichia coli*. *Journal of biological chemistry,* 265**,** 16760-6.

Brown, M. S., Dana, S. E. & Goldstein, J. L. 1975. Cholesterol ester formation in cultured human fibroblasts. Stimulation by oxygenated sterols. *The journal of Biological Chemistry,* 250**,** 4025-4027.

Brown, T. & Brown, O. 1992. Structural basis of DNA mutagenesis. *Current opinion in structural biology,* 2**,** 354-360.

Babu, S. K., Srinivas, P. V. , Praveen, B ., Hara. K. K., Suryanarayana, M.U., Madhusudana, R. J. 2003. Antimicrobial constituents from the rhizomes of Rheum emodi. P*hytochemistry,*62, 2, 203-207.

Burden, D. A. & Osheroff, N. 1998. Mechanism of action of eukaryotic topoisomerase II and drugs targeted to the enzyme. *Biochimica et Biophysica Acta (BBA) - Gene Structure and Expression,* 1400**,** 139-154.

Bush, K. 1995. A functional classification scheme for beta-lactamases and its correlation with molecular structure. *Antimicrobial agents and chemotherapy,* 39**,** 1211.

Cao, J., Liu, Y., Sun, H., Cheng, G., Pang, X. & Zhou, Z. 2002. Chromosomal aberrations, DNA strand breaks and gene mutations in nasopharyngeal cancer patients undergoing radiation therapy. *Mutation Research/Fundamental and Molecular Mechanisms of Mutagenesis,* 504**,** 85-90.

Cantwell, M. 1996. A Review of Important Facts about Potato Glycoalkaloids. *Perishables Handling Newsletter Issue* 87. 26-27.

Cassell, G. H. 2001. Development of antimicrobial agents in the era of new and reemerging infectious diseases and increasing antibiotic resistance. *JAMA: the Journal of the American Medical Association,* 285**,** 601-5.

Chatterji, M. & Nagaraja, V. 2002. GyrI: a counter-defensive strategy against proteinaceous inhibitors of DNA gyrase. *EMBO Rep,* 3**,** 261-7.

Centersfordiseasecontrolandprevention. 2014. Centers for Disease Control and Prevention National Center for Emerging and Zoonotic Infectious Diseases (NCEZID). Division of Healthcare Quality Promotion (DHQP). URL: http://www.cdc.gov/drugresistance/about.html. Accessed date: 07-08-2014.

Chen, L.G. & Wang, C. C. 2009. Preparative separation of oligostilbenes from *Vitis thunbergii var*. taiwaniana by centrifugal partition chromatography followed by Sephadex LH-20 column chromatography. *Separation and Purification Technology,* 66**,** 65-70.

Cheng, Y. S. 1979. Purification and characterization of protease III from *Escherichia coli. Journal of biological chemistry,* 254**,** 4698-706.

Chinese academy of sciences 1985. *Flora of china,*74, 326.

Chinese materia medica 1985. *Dictionary of Chinese Materia Medica*, Shanghai Scientific Technological Publishers. 25.

Claudio, O. G., Letizia, B., Attilio, F. & Cynthia, L. P. 2013. *Antibiotics: Targets, Mechanisms and Resistance*: Wiley-VCH. 263-298.

Claxton, L., Umbuzeiro, D. M. & Umbuzeiro, D. 2010. The Salmonella Mutagenicity Assay: The Stethoscope of Genetic Toxicology for the 21st Century. *Environmental health perspectives,* 118**,** 1515-1522.

Cohen, L. S. & Cluff, L. E. 1961. The sulfonamides. *Am J Nurs,* 61**,** 54-8.

Comas, I., Chakravartti, J., Small, P. M., Galagan, J., Niemann, S., Kremer, K., Ernst, J. D. & Gagneux, S. 2010. Human T cell epitopes of Mycobacterium tuberculosis are evolutionarily hyperconserved. *Nat Genet,* 42**,** 498-503.

Corbett, K. D., Shultzaberger, R. K. & Berger, J. M. 2004. The C-terminal domain of DNA gyrase A adopts a DNA-bending beta-pinwheel fold. *Proc Natl Acad Sci U S A,* 101**,** 7293-8.

Couteau, J., Flaman, C. & Minier, J. 2008. Detection of environmental mutagens using the FACIM assay. *Marine environmental research,* 66**,** 62-63.

Cragg, G. & Cragg, D. 2001. Natural Product Drug Discovery in the Next Millennium. *Pharmaceutical biology,* 39**,** 8-17.

Cuddy, P. G. 1997. Antibiotic classification: implications for drug selection. *Crit Care Nurs Q,* 20**,** 89-102.

Daikos, G. K., Kourkoumeli, K. P. & Kekis, B. P. 1961. The value of the quinine test for the differentiation of jaundice. *Am J Med Sci,* 242**,** 351-6.

Daniel, F. & Austin; 2004. *florida ethnobotany*, CRC Press.305.

Davies, J. & Davies, D. 2010. Origins and evolution of antibiotic resistance. *Microbiol Mol Biol Rev,* 74**,** 417-33.

De-Eknamkul, W. & Potduang, B. 2003. Biosynthesis of β-sitosterol and stigmasterol in Croton sublyratus proceeds via a mixed origin of isoprene units. *Phytochemistry,* 62**,** 389-398.

Desbois, A. P. & Lawlor, K. C. 2013. Antibacterial activity of long-chain polyunsaturated fatty acids against Propionibacterium acnes and Staphylococcus aureus. *Mar Drugs,* 11**,** 4544-57.

Dewick, P. M. (ed.) 2001. *Medicinal Natural Products: A Biosynthetic Approach*: John Wiley and Sons.252-255.

Diekema, D. J. & Jones, R. N. 2001. Oxazolidinone antibiotics. *Lancet,* 358**,** 1975-82.

Diggle, S. & Crusz, M. 2007. Quorum sensing. *Current biology,* 17**,** 907-910.

Ding, Z. F., Zhang, H., Tang, W., Tong, C. Y., Li, R. T., Chen, L. X., Pu, L. J., Zhu, Z. B. & Cui, Y. D. 2012. Methylase Genes-Mediated Erythromycin Resistance in *Staphylococcus aureus* from Bovine Mastitis in China. *Israel Journal of Veterinary Medicine,* 67**,** 170-179.

Dixon, D. M. & J., W. T. 1996. *Antifungal Agents*, The University of Texas Medical Branch at Galveston. 4023-4057.

Domagk, G. 1895. Nobel lectures: physology or medicine. 1922-1941. Including presentation speeches and laureates' biographies*.* 2, 1922 - 1941.

Domagk, G. 1950. Mechanism of action of sulfonamides. *Rev Sudam Morfol,* 8**,** 1-39.

Donhofer, A., Franckenberg, S., Wickles, S., Berninghausen, O., Beckmann, R. & Wilson, D. N. 2012. Structural basis for TetM-mediated tetracycline resistance. *Proc Natl Acad Sci U S A,* 109**,** 16900-5.

Dorothy, M. & Bruce, A. 1983. Revised methods for the *Salmonella* mutagenicity test.

Mutation Research, 173-215.

Durata therapeutics. 2014. *Dalvance Prescribing Information*. ULR: http://www.dalvance.com/. Accessded date: 23-07-2014.

Eastmond, D., Eastmond, A., Hartwig, D., Anderson, W. A., Anwar, M. C., Cimino, I., Dobrev, G. R., Douglas, T., Nohmi, D. H. & Phillips, C. 2009. Mutagenicity testing for chemical risk assessment: update of the WHO/IPCS Harmonized Scheme. *Mutagenesis,* 24**,** 341-349.

Edwards, P. J., Frey, D., Bailer, H. & Baltisberger, M. 2006. Genetic Variation in Native and Invasive Populations of *Erigeron annuus* as Assessed by RAPD Markers. *International journal of plant sciences,* 167**,** 93-101.

Evans, M., Evans, S., Kralovic, L., Simbartl, R., Freyberg, D. S., Obrosky, G. & Roselle, R. 2014. Nationwide reduction of health care associated methicillin-resistant *Staphylococcus aureus* infections in Veterans Affairs long-term care facilities. *American journal of infection control,* 42**,** 60-62.

Fairlamb, L. R., Marrison, J., Dickinson, F.-J. & Lu, J. 2004. 2-Pyrones possessing antimicrobial and cytotoxic activities. *Bioorganic & Medicinal Chemistry,* 12**,** 4285-4299.

Fan, C. S. & Zhu, Y. Y. 1975. *National Herbal Compilation,* Beijing, People's Health Publishing House. 21.

Faye, M. B. & Anthony, M. 2001. Interaction between DNA Gyrase and Quinolones: Effects of Alanine Mutations at GyrA Subunit Residues Ser83 and Asp87. *Antimicrob Agents Chemother,* 45**,** 1994-2000.

Fink, G. 1969. Simplified Method for Testing Mutagens in Saccharomyces. *Journal of bacteriology,* 100**,** 1126.

Flückiger-Isler, S. & Kamber, M. 2012. Direct comparison of the Ames microplate format (MPF) test in liquid medium with the standard Ames pre-incubation assay on agar plates by use of equivocal to weakly positive test compounds. *Mutation Research/Genetic Toxicology and Environmental Mutagenesis,* 747**,** 36-45.

Flatman, R. H., Howells, A. J., Heide, L., Fiedler, H. P. & Maxwell, A. 2005. Simocyclinone D8, an inhibitor of DNA gyrase with a novel mode of action. *Antimicrob Agents Chemother,* 49**,** 1093-100.

Fleming, A. 1929. On the Antibacterial Action of Cultures of a *Penicillium*, with Special Reference to Their Use in the Isolation of B. influenzae. Reprinted with permission from *British Journal of Experimental Pathology (Now International Journal of Experimental Pathology)***,** 226-236.

Fleming, A. 1945. Penicillin. The Nobel Prize in Physiology or Medicine 1945*.* The Nobelprize

org.

Forterre, P., Gribaldo, S., Gadelle, D. & Serre, M. C. 2007. Origin and evolution of DNA topoisomerases. *Biochimie,* 89**,** 427-46.

Fox, J. 2014. First vanguard anti-MRSA agent approved. *Nature biotechnology,* 32**,** 603-603.

Friedman, S. M., Malik, M. & Drlica, K. 1995. DNA supercoiling in a thermotolerant mutant of *Escherichia coli*. *Mol Gen Genet,* 248**,** 417-22.

Fuda, C., Hesek, D., Lee, M., Morio, K., Nowak, T. & Mobashery, S. 2005. Activation for catalysis of penicillin-binding protein 2a from methicillin-resistant *Staphylococcus aureus* by bacterial cell wall. *J Am Chem Soc,* 127**,** 2056-7.

Gao, M., Gu, M. & Liu, C.-Z. 2006. Two-step purification of scutellarin from *Erigeron breviscapus* (vant.) Hand. Mazz. by high-speed counter-current chromatography. *Journal of Chromatography B,* 838**,** 139-143.

Gatto, B., Richter, S., Moro, S., Capranico, G. & Palumbo, M. 2001. The topoisomerase II poison clerocidin alkylates non-paired guanines of DNA: implications for irreversible stimulation of DNA cleavage. *Nucleic Acids Res,* 29**,** 4224-30.

Gedvilaite, A. & Sasnauskas, K. 1994. Control of the expression of the *ADE2* gene of the yeast *Saccharomyces cerevisiae*. *Current Genetics,* 25.

Georgopapadakou, N. H. 1982. Penicillin-binding proteins in a *Staphylococcus aureus* strain resistant to specific beta-lactam antibiotics. *Antimicrobial agents and chemotherapy,* 22**,** 172-5.

Ghannoum, M. A. 1999. Antifungal agents: mode of action, mechanisms of resistance, and correlation of these mechanisms with bacterial resistance. *Clinical microbiology reviews,* 12**,** 501-17.

Gilbert, E. J. & Maxwell, A. 1994. The 24 kDa N-terminal sub-domain of the DNA gyrase B protein binds coumarin drugs. *Mol Microbiol,* 12**,** 365-73.

Greenstein, T. M., Speth, J. I. & Maiese, W. M. 1981. Mechanism of Action of Cinodine, a Glycocinnamoylspermidine Antibiotic. *Antimicrobial agent and chemotherapy,* 20**,** 425-432.

Gubaev, A., Hilbert, M. & Klostermeier, D. 2009. The DNA-gate of *Bacillus subtilis* gyrase is predominantly in the closed conformation during the DNA supercoiling reaction. *Proc Natl Acad Sci U S A,* 106**,** 13278-83.

Gubaeva, A. & Klostermeier, D. 2011. DNA-induced narrowing of the gyrase N-gate coordinates T-segment capture and strand passage. *PNAS,* 108**,** 14085-14090.

Halloran, S., Halloran, K., Mauck, S. & Fleisher, J. 2013. Volatiles from Intact and Lygus-Damaged *Erigeron annuus* (L.) Pers. are Highly Attractive to Ovipositing Lygus and its Parasitoid Peristenus relictus Ruthe. *Journal of chemical ecology,* 39**,** 1115-1128.

Hamilton, G. R. & Baskett, T. F. 2000. In the arms of Morpheus the development of morphine for postoperative pain relief. *Can J Anaesth,* 47**,** 367-74.

Hammer, K. A., Carson, C. F., Riley, T. V. 2012. Effects of *Melaleuca alternifolia* (Tea Tree) Essential Oil and the Major Monoterpene Component Terpinen-4-ol on the Development of Single- and Multistep Antibiotic Resistance and Antimicrobial Susceptibility. *Antimicrob Agents Chemother.* 56 (2), 909-915.

Hannan, M. A. 1978. Mutagenic and recombinogenic effects of the antitumor antibiotic anthramycin. *Cancer research,* 38**,** 2795-9.

Hashidoko, Y. 1995. Pyromeconic acid and its glucosidic derivatives from leaves of Erigeron annuus, and the siderophile activity of pyromeconic acid. *Biosci Biotechnol Biochem,* 59**,** 886-90.

Hashimi, S. M., Wall, M. K., Smith, A. B., Maxwell, A. & Birch, R. G. 2007. The Phytotoxin Albicidin is a Novel Inhibitor of DNA Gyrase. *Antimicrobial agent and chemotherapy,* 51**,** 181.

Haynes, R. K. & Krishna, S. 2004. Artemisinins: activities and actions. *Microbes Infect,* 6**,** 1339-46.

Healthcarege 2006. Sephadex LH20 Introductions 56-1190-97.

Heddle, J. G., Mitelheiser, S., Maxwell, A. & Thomson, N. H. 2004. Nucleotide binding to DNA gyrase causes loss of DNA wrap. *Journal of Molecular Biology* 337**,** 597-610.

Heide, L. 2009. Genetic engineering of antibiotic biosynthesis for the generation of new aminocoumarins. *Biotechnology Advances,* 27**,** 1006-1014.

Heide, L. 2013. New aminocoumarin antibiotics as gyrase inhibitors. *International Journal of Medical Microbiology*.304,31-36.

Henry, R. J. 1943. The Mode of Action of Sulfonamides. *Bacteriol Rev,* 7**,** 175-262.

Hiramatsu, K., Igarashi, M., Morimoto, Y., Baba, T., Umekita, M. & Akamatsu, Y. 2012. Curing bacteria of antibiotic resistance: reverse antibiotics, a novel class of antibiotics in nature. *Int J Antimicrob Agents,* 39**,** 478-85.

Hockings, S. C. & Maxwell, A. 2002. Identification of four GyrA residues involved in the DNA breakage-reunion reaction of DNA gyrase. *J Mol Biol,* 318**,** 351-9.

Hossion, A. M., Zamami, Y., Kandahary, R. K., Tsuchiya, T., Ogawa, W., Iwado, A. & Sasaki, K. 2011. Quercetin diacylglycoside analogues showing dual inhibition of DNA gyrase and topoisomerase IV as novel antibacterial agents. *J Med Chem,* 54**,** 3686-703.

Huang, H. 2006. Comparisons of Community-Associated Methicillin-Resistant *Staphylococcus aureus* (MRSA) and Hospital-Associated MSRA Infections in Sacramento, California. *Journal of clinical microbiology,* 44**,** 2423.

Ignacimuthu, S. & Pavunraj, M. 2009. Antibacterial activity of a novel quinone from the leaves of *Pergularia daemia* (Forsk.), a traditional medicinal plant. *Asian Journal of Traditional Medicines,* 4**,** 36-40.

Iijima, T., Yaoita, Y. & Kikuchi, M. 2003a. Five new sesquiterpenoids and a new diterpenoid from *Erigeron annuus* (L.) PERS., *Erigeron philadelphicus* L. and *Erigeron sumatrensis* RETZ. *Chem Pharm Bull (Tokyo),* 51**,** 545-9.

Iijima, T., Yaoita, Y. & Kikuchi, M. 2003b. Two new cyclopentenone derivatives and a new cyclooctadienone derivative from *Erigeron annuus* (L.) PERS., *Erigeron philadelphicus* L., and *Erigeron sumatrensi*s RETZ. *Chem Pharm Bull (Tokyo),* 51**,** 894-6.

Inoue, Y., Hada, T., Shiraishi, A., Hirose, K., Hamashima, H. & Kobayashi, S. 2005. Biphasic effects of geranylgeraniol, teprenone, and phytol on the growth of Staphylococcus aureus. *Antimicrob Agents Chemother,* 49**,** 1770-4.

Inspiralis. *Inspiralis company technical information*. Inspiralis company. URL: http://www.inspiralis.com/.Accessed date: 16-02-2014.

Jack, D., Jack, N. & Yang, M. 2001. The drug/metabolite transporter superfamily. *European journal of biochemistry,* 268**,** 3620-3639.

Jacoby, G. A. 2009. AmpC beta-lactamases. *Clin Microbiol Rev,* 22**,** 161-82.

Jang, D. S., Yoo, N. H., Kim, N. H., Lee, Y. M., Kim, C. S. & Kim, J. 2010. 3,5-Di-O-caffeoyl-epi-quinic Acid from the Leaves and Stems of *Erigeron*. *Biol Pharm Bull,* 33**,** 329-333.

Jang, D. S., Yoo, N. H., Lee, Y. M., Yoo, J. L., Kim, Y. S. & Kim, J. S. 2008. Constituents of the flowers of *Erigeron annuus* with inhibitory activity on the formation of advanced glycation end products (AGEs) and aldose reductase. *Arch Pharm Res,* 31**,** 900-4.

Janid, A. A., Andrew, P. J., Alison, J. H. & Anthony, M. 1993. The 43-kilodalton N-terminal fragment of the DNA gyrase B protein hydrolyzes ATP and binds coumarin drugs. *Biochemistry,* 32**,** 2717-2724.

Jensen, P. R., Loman, L., Petra, B., Van Der Weijden, C. & Westerhoff, H. V. 1995. Energy buffering of DNA structure fails when *Escherichia coli* runs out of substrate. *J Bacteriol,* 177**,** 3420-6.

Jeong, G.-S., Li, B., Lee, D.-S., Kim, K. H., Lee, I. K., Lee, K. R. & Kim, Y.-C. 2010. Cytoprotective and anti-inflammatory effects of spinasterol via the induction of heme oxygenase-1 in murine hippocampal and microglial cell lines. *International Immunopharmacology,* 10**,** 1587-1594.

Jo, M. 2013. Roots of *Erigeron annuus* Attenuate Acute Inflammation as Mediated with the Inhibition of NF-β-Associated Nitric Oxide and Prostaglandin E2 production. *Evidence-based complementary and alternative medicine,* 1-10.

Joyce, M., Edmund, C., Edith, Y. & Bruce, A. 1975. Detection of carcinogens as mutagens in the *Salmonella*/microsome test: Assay of 300 chemicals. *Proceedings of the National Academy of Sciences,* 72**,** 5135-5139.

K. Rébora, C. Desmoucelles, F. Borne, B. Pinson, A., Daignan-Fornier, B. & 2001. Yeast AMP Pathway Genes Respond to Adenine through Regulated Synthesis of a Metabolic Intermediate. *molecular and cellular biology,* 21**,** 7901-7912.

Kagawa, M., Minami, H., Nakahara, M. & Takahashi, H. 1998. Oleanane-type triterpene from *Viburnum awabuki*. *Phytochemistry,* 47**,** 1101-1105.

Kallen, A. 2010. Health Carea€'Associated Invasive MRSA Infections, 2005-2008. *JAMA: the Journal of the American Medical Association,* 304**,** 641-8.

Kampranis, S. C., Bates, A. D. & Maxwell, A. 1999. A model for the mechanism of strand passage by DNA gyrase. *Proc Natl Acad Sci U S A,* 96**,** 8414-8419.

Karkare, S., Chung, T. T. H. & Collin, F. 2012. The Naphthoquinone Diospyrin Is an Inhibitor of DNA Gyrase with a Novel Mechanism of Action. *The Journal of Biological Chemistry,* 288**,** 5149-5156.

Kasper, D. L. 1986. Bacterial capsule-old dogmas and new tricks. *J Infect Dis,* 153**,** 407-15.

Kemshead, J. & Kemshead, A. 1976. Degradation of Abnormal Proteins in *Escherichia coli*. Differential Proteolysis in vitro of *E. coli* Alkaline Phosphatase Cyanogen-Bromide-Cleavage Products. *European journal of biochemistry,* 71**,** 185-192.

Khazir, J., Khazir, B., Mir, S. & Mir, D. 2013. Natural products as lead compounds in drug discovery. *Journal of Asian natural products research,* 15**,** 764-788.

Kim, D. H., Jung, S. J., Chung, I. S., Lee, Y. H., Kim, D. K., Kim, S. H., Kwon, B. M., Jeong, T. S., Park, M. H., Seoung, N. S. & Baek, N. I. 2005. Ergosterol peroxide from flowers of *Erigeron annuus* L. as an anti-atherosclerosis agent. *Arch Pharm Res,* 28**,** 541-5.

Kim, H. Y. & Kim, K. Y. 2003. Protein Glycation Inhibitory and Antioxidative Activities of Some Plant Extracts in Vitro. *Journal of Agricultural and Food Chemistry,* 51**,** 1586-1591.

Kim, K. Y., Park, J. H., Kwak, H. S. & Woo, G. J. 2011. Characterization of the quinolone resistance mechanism in foodborne Salmonella isolates with high nalidixic acid resistance. *Int J Food Microbiol,* 146**,** 52-6.

Kim, O., Kim, Y., Kim, D., Jang, N. & Yoo, J. 2009. Cytoprotection against hydrogen peroxide-induced cell death in cultured mouse mesangial cells by erigeroflavanone, a novel compound from the flowers of *Erigeron annuus*. *Chemico-biological interactions,* 180**,** 414-420.

Klous, M., Van Den Klous, W., Van Brink, J. & Ree, J. 2005. Development of pharmaceutical heroin preparations for medical co-prescription to opioid dependent patients. *Drug and alcohol dependence,* 80**,** 283-295.

Kohanski, M. A., Dwyer, D. J. & Collins, J. J. 2010. How antibiotics kill bacteria: from targets to networks. *Nature Reviews Microbiology,* 8**,** 423-435.

Kollár, R. 1997. Architecture of the yeast cell wall. Beta(1-->6)-glucan interconnects mannoprotein, beta(1-->)3-glucan, and chitin. *Journal of biological chemistry,* 272**,** 17762-75.

Kongduang , D., Wungsintaweekul, J. & Eknamkul, W. D. 2008. Biosynthesis of b-sitosterol and stigmasterol proceeds exclusively via the mevalonate pathway in cell suspension cultures of *Croton stellatopilosus*. *Tetrahedron Letters,* 49**,** 4067-4072.

Kumar, V., Kumar, C. S., Mathela, G., Tewari, D., Singh, A. K. & Tewari, K. S. 2014. Chemical composition and antifungal activity of essential oils from three Himalayan Erigeron species. *Food science & technology,* 56**,** 278-283.

Kuroda, T. 2009. Multidrug efflux transporters in the MATE family. *Biochimica et biophysica acta. Proteins and proteomics,* 1794**,** 763-768.

Laponogov, I., Sohi, M. K., Veselkov, D. A., Pan, X.S., Sawhney, R., Thompson, A. W., Mcauley, K. E., Fisher, L. M. & Sanderson, M. R. 2009. Structural insight into the quinolone-DNA cleavage complex of type IIA topoisomerases. *Nat Struct Mol Biol,* 16**,** 667-669.

Latorre, M., Rojo, P. M., Unzaga, M. J. & Cisterna, R. 1993. *Staphylococcus schleiferi*: a new opportunistic pathogen. *Clin Infect Dis,* 16**,** 589-90.

Lazzaroni, J.C. & Portalier, R. 1992. The excC gene of *Escherichia coli* K-12 required for cell envelope integrity encodes the peptidoglycan-associated lipoprotein (PAL). *Molecular Microbiology,* 6**,** 735-742.

Leclercq, R. 2002. Mechanisms of Resistance to Macrolides and Lincosamides: Nature of the Resistance Elements and Their Clinical Implications. *Clinical infectious diseases,* 34**,** 482-492.

Lee, H. & Lee, Y. 2006. Antioxidant properties ofErigeron annuus extract and its three phenolic constituents. *Biotechnology and bioprocess engineering,* 11**,** 13-18.

Lee, M. 2003. A mechanism-based inhibitor targeting the DD-transpeptidase activity of bacterial penicillin-binding proteins. *Journal of the American Chemical Society,* 125**,** 16322-6.

Lee, N. S., Yuen, K. Y. & Kumana, C. R. 2001. B-lactam antibiotic and β-lactamase inhibitor combinations. *JAMA,* 285**,** 386-388.

Leicach, S. R. & Chludil, H. D. 2014. Plant Secondary Metabolites: Structure–Activity Relationships in Human Health Prevention and Treatment of Common Diseases. *Elsevier*. 267-297.

Leski, T. 2005. Role of Penicillin-Binding Protein 2 (PBP2) in the Antibiotic Susceptibility and Cell Wall Cross-Linking of *Staphylococcus aureus*: Evidence for the Cooperative Functioning of PBP2, PBP4, and PBP2A. *Journal of bacteriology,* 187**,** 1815.

Lewis, D. F. V. & Lewis, A. 2005. A selective review of bacterial forms of cytochrome P450 enzymes. *Enzyme and microbial technology,* 36**,** 377-384.

Lewis, M. 2011. Agarose gel electrophoresis (basic method),Biological Protocols.

Lewis, R. J., Singh, O. M., Smith, C. V., Skarzynski, T., Maxwell, A., Wonacott, A. J. & Wigley, D. B. 1996. The nature of inhibition of DNA gyrase by the coumarins and the cyclothialidines revealed by X-ray crystallography. *EMBO J,* 15**,** 1412-20.

Li, B., Li, W., Tao, C., Zheng, P., Shar, C., Huang, Y. & Fu, Y. 2014. Systems pharmacology-based approach for dissecting the addition and subtraction theory of traditional Chinese medicine: An example using Xiao-Chaihu-Decoction and Da-Chaihu-Decoction. *Computers in biology and medicine,* 53**,** 19-29.

Li, X., Pan, J. & Gao, K. 2006. Gamma-pyranone derivatives and other constituents from *Erigeron annuus*. *Pharmazie,* 61**,** 474-7.

Li, X., Yang, M., Han, Y. F. & Gao, K. 2005. New sesquiterpenes from *Erigeron annus*. *Planta Med,* 71**,** 268-72.

Li, X., Zhang, Q. K. & Gao, K. 2004. Chemical constituents of *Erigeron annus. Acta Bot Boreal.,* 24**,** 2096-2099.

Ling, R. & Chen, Y. L. 1985. *Flora Reipublicae Popularis Sinicae,* Beijing, Science press.295-299

Lipke, P. 1998. Cell Wall Architecture in Yeast: New Structure and New Challenges. *Journal of bacteriology,* 180**,** 3735.

Lis, A., Lis, J., Mielczarek, D. & Kalemba, J. 2011. Chemical Composition of the Essential Oil

from the Herb of *Erigeron annuu*s (L.) Pers. *The Journal of essential oil research,* 20**,** 229-232.

Liu, J. X., Peng, S., Faivre-Vuillin, B., Xu, Z. H., Zhang, D. Q. & Zhou, G. Y. 2008. *Erigeron annuus* (L.) Pers., as a green manure for ameliorating soil exposed to acid rain in Southern China. *J Soils Sediments,* 8**,** 452-460.

Liu, Y. H., Xue, C. Y., Zhang, Y., Xu, Q., Yu, X. M., Zhang, X. S., Wang, J., Zhang, R. X., Gong, X. & Guo, C. J. 2011. Triglyceride with Medium-Chain Fatty Acids Increases the Activity and Expression of Hormone-Sensitive Lipase in White Adipose Tissue of C57BL/6J Mice. *Bioscience, Biotechnology, and Biochemistry,* 75**,** 1939-1944.

Lo, P.-R., Yu, R.-C., Chou, C.-C. & Huang, E. C. 2004. Determinations of the antimutagenic activities of several probiotic bifidobacteria under acidic and bile conditions against benzo[a]pyrene by a modified Ames test. *International Journal of Food Microbiology,* 93**,** 249-257.

Lubbers, T., Angehrn, P., Gmunder, H. & Herzig, S. 2007. Design, synthesis, and structure-activity relationship studies of new phenolic DNA gyrase inhibitors. *Bioorg Med Chem Lett,* 17**,** 4708-14.

Lubelski, J. 2007. Distribution and Physiology of ABC-Type Transporters Contributing to Multidrug Resistance in Bacteria. *Microbiology and molecular biology reviews,* 71**,** 463.

Luo, P., Tan, Z. H., Zhang, Z. F., Zhang, H., Liu, X. F. & Mo, Z. J. 2008. Scutellarin Isolated from *Erigeron multiradiatue* Inhibits High Glucose-mediated Vascular Inflammation. *The Pharmaceutical Society of Janpan. ,* 128**,** 1293-1299.

Luo, Z.-Q. 2003. In Situ Activation of the Quorum-Sensing Transcription Factor TraR by Cognate and Noncognate Acyl-Homoserine Lactone Ligands: Kinetics and Consequences. *Journal of bacteriology,* 185**,** 5665.

Lwata, N. G., Pham, M., Rizzo, N. O., Cheng, A. M., Maloney, E. & Kim, F. 2011. Trans Fatty acids induce vascular inflammation and reduce vascular nitric oxide production in endothelial cells, *Plos one,* 6.

Lyubchenko, Y., L. & Shlyakhtenko, L. S. 1988. Early melting of supercoiled DNA. *Nucleic Acids Res,* 16**,** 3269-81.

Mahendran, K., Mahendran, M., Kreir, H., Weingart, N. & Fertig, M. 2010. Permeation of Antibiotics through *Escherichia coli* OmpF and OmpC Porins: Screening for Influx on a Single-Molecule Level. *Journal of biomolecular screening,* 15**,** 302-307.

Malik, M., Marks, K. R., Mustaev, A., Zhao, X., Chavda, K., Kerns, R. J. & Drlica, K. 2011. Fluoroquinolone and quinazolinedione activities against wild-type and gyrase mutant strains of Mycobacterium smegmatis. *Antimicrob Agents Chemother,* 55**,** 2335-43.

Maron, D., Katzenellenbogen, J. & Ames, B. N. 1981. Compatibility of organic solvents with the Salmonella/microsome test. *Mutat Res,* 88**,** 343-50.

Martin, A. L. & Dagmar, K. 2011. Guiding strand passage: DNA-induced movement of the gyrase C-terminal domains defines an early step in the supercoiling cycle. *Nucl. Acids Res,* 39**,** 9681-94.

Martin, E., Hine, R. 2008. Gibberellin. *A Dictionary of Biology*. 6 ed. Oxford University Press. URL:http://www.oxfordreference.com. Accessed date: 08-09-2014.

Martin, E., Mcferran, T. 2008. Camphor. *A Dictionary of Nursing*. 5 ed.Oxford University Press. URL:http://www.oxfordreference.com. Accessed date: 08-09-2014.

Masters, M. 1989. The Escherichia coli chromosome and its replication. *Curr Opin Cell Biol,* 1**,** 241-9.

Mathela D.K., Pant A.K., Mathela C.S., 1984, A pyrone glycoside from *Erigeron karwinskyanus*. *Phtochemistry ,*23, 2090-2091.

Maxwell, A. 1997. DNA gyrase as a drug target. *Trends Microbiol,* 5**,** 102-9.

Mcclanahan, C. 2009. Antifungals. *BioFiles.* Sigma-Aldrich. ULR: http://www.sigmaaldrich.com/china-mainland/zh/technical-documents/articles/biofiles/antifungals.html. Accessed date: 20-07-2014.

Mcclendon, A. K. & Osheroff, N. 2007. DNA topoisomerase II, genotoxicity, and cancer. *Mutat Res,* 623**,** 83-97.

Mika, F. N., Hideaki, I., Yoshihiro, O., Takeshi, N. & Jun-Ichi, Y. 2005. Accumulation of mutations in both gyrB and parE genes is associated with high-level resistance to novobiocin in *Staphylococcus aureus*. *Antimicrob Agents Chemotherapy,* 49**,** 3810-3815.

Milavetz, B. I. & Carter, W. A. 1977. Streptovaricins. *Pharmacology & Therapeutics. Part A: Chemotherapy, Toxicology and Metabolic Inhibitors,* 1**,** 289-305.

Mishima, S., Inoh, Y., Narita, Y., Ohta, S., Sakamoto, T., Araki, Y., Suzuki, K.-M., Akao, Y. & Nozawa, Y. 2005. Identification of caffeoylquinic acid derivatives from Brazilian propolis as constituents involved in induction of granulocytic differentiation of HL-60 cells. *Bioorganic & Medicinal Chemistry,* 13**,** 5814-5818.

Mohamed, H. & Abd, E. R. 2006. A New Flavan from the Aerial Part of *Erigeron annuus*. *The Chinese Pharmaceutical Journal,* 58**,** 95-104.

Mukherjee, A., Sen, S. & Agarwal, K. 1993. Ciprofloxacin: mammalian DNA topoisomerase type II poison in vivo. *Mutation Research Letters,* 301**,** 87-92.

Muller-Waldeck, F., Sitzmann, J., Schnitzler, W. H. & Grassmann, J. 2010. Determination of toxic perilla ketone, secondary plant metabolites and antioxidative capacity in five Perilla frutescens L. varieties. *Food Chem Toxicol,* 48**,** 264-70.

Murphy, B. E. P. & D'aux, R. C. D. 1975. The use of sephadex LH-20 column chromatography to separate unconjugated steroids. *Journal of Steroid Biochemistry,* 6**,** 233-237.

Nair, M. S. R. & Anchel, M. 1972. An antibacterial quinone hydroquinone pair from the ascomycete, nectria coryli. *Tetrahedron Letters,* 13**,** 795-796.

Nakada, N., Gmunder, H., Hirata, T. & Arisawa, M. 1994. Mechanism of inhibition of DNA gyrase by cyclothialidine, a novel DNA gyrase inhibitor. *Antimicrob Agents Chemother,* 38**,** 1966-73.

Nanjing military ministry of health 1969. Nanjing common used herbal medicines. Nanjing Military Ministry of Health. 71.

National toxicology program. 2011. *RE: Report on Carcinogens.* URL: http://ntp.niehs.nih.gov/ntp/roc/content/profiles/ethylmethanesulfonate.pdf.Accessed date: 02-01-2014.

Nazaruk, J. & Kalemba, D. 2009. Chemical composition of the essential oils from the roots of *Erigeron acris* L. and *Erigeron annuus* L. Pers. *Molecules,* 14**,** 2458-65.

Nelson, M. L. & Levy, S. B. 2011. The history of the tetracyclines. *Ann N Y Acad Sci,* 1241**,** 17-32.

Neu, H. C. 1988. Quinolones: a new class of antimicrobial agents with wide potential uses. *Med Clin North Am,* 72**,** 623-36.

Newsom, S. W. 1982. Vancomycin. *Journal of antimicrobial chemotherapy,* 10**,** 257-9.

Nikaido, H. & Nikaido, Y. 2009. Mechanisms of RND multidrug efflux pumps. *Biochimica et biophysica acta. Proteins and proteomics,* 1794**,** 769-781.

Nikaido, H. & Vaara, M. 1985. Molecular basis of bacterial outer membrane permeability. *Microbiol Rev,* 49**,** 1-32.

Oblak, M., Grdadolnik, S. G., Kotnik, M., Poterszman, A., Atkinson, R. A., Nierengarten, H., Desplancq, D., Moras, D. & Solmajer, T. 2006. Biophysical characterization of an indolinone inhibitor in the ATP-binding site of DNA gyrase. *Biochem Biophys Res Commun,* 349**,** 1206-13.

Oh, H., Lee, S., Lee, H. S., Lee, D. H., Lee, S. Y., Chung, H. T., Kim, T. S. & Kwon, T. O. 2002. Germination inhibitory constituents from *Erigeron annuus*. *Phytochemistry,* 61**,** 175-9.

Ohnishi, G., Endo, K., Doi, A., Fujita, A., Daigaku, Y., Nunoshiba, T. & Yamamoto, K. 2004. Spontaneous mutagenesis in haploid and diploid *Saccharomyces cerevisiae*. *Biochem Biophys Res Commun,* 325**,** 928-33.

Osbourn, A. E. & Lanzotti, V. 2009. *Plant-derived Natural Products: Synthesis, Function, and Application* Springer. 3-10.

Osburne, M. S., Maiese, W. M. & Greenstein, M. 1990. In vitro inhibition of bacterial DNA gyrase by cinodine, a glycocinnamoylspermidine antibiotic. *Antimicrob Agents Chemother,* 34**,** 1450-2.

Otero, L., Otero, A., Rojas-Altuve, L. I., Llarrull, C., Carrasco Lopez, M., Kumarasiri, E., Lastochkin, J., Fishovitz, M., Dawley, D., Hesek, M., Lee, J. W., Johnson, J. F., Fisher, M., Chang, S. & Mobashery, J. A. 2013. How allosteric control of *Staphylococcus aureus* penicillin binding protein 2a enables methicillin resistance and physiological function. *Proceedings of the National Academy of Sciences of the United States of America,* 110**,** 16808-16813.

Oteroa, L. H., Altuvea, A. R., Llarrull, L. I. & Lópeza, C. C. 2013. How allosteric control of *Staphylococcus aureus* penicillin binding protein 2a enables methicillin resistance and physiological function. *PNAS,* 110**,** 16808-16813.

Pao, S. 1998. Major Facilitator Superfamily. *Microbiology and molecular biology reviews,* 62**,** 1.

Paques, F. & Haber, J. E. 1999. Multiple pathways of recombination induced by double-strand breaks in *Saccharomyces cerevisiae*. *Microbiol Mol Biol Rev,* 63**,** 349-404.

Pato, M. L. & Brown, G. M. 1963. Mechanisms of Resistance of *Escherichia Coli* to Sulfonamides. *Arch Biochem Biophys,* 103**,** 443-8.

Paul, N. M. 2001. Two-Hybrid Systems: Methods and Protocols, *A product of Humana Press*. 10.

Perry, J. J., Staley, J. T. & Lory, S. 2002a. *Microbial life,* Sunderland, Sinauer Associates. 629.

Perry, J. J., Staley, J. T. & Lory, S. 2002b. *Microbial life,* Sunderland, Sinauer Associates. 91.

Perry,J.J., Staley, J. T. & Lory, S. 2002c. *Microbial life,* Sunderland, Sinauer Associates. 765-782.

Pflanzenbilder. 2014. *Imagines Plantarum*. URL: http://www.imagines-plantarum.de/ Accessed Date: 2014-7-016.

Phillips, I. 1982. Aminoglycosides. *Lancet (London, England),* 320**,** 311-315.

Phillips, J. W., Goetz, M. A., Smith, S. K., Zink, D. L., Polishook, J., Onishi, R., Salowe, S., Wiltsie,

J., Allocco, J., Sigmund, J., Dorso, K., Lee, S., Skwish, S., De La Cruz, M., Martin, J., Vicente, F., Genilloud, O., Lu, J., Painter, R. E., Young, K., Overbye, K., Donald, R. G. & Singh, S. B. 2011. Discovery of kibdelomycin, a potent new class of bacterial type II topoisomerase inhibitor by chemical-genetic profiling in *Staphylococcus aureus*. *Chem Biol,* 18**,** 955-65.

Pieribattesti, J.C., Conan, J.-Y., Buil, P., Garnero, J. & Joulain, D. 1981. Terpenoids and polyacetylenic esters of the essential oil of *Erigeron naudini*. *Phytochemistry,* 20**,** 507-508.

Plaper, A., Golob, M., Hafner, I., Oblak, M., Solmajer, T. & Jerala, R. 2003. Characterization of quercetin binding site on DNA gyrase. *Biochem Biophys Res Commun,* 306**,** 530-6.

Pommier, Y. 1998. Diversity of DNA topoisomerases I and inhibitors. *Biochimie,* 80**,** 255-70.

Porter, W. R. & Trager, W. F. 1982. 4-Hydroxycoumarin/2-hydroxychromone tautomerism: Infrared spectra of 3-substituted-2-13c-4-hydroxycoumarins. *Journal of Heterocyclic Chemistry,* 19**,** 475-480.

Ragasa, C. Y., Espineli, D. L., Mandia, E. H., Don, M.-J. & Shen, C.-C. 2012. A new triterpene from Glinus oppositifolius. *Chinese Journal of Natural Medicines,* 10**,** 284-286.

Ragasa, C. Y., Rideout, J. A., Sy, J. O., Alcachupas, D., Inte, V. M. L. & Coll, J. C. 1997. Bioactive monoterpene glycosides from Erigeron linifolius. *Phytochemistry,* 46**,** 151-154.

Rahmoun, N. M., Boucherit-Otmani, Z., Boucherit, K., Benabdallah, M., Villemin, D. & Choukchou-Braham, N. 2012. Antibacterial and antifungal activity of lawsone and novel naphthoquinone derivatives. *Med Mal Infect,* 42**,** 270-5.

Rajendram, M., Hurley, K. A., Foss, M. H., Thornton, K. M., Moore, J. T., Shaw, J. T. & Weibel, D. B. 2014. Gyramides Prevent Bacterial Growth by Inhibiting DNA Gyrase and Altering Chromosome Topology. *ACS Chem Biol*. 9,(6), 1312-9.

Rao, K. S., Xu, Y., Shaw, E. & Parton, J. W. 2000. MutagenicityTesting Applied for Regulation of Developing Products. *In:* SEPARATIONS, C. (ed.). Greenfield: MicaGenix. 141-144.

Reece, R. J., Maxwell, A. & Wang, J. C. 1991. DNA Gyrase: Structure and Function. *Critical Reviews in Biochemistry and Molecular Biology,* 26**,** 335-375.

Reguera, R. M., Redondo, C. M., Gutierrez De Prado, R., Perez-Pertejo, Y. & Balana-Fouce, R. 2006. DNA topoisomerase I from parasitic protozoa: a potential target for chemotherapy. *Biochim Biophys Acta,* 1759**,** 117-31.

Reusser, F. & Dolak, L. A. 1986. Novenamine is the active moiety in novobiocin. *J Antibiot (Tokyo),* 29**,** 272-4.

Revolutionary Health Committee of Anhui Province 1975. *Anhui herbology (Botanicals Parts)*,

Anhui People's Publishing House. 558.

Revolutionary Health Committee of Zhejiang Province,1970. *Zhejiang common used herbal medicine*, Zhejiang People's Publishing Press. 410.

Rhaese, H.-J. & Rhaese, N. 1973. The Molecular Basis of Mutagenesis by Methyl and Ethyl Methanesulfonates. *European journal of biochemistry,* 32**,** 166-172.

Roberfroid, M. B. 2005. Introducing inulin-type fructans. *Br J Nutr,* 93 Suppl 1**,** S13-25.

Roca, J. 2009. Topoisomerase II: a fitted mechanism for the chromatin landscape. *Nucleic Acids Res,* 37**,** 721-30.

Royer, M. & Costet, L. 2004. Xanthomonas albilineans Is Encoded by Three Large PKS and NRPS Genes Present in a Gene Cluster Also Containing Several Putative Modifying, Regulatory, and Resistance Genes. *MPMI,* 17**,** 414-427.

Rustamadji 2000. Family medicine between west and east. *The Lancet,* 356, Supplement 1**,** 29.

Saccharomyces Genome Database: SGD-Wiki. ULR: http://www.yeastgenome.org/. Accessed date: 18-05-2014.

Saga, T. & Yamaguchi, K. 2009. History of Antimicrobial Agents and Resistant Bacteria. *Japan Medical Association Journal,* 52**,** 103-108.

Sasaki, Y. F., Nakamura, T. & Kawaguchi, S. 2007. What is better experimental design for in vitro comet assay to detect chemical genotoxicity. *World Congress on Alternatives & Animal Use in the Life Sciences,* 14**,** 449-504.

Savoia, D. 2012. Plant-derived antimicrobial compounds: alternatives to antibiotics. *Future Microbiol.* 7(8), 979-990.

Sawa, R., Takahashi, Y., Hashizume, H., Sasaki, K., Ishizaki, Y., Umekita, M., Hatano, M., Abe, H., Watanabe, T., Kinoshita, N., Homma, Y., Hayashi, C., Inoue, K., Ohba, S., Masuda, T., Arakawa, M., Kobayashi, Y., Hamada, M., Igarashi, M., Adachi, H., Nishimura, Y. & Akamatsu, Y. 2012. Amycolamicin: a novel broad-spectrum antibiotic inhibiting bacterial topoisomerase. *Chemistry,* 18**,** 15772-81.

Schaefler, S. 1979. Methicillin-Resistant Strains of *Staphylococcus aureus* Phage Type 92. *Antimicrobial agents and chemotherapy,* 15**,** 74.

Schleifer, K. H. & Kandler, O. 1972. Peptidoglycan types of bacterial cell walls and their taxonomic implications. *Bacteriol Rev,* 36**,** 407-77.

Schlitzer, M. 2007. Malaria chemotherapeutics part 1: History of antimalarial drug

development, currently used therapeutics, and drugs in clinical development. *Chemmedchem,* 2**,** 944-986.

Schmitz, R. 1985. Friedrich Wilhelm Sertrner and the discovery of morphine. *Pharmacy in history,* 27**,** 61-74.

Seki, T. & Sugase, T. 1969. Chromatographic separation of 17-ketosteroids and 17-hydroxycorticosteroids on sephadex LH-20. *J Chromatogr,* 42**,** 503-8.

Sen, D. J., Shishoo, C. J. & Lahiri, A. 2011. Three musketeers of genotoxicity: carcinogen, mutagen & teratogen. *NSHM Journal of pharmacy and Healthcare Management,* 2**,** 13-25.

Sen, S., Lahiri, A. & Majumdar, R. 1992. Melting characteristics of highly supercoiled DNA. *Biophys Chem,* 42**,** 229-34.

Sengupta, S. & Nagaraja, V. 2008. YacG from *Escherichia coli* is a specific endogenous inhibitor of DNA gyrase. *Nucleic Acids Res,* 36**,** 4310-6.

Sengupta, S., Shah, M. & Nagaraja, V. 2006. Glutamate racemase from *Mycobacterium tuberculosis* inhibits DNA gyrase by affecting its DNA-binding. *Nucleic Acids Res,* 34**,** 5567-76.

Seow, L. J., Beh, H. K., Sadikun, A., Asmawi, M. Z. 2013. Preliminary Phytochemical and Physicochemical Characterization of *Gynura segetum* (Lour) Merr (Compositae) Leaf. *Tropical Journal of Pharmaceutical Research*, 12 (5)**,** 777-782.

Shandilya, A., Shandilya, S., Chacko, B. & Jayaram, I. 2013. A plausible mechanism for the antimalarial activity of artemisinin: A computational approach. *Scientific Reports,* 3**,** 2513.

Shanghaipeople'spublishinghouse 1972. *Identification of common herbs,* shang hai, Shanghai People's Publishing House. 46.

Shanghaiscientifictechnologicalpublishers 1985. Dictionary of Chinese Materia Medica. 25.

Sigma-Aldrich,CHP20P datasheet. Sigma-Aldrich MCI Gel. URL: http://www.sigmaaldrich.com/catalog/product/supelco/13630u?lang=en&region=G B. Accessed date: 29-05-2014.

Sigma-Aldrich. 2014. *Glycobiology Analysis Manual* . Sigma-Aldrich. URL: http://www.sigmaaldrich.com/technical-documents/articles/biology/glycobiology/p eptidoglycans.html. Accessed date: 19-07-2014.

Silverman, M. H. & Ostro, M. J. 1999. Bacterial Endotoxin in Human Disease. 1-2.

Singh, S. B., Goetz, M. A., Smith, S. K., Zink, D. L., Polishook, J., Onishi, R., Salowe, S., Wiltsie,

J., Allocco, J., Sigmund, J., Dorso, K., De La Cruz, M., Martin, J., Vicente, F., Genilloud, O., Donald, R. G. & Phillips, J. W. 2012. Kibdelomycin A, a congener of kibdelomycin, derivatives and their antibacterial activities. *Bioorg Med Chem Lett,* 22**,** 7127-30.

Sissi, C., Perdonà, E., Domenici, E., Feriani, A., Howells, A. J., Maxwell, A. & Palumbo, M. 2001. Ciprofloxacin affects conformational equilibria of DNA gyrase A in the presence of magnesium ions. *Journal of Molecular Biology,* 311**,** 195-203.

Smith, C. G., Dietz, A., Sokolski, W. T. & Savage, G. M. 1956. Streptonivicin, a new antibiotic. I. Discovery and biologic studies. *Antibiot Chemother (Northfield Ill),* 6**,** 135-42.

Sreejith, S. R., Nair, M. G. & Rao, D. D. 2014 Evaluation of sample pretreatment methods for analysis of polonium isotopes in herbal medicines. *Journal of Environmental Radioactivity*. 138, 417-20.

Srivastava, J. Chandra, H. Nautiyal, A. R. Kalra, S. J. S. 2014. Antimicrobial resistance (AMR) and plant-derived antimicrobials (PDA$_m$s) as an alternative drug line to control infections. *Biotech*. 4**,** 451-460.

Stace, C. (ed.) 1992. *New Flora of the British Isles*. 171-172.

Steinberg, R. A. 1940. Mutations and Reversions in Reproductivity of Aspergilli with Nitrite, Colchicine and d-Lysine. *Proceedings of the National Academy of Sciences of the United States of America,* 26**,** 363-6.

Stewart Tull, D. E. 1980. The immunological activities of bacterial peptidoglycans. *Annual review of microbiology,* 34**,** 311-40.

Sti, C. 2002. A Nucleotide-dependent molecular switch controls ATP binding at the C-terminal domain of Hsp90. N-terminal nucleotide binding unmasks a C-terminal binding pocket. *Journal of biological chemistry,* 277**,** 7066-75.

Still, W. C., Kahn, M. & Mitra, A. 1978. *J. Org. Chem,* 43**,** 2923-2925.

Stotz, A. & Linder, P. 1990. The ADE2 gene from *Saccharomyces cerevisiae*: sequence and new vectors. *Gene,* 95**,** 91-8.

Tan, J., Wang, B. & Zhu, L. 2009. DNA binding, cytotoxicity, apoptotic inducing activity, and molecular modeling study of quercetin zinc(II) complex. *Bioorg Med Chem,* 17**,** 614-20.

Tanitame, A., Oyamada, Y., Ofuji, K., Fujimoto, M., Iwai, N., Hiyama, Y., Suzuki, K., Ito, H., Terauchi, H., Kawasaki, M., Nagai, K., Wachi, M. & Yamagishi, J. 2004. Synthesis and antibacterial activity of a novel series of potent DNA gyrase inhibitors. Pyrazole derivatives. *J Med Chem,* 47**,** 3693-6.

Torrence, M. E. & Isaacson, R. E. 2003. *Microbial Food Safety in Animal Agriculture: Current*

Topics, Ames, Iowa State Press. 53.

Tran, J. H., Jacoby, G. A. & Hooper, D. C. 2005. Interaction of the plasmid-encoded quinolone resistance protein Qnr with *Escherichia coli* DNA gyrase. *Antimicrob Agents Chemother,* 49**,** 118-25.

Trtikova, M. 2009. Effects of competition and mowing on growth and reproduction of the invasive plant *Erigeron annuus* at two contrasting altitudes. *Botanica Helvetica,* 119**,** 1-6.

Trzcinski, K. 2000. Expression of resistance to tetracyclines in strains of methicillin-resistant *Staphylococcus aureus*. *Journal of antimicrobial chemotherapy,* 45**,** 763-770.

Tu, Y. 2011. The discovery of artemisinin (qinghaosu) and gifts from Chinese medicine. *Nature medicine,* 17**,** 1217-1220.

Velmurugan, P., Velmurugan, M., Cho, S.-M., Lee, J.-H., Park, S. & Bae, B.-T. 2014. Antimicrobial fabrication of cotton fabric and leather using green-synthesized nanosilver. *Carbohydrate polymers,* 106**,** 319-325.

Verghese, J., Nguyen, T., Oppegard, L. M., Seivert, L. M., Hiasa, H. & Ellis, K. C. 2013. Flavone-based analogues inspired by the natural product simocyclinone D8 as DNA gyrase inhibitors. *Bioorganic & Medicinal Chemistry Letters,* 23**,** 5874-5877.

Vivien, E., Pitorre, D., Cociancich, S., Pieretti, I., Gabriel, D. W., Rott, P. C. & Royer, M. 2007. Heterologous production of albicidin: a promising approach to overproducing and characterizing this potent inhibitor of DNA gyrase. *Antimicrob Agents Chemother,* 51**,** 1549-52.

Waksman, S. A. 1941. Antagonistic Relations Of Microorganisms. *Bacteriological reviews,* 5**,** 231-291.

Waksman, S. A. 1943. Production and Activity of Streptothricin. *J Bacteriol,* 46**,** 299-310.

Waksman, S. A. 1947. What is an antibiotic or an antibiotic substance *Mycologia,* 39**,** 565-569.

Walsh, C. 2000. Molecular mechanisms that confer antibacterial drug resistance. *Nature,* 406**,** 775-781.

Watanabe, K., Sasaki, T. & Kawakami, K. 1998. Comparisons of chemically-induced mutation among four bacterial strains, *Salmonella typhimurium* TA102 and TA2638, and *Escherichia coli* WP2/pKM101 and WP2 uvrA/pKM101: collaborative study III and evaluation of the usefulness of these strains. *Mutat Res,* 416**,** 169-81.

Watson, N. 1988. A new revision of the sequence of plasmid pBR322. *Gene,* 70**,** 399-403.

Watt, P. M. & Hickson, I. D. 1994. Structure and function of type II DNA topoisomerases. *Biochem J,* 303 (Pt 3)**,** 681-95.

Weeks, H. F. 1980. Chloramphenicol. *MCN, the American journal of maternal child nursing,* 5**,** 280.

Wehrli, W., Nuesch, J., Knusel, F. & Staehelin, M. 1968. Action of rifamycins on RNA polymerase. *Biochim Biophys Acta,* 157**,** 215-7.

Wexler, P. 2014. *Encyclopedia of Toxicology*, Elsevier Science Publishing Co Inc 187.

Wilson, J. W., Schurr, M. J., Leblanc, C. L., Ramamurthy, R., Buchanan, K. L. & Nickerson, C. A. 2002. Mechanisms of bacterial pathogenicity. *Postgrad Med J,* 78**,** 216-24.

Wong, L.-L. 1998. Cytochrome P450 monooxygenases. *Current opinion in chemical biology,* 2**,** 263-268.

Worthington, R. & Worthington, C. 2013. Overcoming Resistance to β-Lactam Antibiotics. *Journal of organic chemistry,* 78**,** 4207-4213.

Wu, L. J. & Wu, J. Z. 2003. *Medicinal Chemistry of Natural Products,* Beijing, People's medical publishing house.283.

Wu, R. & Wu, T. 1996. A novel intact circular dsDNA supercoil. *Bull Math Biol,* 58**,** 1171-85.

Xi, Z. X., Wang, Y., Li, X., Wu, Z. J., Sun, L. N. 2011. Chemical constituents of petroleum ether fractions of *Gnaphalium affine* D. Don. *Academic Journal of Second Military Medical University.* 32, 3, 311-313.

Yang, S. C., Pu, J. X., Lu, Y., Xiao, F. H., Xiao, W. L. & Sun, H. D. 2008. A new lipophilic monosaccharide from *Erigeron annuus*. *Chinese Chemical Letters,* 19**,** 1231-1233.

Yoo, N. H., Jang, D. S., Yoo, J. L., Lee, Y. M., Kim, Y. S., Cho, J. H. & Kim, J. S. 2008. Erigeroflavanone, a flavanone derivative from the flowers of *Erigeron annuus* with protein glycation and aldose reductase inhibitory activity. *J Nat Prod,* 71**,** 713-5.

Yu, J., Cui, M., Li, H. Y. & Ye, Z. G. 2011. The Safety-influencing Factors in Use of the Tonics of Chinese Medicine: A Meta-analysis Based on the Case Reports in Periodicals. *Journal of Traditional Chinese Medicine,* 21**,** 130-135.

Yue J.M., Lin Z.W., Wang D.Z., Sun H.D. 1994. A sesquiterpene and other constituents from *Erigeron breviscapus*. *Phytochemistry,* 36:,717-719.

Zheng, X., Wang, W., Piao, H., Xu, W., Shi, H., Zhao, C. 2013. The Genus *Gnaphalium* L. (Compositae): Phytochemical and Pharmacological Characteristics. *Molecules*. 18, 8298-8318.

Zimmermann, F. 1977. Genetic effects of nitrous acid. *Mutation research - Fundamental and Molecular Mechanisms of Mutagenesis,* 39**,** 127-48.

Zimmermann, F. K. 1973. A yeast strain for visual screening for the two reciprocal products of mitotic crossing over. *Mutation Research/Environmental Mutagenesis and Related Subjects,* 21**,** 263-269.

Zimmermann, F. K. 1975. Procedures used in the induction of mitotic recombination and mutation in the yeast Saccharomyces cerevisiae. *Mutation research - Fundamental and Molecular Mechanisms of Mutagenesis,* 31**,** 71-86.